ISTANBUL TECHNICAL UNIVERSITY ★ GRADUATE SCHOOL

PREDICTION OF EARLY-AGE MECHANICAL PROPERTIES OF HIGH STRENGTH CONCRETE WITH POZZOLANS BY USING STATISTICAL METHODS

M.Sc. THESIS

Muzaffer Umur DALGIC

Department of Civil Engineering

Structure Engineering Programme

JUNE 2022

ISTANBUL TECHNICAL UNIVERSITY ★ GRADUATE SCHOOL

PREDICTION OF EARLY-AGE MECHANICAL PROPERTIES OF HIGH STRENGTH CONCRETE WITH POZZOLANS BY USING STATISTICAL METHODS

M.Sc. THESIS

Muzaffer Umur DALGIC
(501181029)

Department of Civil Engineering

Structure Engineering Programme

Thesis Advisor: Prof. Dr. Yılmaz AKKAYA

JUNE 2022

ISTANBUL TEKNİK ÜNİVERSİTESİ ★ LİSANSÜSTÜ EĞİTİM ENSTİTÜSÜ

İSTATİSTİK YÖNTEMLER KULLANILARAK PUZOLAN KATKILI YÜKSEK DAYANMLI BETONLARIN ERKEN YAŞ MEKANİK ÖZELLİKLERİNİN TAHMİNİ

YÜKSEK LİSANS TEZİ

Muzaffer Umur DALGIÇ
(501181029)

İnşaat Mühendisliği Anabilim Dalı

Yapı Mühendisliği Programı

Tez Danışmanı: Prof. Dr. Yılmaz AKKAYA

HAZİRAN 2022

Muzaffer Umur DALGIC, a M.Sc./a Ph.D. student of ITU Graduate School student ID 501181029, successfully defended the thesis/dissertation entitled "PREDICTION OF EARLY-AGE MECHANICAL PROPERTIES OF HIGH STRENGTH CONCRETE WITH POZZOLANS BY USING STATISTICAL METHODS", which he/she prepared after fulfilling the requirements specified in the associated legislations, before the jury whose signatures are below.

Thesis Advisor :	**Prof. Dr. Yılmaz AKKAYA** İstanbul Technical University	.....
Jury Members :	**Dr. Oğuz GÜNEŞ** Istanbul Technical University	.....
	Dr. Yuşa ŞAHİN Yozgat Bozok University	.....

Date of Submission : 02 June 2022
Date of Defense : 14 June 2022

To my beloved family,

FOREWORD

Above all, I really would like to show my all-hearty thankfulness to my thesis advisor Prof. Dr. Yılmaz AKKAYA for leading me in this study. His supervising and examining in the concept of this thesis are very appreciated. In addition, I am also grateful to my thesis jury members Dr. Oğuz GÜNEŞ and Dr. Yuşa ŞAHİN for sharing their time to attend in my thesis jury.

I kindly thank to Res. Asst. Yonca BAB for her encouragement and support in my entire thesis study. Moreover, I honestly remark the help of my friend Ozlem Ezgi DURAN throughout the time from the beginning and to the end of the graduate program.

Besides, it is truly hard to describe my sincere gratitude to my family for their unconditional and undeniable support which is full of family bliss for my entire life.

June 2022

Muzaffer Umur DALGIC
(Civil Engineer)

TABLE OF CONTENTS

Page

ABBREVIATIONS

AD.1 , AD.2	**:** Superplasticizer
ANFIS	**:** Adaptive-Network-Based Fuzzy Inference System
ANN	**:** Artificial Neural Network ANN
BP	**:** Backpropagation
BPNN	**:** Backpropagation Neural Network
BR	**:** Bayesian Regularization
C	**:** Cement, Cement Content, Cement Type, and Cement Dosage
Ç	**:** Çimento
CA	**:** Coarse Aggregate
CA/A	**:** Coarse Aggregate to Aggregate Ratio
CEM 32.5N	**:** Class S Cement Type
CEM 32.5R	**:** Class N Cement Type
CEM 42.5N	**:** Class N Cement Type
CEM 42.5R	**:** Class R Cement Type
CEM 52.5N	**:** Class R Cement Type
CEM 52.5R	**:** Class R Cement Type
CEMI 42.5N	**:** Cement Type
CEMI 52.5LA	**:** Cement Type
CEMI 52.5N	**:** Cement Type
CEMIII BS	**:** Cement Type
CEMI	**:** Cement Type
CEMIII	**:** Cement Type
CFGPC	**:** Class F Fly Ash Based Geopolymer Concrete
CS	**:** Compressive Strength, and Crushed Sand
E	**:** Modulus of Elasticity, and Water Content
FA	**:** Fine Aggregate, and Fly ash
FA/A	**:** Fine Aggregate to Aggregate Ratio
GGBS	**:** Ground Granulated Blast Furnace Slag
H	**:** Air Content

HKOK : Hata Karelerin Ortalama Kökü

HKT : Hataların Kareler Toplamı

İNA : İnce Agrega

İRA : İri Agrega

LM : Levenberg-Marquardt

ME : Modulus of Elasticity

MLA : Machine Learning Algorithm

MLR : Multiple Regression Analysis

MRA : Multivariate Regression Analysis

MS : Micro Silica

MSE : Mean Square Error

NAB : Normal Ağırlıklı Beton

NNF : Neural Net Fitting

NO:0 , NO:1 , NO:2 : Coarse Aggregate

NS : Natural Sand

NSE : Nash–Sutcliffe Efficiency

NWC : Normal Weight Concrete

ÖGYFC : Öğütülmüş Granüle Yüksek Fırın Cürufu

OKH : Ortalama Kök Hata

OPCC : Ordinary Portland Cement Concrete

PCS : Predicted Compressive Strength

PME : Predicted Modulus of Elasticity

PSTS : Predicted Splitting Tensile Strength

RBFNN : Radial Basis Function Neural Netwrok

RCA : Re-cycled Coarse Aggregate

RMSE : Root Mean Square Error

SAU : Sinir Ağı Uyumu

SSE : Sum of Squared of Errors

STS : Splitting Tensile Strength

SVM : Support Vector Machine

T : Theoretical Concrete Weight Computed on an Air-free Basis

UK : Uçucu Kül (UK)

URA : Univariate Regression Analysis

W : Water

W/B	**:** Water to Binder Ratio
W/C, and w/c	**:** Water to Cement Ratio
W_1	**:** Total Weight of All Materials Batched
$W_{concrete}$	**:** Unit Weight of Concrete

SYMBOLS

$\%$	: Percentage
$\bar{x}$, $\hat{y}$	: Predicted/Estimated data results
$\bar{y}$	: Actual Mean Value
±	: Plus, and Minus
≈	: Approximate equality
^{o}C	: Celsius Degree
∞	: Infinite Number
a	: Cement, and Aggregate Type Coefficient
A	: Strength Gain Constant Rate (Regression Line Slope)
a, A	: Constant, and Regression Coefficient/Constant
$a, A\ [\%]$	: Air Proportion
A_0	: Immediate Dissolution
A_1	: Diffusion-controlled Transporting
A_2	: Long-term Kinetical Dissolution
B	: Strength Constant Level (Grade Constant)
b, B	: Regression Coefficient/Constant
c	: Cement Proportion
C_{ca}	: Coarse Aggregate Coefficient
d	: Diameter
d_{max}	: Maximum Diameter
E_0 , E_c , E_d	: Modulus of Elasticity
E'_c	: Predicted/Estimated Modulus of Elasticity
E_{c0}	: 21500 MPa
E_{ci}	: Modulus of Elasticity at day-28
E_{cj}	: Modulus of Elasticity in an Appropriate Age
E_{cm}	: Mean Modulus of Elasticity in GPa
E_{cmt}	: Predicted/Estimated Modulus of Elasticity
f	: Compressive Strength, and Long-term Leaching Characteristics

f'_c : Characteristic Compressive Strength, and Predicted/Estimated Compressive Strength

f_c , f'_c , f_t : Compressive Strength

f_{c28} : Predicted/Estimated Compressive Strength at day-28

f_{c28} : Compressive Strength at day-28

f_{cc} : Cement Norm Strength

f_{cm} : Mean Compressive Strength

$f_{cm}(t)$: Compressive Strength at Age t

f_{cm28} : Mean Compressive Strength at day-28

f_{cmt} : Predicted/Estimated Compressive Strength

f_{ctm} , f_{stp} , f'_t : Splitting Tensile Strength

f'_t : Predicted/Estimated Splitting Tensile Strength

ft. : Feet

GPa : Gigapascal (GN/mm^2) (Pressure)

h : Specimen Height

j^{th} : Compressive Strength Age

K : Constant between 18000 and 23000

k : Correction Factor

K : Regression Constant

k' : Secondary Constant

K_0 : Constant between 4 and 10

k_1 : Aggregate Coefficient

k_2 : Binder Coefficient

K_B : Concrete Age

K_G : Cement Type Coefficient

l : Gauge Length

lb. : Pound

$lb./ft.^3$: Unit Weight

m : Input Number

m : Equation Degree

m^3 : Meter Cube

mm : Millimeter

MPa : Megapascal (N/mm^2) (Pressure)

MPa/s : Pressure at Unit Time (Second)

n	: Function/Equation Degree, Independent Variable, Observation Number, and Output Number
N	: Total Specimen Number
p	: Parameter Number
R	: Correlation of Coefficient, and Korelasyon Katsayısı
R^2	: Coefficient of Determination, and Belirginlik Katsayısı
R^2_{adj}	: Adjusted Correlation of Determination, and Ayarlanmış Belirginlik Katsayısı
R_s	: 150X300 mm Cylinder Compressive Strength
s	: Coefficient, Cement Strength Class
t	: Age/Time, Concrete Age, and Leaching Duration
th	: Function/Equation Degree
w	: Water Proportion
x	: Actual Data Value, Curve Fitting Axis, and Independent Variable
X	: Accelerated Strength, Exponential Value, and Independent Variable
y	: Actual Data Value, Curve Fitting Axis, Compressive Strength, Dependent Variable, Modulus of Elasticity,
Y	: Predicted/Estimated Concrete Strength at day-28, Response Variable in Logarithmic Calculation, and Splitting Tensile
α , β	: Regression Constants
α_E	: Aggregate Coefficient
β	: Estimable Parameter
$\beta_{cc}(t)$	: Time Dependent Strength Development
γ , ρ	: Concrete Unit Weight
ε_{01} , ε_{02}	: Strain
σ	: Standard Deviation
σ_0	: 0.5 MPa Basic Stress
σ_{01} , σ_{02}	: Compressive Strength
σ_1	: Compressive Strength ($0.45f_{cm}$ MPa)
σ_2	: Compressive Strength ($f_{cm}/3$ MPa)
	: Compressive Strength
Δf	: 8 MPa Mean Compressive Strength

LIST OF TABLES

Page

LIST OF FIGURES

Page

PREDICTION OF EARLY-AGE MECHANICAL PROPERTIES OF HIGH STRENGTH CONCRETE WITH POZZOLANS BY USING STATISTICAL METHODS

SUMMARY

The developments in concrete technology are becoming more important and effective with the help of innovative approaches on materials and computer sciences and their applications. With advanced calculation methods, computing programs/softwares and supercomputers, the mechanical behavior of concrete is better understood in many aspects, today. In addition, the materials used in concrete technology are now much more diverse, more useful, and much more effective than in the past by the opportunities provided from the industry. On the other hand, this level of development and effectiveness still depends on specific needs of concrete. However, this natural limitation does not prevent performance improvement, durability, sustainability, environmental and budget-friendly expectations of concrete in a planned service life. Accordingly, while cement types, aggregates, moisture contents of aggregates, and air contents in concrete mixtures maintain their importance, the concrete mixture designs can be rearranged by weight and/or concrete mixing ratios according to the relevant pioneer test results, and new concrete matrices can be obtained by using fly ash, micro silica, nano silica, ground blast furnace slag, fiber, glass, wood, etc. Moreover, recyclable materials such as water, aggregate, glass, fiber, wood, etc. and even living organic materials are the topics that the concrete industry has recently focused on. In this context, the idea of using new construction materials may arise depending on relevant test results of special concretes produced for special projects. However, willing to change the concrete mixture designs and/or building materials based on test results can be quite difficult, because of time and budget concerns. For this reason, the most used type of concrete in the ready mixed concrete world is normal weight concrete (NWC), which is adapted by the concrete industry. Considering this fact, despite all the possibilities, determining a right concrete mixture design still differs in many ways depending on time, material, and external factors. In this idea, in general, specimens of hardened concrete in the form of cubes, cylinders, and rectangular prisms are tested at an early age to obtain results of mechanical properties such as compressive strength, splitting tensile strength, and modulus of elasticity so that further investigations and predictions of the concrete can be made. According to these test results, statistical methods come to the fore in many cases in terms of time and cost efficiency, and deep analysis to predict results of concrete performance depending on time and material to decide whether these concrete mixture designs comply with standards and regulations. Because, in regression analysis, which is one of these statistical methods, it is possible to predict a mechanical property of concrete without using destructive or non-destructive methods with enough concrete samples. In this way, the gains are obtained in terms of space, time, and cost. As a further step from the regression analysis, the use of machine learning methods such as Neural Net Fitting (NNF) to predict a data has become quite common today in the concrete world.

Before statistical estimation of a data set, the concrete mixture designs should be cared for their validations. Furthermore, the atmospheric conditions at work sites where the concrete is casted are very important to obtain realistic test results from the concrete

casting process. Therefore, the experiments such as slump, flow, unit weight, air content, ambient temperature, bleeding, adiabatic process, setting time etc. for fresh concrete samples can be carried out in the work fields. For this thesis, fresh concrete samples were taken for 33 different concrete mixture designs in 150X300 mm cylindrical sample containers in the numbers allowed by national standards and regulations. Besides, two distinct types of fine aggregates (FA) and three diverse types of coarse aggregates (CA) were used in these mixture designs with fly ash (FA) + micro silica (MS), ground granulated blast furnace slag (GGBS), and five different cement (C) types were used as binding material for these designs. The samples prepared within this framework were also kept in safe places in the worksites for the first setting process of the concrete, right after the sampling process was completed. Subsequently, the concrete samples, when the initial setting process were completed, were transferred to the laboratory environment for the hardened concrete tests in the international standards for 0.5, 1, 2, 3, 7, 14 and 28 days. And, the samples were prepared for the compressive strength, splitting tensile strength and modulus of elasticity tests for statistical analysis and estimations.

In this thesis, as one of the statistical analysis models, regression analysis based on convergence of the obtained estimation results to real data (drawing curves) are used. The properties such as age of concrete samples (time), unit weights of mixture components, unit volumes of mixture components, mixing ratios and/or coefficients of an estimation methods etc. were analyzed individually and cumulatively. Accordingly, the relations of the predicted data with the concrete mixture designs are studied with linear or non-linear equations in univariate and multivariate regression models. In addition to the equations used for the estimation of the test results, other statistical results such as R (Correlation of Coefficient), R^2 (Coefficient of Determination), R^2_{adj} (Adjusted Correlation of Determination), Sum of Squared of Errors (SSE), Mean Square Error (MSE), and Root Mean Square Error (RMSE) were obtained. The relationships between the actual test results, and predicted results were examined at the end.

Due to the nature of the models used in the univariate regression analysis, only one variable was considered, and the results were estimated accordingly. The number of variables taken into consideration was analyzed individually for each mixture design. Although such individual analyzes were possible, many sequential studies on the actual, and estimated results had been the cost of time. Therefore, predicting the actual results required more complex analyzes like the multivariate regression analysis in this study. Before the more complex analyses, the variables were studied one-by-one and/or in combinations for the multiple regression analyses. The substantial number of these combinations let the study to the machine learning process, and the effect of hidden layers between the input (mixture designs) values and the target (test) values four output values (algorithm results) were observed in the machine learning process. Although it was really complicated to detect these hidden layers by the individual calculations, only the input values, and target data values were chosen in the machine learning procedure without stepping directly into the hidden layers. On the other hand, it was understood that increasing the number of hidden layers deviated the estimation results from the target values.

Therefore, to obtain more accurate results, the number of samples in the machine learning algorithms were changed as much as possible, while the number of hidden layers was increased. Yet, it was revealed that increasing the number of samples and/or hidden layers at the same time caused undesirable estimation results. It was also

determined that an infinite number of experiments could be made with the machine learning to predict the target values. But, since it was not possible to conduct an infinite number of trials one-by-one, all trials were recorded first, and then evaluated from the best to the worst and/or in the Levenberg-Marquardt (LM) algorithm form the NNF machine learning process. In addition to this, R and MSE values in the NNF machine learning process, training, validation, test, and all correlation results were displayed in the x - y planes. Finally, in this framework, the best results were shared in association with the statistical results with physical meanings specific to mixture designs.

İSTATİSTİK YÖNTEMLER KULLANILARAK PUZOLAN KATKILI YÜKSEK DAYANMLI BETONLARIN ERKEN YAŞ MEKANİK ÖZELLİKLERİNİN TAHMİNİ

ÖZET

Beton teknolojisindeki gelişmeler, malzeme ve bilgisayar bilimleri ile tüm bunların uygulamaları yardımıyla daha önemli ve etkin hale gelmektedir. Gelişmiş hesap yöntemleri, hesap programları ve süper bilgisayarlar ile de betonun mekanik davranışları bugün, birçok yönden çok daha iyi anlaşılmaktadır. Ayrıca beton teknolojisinde kullanılan malzemeler artık çok daha çeşitli, daha kullanışlı ve endüstrinin sağladığı imkanlarla geçmişe oranla çok daha etkilidir. Öte yandan bu gelişmişlik ve etkinlik seviyesi hala daha üretilmek istenen betonun özelindeki ihtiyaçlara bağlıdır. Fakat bu doğal sınırlama betonun planlanan hizmet ömründeki performans gelişiminin, dayanıklı oluşunun, sürdürülebilirliğinin, çevreci ve bütçe dostu oluşu beklentilerinin önüne geçmemektedir. Buna göre çimento türleri, agregalar ve agregaların nem içerikleri ile beton karışımlarındaki hava içerikleri ilk sıradaki önemini korumakla beraber beton karışım tasarımları, uçucu kül, mikro silika, nano silika, öğütülmüş yüksek fırın cürufu, elyaf, cam, ahşap vb. ilaveler ile de ağırlıkça ve/veya beton karışım oranlarınca ilgili öncü test sonuçlarına göre yeniden düzenlenebilmekte ve yeni beton matrisleri elde edilebilmektedir. İlaveten su, agrega, cam, fiber, ahşap vb. gibi geri dönüştürülebilir malzemeler ve hatta canlı organik malzemeler bile son zamanlarda beton endüstrisinin odaklandığı konulardandır. Bu çerçevede özel projeler için hazırlanan özel betonların ilgili test sonuçlarına bağlı olarak yeni yapı malzemelerinin kullanılması düşüncesi de ortaya çıkabilmektedir. Ancak, beton karışım tasarımlarını ve/veya yapı malzemelerini test sonuçlarına göre değiştirmek istemek, özellikle zaman ve bütçe dengesi açısından oldukça zor olabilir. Bu nedenle hazır beton dünyasında en çok kullanılan beton türü, hemen hemen tüm hazır beton endüstrisinin de uyum sağladığı Normal Ağırlıklı Beton'lardır (NAB). Bu gerçeği düşünerek, sahip olunan bunca imkâna rağmen, doğru beton karışım tasarımını belirlemek hala daha zamana, malzemeye ve dış etkenlere bağlı olarak pek çok konuda farklılık göstermektedir. Bu düşüncede, genel olarak, küp, silindir ve dikdörtgen prizma şeklindeki sertleşmiş beton numuneleri, betona dair ileri tetkikler ve tahminler yapılabilmesi adına basınç dayanımı, yarmada çekme dayanımı ve elastisite modülü gibi mekanik özelliklerin sonuçlarını elde etmek için erken yaşta teste tabi tutulur. Bu test sonuçlarına göreyse betonun zamana ve malzemeye bağlı performansları için sonuçları tahmin etmek ve bu beton karışım tasarımlarının standartlara ve yönetmeliklere uygun olup olmadığına karar vermek için istatistiksel yöntemler, zaman ve maliyet verimliliği ile derin çözümlemeler yapabilme açısından birçok yönden öne çıkmaktadır. Çünkü bu istatistiksel yöntemlerden biri olan regresyon analizinde yeterli sayıda beton numunesi ile tahribatlı veya tahribatsız yöntemler kullanmadan betonun mekanik bir özelliğini tahmin etmek mümkündür. Bu sayede yer, zaman ve maliyet açısından kazanç da elde edilir. Regresyon analizinden daha ileri bir adım olarak, bir veriyi tahmin etmek için Sinir Ağı Uyumu (SAU) gibi makine öğrenim yöntemlerinin kullanılması günümüzde iyice yaygınlaşmıştır.

Verilerin istatistiksel tahmininden önce, beton karışım tasarımının güncel ve geçerli olmasına dikkat edilmelidir. Ayrıca beton döküm işleminden gerçeğe yakın test sonuçları elde edilebilmesi için betonun döküldüğü yerdeki atmosfer koşulları da çok önemlidir. Bu nedenle taze beton numuneleri için çökme, yayılma, birim ağırlık, hava

içeriği, ortam sıcaklığı, terleme, adyabatik süreç, priz süresi vb. konularda çalışma sahası içerisinde deneyler yapılır. Bu tez çalışması içinse 33 farklı beton karışım tasarımı kullanılmıştır. Bu karışım tasarımlarında iki farklı tipte ince agrega (İNA) ve üç farklı tipte iri agrega (İRA) kullanılmıştır. Hazırlanan bu tasarımlar için bağlayıcı malzeme olarak, uçucu kül (UK) + mikro silika (MS) ve öğütülmüş granüle yüksek fırın cürufu (ÖGYFC) ile beş ayrı çimento (Ç) türü bulunmaktadır. Bu çerçevede hazırlanan numuneler, numune alım işlemleri tamamlandıktan hemen sonra betonun ilk priz süreci için çalışma alanlarında güvenli yerlerde muhafaza edilmiştir. Akabinde ise ilk priz süreci tamamlanan beton numuneleri 0.5, 1, 2, 3, 7, 14 ve 28 günlük uluslararası standartlarda sertleşmiş beton testlerinin yapılması için laboratuvar ortamına aktarılmıştır. Basınç dayanımı, yarmada çekme dayanımı ve elastisite modülü testleri sonucu elde edilen numuneler istatistiksel olarak çözümlemeler ve tahminler için hazırlanmıştır.

Bu tez çalışmasında istatistiksel çözümleme modellerinden biri olarak, elde edilen tahmin sonuçlarını gerçek verilere yakınsamaya (eğri çizme) dayanan regresyon analizi kullanılmıştır. Beton numunelerinin yaş (zaman), karışım bileşenlerinin birim ağırlıkları, karışım bileşenlerinin birim hacimleri, karışım oranları ve/veya tahmin yöntemlerinin katsayıları vb. özellikleri tek tek ve toplu olarak incelenmiştir. Buna bağlı olarak da tahmin edilen verilerin beton karışım tasarımlarıyla olan ilişkileri, doğrusal veya doğrusal olmayan denklemler ile hem tek hem de çok değişkenli regresyon modelleri ile çalışılmıştır. Sonuçların tahmini için kullanılan denklemlerin yanı sıra, R (Korelasyon Katsayısı), R^2 (Belirginlik Katsayısı), R^2adj (Ayarlanmış Korelasyon Katsayısı), Hataların Kareler Toplamı (HKT), Ortalama Kök Hata (OKH), Hata Karelerin Ortalama Kökü (HKOK) gibi diğer istatistiksel sonuçlara ulaşılmış, bu sonuçlar bir silsile içerisinde derlenmiş ve test sonuçları ile tahmin edilen sonuçlar arasındaki ilişkiler irdelenmiştir.

Tek değişkenli regresyon analizlerinde kullanılan modellerin doğası gereği tek bir değişken dikkate alınmış ve sonuçlar buna bağlı olarak tahmin edilmiştir. Değerlendirmeye alınan değişken sayısı kere her bir karışım tasarımı için tek tek analiz yapılmıştır. Bu gibi tek tek analizler mümkün olsa da gerçek ve tahmini sonuçlarda pek çok ardışık çalışma yapmak fazlaca zaman kaybına sebep olmuştur. Bu nedenle sonuçların öngörülmesi, bu çalışmada olduğu gibi çok değişkenli regresyon analizi ya da buna benzer şekilde daha karmaşık analizlere ihtiyaç duyulmuştur. Daha karmaşık analizlerden önce çoklu regresyon analizleri ile değişkenler toplu ve/veya kombinasyonlar halinde çalışılmıştır. Bu kombinasyonların sayıca çokluğu çalışmayı makine öğrenmesi sürecine yönlendirmiş ve makine öğrenmesi sürecinde girdi (karışım tasarımları) değerler ile hedef (gerçek) değerlerin sonuçlara (algoritma sonuçları) götüren gizli katmanlardaki etkisi görülmüştür. Bu gizli katmanların tek tek hesaplamalar ile tespit edilmesi çok karmaşık olmakla birlikte makine öğrenmesi sürecinde gizli katmanlara doğrudan adım atılmadan sadece girdi (karışım tasarımları) değerler ve hedef veriler (gerçek) değerler kullanılmıştır. Öte yandan, gizli katmanların sayısının arttırılmasının, tahmin sonuçlarının hedef değerlerden uzaklaştırdığı anlaşılmıştır. Bu nedenle, daha doğru sonuçlar elde etmek için algoritmalardaki örnek sayıları mümkün olduğunca değiştirilirken gizli katman sayıları da artırılmıştır. Ancak örneklerin ve/veya gizli katmanların sayılarının aynı anda arttırılmasının istenmeyen düşük tahmin sonuçlarına neden olduğu ortaya çıkmıştır. Hedef değerleri tahmin etmek adına makine öğrenmesi ile sonsuz sayıda deneme yapılabileceği de ayrıca saptanmıştır. Fakat sonsuz sayıda deneme yapılması mümkün olmayacağı için yapılan tüm denemeler önce kaydedilmiş ve daha sonra SAU

makine öğrenmesi sürecinde Levenberg-Marquardt algoritmasında en iyiden en kötüye ve/veya tam tersi şeklinde değerlendirilmiştir. İlave olarak SAU makine öğrenmesi sürecinde R ve OKH değerleri ile x – y düzlemi içerisinde deneme, doğrulama, test ve nihai korelasyon sonuçları alınmıştır. Son olaraksa bu çerçevede, istatistiksel sonuçların karışım tasarımlarına özgü fiziksel anlamlarla ilişkilendirilmesi için en iyi sonuçlar paylaşılmıştır.

1. INTRODUCTION

Concrete is a mass of medium of cementing in common sense. In general, this medium product is an exothermic chemical reaction of water with hydraulic cement (Neville and Brooks., 2010). This chemical reaction is also explained as binding fine and coarse aggregates, cement, and water together in a harmony (Akman, 1990). However, in previous types of concrete, fine aggregate was not a mixture element. Except absence of fine aggregate, for some special cases, concrete has also some cementitious supplements and/or chemical admixtures (Ghafoori and Dutta, 1995). In these previous and present types of concrete, the main binder material is cement. Contrast the past, recently, for compactness, sand as fine aggregate fills the gaps between coarse aggregates. Furthermore, the general frame of concrete is made of gravel or crushed stone to resist the external forces applied on concrete (Akman, 1990).

In addition to the components and effects, producing concrete has undeniable effects in climate change crisis. Heat emission of cement manufacturing and groundwater recharging to use in concrete products are serious worries for environmental concerns (Ibrahim et al., 2014). To decrease the negative effects of concrete producing and for sustainable development in green concrete technology, the industry supplies opportunities such as cements in several types and aggregates in different sizes as products of construction materials (ACI Materials Journal., 2011; Bingol et al., 2013).

Besides the conventional concrete materials, some of waste products from the heavy industry are now widely preferred in concrete technology. Especially slag and fly ash are almost used in every concrete production process, now. Why slag is preferred in concrete mixture designs as a pozzolan is its calcium oxide content which is considerably low. Also, it has perfect chemical and mechanical aspects which are determined as eco-friendly choice to be replaced with fine aggregates. Although fly ash is generally not a binder alone, it is another artificial pozzolan that hardens in water by a hydration reaction with slaked lime. In this perspective, fly ash can be used with cement or directly added to concrete instead of sand, which is also considered as environmental practice (Yilmaz, 2014). Because of these kinds of benefits, use of slag

and fly ash is now increased in normal weight and heavy weight concretes (Ambily et al., 2015 ; Gorai et al., 2003 ; Al-Jabri et al., 2009 ; Khanzadi and Behnood, 2008 ; Wei, 2009).

In addition to the damages of concrete production process and use of groundwater, and even benefits of use of industrial wastes in concrete technology, there is another point of focus as a trend which is expedition of concrete works in construction fields. Because of this issue, fast concrete casting for again time and budget/cost limitations, there may be quite dangerous factors for construction and structure health. Because of the dispatch of construction works, it may not be possible to reverse or overly expensive to fix the works that have problems. For why until concrete samples are taken, and then tested, the construction works are not or cannot be stopped. Nevertheless, under standard methods, the concrete samples are needed to be cured, and then tested to get the results of early age strength developments of concrete. Until the time that the test results are released, at worksites, there can be some critical problems in concrete health based on human factors. Because of this, to take actions in advance for unexpected situations, to check the quality of concrete on time is necessary to estimate the strength of concrete at day-28. To make this estimation, again, it is also another necessity to apply accelerated curing methods. Yet, every construction site may not have an opportunity to apply standard curing methods for concrete samples previously taken. That is why, prediction methods such as regression analysis from statistics and machine learning process in computing sciences to illuminate the close future of concrete health come forward to save time, money, place and to eliminate human based risks in construction works (Arioglu et al., 1994).

To extrapolate a mechanical property of an early age concrete needs conjectures by using either statistical models or machine learning algorithms. For this extrapolation, a premise data collection is required at laboratory conditions. Under standard curing methods, the samples in exact dimensions for an exact mechanical test are taken in-situ conditions. And then they are tested by applying external forces until they are reached to the load bearing capacity (NT BUILD 200, 1984; NT BUILD 201, 1984; NT BUILD 202, 1984; NT BUILD 203, 1984; NT BUILD 204, 1984; NT BUILD 205, 1984).

For the compressive strength, splitting tensile strength and modulus of elasticity tests, cube and/or cylinder samples are molded in-situ conditions (NT BUILD 200, 1984;

NT BUILD 201, 1984; NT BUILD 202, 1984; NT BUILD 203, 1984; NT BUILD 204, 1984; NT BUILD 205, 1984). After completing the tests, the results are revealed with the concrete specimen ages. By the help of statistical methods and/or machine learning potentialities, these data sets can be predicted and analyzed to express the strength developments of concrete at early ages for concrete mixture designs with optimizations. Because those optimizations may lead producing of concrete in less cost and environmentally friendly which are now highly recommended in modern concrete technology (Arioglu et al., 1994).

On the other hand, there are many computational techniques in addition to the statistical model by using artificial intelligence as machine learning. (Bendapudi, 2019) To elaborate the machine learning, artificial neural network (ANN), adaptive-network-based fuzzy inference system (ANFIS), neural net fitting (NNF) and support vector machine (SVM) step forward as some of the mostly chosen software methods to predict a data set by using mechanical properties of concrete (Kockal and Aydogdu., 2020).

Presuming these mechanical properties of concrete is important for either modern construction works or structural members. Transporting those members from a place to another, mechanical loading, placing joints of precast members and removing formworks are the several topics of early age strength developments of concrete for the reasons of safety and economy. Especially in sub-zero air conditions, having pre-knowledge of strength developments of concrete is very essential (Price et al., 1996).

Although the strength gaining of concrete is externally complicated with many factors, statistical models are studied to predict early age strengths of concrete in the regression analysis. In the regression analysis, mixture designs of concrete have an opportunity to be optimized by using univariate and multivariate regression models. By these models, studied mechanical properties of concrete and their applications, are predicted to see linear and non-linear behaviors and their correlations for the strength developments of concrete based on concrete mixture designs (Zain et al., 2008).

Herewith, both statistical models, and machine learning algorithms are decided as the main focuses to predict early age strength developments of concrete. To work in a plan with time, budget and place limitations, computing methods such as univariate and multivariate regression analysis, and machine learning algorithms are recently the

most preferred methods for engineering calculations to optimize the mixture designs of concrete for necessities of strength gaining and performance of concrete.

1.1 Aims and Scope of Thesis

The main objective of this study is to predict the mechanical properties which are the compressive strength, splitting tensile strength and modulus of elasticity by comparing with the strength development of concrete in computing models and tools to find the most suitable concrete mixture designs including fly ash (FA) + micro silica (MS) and ground granulated blast furnace slag (GGBS) ingredients for the strength gaining analysis. In this frame, the same size and shape hardened concrete samples were tested under perpendicular loads to the specimens located at testing plates with millimetric accuracies. For this study, these sample blocks were produced by following the concrete mixture designs which are composed of binder, water, aggregate and admixtures with a wide range. And the mechanical test results are obtained in a very wide range, as well. Because of this, with neural net fitting (NNF) algorithms as machine learning procedure, univariate and multivariate regression analysis models were applied. Firstly, the univariate regression analysis (URA) models were studied on each dependent variable by using the test results. Further, multivariate regression analysis (MRA) models were operated on the dependent variables at once by organizing the mechanical properties of hardened concrete specimens. And then, NNF algorithms were constructed with the help of the concrete mixture designs within the practices in the tests. Finally, the results of the prediction models were established with the linear correlations for the strength developments of concrete to build a bridge between physical and statistical meanings.

The total number of models used for every mechanical property was eight in the URA. However, for the MRA, there were four models used for all the mechanical properties. In NNF algorithms for this study, there was only one basic algorithm used as machine learning route. The results of all estimation models and tools were represented in a logic manner to check against the test results by using statistical expressions to find a way for physical meaning either in the test results or in the concrete mixture designs for the strength gaining comments. In these kinds of investigations, the whole target was to state the most sense mixture designs for future suggestions in different cases and conditions in concrete works for the strength development concerns. Because

those concerns are the priorities for durable, sustainable, safe, green and cheap structures and/or construction efforts.

1.2 Organization of Study

The first chapter of this study explains widespread knowledge of models, methods and tools by using the actual test results to predict the compressive strength, splitting tensile strength and modulus of elasticity for the strength developments of concrete.

The second chapter details an omnibus literature brief of the presuming regression analysis models and machine learning tools used in preferences of civil engineering profession to estimate a data set by using the real test results within the concrete mixture designs prepared.

The third chapter shows the experiments done in this thesis. The concrete materials, concrete mixture designs, production procedure of concrete, fresh and hardened concrete tests in-situ and at laboratory conditions are represented. The regression analysis models, and machine learning tool are explicated in the part of hardened concrete specimen tests.

The fourth chapter sums the results of hardened concrete sample tests. In-situ condition practices with their mechanical test results, the regression analysis methods and machine learning tools are exposed in divided sections.

The fifth chapter spotlights the compressive strength, splitting tensile strength and modulus of elasticity predictions in univariate and multivariate regression analysis. Both linear and non-linear equations as regression analysis models are presented in a manner of discussion for the mechanical properties of concrete by age, amounts used in mixtures and proportions used in mixtures as independent variables to make a contact between the test results and statistical results. Followingly, the machine learning algorithms are also shown for a searching to understand how concrete mixture designs are effective on the test results by comparing with the estimated results. Even though the fifth chapter especially targets the strength developments of concrete, the last section of the chapter analyzes the linear correlations between the test and estimated results for all kind of models, methods and algorithms studied in this thesis.

The sixth and the last chapter concludes all efforts and gives suggestions for upcoming research and studies.

2. REVIEW OF LITERATURE

In this part of the study, an inclusive brief of literature about data prediction which is based on regression analysis and machine learning algorithms from test results of the compressive strength, splitting tensile strength and modulus of elasticity is put forth in a chronology with subsections.

2.1 Univariate Regression Analysis for Mechanical Properties of Concrete

The univariate regression analysis (URA) methods have a potential to predict the mechanical properties of concrete by evaluating the actual test results. Without using any destructive and/or non-destructive methods on an existing concrete structure, it is possible to estimate a data set by deciding which independent variable for strength gaining is appropriate to be reclaimed. In this way, time, cost and place limitations are discarded to understand how concrete behaves at an early age period of concrete to gain its strength. Analyzing the test results of the compressive strength, splitting tensile strength and modulus of elasticity by data predictions with statistical results, the exact numbers of errors are also defined to see how close or far the estimated results are to the actual test results.

A model; studied by Pleaces and Dimovic (2009), depending on a polynomial equation to search for a well leaching conduct of ^{137}Cs from the formation of waste in radioactivity by using leach testing of immobilized radioactive waste as suggested in IAEA adopted (Plecas and Dimovic, 2009; Hespe, 1971). In this perspective, the authors prepare concrete samples with Portland cement PC-20-Z-45 MPa, 0-2 mm sand friction; 2-4, 4-8, and 8-15 granulation, bentonite clay, and water. ^{137}Cs as an artificial radioactivity in the composition of $CsNO_3$ is added to the cement by them. Further, they casted the samples in 50X50 mm cylindrical molds. Moreover, they cast the samples in approximately ten minutes. And then, the specimens are sealed and cured by the authors for leaching tests at day-28. After the radioactive process, the leaching process is measured with ER&G-ORTEC spectrometry system and a one-dimensional computing method (Plecas and Dimovic, 2009). They use more than 100

grout formulations to examine the suction and mechanical properties for optimizations of concrete mixtures. Moreover, they focus on four representative formulations and four ^{137}Cs included samples. And then finally, they conclude the study in a result of mathematical analysis by a time dependent polynomial equation to see how the results are well fitted to the literature. They also prove that the one-dimensional model can be used to calculate the migration process parameters and the linear regression model pioneers the results with a minor effect of time variable.

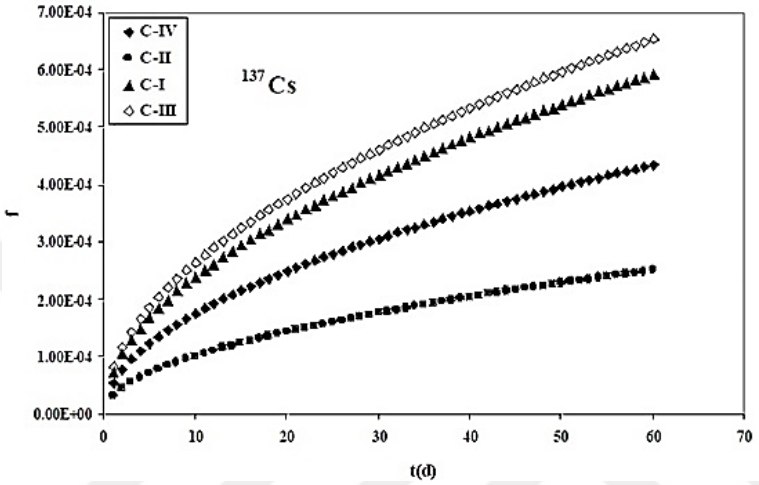

Figure 2.1 : *f* vs. *t* to leach ^{137}Cs from the four specimens. (Plecas and Dimovic., 2009.)

A direct model to guess compressive strength of concrete in different ages is feasible (Abd elaty, 2014). This direct model has two constants in a logarithmic equation to show the strength developments in different conditions of concrete at any age without getting any data at those same ages. He prepares five pastes made of C_3S, C_2S, C_3A and C_4AF. Also, the results are divided into normal and logarithmic scales for concrete mixtures. The author defines the constants used in the model as *A* and *B*. He explains the constant *A* as a denotation of the regression line slope which could be named as the rate of strength gaining constant representing the rate constant. For the constant *B*, the researcher explains that it is an intersection of strength axis by the line of regression. Because it differs from a mixture design to age of compressive strength values. He also adds that the constant *B* is also named as the grade constant. In his study, the results are shown that the logarithmic model with two constants is useful to predict the strength gaining of concrete mixtures that have Portland cement at an age with normal temperature. The model also shows that the strength developments for Portland cement and silica fume added mixtures of concrete at 20 ºC could be

observed. In addition to this, by curing the samples in water at normal temperature 20 ºC, the model is also beneficial to predict the compressive strength for concrete mixtures including nano silica fumes and Portland cement. The author also adds that the constants of the model are the characteristic properties of a mixture of concrete.

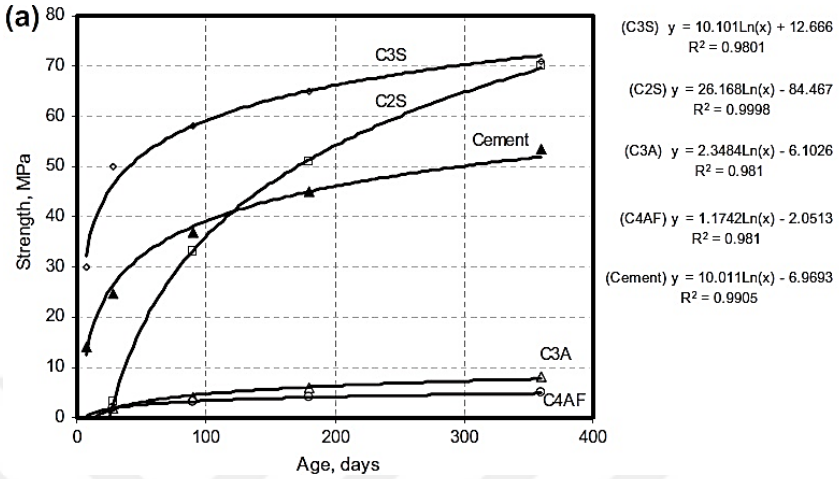

Figure 2.2 : The age vs. compressive strength for mixtures. (a) Normal scale. (Abd elaty, 2014.)

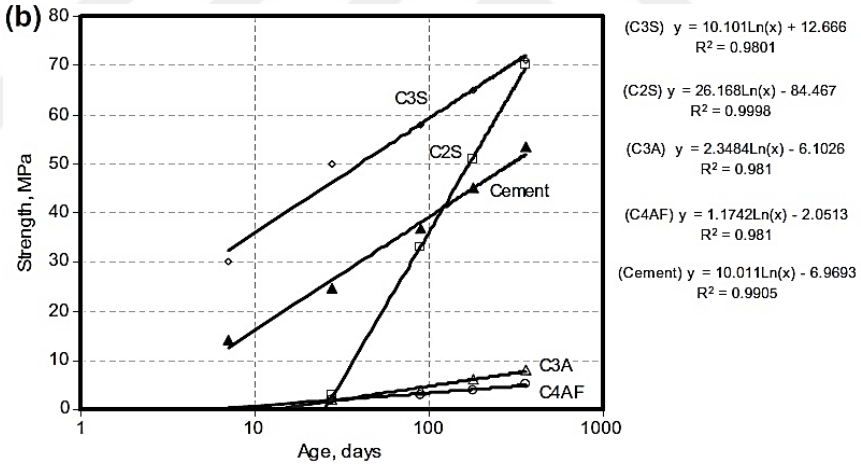

Figure 2.3 : The age vs. compressive strength for mixtures. (b) Log scale. (Abd elaty, 2014.)

Besides, the construction pace has been quickened since the last decade. Because of this, the authors suggest use of 7-day and 28-day tests to make reasonable judgements on the controlling of concrete quality (Resheidat and Ghanma., 1997). In this view, they prepare the concrete mixture designs composed of pozzolanic Portland cement, white cement, crushed aggregates out of limestone, medium and coarse aggregates, valley sand as fine aggregates, pumping facilitator as a superplasticizer admixture for good workability in concrete mixture designs. When the concrete mixture designs are ready, the researchers aim to have the nominal compressive strength of 28-day test

results based on standard cube shaped samples. In this perspective, the author studies the ratio, linear function, power function and exponential models. The results of the authors' study give details about using the Boiling Water Method for accelerated strength tests for concrete in a reliable prediction of 28-day strength for the quality control of concrete. Beyond this method, the study shows enough that the Statistical Ratio Model is a quick way for a data estimation without using more complex solutions. On the other hand, the regression models as linear, power and exponential methods represent close value predictions to the test results. The researchers most importantly add that the test results are more accurate than the tests controlled in laboratory conditions. At the same time, the estimation models and/or methods are the reflections of the real extrapolations of 28-day strength of concrete.

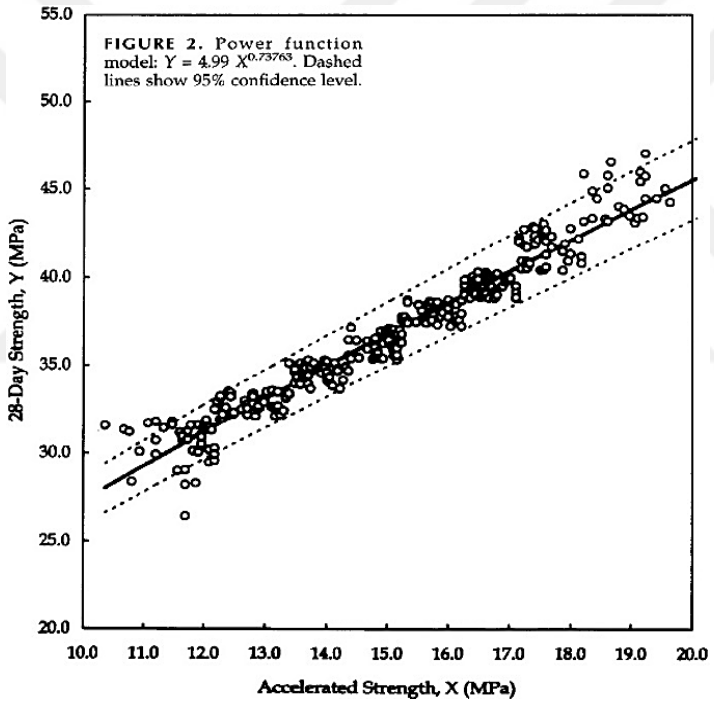

Figure 2.4 : The power function model with 95% confidence level on dashed lines. (Resheidat and Ghanma., 1997.)

McKinney (2009) firstly describes what regression means for engineering applications. The author briefs that regression methods can be explained to construct functions to fit and draw curves for a data set on *x-y* planes. Without focusing an individual point of data sets, the regression methods trend to draw lines and/or curves to drive those same data sets by using the constructed functions. This procedure needs a criterion to measure goodness of a fit of lines and/or curves to the data. This technique is called as least-squares regression. In this approach, the author proposes linear least squares and polynomial regression models. At the same time, he claims

linearization of non-linear relationships to apply the models by searching for the approximated coefficients of the models as a must in linear behavior. The researcher exercises carbon absorption and population growth in suggested models. One of them has the constants *a* and *b* for growth rate in population with limiting conditions where *y* axis aligns saturations in populations with an increase in *x* axis. In this context, Hope et al. and ACI 209.2R-08 (2008) bring that function to the ground by defining the *y* axis as the compressive strength values against to developing concrete age in *x* axis again with the empirical constants *a* and *b* in terms of the cement and curing types for the normal weight, sand weight and light weight concretes.

In the *fib* Model Code for Concrete Structures 2010 (2010), for the time effects on the developments of normal weight concrete strengths, it is functioned at an age which is in days for the mean values of compressive strength in MPa. To detail that equation as a function, the model code uses cement types depend on coefficient *s* with an adjusted age *t* in temperature conditions for curing periods. The research in the model shows that the compressive strengths at ages *t* are based on cement types and classes, admixtures amounts and types, water/cement ratios and external conditions such as humidity with temperature. The proposed model is also obtained from CEM I and CEM III type cements. Whether the other types of cements are decided to be used or pozzolans with excessive amounts are the replacements of CEMI type cement, there is a significant importance for the designs in the compressive strength developments for additional experimental processes. Moreover, using fly ash, natural pozzolans and/or ground granulated blast furnace slag cause decreasing in the compressive strength results at early ages and increasing strength gaining for upcoming ages. In the experimental progress, the model code uses 150 mm size cube molds for concrete casting.

Parallel to the *fib* Model Code for Concrete Structures 2010 (2010), TS802 (2016) offers the similar procedure. With a nuance from *fib* Model Code for Concrete Structures 2010 (2010), British Standards Institution (2004) studies the characteristic compressive strength in a limitation of concrete age which is greater than day-3 and less than day-28. In this manner, the concrete age is still a determinant factor for the characteristic compressive strength.

Table 5.1-9 :	Coefficients to be used in Eq. (5.1-51) for different types of cement	
f_{cm} [MPa]	Strength class of cement	s
≤ 60	32.5 N	0.38
	32.5 R, 42.5 N	0.25
	42.5 R, 52.5 N, 52.5 R	0.20
> 60	All classes	0.20

Table 2.1: The coefficients depending on cement types for compressive strength.
(*fib* Model Code for Concrete Structures 2010, 2010.)

To find a conceivable solution, the code also uses the mean value of compressive strength at an age *t* with the coefficient *s* depends on the cement types. The code also additively suggests for the time early from day 3, more precise calculations ought to be examined.

Table 5.1-3 :	Characteristic strength values of normal weight concrete [MPa]								
Concrete grade	**C12**	**C16**	**C20**	**C25**	**C30**	**C35**	**C40**	**C45**	**C50**
$\mathbf{f_{ck}}$	12	16	20	25	30	35	40	45	50
$\mathbf{f_{ck,cube}}$	15	20	25	30	37	45	50	55	60
Concrete grade	**C55**	C60	**C70**	**C80**	**C90**	**C100**	**C110**	**C120**	
$\mathbf{f_{ck}}$	12	16	20	25	30	35	40	45	
$\mathbf{f_{ck,cube}}$	15	20	25	30	37	45	50	55	

Table 2.2: The norm strengths depending on the cement types
(*fib* Model Code for Concrete Structures 2010, 2010.)

In addition to the univariate regression models to predict the compressive strength, McKinney (2009) indicates for the least square regression approach, the polynomial regression analysis such as a parabola or a cubic function come forward to estimate the splitting tensile strength. Because, in his study, a straight line is weak representation for data fitting rather than a curve fitting. By thinking this proof, a polynomial function in an m^{th} degree with coefficients could be useful to estimate the mechanical properties of concrete. In this frame, whether *x*-*y* axis relationship is truly in m^{th} degree polynomial, and there are not error values, the polynomial curve passes through all data points. In the basis of this sight, Ahmet et al. (2020) tries polynomial regression models due to the concerns of data forecasting in civil engineering. In their estimation models, they use experimental results of the compressive strength as *x* axis

to fit the splitting tensile strength results as *y* axis. In the experimental timeline, the cubic and cylindrical samples are used to collect the data. At the end, it is an obvious result that the compressive strengths of cubic samples are higher than the cylindrical ones. Because of the differences in the results, they multiply the compressive strength results of cubic samples with the factor 0.8 to adjust all results in four different polynomial cases.

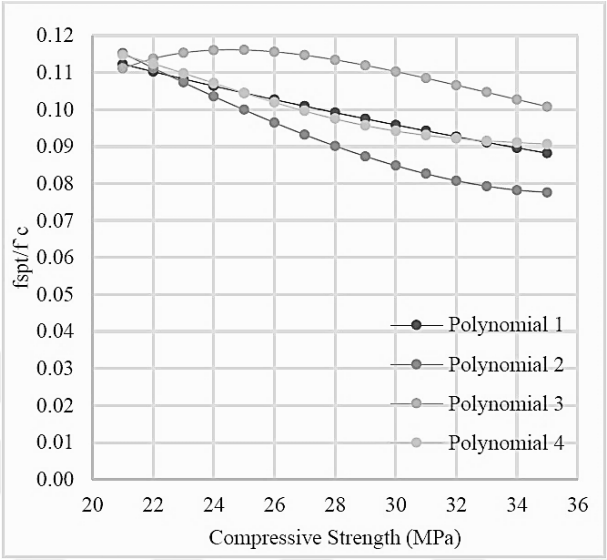

Figure 2.5 : The comparison of different polynomial model ratios for the strengths. (Ahmed et al., 2020.)

The authors also give details about the age of the samples tested. For both 7-day and 28-day of specimen tests, having low water/binder ratio with high compressive strength condition, the splitting tensile strength of concrete and the compressive strength ratio is less than the high water/binder ratio with the low compressive strength condition for the lower strength of concrete. They also add that while the compressive strength increase, the splitting tensile strength and compressive strength proportion decrease. However, this non-linear result changes for all models as the authors' practice. Kim et al. (2002) experiments for concrete 100X200 mm cylinder specimens to realize the effects of water/cement ratios, curing temperatures and cement types with pozzolans on the splitting tensile strength in developing concrete ages. In the study, for the non-linear regression analysis, the power function was chosen for a univariate model. The relationship between the compressive strength and splitting tensile strength is subjected to the elevated temperatures for cuing at early ages again with the high mechanical properties. But the low temperatures for cuing at later ages in lower mechanical properties are also the same. On the other hand, there is no large effects by

using different concrete ages, cement types and curing temperatures on the compressive strength and splitting tensile strength relationships. Finally, the authors conclude the study using power function for a proper estimation of the splitting tensile strength.

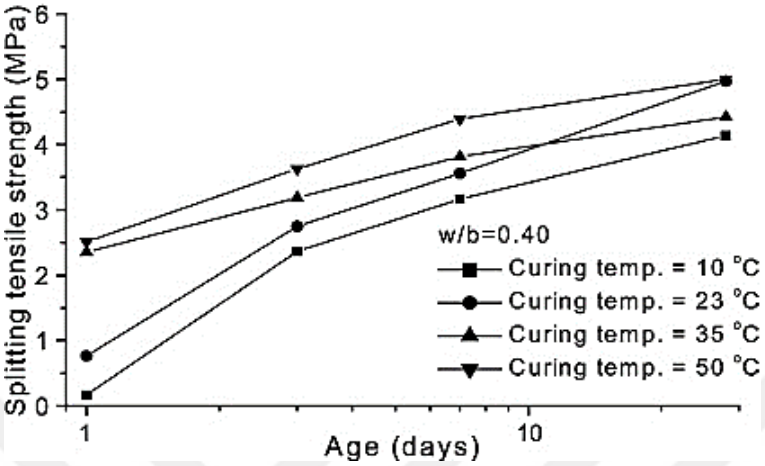

Figure 2.6 : The strength development under different curing temperatures. (Kim et al., 2002.)

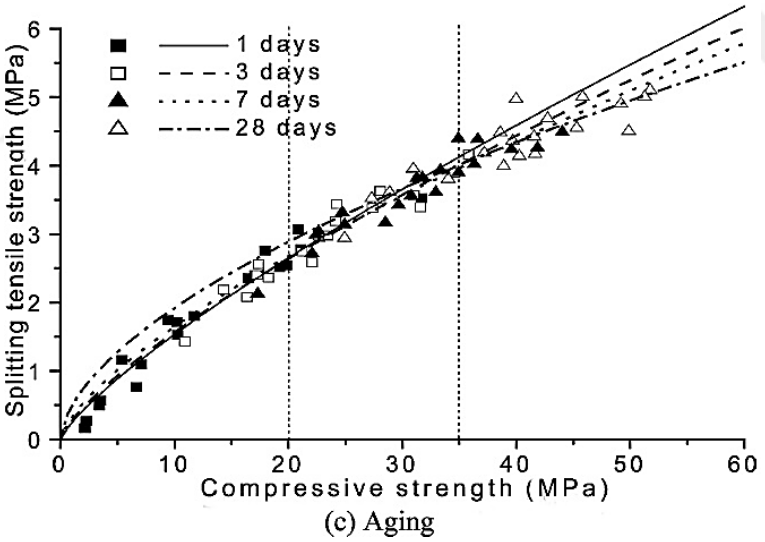

(c) Aging

Figure 2.7 : The strength development at different ages. (Kim et al., 2002.)

AS3600 (2001), Shah et al. (1985), Parrott (1988), Crouch et al., Iravani (1996) and Raphael (1984) also promote the use of power function by testing again cylindrical concrete samples in different mixture designs and/or curing conditions with strength development limitations to estimate the splitting tensile strength. In AS3600 (2001), to use power function in 0.5^{th} degree with an experimental coefficient, it is significant to have 28-day of compressive strength under standard curing procedure. Depending on the data set Shah et al. (1985) works, Parrott (1988) recommends the use of power

function up to 120 MPa cylindrical compressive strength. Crouch et al. designs previous gravel and limestone aggregate concretes and studies the splitting tensile strength developments in use of aggregate types. Additionally, Iravani (1996) operates the concrete samples at 56-day compressive strength from 65 MPa to 120 MPa with or without silica fume additions. He takes care the concrete age, cement types, drying effects, specimen size effects, Poisson's Ratio, and the mechanical properties of concrete. For the estimation of splitting tensile strength, the power function is basis for extension of high-performance concretes with or without cementitious modifiers with 28-day of compressive strength up to 120 MPa. In another research, Raphael (1984) examines thousands of samples in varied sizes and shapes produced between 1928 and 1965 in different water/binder ratios and aggregate sizes. He results the top limit of the cylindrical compressive strength in use of power function analysis at 65 MPa.

Externally, Arioglu and Arioglu (2005) estimate the splitting tensile strength by using logarithmic function which is propounded by Arioglu and Koyluoglu (1997) in regression analysis for univariate models. As independent variable, the compressive strength is used between 1 MPa and 122 MPa. To collect data, they use 150X300 mm cylinder shape concrete samples. They also execute by cross checking the literature suggestions that their studies to forecast the mechanical properties of concrete with different statistical relations end up with the comparable results. They also remind for the colleagues that engineers should be always aware of error margins. With laboratory tests, civil engineers need to search for the literature to analyze physical and mechanical properties of concrete by taking importance of engineering projects with time and cost limitations into account.

In univariate regression analysis, the modulus of elasticity is also another topic of searching for data prediction in civil engineering. Even though this mechanical property is the least studied and the hardest to examine, the literature supports details about getting knowledge on the modulus of elasticity by using the compressive strength test results. As previously mentioned above, McKinney (2009) studies an overview of diverse functions and/or equations able to be used for data forecasting in civil engineering. Those models are adequate to calculate a data set based on independent variables such as the concrete age and compressive strength. Nonetheless, the literature gathers the studies at some basic points such as data analysis for the splitting tensile strength and modulus of elasticity based on compressive strength.

Except this, to predict the compressive strength, the early ages for concrete are another direct factor as independent variables. In ACI Committee 318 (2014), for ordinary Portland cement concrete, it is suggested to use of power function to presume the modulus of elasticity for the lightweight concrete specimens that has unit weights between 90 and 160 lb./ft^3. For the NWC, in the function, there is only experimental coefficient. For a specific task, Diaz et al. (2011) studies class F fly ash based geopolymer concrete (CFGPC) to compare with ordinary Portland cement concrete (OPCC) which are correlated by using the compressive strength test results. Depending on this method, Cui et al. (2020) reveals that the mean elastic modulus of CFGPC is lower than OPCC mixtures. Although the aggregates and aggregate proportions used in the mixtures are the same to the total masses, the difference results observed in the mixtures are because of the attribution of ordinary Portland cement (OPC) and geopolymer binders. They find out that the power function driven in the study which is correlation of the compressive strength and modulus of elasticity is quite adequate in the light of the statistical results (R^2) to estimate the modulus of elasticity.

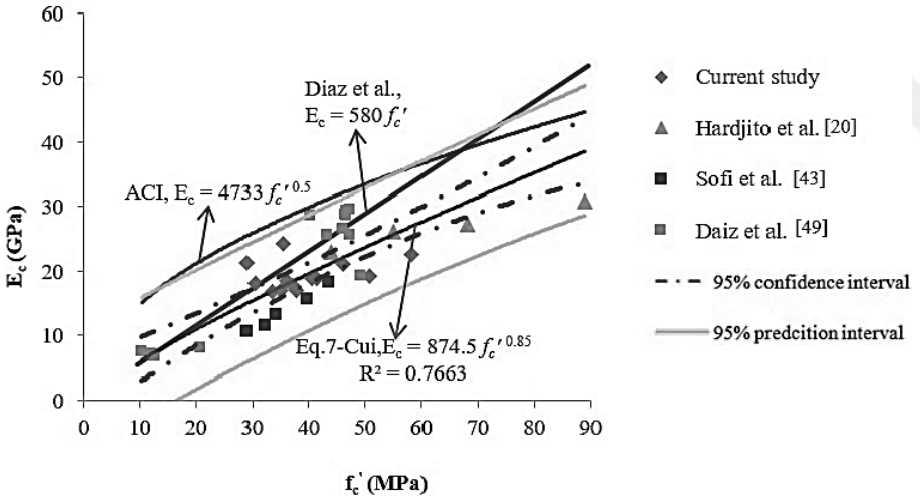

Figure 2.8 : The correlations of compressive strength and modulus of elasticity. (Cui et al., 2020.)

Furthermore, Haque and Rasel-Ul-Alam (2018) refer to operate polynomial, logarithmic and exponential models for the modulus of elasticity calculations. According to the authors, under standard curing methods, the concrete age is the main idea to evaluate the results. The main goal of their study is to characterize the compressive strength with the pattern of diverse specified concrete designs in different strengths. Without additional experiments, by using only standard curing methods, the compressive strength is developed to predict the modulus of elasticity in short term.

For this prediction, the mentioned non-linear models are preferred with the statistical results (R^2, RMSE, NSE) to see how the compressive strength is effective on the modulus of elasticity in an increasing concrete age. They last the results that the regression analyses as non-linear models are possible to illuminate the short-term behaviors of concrete strengths without necessity of more experiments.

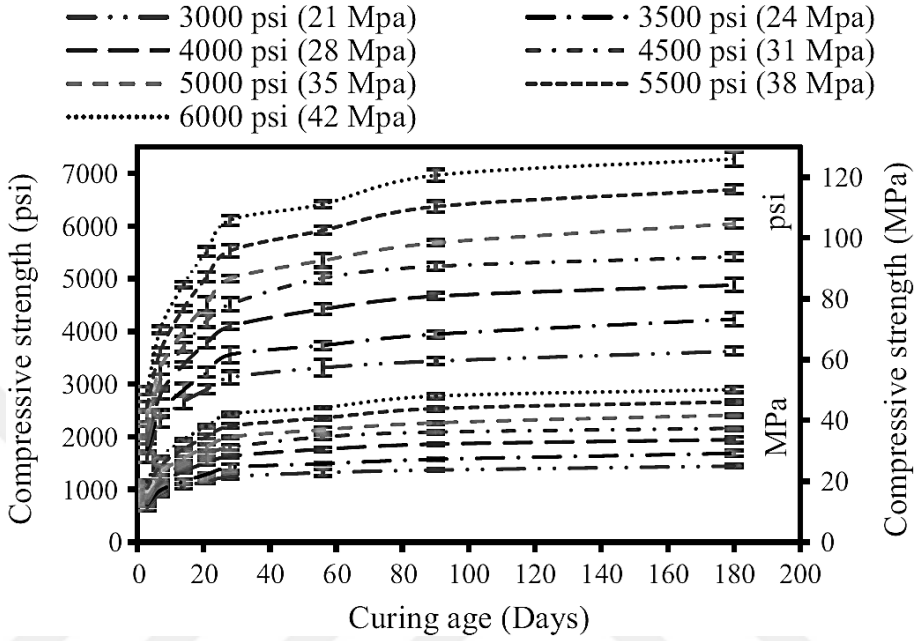

Figure 2.9 : The compressive strength profiles of specified design strengths. (Haque and Rasel-Ul-Alam., 2018.)

Likewise, like the other studies referred above, ACI Committee 363 (2010), CEB – FIB 1990 (1993), and TS500 (2000) also mention the use of univariate regression models to conjecture the modulus of elasticity. The effects of crushed limestone, bauxite, crushed quartzite, crushed andesite, crushed basalt, crushed clay slate, crushed cobblestone aggregates and coarse aggregates are focuses. ACI Committee 363 (2010) derives a power function for the NWC. Beyond the aggregate effects, it studies silica fume, slag, cement and fly ash effects on the development of modulus of elasticity. Although the first impression of the model seems multivariate, the study simplifies the equations by the mathematical calculations to reach univariate effects on the mechanical properties. In CEB-FIP 1990 (1993), the modulus of elasticity for the NWC is calculated from the characteristic compressive strength of concrete at age 28-day. In the calculation, the power function again is the choice of regression models.

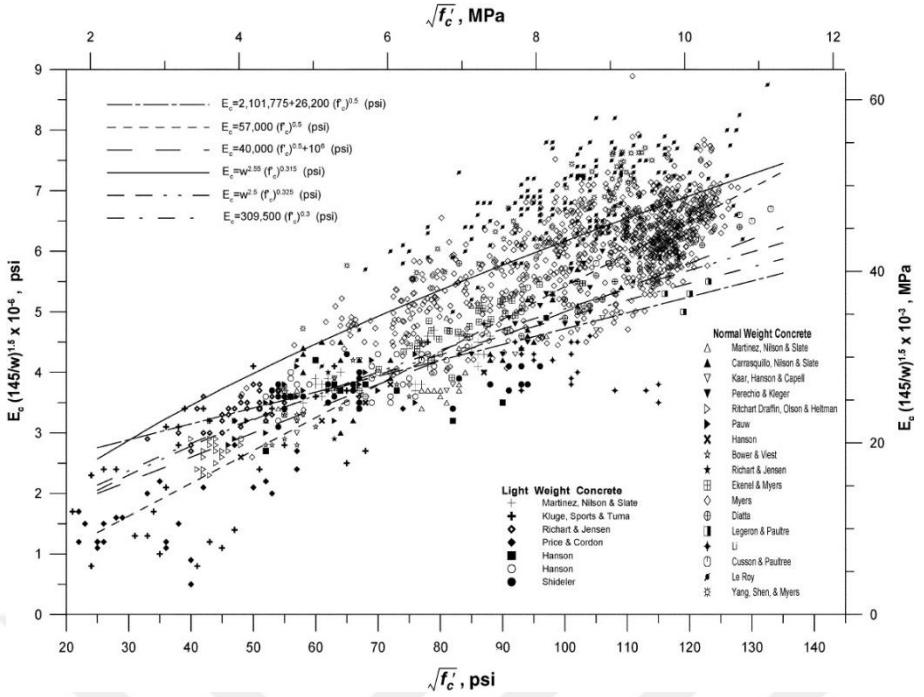

Figure 2.10 : The modulus of elasticity vs. square root of compressive strength. (ACI Committee 363, 2010.)

Though the mean strength of compressive strength is necessary, it is more complex to calculate the modulus of elasticity. Rather than the literature, the code prefers to get tangent moduli to make a comparison for the modulus of elasticity (reduced moduli of elasticity). In this perspective, the code draws a comparison table for different concrete grades.

Table 2.1.6.	**Tangent moduli and reduced moduli of elasticity**							
Concrete grade	**C12**	**C20**	**C30**	**C40**	**C50**	**C60**	**C70**	**C80**
E_{ci} (10^3 MPa)	27	30	34	36	39	41	43	44
E_c (10^3 MPa)	23	26	29	31	33	35	36	38

Table 2.3: The tangent moduli and moduli of elasticity for concrete grades. (CEB-FIP 1990, 1993.)

TS500 (2000) examines the NWC at a j^{th} days for the modulus of elasticity calculations. For j^{th} day, the characteristic compressive strength of cylinder is used. On the other hand, the characteristic compressive strength is multiplied by 0.4 for the stress level corresponding to conformity of secant modulus of elasticity. It also shares 28-day concrete strengths which help to estimate the modulus of elasticity in the Figure 2.13 for the cube and cylinder shape concrete sample values. The calculation function is also in the power form.

ÇİZELGE 3.2 – Beton Sınıfları ve Dayanımları				
Beton Sınıfı	Karakterististik Basınç Dayanımı, f_{ck} MPa	Eşdeğer Küp (200 mm) Basınç Dayanımı MPa	Karakteristik Eksenel Çekme Dayanımı, f_{ctk} MPa	28 Günlük Elastisite Modülü, E_c MPa
C16	16	20	1.4	27000
C18	18	22	1.5	27500
C20	20	25	1.6	28000
C25	25	30	1.8	30000
C30	30	37	1.9	32000
C35	35	45	2.1	33000
C40	40	50	2.2	34000
C45	45	55	2.3	36000
C50	50	60	2.5	37000

Table 2.4: The concrete grades and strengths.
(TS500, 2000.)

In British Standards Institution (2004), like in the data prediction of the compressive strength, there are three different coefficient values depending on different cement types [CEM 42.5R, CEM 52.5N, CEM 52.5R (class R), CEM 32.5R, CEM 42.5N (class N), CEM 32.N (class S)] driven in the time dependent mean compressive strength values which are calculated from an exponential function. In this frame, under standard curing methods, the concrete age and cement types are important factors to manipulate the regression analysis results of modulus of elasticity. However, from complex to simple form, it is also another factor to have the mean value of modulus of elasticity in the power function form to predict the results. At the end of this procedure, the compressive strength is again the prior independent factor for the correlation. In this manner, the characteristic compressive strength of concrete comes forth to construct a regression model to presume an early age concrete strength development for the modulus of elasticity. Besides, to understand the mechanism of elastic deformation of concrete, the code reviews that the mean compressive strength needs to be reduced due to use of distinct types of aggregates such as quartzite, limestone, sandstone and basalt for calculations.

2.2 Multivariate Regression Analysis for Mechanical Properties of Concrete

The univariate regression analysis is one of the mostly preferred methods to predict a data set especially in civil engineering. However, the mechanical properties of concrete are dependent on many factors because of the nature of mixture designs. Due

to this, it is hard to analyze and understand the effects of mixture design materials on concrete strength just because using one independent variable in regression analysis. For instance, time as concrete age; amounts of binders, water, aggregates, admixtures; proportions of materials such as water/cement, water/binder, fine aggregate/aggregate, coarse aggregate/aggregate, and air content as independent variables are the tasks of univariate regression analysis for each. Moreover, univariate regression models can calculate the compressive strength. In this perspective, more complex data analysis is needed for further investigations. As a complicated method, the multivariate regression analysis is the other mostly preferred method for data analysis. In data predictions, the linear and non-linear regression analysis models/functions are operated. For the non-linear functions, there are power, exponential, and logarithmic models. In this view, Abrams (1919) pioneers the importance of use of water to cement ratio for the compressive strength of fully compacted with 1% of air voids concrete in the power function form. With this reference, Ozturan et al. studies the multiple regression analysis with two experimental coefficients and artificial neural network (ANN) approach for the prediction of compressive strength at day-28 with a wide range of concrete mixture properties. In the ANN approach, they examine accurate numbers of hidden neuron numbers and hidden layers. They find out that Abrams' law results have lower correlation of determination than the ANN approach results. Because in the regression analysis water to cement ratio is the only independent variable. Nonetheless, the ANN approach uses all properties of mixture design properties in its hidden neurons and layers. The authors also indicate that the lower correlation of determination may be caused because of plasticizers effects on the concrete microstructures.

Akhtar et al. (2014, 2015) gives details about the multiple regression analysis (MLR) by referring Chau et al. (2005) who identify that the MLR is a casual and time invariant representation of relationships between input and output values. On the other hand, Akhtar et al. (2014, 2015) signifies that the MLR can be studied with two or more dependent and independent variables with linear fitting regression functions for examined data. In this representation, the authors forecast the compressive strength of concrete by using amount of cement (C), fly ash (FA), ground granulated blast furnace slag (GGBS) and water/cement ratio (W/C) for 3-day, 7-day, 14-day, and 28-day age concrete in the MLR form. At the end, they result that use of different amount of FA

and GGBS in replacement of cement leads increase of the compressive strength for high strength concretes at different ages.

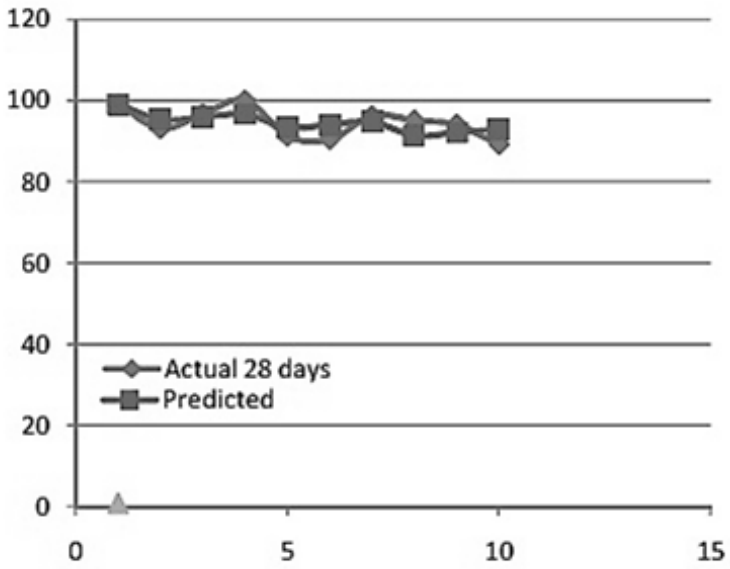

Figure 2.11 : The actual data to predicted data of the compressive strength at day-28. (Akhtar et al.; 2014, 2015.)

As following method, Haranki (2009) refers another power function form for the multivariate regression analysis in volumetric proportions of cement, water, and air. He also uses the coefficient which is from the regression calculations. In the compressive strength equation, Ziolkowski et al. (2021) mentions the mean compressive strength. And the coefficient used in the function is for the aggregate type and cement strength class. Furthermore, Turkel (2002) and Bedirhanoglu (2011) cite that Feret's formula is in second degree. Ziolkowski et al. (2021) also adds that according to the consistency equation Abdelgader et al. (2013), Rajamane et al. (2014) and Zhang et al.(2007) who study ingredient volumes for an analytical method with valid destructive laboratory tests, it is allowable to decide the amount of water, cement, and aggregate per unit volume by weight. In this perception, there are three different methods which are in linear forms. The one of them is incorporated with water demand for water-cement and water-aggregate indexes with cement and aggregate weights in 1 m^3 of concrete. The last method is Bolomey's formula as Gołaszewski et al. (2016) and Abdelgader et al. (2013) put forth. It also seems like the second method based on Feret's formula. For these two methods, the cement to water ratio is necessary with the air content in 1 m^3 of concrete. In addition to this, there is another numerical value named as *a* for the types of aggregates and cements used in concrete. However, Feret's formula is accurate when the strength of aggregate is lower than the strength of grout

and applies to concrete porous (Gołaszewski et al., 2016; Abdelgader et al., 2013). By using Bolomey's formula, Ziolkowski et al. (2021) predict the test results in types of

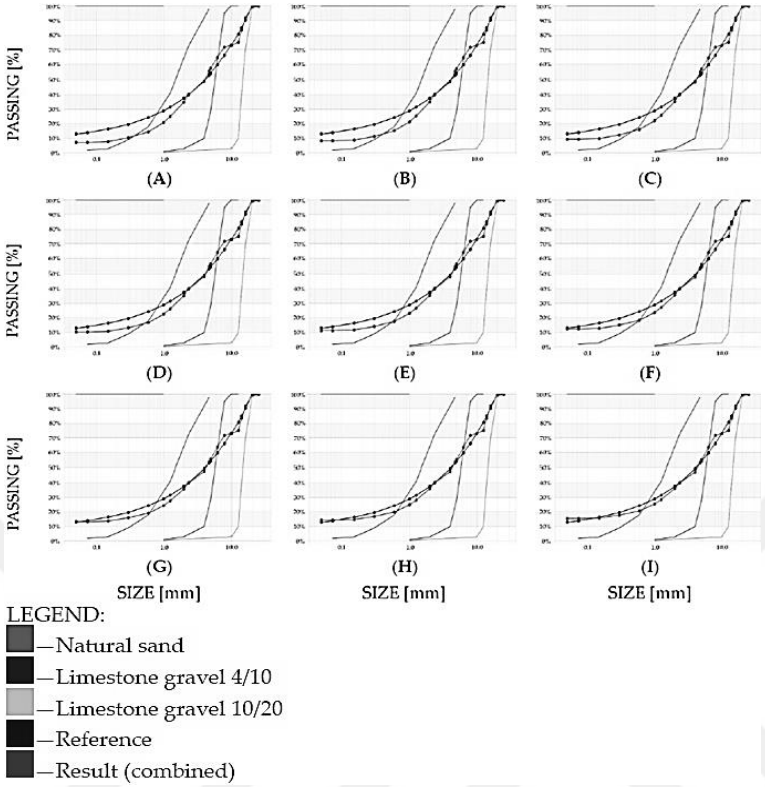

Figure 2.12 : For recipe number 1, fitting curves and gradings. (Ziolkowski et al., 2021.)

aggregates for data fitting with the aggregate sizes in mm to the aggregate passing in percentages from the sieve analysis.

In Graf's formula, there is a correlation in second degree between cement to water ratio and norm strength of cement. In the calculations, the standard values are considered for the norm strength of cement. For instance, the coefficient K_G in the correlation changes between four and ten for CEMI 42.5 cement type (Akman, 1990). As a power function solution, Turkel (2002) also proposes to use the cylinder compressive strength as an output solved by using the cement to water ratio in a fraction value degree. As a result of the study, Turkel (2002) gets high correlation of determination results which are coherent with the test results. Like Abrams' formula, Colak (2006, 2013) studies another non-linear regression model based on the water to cement ratio. At the same time, he finds out that there are two main paths for the compressive strength prediction. The first projection works when the water/cement ratio is known. In this way, the maximum compressive strength is essential to use any water/cement ratio in the equation of estimation. However, the second one is operated

when the maximum compressive strength is absent. For both situations, the Portland cement is also necessary. With Abrams' formula and Colak's correlation, Seitablaiev

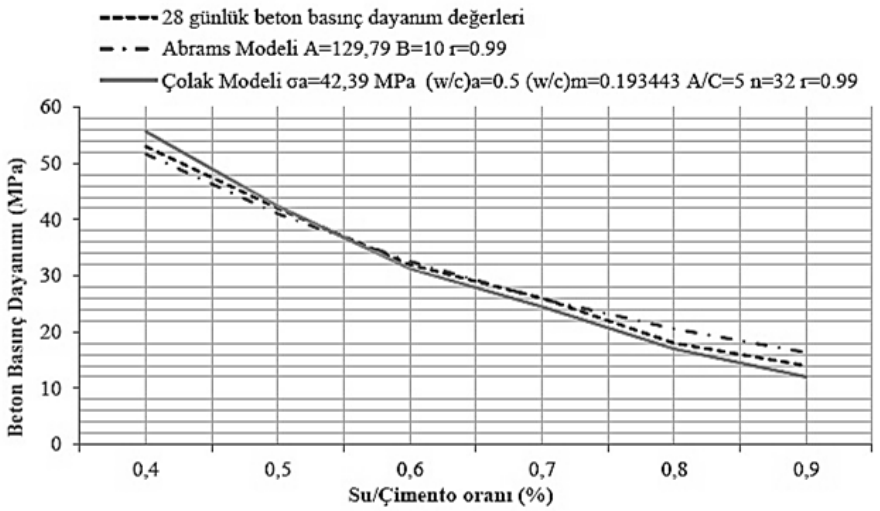

Figure 2.13 : Abrams' and Colak's models for the compressive strength at day 28. (Experimental values are from Neville's book (1996).) (Seitablaiev, 2019.)

(2019) examines 28-day compressive strength analysis for the water/cement ratio to the compressive strength with very high correlation of determinations.

One of the further non-linear regression analysis models for the mechanical properties of concrete could be rearranged in the general linear regression model form. For this rearrangement, the logarithm of the response variable Y is needed to be taken. By this logarithmic calculation, the general form of the linear model turns out to be non-linear form of multiplication of every independent variable in the power form. Those independent variables are called covariate vectors such as concrete mixture design ingredients. At the same time, the exponential values X is called estimable parameter vectors from calculations. Briefly, the logarithmic transformation is operated for the non-linear behavior of mechanical properties of concrete. In this approach, Behnood et al. (2015) examines the splitting tensile strength prediction for the plain and steel fiber-reinforced concrete based on the compressive strength tests.

In general, civil engineers studies the compressive strength for the strength development of concrete. Because it is the most efficient guide for further analysis in concrete behavior for both early and late date provisions of the strength development of concrete. One of the provisions is to presume the modulus of elasticity based on elastic behavior of concrete. For this forecasting, the mostly used prior data is the compressive strength. In another saying, the modulus of elasticity is driven from the

compressive strength. From the line of this sight, Iravani (1996) proposes use of cylinder compressive strength between 55 and 125 MPa which is in the power form model with the empirical coefficient based on stiffness tests for the high-performance concrete at day-56 with well fitted relationships. The literature also modifies the equation which has also the type of coarse aggregate coefficient C_{ca} depending on empirical work (Razak and Wong.). For the relationships between the compressive strength and modulus of elasticity, Razak and Wong study the general form of power function model for the modulus of elasticity based on Iravani's proposal (1996). They also see that the model has good correlation of determination which are above 080. At the end, in the cross checking of the model, the authors try ACI 318R-99 (1999) and ACI 363R-92 (1992) to suggest with the modifications based on their test results.

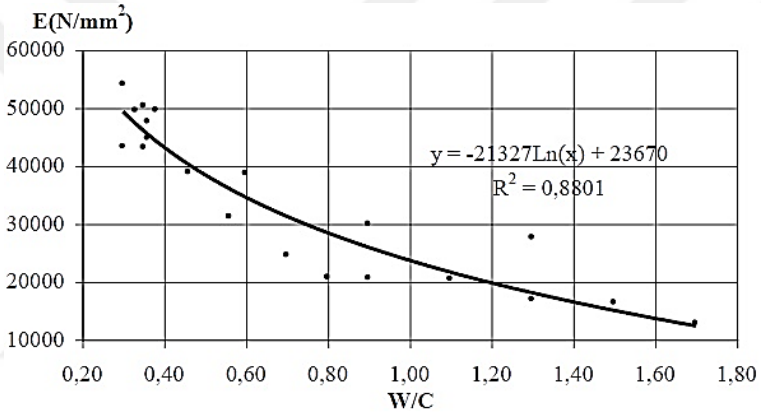

Figure 2.14 : The best fitting curves for static modulus of elasticity. (Razak and Wong.)

Additionally, Turkel (2002) explains in his study that the higher water to cement ratio means the lower characteristic compressive strength. By drawing a curve, he proposes a logarithmic function of the modulus of elasticity with the very high R^2 value for accuracy between the test and prediction results depending on the water/cement ratio. Differently, Noguchi and Tomosawa (1995) say that before analyzing any group of data, the creation of a basic form of equation for the modulus of elasticity is a need. In their regression analysis, the authors use the unit weight of concrete and compressive strength values in a non-linear equation form which is exponential. Addition to this, they evaluate correction factors of *k* in the multiplication form for the aggregate and admixture effects on the modulus of elasticity results. Blick (1973) and ACI Committee 363 (2010) also indicate that previous examinations are the compositions of low water to cement ratio with high cementitious content, and the maximum coarse

aggregate size in 10-mm or 13-mm. However, Cook (1982) successfully proposes the maximum size of the coarse aggregate in 19-mm and 25-mm.

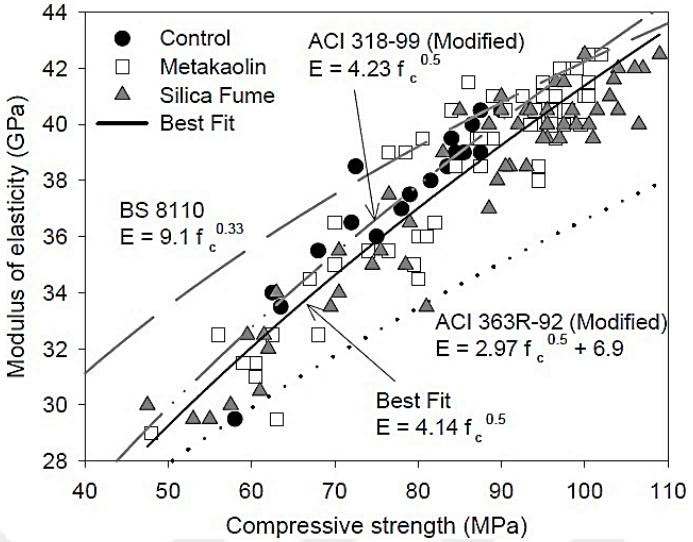

Figure 2.15 : The relationship between w/c ratio and the modulus of elasticity. (Turkel, 2002.)

For fine aggregates, Wills et al. (1967) discuss that the rounded shape of particle and smoothness of texture are beneficial for less water in concrete mixtures for high strength concretes. In this perspective, the use of less water and greater area of smaller size of aggregate increase the strength of concrete due to the water to cement ratio and bond of cement and surface area of aggregate content.

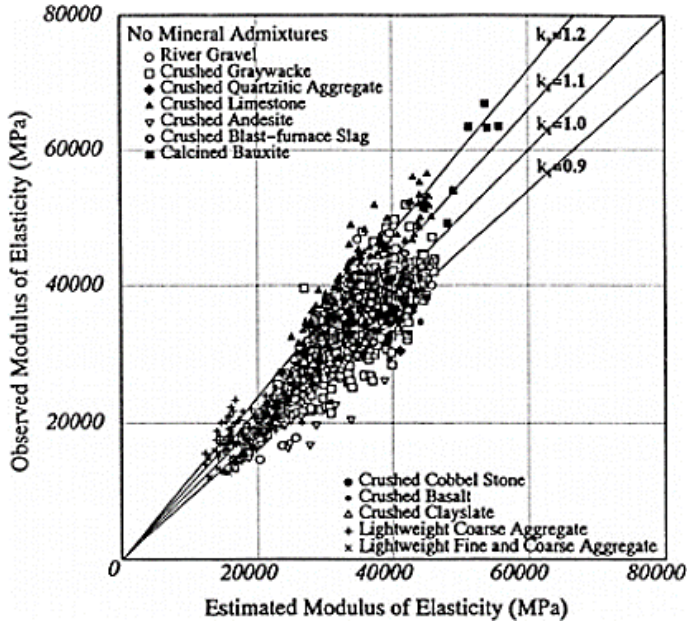

Figure 2.16 : The correlations of estimated and test data of the modulus of elasticity. (Noguchi and Tomosawa, 1995.)

Regarding of this, Cook (1982) studies the modulus of elasticity based on the compressive strength less than 84 MPa and unit weight of concrete in the non-linear model form from an exponential equation. Onto these studies, CEB – FIB 1990 (1993) and ACI Committee 363 (2010) develop the same model by caring aggregate and admixtures effects on the modulus of elasticity like in Noguchi and Tomosawa (1995) study. It signifies that the coefficient k_1 is for crushed limestone, calcined bauxite, crushed quartzite, crushed andesite, crushed basalt, crushed clay slate, crushed cobblestone aggregates, and the coefficient k_2 is for silica fume, slag cement and fly ash fume. There are also other acceptances for the coefficients for limitations in aggregates and admixtures.

2.3 Machine Learning Algorithms for Mechanical Properties of Concrete

In model fitting, the multiple regression algorithms are applied in use of many statistical methods for assessments of performance. In the Figure 2.21, the metrics of potential statistical are displayed for the multiple regression model evaluations with the corresponding expressions of mathematics. These metrics also prove that how predicted data fits with real data (Chaabene et al., 2020). Further, the multivariate regression models which figure each input variable weight in estimation progress out could be computed in sensitive analysis (Xu et al., 2019; Van Dao et al., 2019). Intercalarily, the statistical metrics are for both performances assess of the multivariate regression techniques and reference of effectiveness comparisons of a lot of algorithms.

Like human brain working framework, the artificial neural network (ANN) is an inspired non-linear model in machine learning (Reza et al., 2019; Pliego Marugán et al. 2019). In the ANN algorithms, the propagation of data is set throughout the connections having the information of element procedure called neuron to send them to the follow-up neurons. In this process, every bit of information is weighted by the importance of input variables to outputs in reflections (Derousseau et al., 2018). When a neuron is given an information, the neuron merges that information with the other following information coming from different neurons in a combination equation. After that, the combined data is sent to the coming nodes. This cycle continues until the algorithm fits the actual data. This process is indicated by the error rate convergence and/or when the maximum numbers of iterations are received (Bourdeau et al., 2019).

Statistical metric.	
Statistical parameter	Formula
Correlation coefficient (R)	$R = \frac{n\sum xy - (\sum x)(\sum y)}{\sqrt{[n\sum x^2 - (\sum x)^2]\,[n\sum y^2 - (\sum y)^2]}}$
Coefficient of deermination (R^2)	$R^2 = 1 - \frac{\sum_{i=1}^{N}(y_i - \hat{y}_i)^2}{\sum_{i=1}^{N}(y_i - \overline{y})^2}$
Mean square error (MSE)	$MSE = \frac{1}{n}\sum_{i=1}^{n}(y_i - \hat{y}_i)^2$
Root mean square error (RMSE)	$RMSE = \sqrt[2]{\frac{(y_i - \hat{y}_i)^2}{n - p}}$
Mean absolute error (MAE)	$MAE = \frac{1}{n}\sum_{i=1}^{n}\lvert y'_i - y_i\rvert$
Mean absolute percentage error (MAPE)	$MAPE\ (\%) = \frac{1}{n}\sum_{i=1}^{n}\lvert\frac{y'_i - y_i}{y_i}\rvert$
Mean (μ)	$\mu = \frac{1}{n}\sum_{i=1}^{n}\frac{y_i}{y'_i}$
Standard deviation (σ)	$\sigma = \sqrt{\frac{1}{n}\sum_{i=1}^{n}(\frac{y_i}{y'_i} - \mu)^2}$
Coefficient of variation (COV)	$COV\ (\%) = \frac{\sigma}{\mu}x\ 100$

Table 2.5 : The correlations of estimated and test data of the modulus of elasticity. (Chaabene et al., 2020.)

An input layer with hidden layers and output layers, there are three typical layer compositions (Fadaei et al., 2018). In the Figure 2.22, the general frame of the ANN is shared. In this structure, the parameters of input are conveyed to testing and training of a model. The relationships between the input and output layers are linked by hidden layers. For these relationships, a function of a model is necessary to produce neuron outputs and data transferring throughout the hidden and output layers (Reza et al., 2019; Hemmat Esfe et al., 2015). In this concept, training of the ANN is bridged via algorithms of learning processes which lead solutions for the problems put forth. Thus, the general body structure of the ANN differs due to the types of algorithms used for learning. The mechanical properties of concrete can be forecasted by using machine learning algorithms. In the existence of concrete ingredients and proportions of mixture compositions, the input variables are used in the ANN models. For example, this approach is used by Ziółkowski and Niedostatkiewicz (2019) for four main components such as cement, fine and coarse aggregates, and water for the compressive strength estimation. They also use 28-day strength of concrete to define the prediction process in the ANN structure. In the structure, they divide their study into three subsets

which are the training data set, data set selection and data set tests. To create a neural network, the training data set is used.

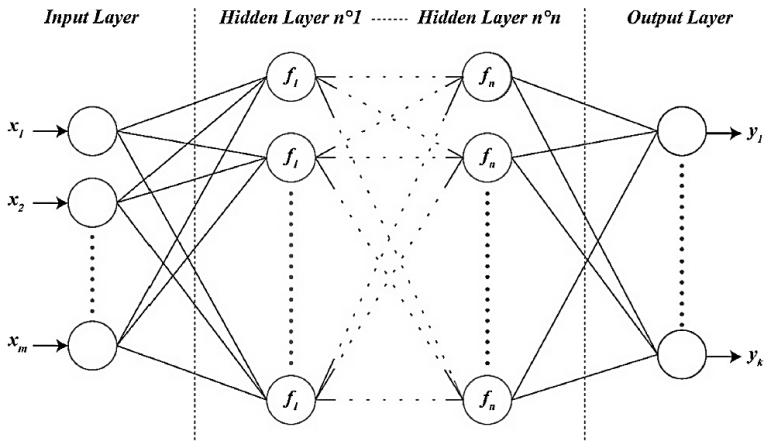

Figure 2.17 : The frame of ANN with m number of inputs and n number of outputs. (Chaabene et al., 2020.)

For the data set selection, the parameters are adjusted for the neural network. Lastly, for the evaluation of the network efficiency, the data set testing is used. In this path, they have many records for an exclusive result. Also, like in the following figure, they construct their ANN structure.

At the end, they reach the result that the machine learning application could be a choice for an engineering practice in mixture designs of concrete. In the algorithms, they use fifteen equations and fourteen required auxiliary variables. However, even though they evaluate an equation to quickly check the concrete mixture designs in this condition out, the method they follow does not let to reflect all the relationships between the boundary conditions and inputs. Because they use only four components for their algorithms (Ziółkowski and Niedostatkiewicz., 2019). To train the ANN models, the backpropagation neural network (BPNN) is a local search method.

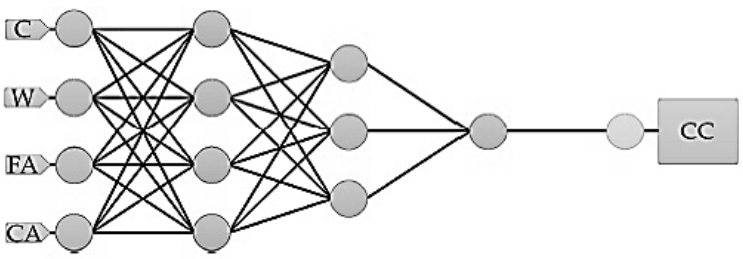

Figure 3. The initially used architecture of the ANN. The figure shows the network architecture, which includes the following parts, principal components (blue), perceptron neurons (red), and, because we use feature scaling, there are scaling and unscaling layers. The scaling and unscaling neurons are green and yellow, respectively. Abbreviations: C, cement; W, water; FA, fine aggregate; CA, coarse aggregate; CC, full compressive strength of concrete.

Figure 2.18 : The ANN structure for the prediction of compressive strength. (Ziółkowski and Niedostatkiewicz., 2019.)

For instance, the Levenberg-Marquardt (LM) algorithm is one of the BPNN method to upgrade the ANN biases and weights. The authors also refer that backpropagation (BP) is employed for the compressive strength of high-performance concretes. In this employment, the age of concrete and the components of concrete are essential as input parameters. Also, the authors indicated for the assessment of performance, BPNN would show good presuming in terms of the precision rather than the regression models (Ziółkowski and Niedostatkiewicz., 2019). Except the compressive strength of concrete, the splitting tensile strength is also applicable in the BPNN techniques. What Behnood et al. (2015) proposes to predict the splitting tensile strength is based on steel fiber-reinforced concrete. His model introduces the actual compressive strength results as input parameter. Parallel to him, Mohammadi et al. (2018) develops a comparison of the effectiveness of the radial basis function neural network (RBFNN) and BPNN for the modulus of elasticity. In the authors' efforts, the LM algorithm is preferred in the BPNN. At the end, they report that the BPNN is more effective than the RBFNN to practice forecasting of the modulus of elasticity (Mohammadi et al., 2018).

As another artificial intelligence tool, the Bayesian Regularization (BR) algorithm is one of the possible analysis methods. The use of BR in the ANN has more potential than the standard BP methods. Because the BR method increases or decreases extensively the cross-validation requirements (Burden and Winkler., 2009). Also, the BR conducts the non-linear regression models into a postured-well statistic manners like the non-linear regression models do (Kaur and Salaria., 2013). Additionally, the BR proposes better generalization when the data sets are hard to be analyzed (Burden and Winkler., 2008). By thinking of this, the BR training method displays better solutions than the LM method does may be because of the heterogeneity of the input variables which are justified by the diverse properties and/or amounts of ingredients of the concretes tested. Because the BR typically spends more time for a generalized solutions for the data sets which are noisy and small (Kaviya et al., 2019).

Hadzima-Nyarko and Trinh (2022) construct nine variable input data base for an output through the hidden layers with ten variables to one output computing process. At the end, they report that for the age 28-day, the compressive strength is predicted by using the BR method at feverish temperatures. The wide range of experimental data were collected from the actual data sets to build a BR structure by using water, cement, fine and coarse aggregates, fly ash, nano silica, silica fume, super plasticizer and

temperature records as variables in the input database. Finally, the authors give advice to use the ANN models for saving budget and time to avoid setting more experiments for data collection and prediction.

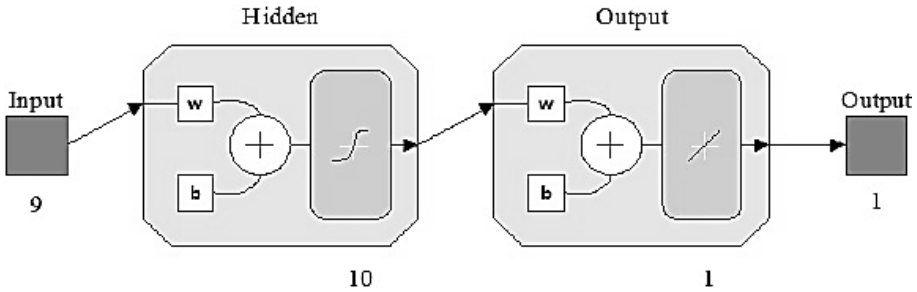

Figure 2.19 : The ANN structure for the prediction of compressive strength. (Hadzima-Nyarko and Trinh., 2022.)

Like in Hadzima-Nyarko and Trinh (2022) study, Suescum-Morales et al. (2021) puts eleven input variables which are also from the concrete mixture design water, cement, fine (natural) and coarse (natural and/or re-cycled) aggregates with the fineness modulus of sand, fly ash, superplasticizer, capacity of water absorption, dry density of saturated surface of the coarse aggregates and the maximum size of coarse aggregate particles. In their BR method, the authors construct twenty hidden layers for enough accuracy of the actual data set. They criticize the study that at the age 28-day, the compressive strength is hard to be estimated for producing new concrete because of the heterogeneity of the presence of the re-cycled coarse aggregate (RCA).

In this light of modelling, Kaviya et al. (2019) also suggests using the BR structure to predict the compressive strength of concrete rather than using the multiple regression analysis models due to the marginal differences between the real and estimated values for the high-performance concrete including supplementary cementitious materials. In the Table 2.6, a wide range of prediction models for the mechanical properties of concrete is referred from the literature.

Table 2.6: The review of literature for concrete mechanical properties prediction.

Reference	Model	Equation	Parameter	Source	Data Set	Model Evaluation
Plecas and Dimovic (2009)	Least Square Regression	$f = A_0 + A_1 t^{1/2} + A_2 t$	$\boldsymbol{A_0}$ for immediate dissolution, $\boldsymbol{A_1}$ for diffusion-controlled transporting, $\boldsymbol{A_2}$ for long-term kinetical dissolution, $\boldsymbol{t}$ for leeching duration, $\boldsymbol{f}$ for long-term leaching characteristics	Laboratory	4	IAEA
Abd elaty (2014)	Univariate Regression Analysis	$f_t = Aln(t) + B$	$\boldsymbol{A}$ for strength gain constant rate (regression line slope), $\boldsymbol{B}$ for strength constant level (grade constant), $\boldsymbol{t}$ for concrete age, $\boldsymbol{f_t}$ for compressive strength	Literature	89	R^2
Resheidat and Ghanma (1997)	Univariate Regression Analysis	$Y = \alpha + \beta X$, $Y = \alpha X^{\beta}$, $Y = \alpha^{\beta X}$	$\boldsymbol{\alpha}$ and $\boldsymbol{\beta}$ for regression constants, $\boldsymbol{X}$ for accelerated strength, $\boldsymbol{Y}$ for predicted 28-day concrete strength	Laboratory	4	σ, R, 95% Confidence Interval
McKinney (2009)	Least Square Regression	$y = ae^{bx}$, $y = ax^b$, $y = a_0 + a_1 x + a_2 x^2 + \ldots + a_m x^m$	$\boldsymbol{a}$ and $\boldsymbol{b}$ for regression constants, $\boldsymbol{m}$ for equation degree, $\boldsymbol{x}$ for independent variable, $\boldsymbol{y}$ for predicted result	Laboratory	8	-
ACI 209.2R-08 (2008)	Univariate Regression Analysis	$f_{cmt} = [t / (a + bt)] f_{cm28}$, $E_{cmt} = a + b\sqrt{(f_{cmt})}$	$\boldsymbol{a}$ and $\boldsymbol{b}$ for regression constants, $\boldsymbol{t}$ for concrete age, $\boldsymbol{f_{cm28}}$ for mean compressive strength, $\boldsymbol{f_{cmt}}$ for predicted compressive strength, $\boldsymbol{E_{cmt}}$ for predicted modulus of elasticity	Literature	-	-

Table 2.6 (continued): The review of literature for concrete mechanical properties prediction.

Reference	Model	Equation	Parameter	Source	Data Set	Model Evaluation
fib Model Code for Concrete Structures 2010 (2010); TS802 (2016)	Univariate Regression Analysis	$f_{cm}(t) = \beta_{cc}(t) f_{cm}$, $\beta_{cc}(t) = exp\{s[1-(28/t)^{0.5}]\}$ $f_{ctm} = 0.3 f_{ck}^{2/3}$; $f_{ck} < C50$, $f_{ctm} = 2.12 ln(1 + 0.1(f_{ck} + \Delta f)$; $f_{ck} \geq C50$ $E_{ci} = E_{c0} \alpha_E [(f_{ck} + \Delta f)/10]^{1/3}$	***s*** for cement strength class, ***t*** for concrete age, $\boldsymbol{\beta_{cc}(t)}$ time dependent strength development, $\boldsymbol{f_{cm}}$ for mean compressive strength at day-28, $\boldsymbol{f_{cm}(t)}$ for compressive strength at age ***t***, $\boldsymbol{f_{ctm}}$ for splitting tensile strength, $\boldsymbol{\Delta f}$ *for mean compressive strength as* ***8 MPa***, $\boldsymbol{E_{c0}}$ for **21500 MPa**, $\boldsymbol{\alpha_E}$ for aggregate coefficient, $\boldsymbol{E_{ci}}$ for 28-day modulus of elasticity	Literature	-	-
British Standards Institution (2004)	Univariate Regression Analysis	$f_{cm}(t) = \beta_{cc}(t) f_{cm}$, $\beta_{cc}(t) = exp\{s[1-(28/t)^{0.5}]\}$ $f_{ctm} = 0.3 f_{ck}^{2/3}$; $f_{ck} < C50$, $f_{ctm} = 2.12 ln(1 + 0.1(f_{ck} + \Delta f)$; $f_{ck} \geq C50$ $E_{cm} = 22[(f_{cm})/10]^{1/3}$; $f_{cm} = f_{ck} + \Delta f$	***s*** for cement strength class, ***t*** for concrete age, $\boldsymbol{\beta_{cc}(t)}$ time dependent strength development, $\boldsymbol{f_{cm}}$ for mean compressive strength at day-28, $\boldsymbol{f_{cm}(t)}$ for compressive strength at age ***t***, $\boldsymbol{f_{ctm}}$ for splitting tensile strength, $\boldsymbol{\Delta f}$ *for mean compressive strength as* ***8 MPa***, $\boldsymbol{E_{cm}}$ in **GPa** for mean modulus of elasticity	Literature	-	-
AS3600 (2001)	Univariate Regression Analysis	$E_{cj} = \rho^{1,5}(0.043\sqrt{f'_c})$	$\boldsymbol{\rho}$ for concrete unit weight, $\boldsymbol{f'_c}$ for characteristic compressive strength, $\boldsymbol{E_{cj}}$ for modulus of elasticity in an appropriate age	Literature	-	-

Table 2.6 (continued): The review of literature for concrete mechanical properties prediction.

Reference	Model	Equation	Parameter	Source	Data Set	Model Evaluation
Ozturan et al.	Multivariate Regression Analysis, Artificial Neural Netwrok	$f_{c28} = a_0 + a_1x_1 + a_2x_2 + \ldots + a_nx_n$	***a*** for regression constant, ***n*** for independent variable, ***x*** for independent variable, $\boldsymbol{f_{c28}}$ for predicted compressive strength	Laboratory	60	R^2
Ozturan et al.	Multivariate Regression Analysis	$f_{c28} = A/B^{(w/c)}$	***A*** and ***B*** for regression constants, ***w/c*** for water to cement ratio, $\boldsymbol{f_{c28}}$ for 28-day compressive strength	Laboratory	5	R^2
Haranki (2009)	Multivariate Regression Analysis	$f_c = K(c/(c + w + a))^2$**;** $f_c = K(c/(c + w + a))^n$	***K*** for regression constant, ***c*** for cement ***[%]***, ***w*** for water ***[%]***, ***a*** for air ***[%]***, ***n*** for equation degree, $\boldsymbol{f_c}$ for compressive strength	Laboratory	30	R^2 SSE
Behnood et al. (2015)	Multivariate Regression Analysis	$Y = \beta_0 X_1^{\beta 1} X_2^{\beta 2} \ldots X_n^{\beta n}$**,** $f_{spt} = a f_c^{\,b}$	$\boldsymbol{\beta}$ for estimable parameter, ***n*** for number of independent variables, ***X*** for independent variable, ***Y*** for splitting tensile strength, ***a*** and ***b*** for regression coefficients, $\boldsymbol{f_c}$ for compressive strength, $\boldsymbol{f_{stp}}$ for splitting tensile strength	Laboratory Literature	6	R^2 RMSE
Turkel (2002)	Multivariate Regression Analysis	$f_c = (K_B[(C/(E + h)) - k']$	$\boldsymbol{k'}$ for secondary constant, $\boldsymbol{K_B}$ for concrete age, ***C*** for cement type and dosage, ***E*** for water content, ***h*** for air content, $\boldsymbol{f_c}$ for compressive strength	Laboratory	20	R^2

Table 2.6 (continued): The review of literature for concrete mechanical properties prediction.

Reference	Model	Equation	Parameter	Source	Data Set	Model Evaluation
Turkel (2002)	Multivariate Regression Analysis	$f_c = (f_{cc}/K_0)(C/E)^2$	f_{cc} for cement norm strength, K_0 for between ***4*** and ***10***, ***C*** for cement content, ***E*** for water content, f_c for compressive strength	Laboratory	20	R^2
Turkel (2002)	Multivariate Regression Analysis	$E_d = K\sqrt{R_s}$	***K*** for constant between ***18000*** and ***23000***, R_s for ***150X300 mm*** cylinder compressive strength, E_d for modulus of elasticity	Laboratory	20	R^2
Noguchi and Tomosawa (1995)	Multivariate Regression Analysis	$E = (2.1X10^5)(\gamma/2.3)^{1,5}(f_c/200)^{1/2}$; $E = k_1k_2(3.35X10^4)(\gamma/2.4)^2(\sigma_B/60)^{1/3}$	γ for concrete unit weight, k_1 for aggregate coefficients, k_2 for binder coefficients, σ_B and f_c for compressive strength, ***E*** for modulus of elasticity	Literature Laboratory	3000+	95% Confidence Interval
Chaabene et al. (2020)	Artificial Neural Network	Backpropagation Neural Network (BPNN) Levenberg-Marquardt Algorithm (LM)	**Artificial neural network (ANN)** structures by using concrete mixture design components as input variables in hidden layers through output layers, test results as output variables for compressive strength	Laboratory	5000+	R R^2 MSE RMSE σ
Hadzima-Nyarko and Trinh. (2022)	Artificial Neural Network	Bayesian Regularization Algorithm (BR)	**Artificial neural network (ANN)** structures by using concrete mixture design components as input variables in hidden layers through output layers, test results as output variables for compressive strength	Laboratory	9	R^2 RMSE σ

3. PROCEDURE OF EXPERIMENTS

In this section, the school of thought and methodology of the thesis are expressed. The process of the experiments was studied at Construction Materials Laboratory of the Faculty of Civil Engineering in Istanbul Technical University (I.T.U.).

Various variables effective on the regression analysis models/equations and machine learning algorithms/methods were computed in this thesis. The amount of concrete mixture design ingredients in 1 m^3, the proportions of water to cement (W/C), water to binder (W/B), fine aggregate to aggregate (FA/A), coarse aggregate to aggregate (CA/A), and air (A [%]) were included as investigation tasks in this study for the data prediction. Hence, there were 33 concrete specimens in two main categories which were fly ash (FA) + micro silica (MS) and ground granulated blast furnace slag (GGBS) additions as pozzolans for the comparison purposes of material use effects in the study. At the same time, these specimens had two different concrete grades with five diverse cement types. All the concrete samples were produced in the shape of cylinder (150X300 mm) for the laboratory tests under the standard conditions which were carried out by the literature. With the light of the test results, the mechanical properties of the specimens were forecasted by using the mixture design properties in regression models and artificial intelligence algorithm. In these estimating calculations, the study was focused on which the mixture designs were accurate or not for the aspects of the concrete mixture designs.

The prediction models/methods based on the test results were published with coefficient of correlation (R), determination of correlation (R^2), adjusted determination of correlation (R^2_{adj}), sum of squared errors (SSE), mean square error (MSE), and root mean square error (RMSE) to find out how the performance of the prediction models/methods were efficient.

3.1 Preferences of Material

For the study, as binder materials, cement (C), fly ash (FA) + micro silica (MS), ground granulated blast furnace slag (GGBS) was added to the mixtures. For the types of

cement, CEMI 42.5N, CEMI 52.5LA, CEMI 52.5N, CEMIII BS and CEMIII 32.5 were preferred. The natural sand (NS) and crushed sand (CS) as fine aggregates, and NO:0, NO:1, and NO:2 as coarse aggregates were sieved. The sieve analysis was set by following TS802 (2016) to consider for using the appropriate amounts of aggregates in the mixtures. Moreover, water (W), and two types of superplasticizer admixtures (AD.1 and AD.2) were included for the concrete productions.

3.2 Mixture Designs of Concrete

The concrete mixture designs were prepared to compare the mechanical properties of concrete for presuming of the concrete strengths in the regression analysis, and machine learning algorithm for future strength development investigations. Thus, there were 33 different mixtures of concrete. In these designs, W/C, W/B, FA/A, CA/A, and A [%] ratios were studied for a consistent effort. In the univariate regression analysis (URA), all those specimens were analyzed one by one in the presences of concrete ages and strengths. However, except the four of the specimens, all the other 29 specimens were conducted for the multivariate regression analysis (MRA). Like in the MRA, in the machine learning algorithm (MLA), the same 29 specimens were soft computed for the data estimations. In this perspective, the proportions of W/C were designed to reach the level of the aimed compressive strengths. So, the W/C ratios were differed from 0.35 to 1.11 for the verification of the concrete strengths. At the end, the compressive strength (CS) results ranged from 0.5 MPa to 86.00 MPa. For the splitting tensile strength (STS), the test results varied from 0.10 MPa to 6.55 MPa. And finally, the test results of the modulus of elasticity (ME) ranged from 10.50 GPa to 46.00 GPa. On the other hand, the following Table 3.1, Table 3.2, and Table 3.3 show the amounts and proportions of concrete mixture design substances with the cement types, and concrete grades for the additive distinctions in FA + MS and GGBS.

3.3 Producing of Concrete

33 different mixture specimens including C, FA + MS, GGBS, NS, CS, NO:0, NO:1, NO:2, AD.1 and AD.2 were mixed and produced for the laboratory tests. At the same time, depending on the mixture component amounts, the ingredient proportions were also examined for the mixture design purposes. All the samples were made of the same incorporator materials for consistent research. After producing the concrete samples,

all the specimens were saved, and cured in the laboratory conditions for the hardened concrete tests.

Table 3.1: The identifying properties of concrete mixture designs.

№	Mixing Codes	Additives	Concrete Grades	Cement Types
1	**C45-III-B20**	GGBS	C45/55	CEMIII BS
2	**YM-SEG-03**	FA + MS	C40/50	CEMI 42.5N
3	**YM-SEG-03-FSTC**	FA + MS	C40/50	CEMI 42.5N
4	**MIX-15A-04**	FA + MS	C40/50	CEMI 42.5N
5	**YM-SEG-05**	FA + MS	C40/50	CEMI 42.5N
6	**YM-SEG-08**	FA + MS	C40/50	CEMI 42.5N
7	**MIX-15E-03**	FA + MS	C40/50	CEMI 42.5N
8	**MIX-15AC-04**	FA + MS	C40/50	CEMI 42.5N
9	**YM-SEG-10**	FA + MS	C40/50	CEMI 42.5N
10	**DURABET-PLUS-AIR-AC-03**	GGBS	C40/50	CEMIII 32.5
11	**YM-SEG-10A**	FA + MS	C40/50	CEMI 42.5N
12	**YM-SEG-10E**	FA + MS	C40/50	CEMI 42.5N
13	**YM-DAP-AC-03**	GGBS	C40/50	CEMIII 32.5
14	**MIX-15-AC-03**	FA + MS	C40/50	CEMI 42.5N
15	**MIX-30**	GGBS	C40/50	CEMIII 32.5
16	**MIX-30-03**	GGBS	C40/50	CEMIII 32.5
17	**MIX-30-BRT**	GGBS	C40/50	CEMIII 32.5
18	**MIX-30-07**	GGBS	C40/50	CEMIII 32.5
19	**MIX-34-BRT**	GGBS	C40/50	CEMIII 32.5
20	**MIX-32-03**	GGBS	C40/50	CEMIII 32.5
21	**MIX-32-CEN**	GGBS	C40/50	CEMIII 32.5
22	**MIX-32-CEN-OK**	GGBS	C40/50	CEMIII 32.5
23	**B70-380**	GGBS	C45/55	CEMI 52.5N
24	**B70-420**	GGBS	C45/55	CEMI 52.5N
25	**B47-440**	GGBS	C45/55	CEMI 52.5N
26	**B67-440**	GGBS	C45/55	CEMI 52.5N
27	**B67-440-001**	GGBS	C45/55	CEMI 52.5LA
28	**C45-B25-425**	FA + MS	C45/55	-
29	**B67-440-BEY**	GGBS	C45/55	CEMI 52.5LA
30	**C45-B26-475**	FA + MS	C45/55	-
31	**C45-B25-400**	FA + MS	C45/55	-
32	**C50-B22-460**	FA + MS	C50/60	-
33	**YM-SEG-11**	FA + MS	-	-

3.4 Tests of Fresh Concrete

The slump, unit weight and air content tests as fresh concrete tests were examined, when the concrete samples were produced.

3.4.1 Slump Tests of Concrete

The slump test of concrete is also known as Abrams cone which scales the difference between the heights of fresh concrete when the fresh concrete is fully filled into to the slump mold, and the slump mold is removed. This test is preferred for the concerns of workable concrete mixtures because this test is very cheap and fast to be set for the data collection from the fresh concrete producing. In this assessment, the slump test was experimented in accordance with the standard of TS EN 12350-2 (2019). In the process, the fresh concrete samples were pressed down 25 times with the help of a metal bar and/or rod after each time the samples were poured into to the mold. The mold was filled up in three times of pouring. When the mold was removed the difference was measured for the slump.

3.4.2 Unit Weight Tests of Concrete

According to TS EN 12350-6 (2019), first, the fresh concrete was needed to be filled to a concrete container which had a precise volume. Secondly, after filling process was done, the filled fresh concrete weight was measured to be divided into the inner container volume for the unit weight.

3.4.3 Air Content Tests of Concrete

In TS802 (2016), to calculate the air content in percentage, firstly, the total weights of all materials were calculated by taking the difference between the material weights plus container weights and container weight. Then, the theoretical concrete weight on air-free basis was found by dividing the total weight of all materials to the total absolute subsequent volume. Finally, the air content [%] was found by multiplying the fraction of the difference between the theoretical concrete weight on air-free basis and the concrete unit weight to the theoretical concrete weight on air-free basis with 100.

3.5 Tests of Hardened Concrete

In this section of the thesis, the mechanical properties of hardened concretes which were cured under standard laboratory conditions were studied. The compressive strength, splitting tensile strength and modulus of elasticity tests were conducted for each 150X300 mm cylinder concrete samples. With subsections, these tests are expressed in this part of the study.

Table 3.2: The concrete mixture designs.

Ingredients of Concrete Mixtures												
Mixing Codes	**C [kg/m^3]**	**FA [kg/m^3]**	**MS [kg/m^3]**	**GGBS [kg/m^3]**	**W [kg/m^3]**	**NS [kg/m^3]**	**CS [kg/m^3]**	**NO:0 [kg/m^3]**	**NO:1 [kg/m^3]**	**NO:2 [kg/m^3]**	**AD.1 [kg/m^3]**	**AD.2 [kg/m^3]**
C45-III-B20	380.00	-	-	-	141.00	426.00	474.00	-	495.00	495.00	5.32	-
YM-SEG-03	360.00	60.00	20.00	-	142.00	297.00	534.00	-	516.00	479.00	3.74	-
YM-SEG-03-FSTC	-	-	-	-	-	-	-	-	-	-	-	-
MIX-15A-04	285.00	50.00	30.00	-	102.00	402.00	469.00	-	514.00	495.00	3.89	0.35
YM-SEG-05	340.00	60.00	40.00	-	121.00	304.00	542.00	-	525.00	490.00	3.36	-
YM-SEG-08	340.00	60.00	40.00	-	121.40	303.40	541.70	-	524.90	489.20	2.94	-
MIX-15E-03	285.00	50.00	30.00	-	102.00	514.00	495.00	-	402.00	469.00	3.56	0.42
MIX-15AC-04	285.00	50.00	30.00	-	102.00	514.00	495.00	-	402.00	469.00	3.89	0.55
YM-SEG-10	320.00	60.00	50.00	-	112.50	356.20	372.70	-	561.20	563.30	2.00	-
DURABET-PLUS-AIR-AC-03	-	-	-	-	-	-	-	-	-	-	-	-
YM-SEG-10A	320.00	60.00	50.00	-	112.20	367.10	372.60	-	561.00	563.10	2.60	-
YM-SEG-10E	320.00	60.00	50.00	-	112.30	357.50	372.70	-	561.10	561.10	2.40	-
YM-DAP-AC-03	380.00	-	-	-	140.00	462.00	415.00	-	471.00	452.00	4.94	0.68
MIX-15-AC-03	285.00	50.00	30.00	-	102.00	402.00	469.00	-	514.00	495.00	3.56	0.28
MIX-30	360.00	-	-	-	132.00	444.00	420.00	-	480.00	482.00	4.86	-
MIX-30-03	380.00	-	-	-	132.00	444.00	420.00	-	480.00	482.00	5.70	0.40
MIX-30-BRT	380.00	-	-	-	139.00	485.00	397.00	-	909.00	-	6.08	0.36
MIX-30-07	390.00	-	-	-	137.00	510.00	414.00	-	475.00	404.00	6.63	0.55

Table 3.2 (continued): The concrete mixture designs.

Ingredients of Concrete Mixtures												
Mixing Codes	**C [kg/m³]**	**FA [kg/m³]**	**MS [kg/m³]**	**GGBS [kg/m³]**	**W [kg/m³]**	**NS [kg/m³]**	**CS [kg/m³]**	**NO:0 [kg/m³]**	**NO:1 [kg/m³]**	**NO:2 [kg/m³]**	**AD.1 [kg/m³]**	**AD.2 [kg/m³]**
MIX-34-BRT	380.00	-	-	-	149.00	479.00	392.00	-	898.00	-	6.65	0.33
MIX-32-03	390.00	-	-	-	137.00	458.00	434.00	-	493.00	423.00	6.24	0.55
MIX-32-CEN	390.00	-	-	-	142.00	540.00	414.00	-	440.00	380.00	7.00	0.60
MIX-32-CEN-OK	390.00	-	-	-	137.00	540.00	415.00	-	450.00	385.00	6.20	0.60
B70-380	114.00	-	-	266.00	126.00	395.00	-	502.00	545.00	486.00	4.10	-
B70-420	126.00	-	-	294.00	140.00	417.00	-	428.00	543.00	468.00	3.90	-
B47-440	146.00	-	-	294.00	138.00	468.00	-	370.00	540.00	465.00	4.70	-
B67-440	146.00	-	-	294.00	138.00	468.00	-	370.00	540.00	465.00	4.70	-
B67-440-001	146.00	-	-	294.00	139.00	570.70	149.70	-	337.10	784.10	2.60	-
C45-B25-425	300.00	105.00	50.00	-	125.00	455.00	360.00	-	524.00	452.00	5.87	1.62
B67-440-BEY	146.00	-	-	294.00	137.00	470.00	372.00	-	540.00	467.00	5.72	-
C45-B26-475	-	-	-	-	-	-	-	-	-	-	-	-
C45-B25-400	280.00	100.00	50.00	-	115.00	554.00	437.00	-	609.00	286.00	6.61	0.72
C50-B22-460	340.00	100.00	50.00	-	115.00	452.00	358.00	-	521.00	451.00	5.17	4.20
YM-SEG-11	-	-	-	-	-	-	-	-	-	-	-	-

Table 3.3: The concrete mixture design proportions.

Mixing Codes	Weight [kg]	Unit Con. Wt. [kg]	Unit Con. Vol. [dm^3]	W_1 [kg]	T [kg/m^3]	$W_{concrete}$ [kg/m^3]	Air [%]	W/B	W/C	FA/A	CA/A
C45-III-B20	23900.00	4609.00	8001.00	19291.00	2411.07	2416.32	0.00	0.37	0.37	0.48	0.52
YM-SEG-03	24164.00	4567.00	7890.00	19597.00	2483.78	2411.74	2.90	0.32	0.39	0.46	0.54
YM-SEG-03-FSTC	19526.00	-	-	-	-	-	-	-	-	-	-
MIX1-5A-04	24050.00	4609.00	8001.00	19441.00	2429.82	2351.24	3.23	0.28	0.36	0.46	0.54
YM-SEG-05	24290.00	4609.00	8001.00	19681.00	2459.82	2425.36	1.40	0.28	0.36	0.45	0.55
YM-SEG-08	24091.00	-	-	-	-	2423.54	-	0.28	0.36	0.45	0.55
MIX-15E-03	23543.00	4609.00	8001.00	18934.00	2366.45	2350.98	0.65	0.28	0.36	0.54	0.46
MIX-15AC-04	23516.00	4609.00	8001.00	18907.00	2363.08	2351.44	0.49	0.28	0.36	0.54	0.46
YM-SEG-10	24233.00	4567.00	7890.00	19666.00	2492.52	2397.90	3.80	0.26	0.35	0.39	0.61
DURABET-PLUS-AIR-AC-03	23703.00	4567.00	7890.00	19136.00	2425.35	-	-	-	-	-	-
YM-SEG-10A	24280.00	4567.00	7890.00	19713.00	2498.48	2408.60	3.60	0.26	0.35	0.40	0.60
YM-SEG-10E	24190.00	-	-	-	-	2397.10	-	0.26	0.35	0.39	0.61
YM-DAP-AC-03	23487.00	4567.00	7890.00	18920.00	2397.97	2325.62	3.02	0.37	0.37	0.49	0.51
MIX-15-AC-03	23614.00	4567.00	7890.00	19047.00	2414.07	2350.84	2.62	0.28	0.36	0.46	0.54
MIX-30	23200.00	4567.00	7890.00	18633.00	2361.60	2322.86	1.64	0.37	0.37	0.47	0.53
MIX-30-03	23546.00	4562.00	7890.00	18984.00	2406.08	2344.10	2.58	0.35	0.35	0.47	0.53
MIX-30-BRT	23536.00	4567.00	7890.00	18969.00	2404.18	2316.44	3.65	0.37	0.37	0.49	0.51
MIX-30-07	23336.00	4567.00	7890.00	18769.00	2378.83	2337.18	1.75	0.35	0.35	0.51	0.49

Table 3.3 (continued): The concrete mixture design proportions.

Mixing Codes	Weight [kg]	Unit Con. Wt. [kg]	Unit Con. Vol. [dm^3]	W_1 [kg]	T [kg/m^3]	$W_{concrete}$ [kg/m^3]	Air [%]	W/B	W/C	FA/A	CA/A
MIX-34-BRT	23770.00	4567.00	7890.00	19203.00	2433.84	2304.98	5.29	0.39	0.39	0.49	0.51
MIX-32-03	23671.00	4567.00	7890.00	19104.00	2421.29	2341.79	3.28	0.35	0.35	0.49	0.51
MIX-32-CEN	22961.00	4567.00	7890.00	18394.00	2331.31	2313.60	0.76	0.36	0.36	0.54	0.46
MIX-32-CEN-OK	23452.00	4567.00	7890.00	18885.00	2393.54	2323.80	2.91	0.35	0.35	0.53	0.47
B70-380	24054.00	4567.00	7890.00	19487.00	2469.84	2438.10	1.28	0.33	1.11	0.20	0.80
B70-420	23979.00	4567.00	7890.00	19412.00	2460.33	2419.90	1.64	0.33	1.11	0.22	0.78
B47-440	24393.00	4567.00	7890.00	19826.00	2512.80	2425.70	3.47	0.31	0.95	0.25	0.75
B67-440	24362.00	4567.00	7890.00	19795.00	2508.87	2425.70	3.32	0.31	0.95	0.25	0.75
B67-440-001	24100.00	4657.00	7890.00	19443.00	2464.26	2423.20	1.67	0.32	0.95	0.39	0.61
C45-B25-425	23554.00	4586.00	7954.00	18968.00	2384.71	2378.49	0.26	0.27	0.42	0.46	0.54
B67-440-BEY	24127.00	4586.00	7951.00	19541.00	2457.68	2431.72	1.06	0.31	0.94	0.46	0.54
C45-B26-475	24006.00	4588.00	7944.00	19418.00	2444.36	-	-	-	-	-	-
C45-B25-400	23390.00	4588.00	7944.00	18802.00	2366.82	2438.33	0.00	0.27	0.41	0.53	0.47
C50-B22-460	23896.00	4588.00	7944.00	19308.00	2430.51	2396.37	1.40	0.23	0.34	0.45	0.55
YM-SEG-11	-	-	-	-	-	-	-	-	-	-	-

3.5.1 Tests of Compressive Strength

The concrete samples were produced for shape, dimension and flatness demands according to NT BUILD 200 (1984). For these samples, before the hardened concrete compressive strength tests, the specimens cured in the direction of NT BUILD 201 (1984) were assessed for the medium values of compressive strengths under the rupture occurred in the test specimens, when the stresses were loaded. In accordance with NT BUILD 203 (1984), the tests were continued until the specimens reached the load bearing capacities which made the specimens broken. It was also important to place the samples in the test machine pressure platen with an accuracy of $\pm$ *1 mm* before the tests. Moreover, the upper loading platen was paralleled to the contact/load bearing surfaces of samples. After those arrangements, the load was progressively increased at the rate of 0.8 ± 2 *MPa/s*. At the end, the maximum loads were noted as ultimate loads. By dividing the ultimate loads into the cross-section areas of the specimens, the compressive strengths of samples were calculated and enlisted in *MPa* (N/mm^2). Before starting the tests, the concrete samples were removed from the water pool at the earliest 30 minutes in advance for testing and were dried to avoid free water on the surfaces of contact. In the Figure 3.1, Figure 3.2 and Figure 3.3, the test requirements in size, shape, and loading procedure are shared with in accordance with NT BUILD 200 (1984).

3.5.2 Tests of Splitting Tensile Strength

The concrete samples were prepared for curing process as suggested in NT BUILD 201 (1984). For these specimens, it was concerned for the cross sections of the samples which were at least four times of the nominal particle size in the specimens. And the heights h of the specimens was equal to two times of diameter d in accordance with NT BUILD 201 (1984). In this light of information, the splitting tensile tests were applied by pulling the samples till the ultimate strengths were reached in the test machine. According to the NT BUILD 204 (1984), the load determinations were permitted in $\pm$ *3%* accuracy, and the load adjusting was increased within *0-0.05 MPa/s*. For the sample preparation process of the tests, the specimens were sawn in both ends after the shorn and grinned specimens were at least two times of square root of the cross-section area. While the samples were prepared, dry-against and water-storing effects were eliminated by wet towels.

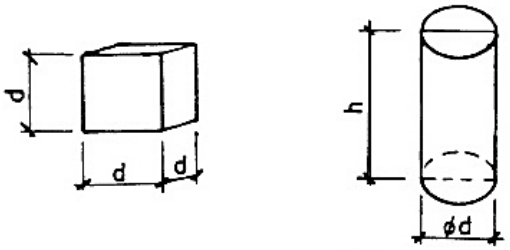

Nominal measures, d		h
Cubes	Cylinders	Cylinders
	50	h = 2d, h = d
	70	
100	100	
150	150	

Figure 3.1: The nominal measure indications of test specimens.

(NT BUILD 200, 1984.)

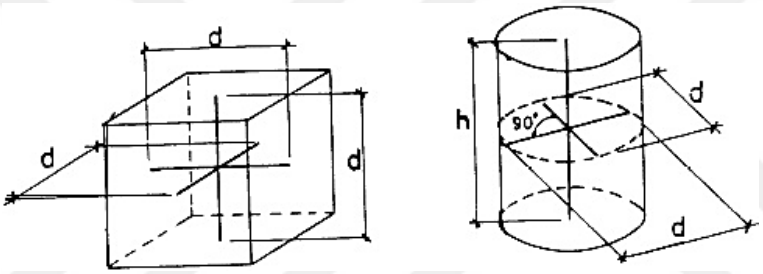

Figure 3.2: The measurement of dimensions of test specimens.
(NT BUILD 200, 1984.)

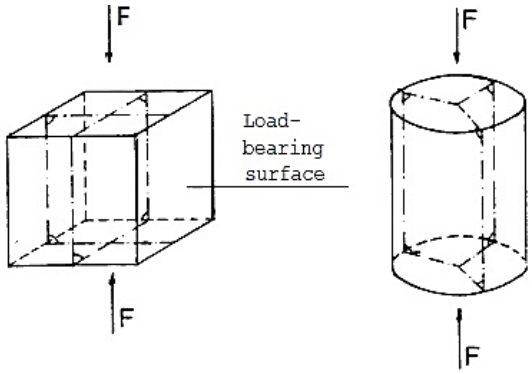

Figure 3.3: The angle examinations. (NT BUILD 200, 1984.)

At the same time, before starting to assess the shape, dimension, and flatness demands according to NT BUILD 200 (1984), the last checks were fulfilled. After that, as given in NT BUILD 204 (1984), the specimens were placed in the center of the test machine within ± *1 mm* precision. The load was continuously increased at the rate of *0.05 MPa/s*. At the end, the maximum loads were noted as ultimate loads, when the breaks occurred. Then, the splitting tensile strengths was calculated by dividing the ultimate loads into the specimen cross section areas. In the Figure 3.4, the sample attachments to the test machine are drawn by NT BUILD 204 (1984).

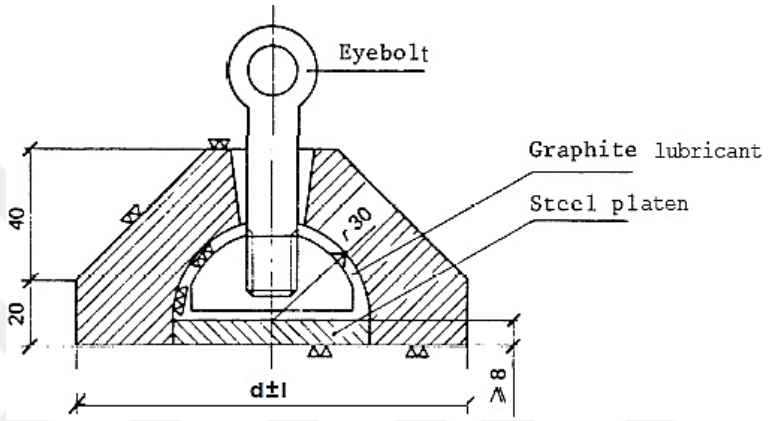

Figure 3.4: The attachment of samples to test machine steel plate.
(NT BUILD 204, 1984.)

3.5.3 Tests of Modulus of Elasticity

The specimens were appropriate according to NT BUILD 200 (1984) for the shape, flatness and measure demands in the half height diameters. For these samples, it was necessary for the cross sections of the samples which were at least four times of the nominal particle size in the specimens. Before the hardened concrete tests were started, the specimens were up rightened. As NT BUILD 205 (1984) expressed that the modulus of elasticity was decided by the relations between the load and deformation. The deformation meter as an extensometer measured the changes in the specimen lengths under the load with the gauge length of *l* where it was between greater or equal than $3d_{max}$, and less or equal than *h* minus *d*. d_{max} was used for the maximum nominal aggregate particle size. And then, the gauge length was centrically placed to the samples. And the differences were measured in two opposite sides of the samples. The accuracy of the measurements was within ± $25X10^{-6}$. Before starting the tests, the concrete samples were removed from the water pool at the earliest 30 minutes in advance for testing and were dried to avoid free water on the surfaces of contact for

loadings. After that, firstly, the compressive strengths were evaluated in accordance with NT BUILD 203 (1984) on three cylindrical specimens in the same sizes and shapes so that the mean compressive strength f_{cm} was calculated in the direction of the compressive strength tests. Furthermore, the test samples with meter of deformation were centrically placed in the compressive strength test machine with $\pm$ *1 mm* precision. After that, the load with the basic stress $\sigma_0 = 0.5\ MPa$ was applied for readings and deformation savings. Then, the stress was progressively applied at the rate of $0.8 \pm 0.2\ MPa/s$ till $\sigma_1 = 0.45 f_{cm}\ MPa$ was found. This step took 60 seconds for the meter of deformation which was again observed for following 30 seconds. After that point, the strain ε_{01} from σ_0, and σ_1 was calculated. When the sufficient centering process was successfully accepted, the specimens were off-loaded at the same rate of $\sigma_{01} = 0.5\ MPa$. After off-loading, the deformation meter was checked 60 seconds later. Followingly, the samples were again loaded until $\sigma_2 = f_{cm}/3$ was found. Then, the samples were off-loaded at the same rate which was found in advance till σ_0 was reached, and when σ_2 and σ_0 were conserved constant for following 60 seconds. This process was cycled once, σ_2 and σ_{02} were paused for 60 seconds in each one-by-one load. Finally, the strain ε_{02} was calculated from σ_2 and σ_{02}. In this frame, the modulus of elasticity E_0 was found by dividing the difference between σ_1 and σ_{01} into the strain ε_{01}. Like in the calculation of E_0, E_c was computed by dividing the difference between σ_2 and σ_{02} into the strain ε_{02}. In the results, the modulus of elasticity was defined in *GPa* (GN/mm^2) and rounded up and down to the closest *0.5 MPa*. (NT BUILD 205, 1984.) In the Figure 3.5, the gauge length, and the maximum nominal aggregate particle size are pictured. And in the Figure 3.6, stress-strain diagram is curved.

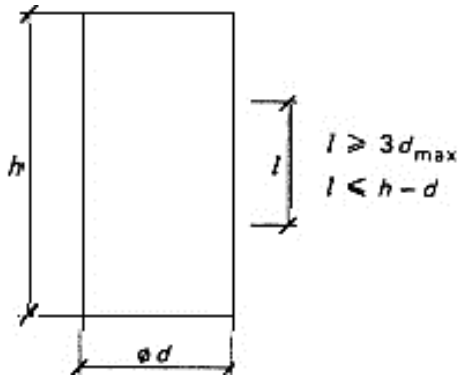

Figure 3.5: The test sample marks with gauge length l and d_{max}.
(NT BUILD 205, 1984.)

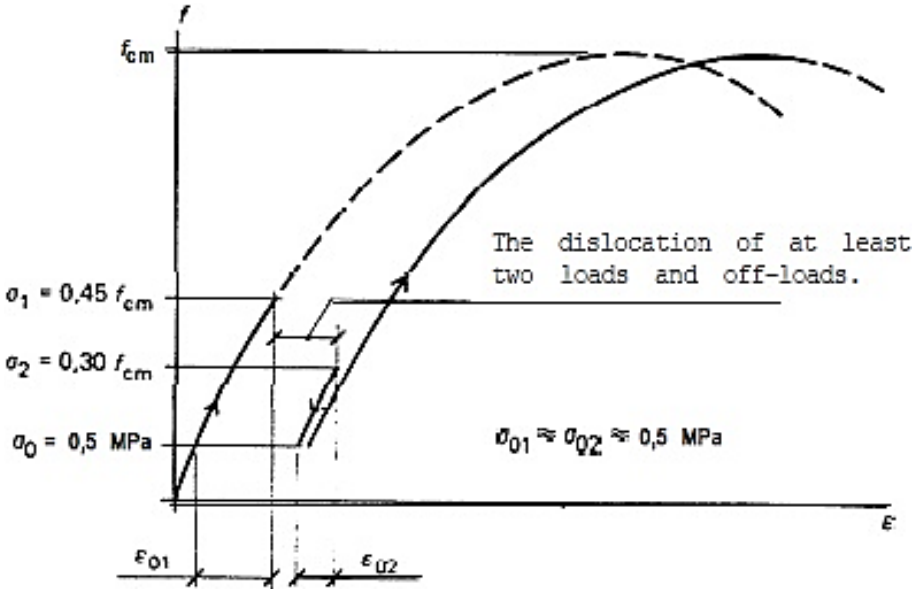

Figure 3.6: The used marks shown in stress and strain diagram. (NT BUILD 205, 1984.)

4. RESULTS OF TESTS

The material properties used in the thesis were given in the anterior section. Additionally, the concrete specimens produced with these materials were also mentioned. Supplementary, the fresh and hardened concrete test samples were represented. In the fresh concrete tests, slump, unit weight and air content tests of concrete were included. Later, the mechanical properties of the concrete samples were examined. Finally, the compressive strength, splitting tensile strength and modulus of elasticity were calculated by following the test procedures. As a result of the tests, the fresh and the hardened concrete tests were enlisted in this section.

4.1 Results of Fresh Concrete Tests

The fresh concrete test results such as slump, unit weight, and air content are released in this section. All three tests were set to determine the fresh concrete features while the concrete samples were produced.

4.1.1 Results of Slump Tests of Concrete

Based on each compressive test result, the concrete slump test results were gathered like in the Figure 4.1. The FA + MS included samples' slump results have a decreasing trend in high strength results. However, for the GGBS added samples' slump test results, there was not a sign like in the FA + MS included results.

4.1.2 Results of Unit Weight Tests of Concrete

Based on each compressive test result, the unit weight test results are displayed in the Figure 4.2. The FA + MS included sample results have an increasing trend in high strength results. However, for the GGBS added samples' results, there was not an open sign like in the FA + MS included results

4.1.3 Results of Air Content Tests of Concrete

Based on each compressive test result, the air content test results are shown in the Figure 4.3. It was understood that the air content was not eligible for an evaluation of the increased compressive strength results for both pozzolans.

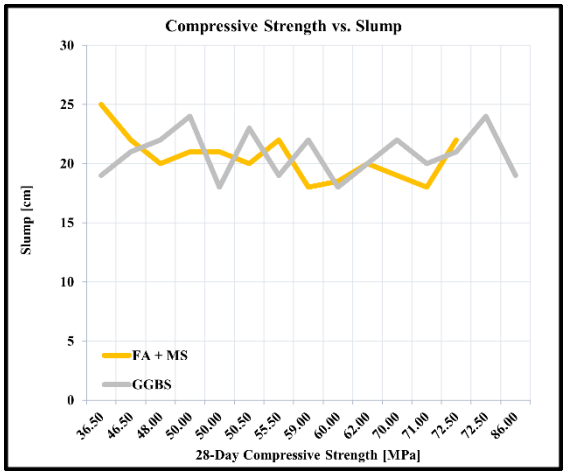

Figure 4.1: The relationship between 28-day CS and slump test result.

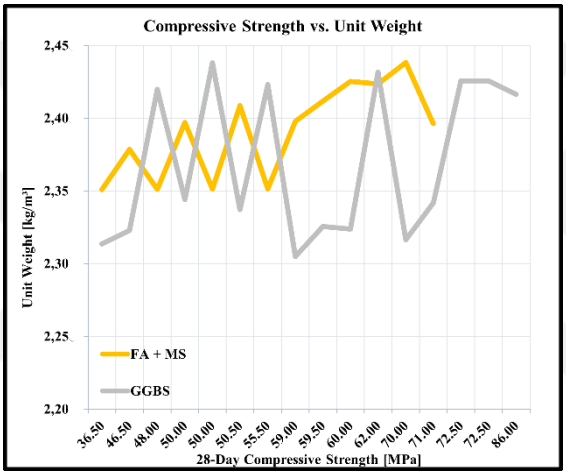

Figure 4.2: The relationship between 28-day CS and concrete unit weight.

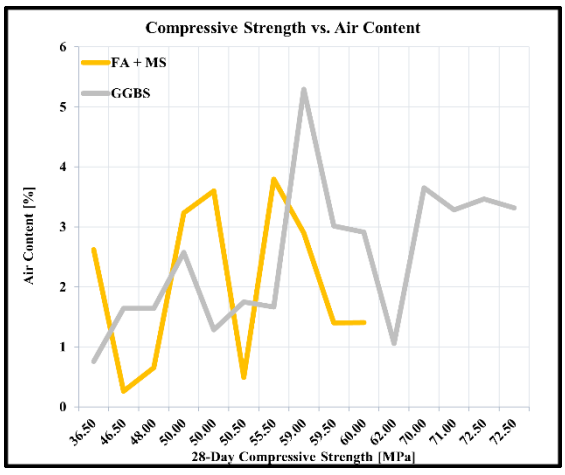

Figure 4.3: The relationship between 28-day CS and air content.

4.2 Actual Results of Mechanical Property Tests

In this section, the Table 4.7, Table 4.8, and Table 4.9 publish the results of the actual laboratory tests. The tested concrete samples were cured under standard curing conditions in a water-filled-tab for 0.5-day, 1-day, 2-day, 3-day, 7-day, 14-day and 28-day strength developments. Both FA + MS and GGBS content including samples are lined up without any additive distinctions.

4.2.1 Actual Results of Compressive Strength Tests

In this section, the compressive strength test results are issued. For both FA + MS and GGBS additives, the results are also ranged in the boxplot for a visual brief in the Figure 4.4; the Table 4.1 and Table 4.2.

In the Figure 4.4, it is noticeably clear that the FA + MS substance included results have higher compressive strength results than the GGBS content leads. Except day-14 and day-28, for all ages, the specimens strengths including the FA + MS substance are close and/or above the median strength values. Only for day-14 and day-28, the specimens strengths including the GGBS content are close and/or above median strength values. However, the whiskers (scores outside median values) of the specimens including GGBS are more evident than the specimens including FA + MS.

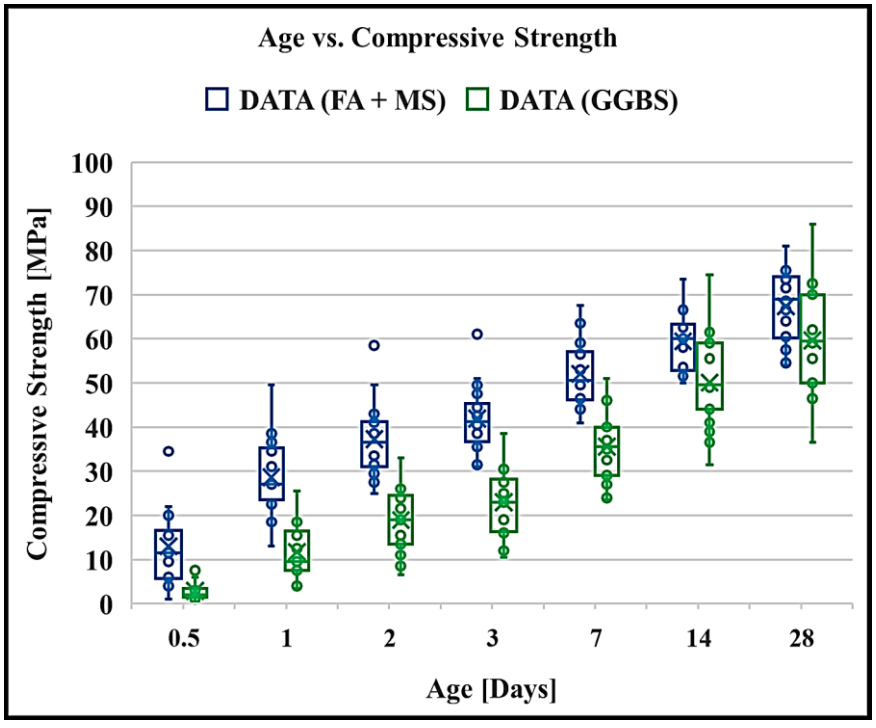

Figure 4.4: The relationship between age and compressive strength.

Table 4.1: The age dependent CS in FA + MS content.

Actual Data [MPa]	0.5-Day	1-Day	2-Day	3-Day	7-Day	14-Day	28-Day
Minimum Value	1.00	13.00	25.00	31.00	41.00	50.00	54.00
1st-Quartile-Value	5.75	23.50	31.00	36.75	36.75	52.75	60.13
Median Value	11.50	27.00	36.50	41.25	41.25	60.00	69.00
3rd-Quartile-Value	16.63	35.25	41.25	45.25	45.25	63.25	74.00
Maximum Value	34.50	49.50	58.50	61.00	61.00	73.50	81.00
Mean Value	13.00	28.60	37.25	41.91	41.91	59.37	67.34
Range	33.50	36.50	33.50	30.00	20.00	23.50	27.00

Table 4.2: The age dependent CS results in GGBS content.

Actual Data [MPa]	0.5-Day	1-Day	2-Day	3-Day	7-Day	14-Day	28-Day
Minimum Value	0.50	3.50	6.50	10.50	23.50	31.50	36.50
1st-Quartile-Value	1.50	7.50	13.50	16.38	29.00	44.00	50.00
Median Value	2.00	9.50	19.00	23.00	35.50	49.50	59.50
3rd-Quartile-Value	3.50	16.50	24.50	28.25	40.00	59.00	70.00
Maximum Value	7.50	25.50	33.00	38.50	51.00	74.50	86.00
Mean Value	2.88	11.71	18.91	22.94	35.59	50.03	59.59
Range	7.00	22.00	26.50	28.00	27.50	43.00	49.50

4.2.2 Results of Splitting Tensile Strength Tests

In this section, the splitting tensile strength test results are represented. In the Figure 4.5, for both FA + MS and GGBS contents, the results are boxploted for an explanatory brief. In the Figure 4.5, it is truly clear that the FA + MS ingredient results have higher splitting tensile strength results than the GGBS content makes. Except day-14 and day-28, for all ages, the specimen strengths including the FA + MS ingredient are close and/or above the median strength values. Except day-3 and day-7, for all ages, the sample strengths including the GGBS subsequent are close and/or above the median strength values. To sum up, the specimens including the GGBS content are more accurate than the specimens including the FA + MS theme.

4.2.3 Results of Modulus of Elasticity Tests

In this section, the modulus of elasticity test results is exposed. For both FA + MS and GGBS pozzolans, the results are revealed in the boxplot for a viewing brief in the Figure 4.6. Moreover, in the Table 4.5, and in the Table 4.6, the numerical results of the tests are tallied for both FA + MS and GGBS contents. In the Figure 4.6, it is certainly open that the FA + MS including results have higher modulus of elasticity results than GGBS theme does. Except day-1, day-2, and day-28, for all ages, the modulus of elasticity developments including the FA + MS ingredient are close and/or

above median strength values. Except day-2 and day-28, for all ages, the modulus of elasticity developments including GGBS are close and/or above median strength values. The whiskers of the specimens having GGBS content are more dependable than the specimens including FA + MS.

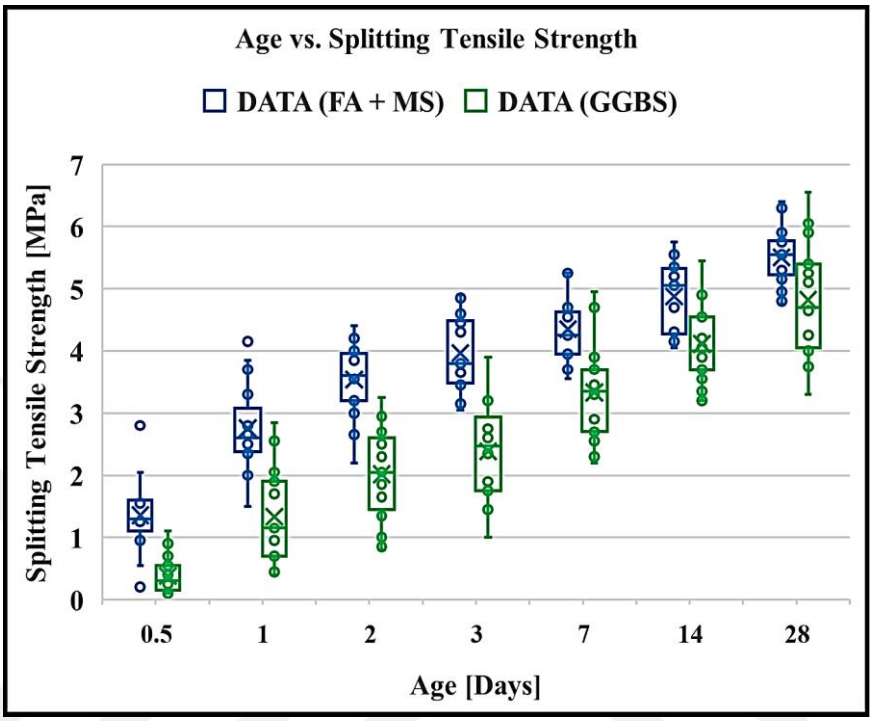

Figure 4.5: The relationship between age and splitting tensile strength.

Table 4.3: The age dependent STS results in FA + MS content.

Actual Data [MPa]	0.5-Day	1-Day	2-Day	3-Day	7-Day	14-Day	28-Day
Minimum Value	0.20	1.50	2.20	3.05	3.55	4.05	4.75
1st-Quartile-Value	1.10	2.38	3.20	3.49	3.95	4.28	5.23
Median Value	1.30	2.60	3.60	3.80	4.25	5.05	5.55
3rd-Quartile-Value	1.60	3.08	3.96	4.49	4.63	5.33	5.78
Maximum Value	2.80	4.15	4.40	4.90	5.25	5.75	6.40
Mean Value	1.36	2.75	3.54	3.97	4.35	4.87	5.50
Range	2.60	2.65	2.20	1.85	1.70	1.70	1.65

Table 4.4: The age dependent STS results in GGBS content.

Actual Data [MPa]	0.5-Day	1-Day	2-Day	3-Day	7-Day	14-Day	28-Day
Minimum Value	0.10	0.40	0.80	1.00	2.20	3.20	3.30
1st-Quartile-Value	0.15	0.70	1.45	1.75	2.70	3.70	4.05
Median Value	0.30	1.15	2.05	2.48	3.35	4.00	4.70
3rd-Quartile-Value	0.55	1.90	2.60	2.94	3.70	4.55	5.40
Maximum Value	1.10	2.85	3.25	3.90	4.95	5.45	6.55
Mean Value	0.38	1.33	2.02	2.38	3.33	4.11	4.82
Range	1.00	2.45	2.45	2.90	2.75	2.25	3.25

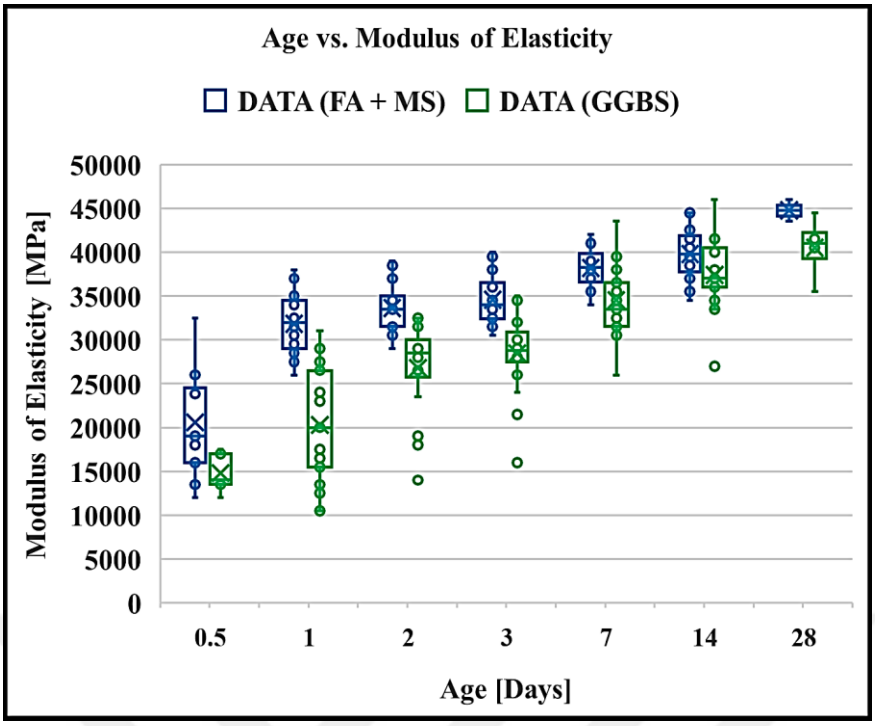

Figure 4.6: The relationship between age and modulus of elasticity.

Table 4.5: The age dependent ME results in FA + MS content.

Actual Data [MPa]	0.5-Day	1-Day	2-Day	3-Day	7-Day	14-Day	28-Day
Minimum Value	12000	26000	29000	30500	34000	34500	38000
1st-Quartile-Value	16000	29000	31500	32375	36625	37750	40375
Median Value	19000	32000	33500	34000	38250	39750	41750
3rd-Quartile-Value	24500	34500	35000	36500	39875	41875	43125
Maximum Value	32500	38000	39000	40000	42000	44500	46000
Mean Value	20593	31833	33615	34563	38188	39786	41844
Range	20500	12000	10000	9500	8000	10000	8000

Table 4.6: The age dependent ME results in GGBS content.

Actual Data [MPa]	0.5-Day	1-Day	2-Day	3-Day	7-Day	14-Day	28-Day
Minimum Value	12000	10500	14000	16000	26000	27000	25000
1st-Quartile-Value	13500	15500	25750	27500	31500	36000	39000
Median Value	14000	20000	28500	28750	33500	37000	40000
3rd-Quartile-Value	17000	26500	30000	30875	36500	40500	42000
Maximum Value	17500	31000	32500	35000	43500	46000	44500
Mean Value	14800	20294	26813	28469	34529	37382	39294
Range	5500	20500	18500	19000	17500	19000	19500

Table 4.7: The actual compressive strength (f'_c) test results [MPa].

Mixing Codes	0.5-Day	1-Day	2-Day	3-Day	7-Day	14-Day	28-Day
C45-III-B20	2.00	9.50	24.00	30.50	51.00	74.50	86.00
YM-SEG-03	20.00	36.50	43.00	49.50	59.00	62.50	71.50
YM-SEG-03-FSTC	22.00	36.00	41.00	43.50	53.00	60.00	68.50
MIX-15A-04	11.50	27.00	38.50	42.50	51.00	-	64.00
YM-SEG-05	9.50	31.00	42.00	42.00	56.50	66.50	73.50
YM-SEG-08	15.50	34.50	40.00	47.50	59.50	64.00	75.50
MIX-15E-03	6.00	23.50	31.50	36.00	45.00	52.00	59.00
MIX-15-AC-04	11.50	27.50	40.00	44.50	54.00	60.00	69.50
YM-SEG-10	-	23.50	33.50	39.00	50.00	60.50	69.50
DURABET PLUS AIR-AC-03	7.50	18.50	22.50	26.50	37.50	55.50	63.50
YM-SEG-10A	15.50	-	33.00	38.50	49.50	58.50	66.50
YM-SEG-10E	-	23.50	29.00	31.00	44.00	53.50	60.50
YM-DAP-AC-03	3.00	13.00	21.50	25.00	37.50	50.00	59.50
MIX-15-AC-03	4.00	22.50	29.50	35.50	45.00	51.50	54.00
MIX-30	1.50	5.50	12.50	16.00	29.00	36.50	46.50
MIX-30-03	7.50	19.50	24.50	27.50	35.50	44.00	50.00
MIX-30-BRT	3.50	16.50	25.50	31.50	46.00	60.50	70.00
MIX-30-07	3.00	12.50	19.00	23.00	32.50	44.00	50.50
MIX-34-BRT	4.00	18.50	26.00	-	37.00	49.00	59.00
MIX-32-03	6.00	25.50	33.00	38.50	47.50	59.00	71.00
MIX-32-CEN	2.00	9.00	14.00	16.00	24.00	31.50	36.50
MIX-32-CEN-OK	2.50	15.50	27.50	31.50	40.00	50.50	60.00
B70-380	1.50	4.00	8.50	12.00	25.00	39.00	50.00
B70-420	1.00	3.50	6.50	10.50	23.50	41.00	48.00
B47-440	1.50	7.50	16.50	23.00	41.50	61.50	72.50
B67-440	1.00	5.50	13.50	20.00	35.00	60.00	72.50
B67-440-001	0.50	7.50	11.00	16.50	27.00	44.50	55.50
C45-B25-425	-	13.00	25.00	37.00	46.50	52.00	57.50
B67-440-BEY	1.00	7.50	15.50	19.00	35.50	49.50	62.00
C45-B26-475	5.00	38.50	49.50	51.00	63.50	68.00	76.50
C45-B25-400	1.00	24.00	34.50	40.50	48.00	58.00	76.00
C50-B22-460	34.50	49.50	58.50	61.00	67.50	73.50	81.00
YM-SEG-11	-	18.50	27.50	31.50	41.00	50.00	54.50

Table 4.8: The actual splitting tensile strength (f'_t) test results [MPa].

Mixing Codes	0.5-Day	1-Day	2-Day	3-Day	7-Day	14-Day	28-Day
C45-III-B20	0.25	1.20	2.70	3.25	4.95	4.20	6.55
YM-SEG-03	1.65	3.85	4.40	4.40	5.25	5.55	5.85
YM-SEG-03-FSTC	-	4.15	4.30	4.60	4.55	5.75	5.65
MIX-15A-04	1.35	2.85	3.55	3.80	4.25	-	4.80
YM-SEG-05	1.25	2.50	3.85	4.30	-	5.05	4.95
YM-SEG-08	2.05	2.80	3.90	4.60	4.70	4.80	6.40
MIX-15E-03	0.95	2.40	3.25	3.65	4.25	4.30	5.25
MIX-15-AC-04	1.30	2.60	4.20	4.45	3.55	5.05	5.90
YM-SEG-10	-	2.60	3.00	3.80	4.05	5.30	5.30
DURABET PLUS AIR-AC-03	0.90	2.15	2.55	2.85	3.45	4.55	5.40
YM-SEG-10A	1.55	-	3.20	3.15	4.60	5.35	5.55
YM-SEG-10E	-	2.35	3.20	3.45	4.65	5.20	5.30
YM-DAP-AC-03	0.55	1.15	2.30	2.75	3.70	4.05	5.15
MIX-15-AC-03	0.55	2.05	3.30	3.75	3.95	4.05	5.15
MIX-30	0.20	0.70	1.35	1.75	2.70	3.80	4.05
MIX-30-03	1.10	2.55	2.75	3.25	3.80	3.90	4.00
MIX-30-BRT	0.40	1.70	2.50	2.65	3.90	5.00	6.05
MIX-30-07	0.40	1.25	2.05	2.60	3.40	4.00	4.35
MIX-34-BRT	0.65	2.05	2.60	-	3.30	4.15	5.25
MIX-32-03	0.70	2.85	3.25	3.90	4.70	5.45	5.90
MIX-32-CEN	0.30	0.95	1.65	1.95	2.70	3.20	3.30
MIX-32-CEN-OK	0.30	1.90	2.95	3.20	3.30	4.90	5.50
B70-380	0.15	0.45	0.80	1.00	2.30	3.20	4.00
B70-420	0.15	0.40	0.85	1.45	2.20	3.55	4.25
B47-440	0.10	1.00	1.85	2.35	3.40	4.90	5.10
B67-440	0.10	0.70	1.70	1.90	3.35	4.00	3.75
B67-440-001	0.10	0.70	1.00	1.55	2.55	3.35	4.70
C45-B25-425	-	1.50	2.20	3.05	3.95	4.15	4.75
B67-440-BEY	0.15	0.95	1.45	1.75	2.90	3.70	4.65
C45-B26-475	1.30	3.30	4.00	4.85	4.55	4.70	6.30
C45-B25-400	0.20	2.65	3.65	3.50	3.70	4.25	5.75
C50-B22-460	2.80	3.70	3.95	4.90	5.25	5.35	5.55
YM-SEG-11	-	2.00	2.65	3.20	3.95	4.25	5.60

Table 4.9: The actual modulus of elasticity (E'_c) test results [MPa].

Mixing Codes	0.5-Day	1-Day	2-Day	3-Day	7-Day	14-Day	28-Day
C45-III-B20	-	22381	30704	35048	41808	45068	46897
YM-SEG-03	26105	32752	37530	39448	41895	42893	43410
YM-SEG-03-FSTC	-	31502	35946	37720	39974	40891	41365
MIX-15A-04	26209	32758	37435	39306	41686	-	43157
YM-SEG-05	17323	24756	-	34674	39156	41151	42227
YM-SEG-08	-	33644	-	38715	40457	41151	41508
MIX-15E-03	20606	27008	31975	34063	36810	37958	38559
MIX-15-AC-04	22371	29806	35745	38288	41677	43108	43860
YM-SEG-10	-	28432	33228	35208	37780	38844	39399
DURABET PLUS AIR-AC-03	17250	24089	30044	32742	36487	38122	38995
YM-SEG-10A	24673	-	34808	36472	38581	39436	39878
YM-SEG-10E	-	25302	30633	32947	36060	37384	38084
YM-DAP-AC-03	-	22478	28449	31213	35111	36836	37764
MIX-15-AC-03	17586	24438	30352	33015	36694	38294	39147
MIX-30	-	19927	25759	28545	32569	34387	35374
MIX-30-03	-	28193	-	33352	35191	35935	36318
MIX-30-BRT	16333	23810	30877	34267	39184	41413	42625
MIX-30-07	15039	21681	27825	30728	34888	36753	37763
MIX-34-BRT	17356	24509	30870	-	37895	39702	40672
MIX-32-03	20003	27164	33086	35679	39188	40689	41484
MIX-32-CEN	-	16999	20946	22703	25110	26150	26703
MIX-32-CEN-OK	-	22805	27022	28796	31133	32110	32622
B70-380	-	11503	18199	22579	31148	36316	39601
B70-420	-	8783	14834	19256	29206	36227	41175
B47-440	-	17658	25601	30117	37720	41664	43963
B67-440	-	16432	24303	28921	36944	41234	43775
B67-440-001	-	14915	21911	25972	32952	36645	38820
C45-B25-425	-	25856	30842	32960	35769	36949	37569
B67-440-BEY	-	16299	23402	27380	33980	37357	39311
C45-B26-475	21348	28266	-	36057	39139	40435	41116
C45-B25-400	-	27398	32250	34273	36920	-	38597
C50-B22-460	32209	37092	40134	41262	42632	43169	43443
YM-SEG-11	-	25667	30892	33142	36150	37423	38094

5. DISCUSSION ON CONCRETE STRENGRH PREDICTION

In the previous section, the mechanical properties of concrete were performed on the cylindrical samples. After the tests, the results were conducted on the regression analysis models. These regression analyses were divided into two main methods which were the univariate regression and multivariate regression analysis. For both methods, linear and non-linear models were studied in this thesis. As independent variables, concrete age, amounts of concrete materials and proportions of concrete materials were related. There were also many regression models used in the study to investigate any relationship between the variables and results through the actual behavior of concrete. However, the range of the study was limited for a better comparison in terms of the test results. In addition to this, one main machine learning algorithm was computed by using again the concrete mixture design properties. The fraction (Equ. 5.1), logarithmic (Equ. 5.2), power logarithmic (Equ. 5.3), and power (Equ. 5.4) forms with their combinations of the univariate regression models were studied for the best data fitting purposes of the test results.

$$y = \frac{a * x}{b + x} \tag{5.1}$$

$$y = a \ln(x)^b \tag{5.2}$$

$$y = a + b * \ln(x) \tag{5.3}$$

$$y = a * x^b \tag{5.4}$$

In these univariate equations, y represents the predicted compressive strength (PCS) (f'_c), predicted splitting tensile strength (PSTS) (f'_t), and predicted modulus of elasticity (PME) (E'_c). The coefficients a and b are from the regression calculations. For the multivariate regression analysis, as general forms, the linear (Equ. 5.5), fraction (Equ. 5.6), logarithmic (Equ. 5.7), and power (Equ. 5.8, Equ. 5.9, and Equ. 5.10), were examined for the best goodness-of-fitting purposes of the test results.

$$y = a + b_1 * x_1 + b_2 * x_2 + b_3 * x_3 + b_n * x_n \tag{5.5}$$

$$y = a * \left(\frac{x_1}{x_2 + x_n} + b\right) \tag{5.6}$$

$$y = a + b * \ln\left(\frac{x_1}{x_2}\right) \tag{5.7}$$

$$y = a * {x_1}^{b_1} * {x_2}^{b_2} * {x_n}^{b_n} \tag{5.8}$$

$$y = a * (\frac{x_1}{x_2 + x_n})^b \tag{5.9}$$

$$y = \frac{a}{b^{\frac{x_1}{x_2}}} \tag{5.10}$$

In the multivariate regression equations, *y* represents the predicted the compressive strength (PCS) (f'_c), predicted splitting tensile strength (PSTS) (f'_t), and predicted modulus of elasticity (PME) (E'_c). The coefficients *a* and *b* are from again regression calculations. In this logic, the regression analysis results may be not always enough for relating variables each other. That is why determination coefficient (R^2) (Equ. 5.11) of a regression analysis model is an incredibly significant parameter without doubt to understand that model like in Chithra et al. (2016) study. R^2 also differs from zero to one for showing how well estimated results fit onto the actual data sets. R^2 additionally represents change percentages in dependent variables which are meant by independent variables. Hence, it is called statistically goodness-of-fit in the regression model calculations. Even though R^2 results are exceedingly high, it is not possible to say that regression model analyzed is always meaningful. In this manner, adjusted coefficient of determination (R^2_{adj}) (Equ 5.12) explains cases which are effective on chosen model. Because of that, there are many academic studies which include R^2_{adj} results like Wilson et al. study. Like R^2, R^2_{adj} is also another goodness-of-fit parameter in this thesis.

$$R^2 = 1 - \frac{\sum_{i=1}^{N}(y_i - \hat{y}_i)^2}{\sum_{i=1}^{N}(y_i - \overline{y})^2} \tag{5.11}$$

$$R^2{}_{adj} = 1 - \frac{n-1}{n-p}(1 - R^2) \tag{5.12}$$

To calculate R^2, actual mean value ($\overline{y}$), and predicted value ($\hat{y}$) of data sets are necessary. And *N* shows the total specimen number in the actual data collection. For R^2_{adj}, *n* explains the observation number, and *p* describes the parameter number used in the regression models. As mentioned above, R^2 may not be accurate because of its sensitivity for data scattering and/or fitting. Because of this issue, use of root means square error (*RMSE*) (Equ. 5.13) comes forward for implying much better model fitting to the actual data sets by using small values as mentioned in Sutherland et al. study. By this thinking, *RMSE* was also used in this study for prediction comparisons as regards R^2_{adj}.

$$RMSE = \sqrt[2]{\frac{(y_i - \hat{y}_i)^2}{n - p}} \tag{5.13}$$

In *RMSE*, *y* indicates the actual data value, and $\hat{y}$ is for the predicted data value. *n* represents the observation number, and *p* corresponds the parameter number used in the regression model. Moreover, sum of squares error (*SSE*) (Equ. 5.14) shows differences between the actual data set and its mean of the group. It is a use of variation measure in a cluster. Whether all the situations are as same as like in the actual data sets, SSE would be equal to zero. Khademi et al. (2016) also experiments *SSE* in their study for artificial neural network (ANN), adaptive neuro-fuzzy inference system (ANFIS), and multiple regression analysis (MRA) in the strength prediction of re-cycled aggregate used concrete.

$$SSE = \sum_{i=1}^{N} (x_i - \bar{x}_i)^2 \tag{5.14}$$

In SSE, *N* explicates the total specimen number in the actual data sets, and x is for the actual data values, and $\bar{x}$ is for the estimated data results. Additionally, for a better fitting trial, mean squared error (MSE) (Equ. 5.15) uses normalization method for the observed data. It depends on the predicted variable units, and changes in an interval between 0.00 and ∞. And it results the differences of average squares between the predicted and the real data values. Gupta et al. (2009) also uses *MSE* criterion in their study for the data calibration. Here, it is used in this study for normalizing of machine learning algorithm results that leads the quality of algorithm chosen.

$$MSE = \frac{1}{n}\sum_{i=1}^{N}(y_i - \hat{y}_i)^2 \tag{5.15}$$

In MSE, *n* explains the observation number, and *N* shows the total specimen number in the actual data sets. On the other hand, y represents the real data, and $\hat{y}$ shows the estimated data. Furthermore, in again machine learning algorithm, correlation coefficient (*R*) (Equ. 5.16) measures how various variables are different in their correlations, and how strong relationship is conducted between variables as Sam (2020) uses in his green technology concrete study.

$$R = \frac{n\sum xy - (\sum x)(\sum y)}{\sqrt{[n\sum x^2 - (\sum x)^2]\,[n\sum y^2 - (\sum y)^2]}} \tag{5.16}$$

In *R* calculations, x means the independent variables, and y means the dependent variables. *n* also indicates the observation number. *R* changes from zero to one to express how the estimated results are close to the actual data values.

Finally, among all the proposed models, the best trials were published in this thesis to narrow the wide range of the model preferences down for the best estimation purposes.

5.1 Univariate Regression Analysis for Compressive Strength

In this section of the thesis, the Table 5.3, Table 5.7, and Table 5.11 publish the regression models with their statistical results come out in the study.

5.1.1 Fraction Power Regression (Model-1)

The fraction power regression model (the Model-1) is one of the univariate regression analysis models depending on concrete age. In this model, for 0.5-day, 1-day, 2-day, 3-day, 7-day, 14-day, and 28-day compressive strength estimations were carried out. Even though the R^2 (btw 0.9427 & 0.9999), and R^2_{adj} results are remarkably high; the SSE, and RMSE results are very low, and the character of the fraction power equation does not fit well to some of the actual data sets. The curve fittings of the specimens in YM-SEG-03, YM-SEG-05, YM-SEG-08, MIX-15E-03, MIX-15-AC-04, MIX-15-AC-03, MIX-34-BRT, MIX-32-03, MIX-32-CEN-OK, C45-B25-425, C45-B26-475, C45-B25-400, and C50-B22-460 mixing codes are especially not accurate between day-7 and day-14. In this bunch of samples, only the samples in MIX-34-BRT, MIX-

32-03, and MIX-32-CEN-OK mixing codes have GGBS substance. The other ones include FA + MS content. In this light of knowledge, the use of FA + MS may lead unexpected strength developments between day-7 and day-14 as shown in the Table 5.4 for the compressive strength. Because it is expected that the concrete should gain it is strength by its age under standard curing methods. Nevertheless, at day-7 and day-14, the compressive strength decreases which is an unwilling situation in this regression model.

In the Figure 5.1, the correlations of the actual data sets and predicted results are given. The correlations clearly describe that the results of the Model-1 are numerically so much satisfying. However, as mentioned above, due to the negative deflections for the strength development in the curve fitting for each specimen test result, the model may not be safe to predict the compressive strength depending on the concrete age.

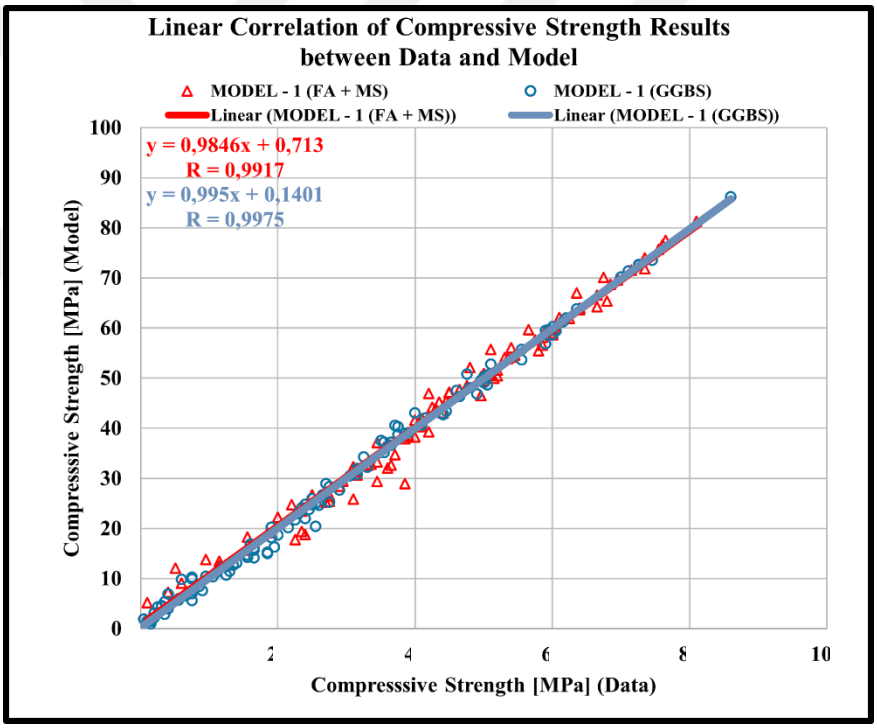

Figure 5.1: The correlations of the compressive strength for the Model-1.

In the Figure 5.2, for the samples including FA + MS ingredient, the Model-1 shows that [(W/C) - (W/B)] result for the maximum R^2 result is greater than for the minimum R^2 value. It is seen that the W/C ratio is more effective than the W/B ratio for data prediction. Also, while [(CA/A) - (FA/A)] result gets smaller, the R^2 result also decreases which means the CA/A ratio is more effective on the data prediction with respect to the FA/A ratio. The figure also indicates that the most powerful data prediction in the R^2 results corresponds to the sample in YM-SEG-10A mixing code.

Besides, the least powerful data prediction corresponds to the sample in YM-SEG-05 mixing code. However, this comparison could not be widened for all the specimens in the compressive strength estimation of the model.

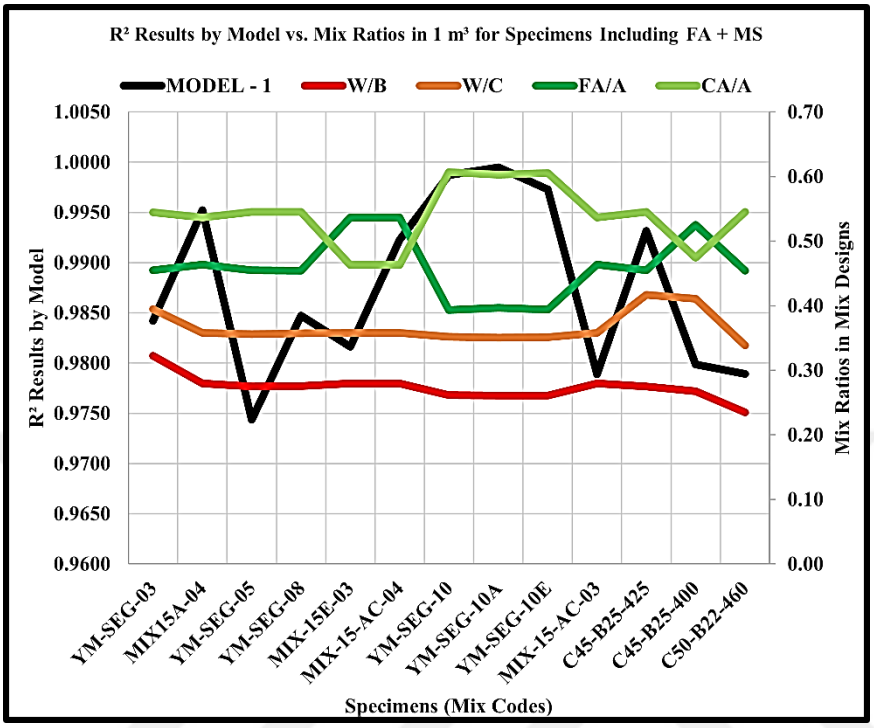

Figure 5.2: The correlations of the mixing ratios of the Model-1 in FA + MS.

In the Figure 5.3, for the samples including FA + MS ingredient, the Model-1 shows that the amounts of CS and NS are very close to each other for the maximum R^2 result. This result teaches that the amounts of fine aggregates may not have any effects on the maximum R^2 value. Oppositely, for the minimum R^2 result, the difference between NS and CS is higher with respect to the maximum R^2 has. Namely, it is understood that the higher [(CS) - (NS)] results decrease the prediction potential of the compressive strength. Moreover, the amounts of NO:1 Agg., and NO:2 Agg. are awfully close to each other for the maximum R^2 result in [(CS) - (NS)] case, too. On the other hand, for the minimum R^2 value, the difference between NO:1 Agg. and NO:2 Agg. is higher as regards the maximum R^2 has. As when the difference between NO:1 Agg., and NO:2 Agg. gets smaller, the R^2 result decreases in the data estimation for the compressive strength. Furthermore, [(FA) - (MS)] of the minimum R^2 result is greater than [(FA) - (MS)] of the maximum R^2 result. As additive, FA + MS existence decreases the data prediction in this model. In addition to this, the maximum amount of MS is 50.00 kg/m^3 for the highest-level R^2 result. However, this is a partial case in the results of the model. Like the high amount of fly ash, the high amount of cement decreases the

potential of the data forecasting which limits the cement use for the strength gaining. Diametrically, the type of cement could not be evaluated, because it is CEMI 42.5 for both. Lastly, there is no direct water and admixtures effects in use for strength gaining.

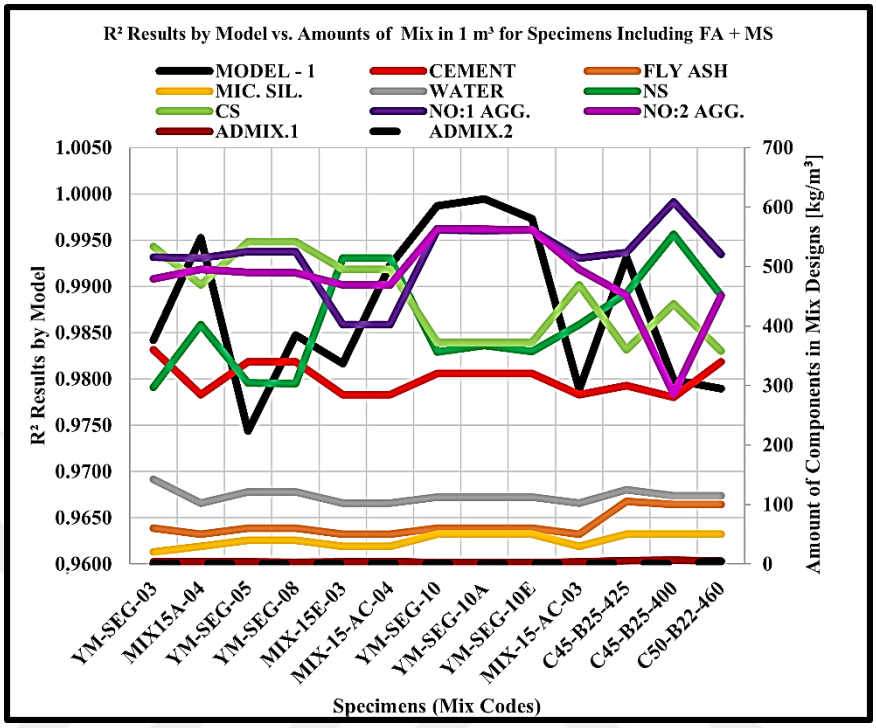

Figure 5.3: The correlation of the mixing amounts of the Model-1 in FA + MS.

In the Figure 5.4, for the samples including GGBS substance, the Model-1 shows that the W/C ratio equals to the W/B ratio for the minimum R^2 result which is the sign of no GGBS effects in the worst strength prediction by the model. Followingly, the minimum W/C ratio is found 0.31 for the maximum R^2 result, and the minimum W/B ratio is spotted 0.35 for the maximum R^2 result. This result takes the model to the use of GGBS which has negative effects for the most well-fitting estimation in strength gaining. It is also figured out that [(W/C) - (W/B)] result of the maximum R^2 result is greater than the minimum R^2 result has. This case could be evaluated as the least GGBS ingredient, the most well-predicted compressive strength. And, while [(CA/A) - (FA/A)] result gets higher, the R^2 result also increases that which means the CA/A ratio is more effective on the data prediction with respect to the FA/A ratio. The figure also clears for the maximum R^2 result that the CA/A ratio is 0.80, and FA/A is 0.20. However, there is no strong sign that the model could be applied on all the specimens except the ones which have the minimum, and the maximum R^2 results. For why, the rest of the results of the samples are not able to be compared.

In the Figure 5.5, for the samples including GGBS substance, the Model-1 also identifies that the amounts of CS and NS are very close to each other for the maximum R^2 value. This result proves that the amounts of fine aggregates may not be effective on the maximum R^2 result.

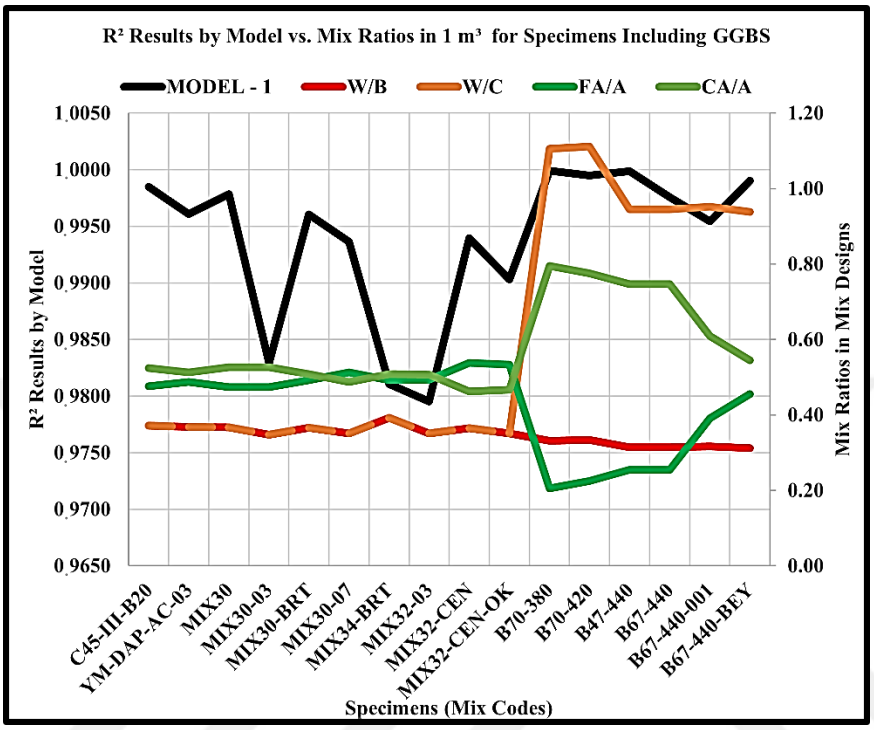

Figure 5.4: The correlation of the mixing ratios of the Model-1 in GGBS.

Differently, [(NS) - (CS)] of the maximum R^2 result is greater than the minimum R^2 result corresponds. This case tells that the NS amount influences the strength prediction in a polite manner. At the maximum R^2 result, the NO:0 Agg., NO:1 Agg., and NO:2 Agg. amounts are the nearest which clarifies that there is no significance sign of coarse aggregate effects on the maximum R^2 result. However, for some specimens, the higher amounts of NO:0 Agg., NO:1 Agg., and NO:2 Agg. get the higher R^2 values. Intercalarily, there is no sign that any amount of water and admixtures affect the results. But again, for some specimens, while the GGBS content is weighted, the cement amount decreases in increasing of the R^2 result. Because GGBS was used as a binder material in the concrete samples and affected the strength gaining and strength estimating in a positive way. In total, for the maximum R^2 result, the amount of cement [114.00 kg/m^3], NO:0 Agg. [486.00 kg/m^3], CS [0.00 kg/m^3], and NS [395.00 kg/m^3], used in the mixture designs are the minimum. For the best data presuming, the amount of GGBS is measured 266.00 kg/m^3. For the highest R^2 value, CEMI 52.5N type cement, and for the lowest R^2 value, CEMIII 32.5 type cement

are stood out. Thus, there is no pointer of the model computation for all the specimens except the ones having the minimum and maximum R^2 results. Because the rest of the sample results are not suitable for different comparisons. In the Model-1, for both contents, the results are shown in the boxplot for an imaginary brief in the Figure 5.6**.**

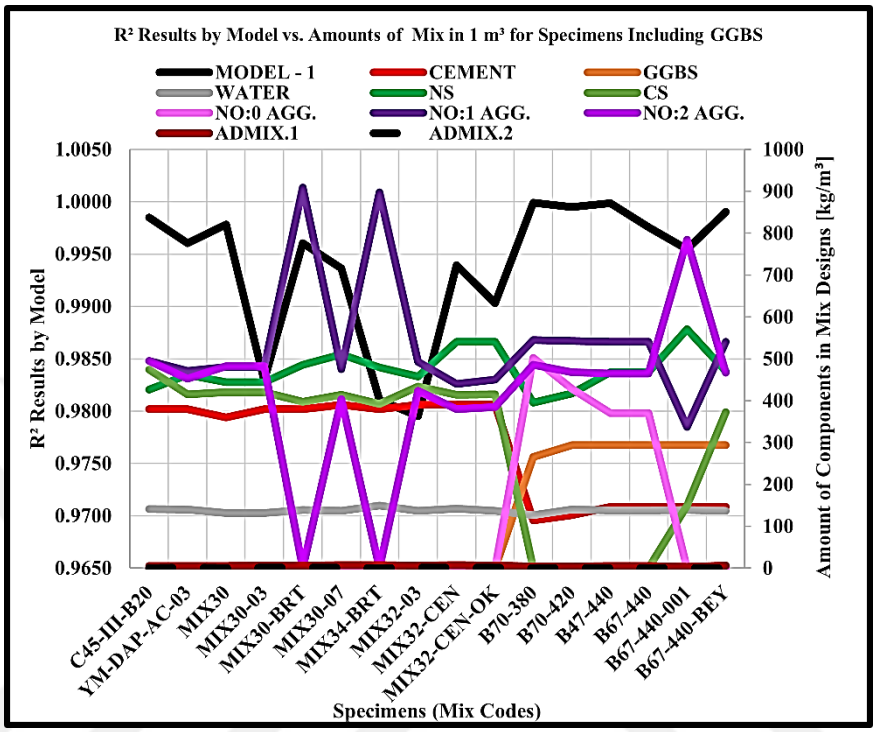

Figure 5.5: The correlation of the mixing amounts of the Model-1 in GGBS.

Moreover, in the Table 5.1, and the Table 5.2, the numerical results of the model are shown for both FA + MS and GGBS contents. In the Figure 5.6, it is certain that the FA + MS ingredient causes higher compressive strength prediction results than the GGBS presence does. Except day-7, day-14, and day-28, for all ages, the strengths of the specimens including FA + MS are close and/or above the median strength values. Except day-28, for all ages, the strengths of the specimens including GGBS ingredient are close and/or above the median strength values. It is proved that the strength estimations for the specimens including FA + MS are kindly incoherent. Hence, the whiskers of the specimens including GGBS subsequent are more dependable than the specimens including FA + MS substance. In the Table 5.4, for the concrete specimens, the regression model shows the strength developments.

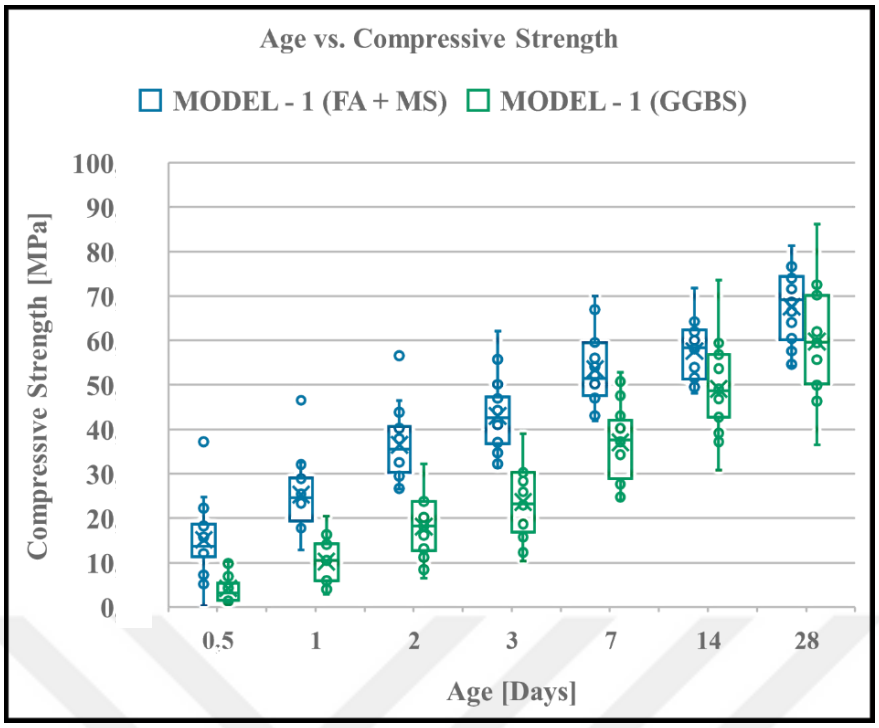

Figure 5.6: The age and the compressive strength relationship for the Model-1.

Table 5.1: The age dependent CS results in FA + MS content for the Model-1.

Model-1 [MPa]	0.5-Day	1-Day	2-Day	3-Day	7-Day	14-Day	28-Day
Minimum Value	0.28	12.81	26.50	31.36	41.97	48.17	54.15
1st-Quartile-Value	11.33	19.30	30.34	36.82	47.58	51.30	60.16
Median Value	13.62	24.60	35.55	42.61	51.50	58.36	69.12
3rd-Quartile-Value	18.72	29.05	40.61	47.35	59.53	62.37	74.42
Maximum Value	37.15	46.53	56.58	62.10	70.05	71.77	81.31
Mean Value	15.11	25.29	36.54	42.98	53.53	57.61	67.58
Range	36.86	33.73	30.08	30.74	28.09	23.60	27.16

Table 5.2: The age dependent CS results in GGBS content for the Model-1.

Model-1 [MPa]	0.5-Day	1-Day	2-Day	3-Day	7-Day	14-Day	28-Day
Minimum Value	0.97	2.90	6.52	10.31	24.10	30.87	36.57
1st-Quartile-Value	1.53	5.98	12.66	16.88	28.92	42.75	50.20
Median Value	3.14	10.46	18.20	23.18	37.55	48.65	59.65
3rd-Quartile-Value	5.36	14.18	23.74	30.25	42.04	56.80	70.18
Maximum Value	10.28	20.43	32.21	39.05	52.79	73.52	86.16
Mean Value	4.20	10.25	18.11	23.61	37.07	49.07	59.75
Range	9.31	17.53	25.69	28.74	28.69	42.65	49.59

Table 5.3: The results of the regression Model-1.

Model-1					
Mixing Codes	**Fraction Power Regression**	**R^2**	**R^2_{adj}**	**SSE**	**RMSE**
C45-III-B20	$f'_c = -18.17 + 28.76t^{0.5} + 0.243t^{1} - 0.3689t^{1.5}$	0.9985	0.9969	9.375	1.768
YM-SEG-03	$f'_c = -12.73 + 60.47t^{0.5} - 16.65t^{1} + 1.556t^{1.5}$	0.9881	0.9761	21.738	2.692
YM-SEG-03-FSTC	$f'_c = 1.233 + 39.76t^{0.5} - 9.862t^{1} + 0.899t^{1.5}$	0.9803	0.9607	28.666	3.091
MIX-15A-04	$f'_c = -32.65 + 80.72t^{0.5} - 25.45t^{1} + 2.579t^{1.5}$	0.9952	0.9881	7.999	2.000
YM-SEG-05	$f'_c = -25.95 + 67.77t^{0.5} - 17.54t^{1} + 1.569t^{1.5}$	0.9744	0.9487	73.389	4.946
YM-SEG-08	$f'_c = -18.72 + 63.59t^{0.5} - 17.06t^{1} + 1.59t^{1.5}$	0.9847	0.9694	37.391	3.530
MIX-15E-03	$f'_c = -25.04 + 58.56t^{0.5} - 15.58t^{1} + 1.422t^{1.5}$	0.9816	0.9633	35.657	3.448
MIX-15-AC-04	$f'_c = -26.73 + 69.58t^{0.5} - 19.25t^{1} + 1.804t^{1.5}$	0.9923	0.9845	18.202	2.463
YM-SEG-10	$f'_c = -5.051 + 35.15t^{0.5} - 6.602t^{1} + 0.4958t^{1.5}$	0.9987	0.9968	1.894	0.973
DURABET PLUS AIR-AC-03	$f'_c = -0.9999 + 15.64t^{0.5} + 0.6141t^{1} - 0.2373t^{1.5}$	0.9872	0.9743	31.717	3.252
YM-SEG-10A	$f'_c = -7.646 + 38.26t^{0.5} - 7.818t^{1} + 0.6118t^{1.5}$	0.9995	0.9987	0.894	0.668
YM-SEG-10E	$f'_c = 12.57 + 9.602t^{0.5} + 1.567t^{1} - 0.3159t^{1.5}$	0.9973	0.9933	2.943	1.213
YM-DAP-AC-03	$f'_c = -15.94 + 32.52t^{0.5} - 5.498t^{1} + 0.3878t^{1.5}$	0.9961	0.9921	9.615	1.790
MIX-15-AC-03	$f'_c = -27.22 + 58.67t^{0.5} - 14.96t^{1} + 1.281t^{1.5}$	0.9789	0.9577	39.730	3.639
MIX-30	$f'_c = -12.78 + 21.22t^{0.5} - 2.593t^{1} + 0.1314t^{1.5}$	0.9978	0.9957	3.623	1.099
MIX-30-03	$f'_c = -10.06 + 33.19t^{0.5} - 7.46t^{1} + 0.6312t^{1.5}$	0.9829	0.9659	21.830	2.698
MIX-30-BRT	$f'_c = -20.10 + 40.69t^{0.5} - 6.957t^{1} + 0.4709t^{1.5}$	0.9961	0.9921	13.509	2.122

Table 5.3 (continued): The results of the regression Model-1.

Model-1					
Mixing Codes	**Fraction Power Regression**	**R^2**	**R^2_{adj}**	**SSE**	**RMSE**
MIX-30-07	$f'_c = -13.02 + 28.05t^{0.5} - 4.664t^{1} + 0.3095t^{1.5}$	0.9936	0.9873	11.052	1.919
MIX-34-BRT	$f'_c = -19.82 + 45.21t^{0.5} - 11.21t^{1} + 1.039t^{1.5}$	0.9810	0.9526	38.767	4.403
MIX-32-03	$f'_c = -24.90 + 59.32t^{0.5} - 15.44t^{1} + 1.449t^{1.5}$	0.9795	0.9590	57.254	4.369
MIX3-2-CEN	$f'_c = -9.926 + 20.90t^{0.5} - 3.595t^{1} + 0.2468t^{1.5}$	0.9939	0.9879	5.530	1.358
MIX-32-CEN-OK	$f'_c = -27.82 + 54.6t^{0.5} - 13.86t^{1} + 1.264t^{1.5}$	0.9903	0.9806	22.790	2.756
B70-380	$f'_c = -2.177 + 2.205t^{0.5} + 4.571t^{1} - 0.5906t^{1.5}$	0.9999	0.9998	0.190	0.251
B70-420	$f'_c = 3.015 - 7.936t^{0.5} + 8.914t^{1} - 1.097t^{1.5}$	0.9995	0.9990	1.110	0.608
B47-440	$f'_c = -10.91 + 15.86t^{0.5} + 3.155t^{1} - 0.5993t^{1.5}$	0.9999	0.9998	0.547	0.427
B67-440	$f'_c = -4.937 + 4.956t^{0.5} + 6.557t^{1} - 0.8921t^{1.5}$	0.9976	0.9951	11.070	1.921
B67-440-001	$f'_c = -5.674 + 9.219t^{0.5} + 2.467t^{1} - 0.3814t^{1.5}$	0.9954	0.9909	11.228	1.935
C45-B25-425	$f'_c = -40.67 + 69.73t^{0.5} - 17.79t^{1} + 1.535t^{1.5}$	0.9932	0.9829	9.846	2.219
B67-440-BEY	$f'_c = -12.60 + 20.21t^{0.5} - 0.494t^{1} - 0.1251t^{1.5}$	0.9990	0.9981	2.946	0.991
C45-B26-475	$f'_c = -46.59 + 103.00t^{0.5} - 30.38t^{1} + 2.90t^{1.5}$	0.9427	0.8854	192.824	8.017
C45-B25-400	$f'_c = -41.73 + 82.07t^{0.5} - 23.95t^{1} + 2.394t^{1.5}$	0.9799	0.9598	70.224	4.838
C50-B22-460	$f'_c = 5.246 + 55.42t^{0.5} - 15.62t^{1} + 1.486t^{1.5}$	0.9789	0.9579	30.315	3.179
YM-SEG-11	$f'_c = -4.204 + 27.64t^{0.5} - 4.58t^{1} + 0.2754t^{1.5}$	0.9973	0.9932	2.584	1.137

Table 5.4: The compressive strength developments of the samples for the Model-1.

Model-1	Strength Development of Actual Data [Day/Day]							Strength Development of Predicted Data [Day/Day]						
Mixing Codes	0.5/28	1/28	2/28	3/28	7/28	14/28	28/28	0.5/28	1/28	2/28	3/28	7/28	14/28	28/28
C45-III-B20	0.0233	0.1105	0.2791	0.3547	0.5930	0.8663	1.0000	0.0250	0.1214	0.2547	0.3535	0.6127	0.8533	1.0000
YM-SEG-03	0.2797	0.5105	0.6014	0.6923	0.8252	0.8741	1.0000	0.2583	0.3789	0.5094	0.5820	0.6909	0.7188	0.8309
YM-SEG-03-FSTC	0.3212	0.5255	0.5985	0.6350	0.7737	0.8759	1.0000	0.2871	0.3717	0.4675	0.5244	0.6272	0.6851	0.7972
MIX-15A-04	0.1797	0.4219	0.6016	0.6641	0.7969	-	1.0000	0.1464	0.2925	0.4399	0.5131	0.5864	0.5591	0.7427
YM-SEG-05	0.1293	0.4218	0.5714	0.5714	0.7687	0.9048	1.0000	0.1596	0.3000	0.4555	0.5451	0.6921	0.7457	0.8589
YM-SEG-08	0.2053	0.4570	0.5298	0.6291	0.7881	0.8477	1.0000	0.2121	0.3412	0.4827	0.5629	0.6912	0.7389	0.8782
MIX-15E-03	0.1017	0.3983	0.5339	0.6102	0.7627	0.8814	1.0000	0.1054	0.2247	0.3556	0.4299	0.5475	0.5854	0.6880
MIX-15-AC-04	0.1655	0.3957	0.5755	0.6403	0.7770	0.8633	1.0000	0.1565	0.2948	0.4442	0.5270	0.6502	0.6803	0.8094
YM-SEG-10	-	0.3381	0.4820	0.5612	0.7194	0.8705	1.0000	0.1936	0.2785	0.3813	0.4480	0.5909	0.6965	0.8072
DURABET PLUS AIR-AC-03	0.1181	0.2913	0.3543	0.4173	0.5906	0.8740	1.0000	0.1193	0.1743	0.2516	0.3099	0.4675	0.6231	0.7404
YM-SEG-10A	0.2331	-	0.4962	0.5789	0.7444	0.8797	1.0000	0.1824	0.2717	0.3779	0.4451	0.5825	0.6744	0.7724
YM-SEG-10E	-	0.3884	0.4793	0.5124	0.7273	0.8843	1.0000	0.2325	0.2719	0.3295	0.3744	0.5001	0.6254	0.7016
YM-DAP-AC-03	0.0504	0.2185	0.3613	0.4202	0.6303	0.8403	1.0000	0.0516	0.1331	0.2339	0.3007	0.4503	0.5696	0.6923
MIX-15-AC-03	0.0741	0.4167	0.5463	0.6574	0.8333	0.9537	1.0000	0.0840	0.2063	0.3419	0.4199	0.5456	0.5799	0.6285
MIX-30	0.0323	0.1183	0.2688	0.3441	0.6237	0.7849	1.0000	0.0113	0.0694	0.1441	0.1959	0.3209	0.4317	0.5382
MIX-30-03	0.1500	0.3900	0.4900	0.5500	0.7100	0.8800	1.0000	0.1149	0.1892	0.2756	0.3288	0.4320	0.4962	0.5827
MIX-30-BRT	0.0500	0.2357	0.3643	0.4500	0.6571	0.8643	1.0000	0.0622	0.1637	0.2886	0.3709	0.5522	0.6896	0.8146

Table 5.4 (continued): The compressive strength developments of the samples for the Model-1.

Model-1	Strength Development of Actual Data [Day/Day]							Strength Development of Predicted Data [Day/Day]						
Mixing Codes	**0.5/28**	**1/28**	**2/28**	**3/28**	**7/28**	**14/28**	**28/28**	**0.5/28**	**1/28**	**2/28**	**3/28**	**7/28**	**14/28**	**28/28**
MIX-30-07	0.0594	0.2475	0.3762	0.4554	0.6436	0.8713	1.0000	0.0533	0.1239	0.2112	0.2690	0.3978	0.4973	0.5881
MIX-34-BRT	0.0678	0.3136	0.4407	-	0.6271	0.8305	1.0000	0.0802	0.1766	0.2859	0.3511	0.4708	0.5435	0.6902
MIX-32-03	0.0845	0.3592	0.4648	0.5423	0.6690	0.8310	1.0000	0.1142	0.2371	0.3738	0.4533	0.5896	0.6592	0.8282
MIX-32-CEN	0.0548	0.2466	0.3836	0.4384	0.6575	0.8630	1.0000	0.0365	0.0885	0.1525	0.1947	0.2876	0.3583	0.4245
MIX-32-CEN-OK	0.0417	0.2583	0.4583	0.5250	0.6667	0.8417	1.0000	0.0500	0.1646	0.2931	0.3684	0.4994	0.5646	0.6998
B70-380	0.0300	0.0800	0.1700	0.2400	0.5000	0.7800	1.0000	0.0169	0.0465	0.0976	0.1426	0.2869	0.4541	0.5800
B70-420	0.0208	0.0729	0.1354	0.2188	0.4896	0.8542	1.0000	0.0171	0.0336	0.0756	0.1197	0.2797	0.4718	0.5580
B47-440	0.0207	0.1034	0.2276	0.3172	0.5724	0.8483	1.0000	0.0194	0.0871	0.1873	0.2659	0.4879	0.7104	0.8421
B67-440	0.0138	0.0759	0.1862	0.2759	0.4828	0.8276	1.0000	0.0178	0.0660	0.1470	0.2168	0.4358	0.6810	0.8439
B67-440-001	0.0090	0.1351	0.1982	0.2973	0.4865	0.8018	1.0000	0.0226	0.0654	0.1302	0.1824	0.3357	0.5035	0.6462
C45-B25-425	-	0.2261	0.4348	0.6435	0.8087	0.9043	1.0000	0.0033	0.1486	0.3099	0.4029	0.5538	0.5987	0.6687
B67-440-BEY	0.0161	0.1210	0.2500	0.3065	0.5726	0.7984	1.0000	0.0162	0.0811	0.1699	0.2353	0.4073	0.5751	0.7193
C45-B26-475	0.0654	0.5033	0.6471	0.6667	0.8301	0.8889	1.0000	0.1402	0.3358	0.5399	0.6469	0.7773	0.7590	0.8991
C45-B25-400	0.0132	0.3158	0.4539	0.5329	0.6316	0.7632	1.0000	0.0600	0.2180	0.3854	0.4760	0.6046	0.6436	0.8895
C50-B22-460	0.4259	0.6111	0.7222	0.7531	0.8333	0.9074	1.0000	0.4312	0.5401	0.6567	0.7207	0.8131	0.8330	0.9437
YM-SEG-11	-	0.3394	0.5046	0.5780	0.7523	0.9174	1.0000	0.1526	0.2220	0.3076	0.3640	0.4871	0.5748	0.6339

5.1.2 Logarithmic Regression (Model-2)

The logarithmic regression model (the Model-2) is one of the univariate regression analysis models depending on concrete age like in the Model-1. In this model, for 0.5-day, 1-day, 2-day, 3-day, 7-day, 14-day, and 28-day compressive strength forecasting were examined. At the end, the R^2 (btw 0.8772 & 0.9996), and R^2_{adj} results are very high; the SSE, and RMSE results are very low as much as in the Model-1. However, unlike the Model-1, the logarithmic equation character fits well to all the actual data sets. In this light of the results, the strength development of the compressive strength is enlisted in the Table 5.8**.** In the strength development, and the strength estimation calculations, there is no very big difference between the actual, and predicted data sets.

In the Figure 5.7, the correlations of the actual, and the predicted data sets are drawn. The correlation no doubtly pictures that the results of the Model-2 is numerically satisfying as much as the Model-1 computes. However, in contrast with the Model-1, the Model-2 could be safe to predict the compressive strength of the concrete because of no negative deflection effects in the data fitting planar except day-0.5. Because the strength results of the samples in C45-III-B20, MIX-30, B70-380, B70-420, B47-440, B67-440, B67-440-001, and B67-440-BEY mixing codes are below zero which is impossible for the strength development of the concrete.

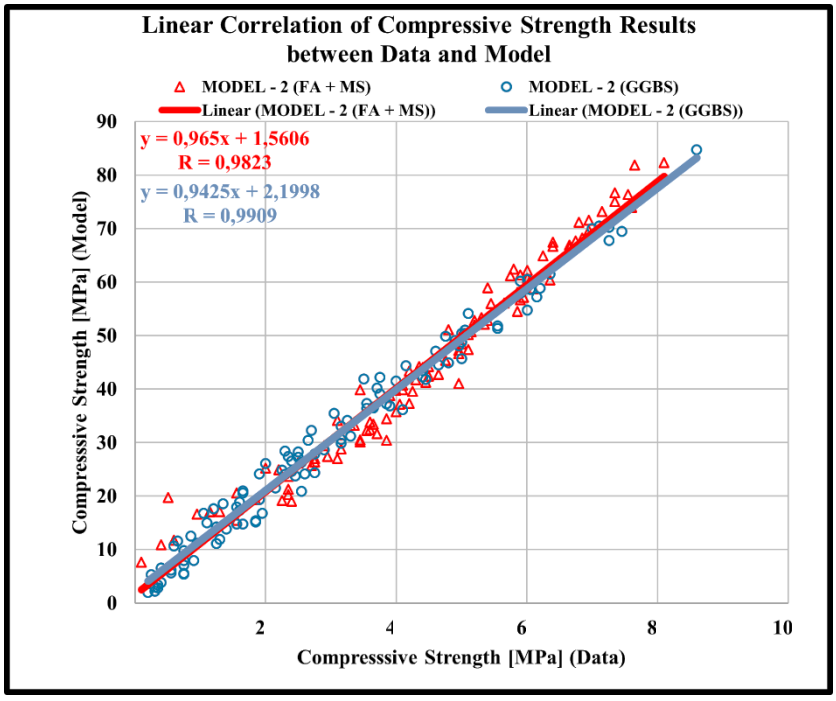

Figure 5.7: The correlations of the compressive strength of the Model-2.

In the Figure 5.8, for the samples including FA + MS substance, the Model-2 describes that [(W/C) - (W/B)] of the maximum R^2 result is greater than [(W/C) - (W/B)] of the minimum R^2 result. It is accounted for that the W/C ratio is more accurate than the W/B ratio for data prediction. Also, while [(CA/A) - (FA/A)] result gets higher, the R^2 result increases which means that the CA/A ratio impacts the data prediction with respect to the FA/A ratio. The figure also adds that the most powerful data prediction projection within the R^2 result answers to the sample in YM-SEG-10A mixing code like in the Model-1. And the weakest data prediction is for the sample in MIX-15-AC-03 mixing code. But this comparison could not be widened on all the specimens in the compressive strength estimations of the model because of the characters of the results.

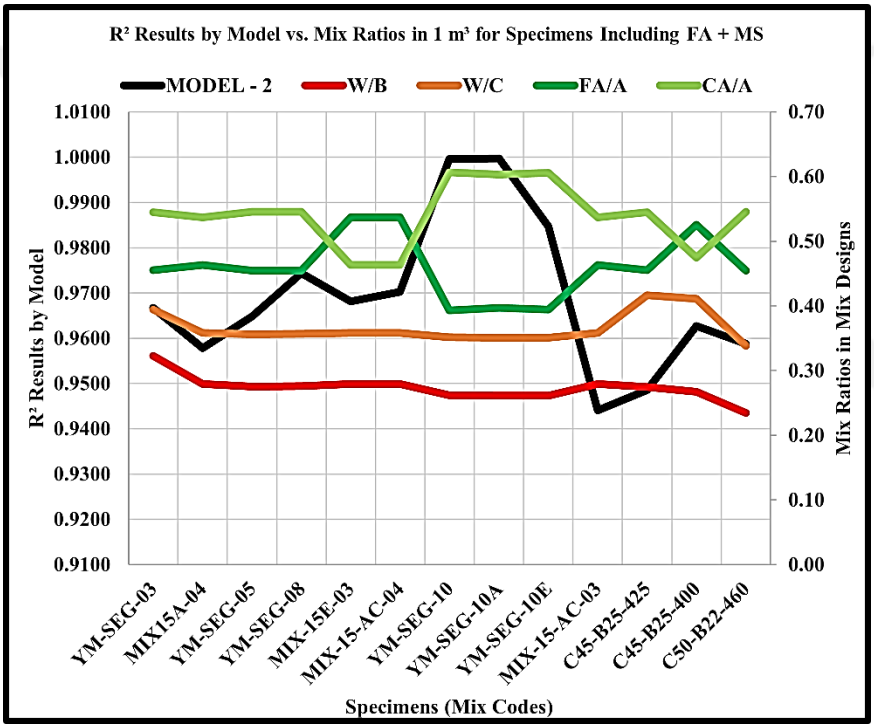

Figure 5.8: The correlations of the mixing ratios of the Model-2 in FA + MS.

In the Figure 5.9, for the samples including FA + MS content, the Model-2 also shows that [(CS) - (NS)] of the minimum R^2 is greater than [(CS) - (NS)] of the maximum R^2. And [(NO:1 Agg.) - (NO:2 Agg.)] of the minimum R^2 is greater than [(NO:1 Agg.) - (NO:2 Agg.)] of the maximum R^2 result. Additionally, for the maximum R^2, NO:1 Agg., and NO:2 Agg. are almost equal which means there are no respectable effects on the maximum R^2. Moreover, the gap between FA and MS decreases the R^2 result. Further, if the amounts of cement increase, the R^2 result increases as well. On the other hand, for the minimum R^2 value, the difference between NO:1 Agg. and NO:2 Agg. is higher with respect to the maximum R^2 cares. In addition to this, the maximum amount

of MS is 50.00 kg/m^3 for the highest-level R^2 result. At the same time, the minimum FA content is 30.00 kg/m^3, and the minimum water theme is 102.00 kg/m^3 for the lowest-level R^2 result. Nonetheless, this is a rare case in the results of the model. The higher amount of cement increases the potential of the data forecasting that which works for the use of cement is at the upper limit for the strength gaining. Thus, there is no evidence for the effects of admixture use in the compressive strength development. Finally, the highest and lowest R^2 values have an impact of CEMI 42.5 type of cement use. Because of that, the type of cement is not the topic of the comparison.

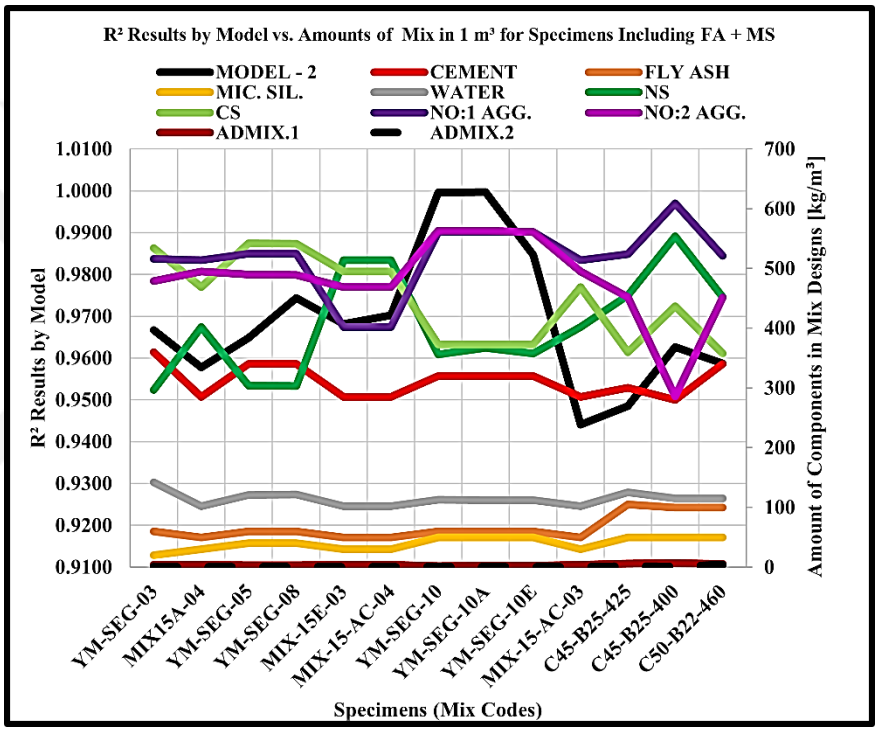

Figure 5.9: The correlations of the mixing amounts of the Model-2 in FA + MS.

In the Figure 5.10, for the samples including GGBS subsequent, the Model-2 estimates that [(W/C) – (W/B)] of the minimum R^2 is greater than [(W/C) – (W/B)] of the maximum R^2. Continuously, the maximum W/C ratio is found 1.11 for the minimum R^2 result, and there is no evidence of GGBS effects on the compressive strength estimation. And, while [(CA/A) - (FA/A)] result gets higher, the R^2 result decreases which means the CA/A ratio is more effective on the data prediction with respect to the FA/A ratio. The figure also ripostes that the FA/A ratio is almost equal to the CA/A ratio in maximum R^2 result.

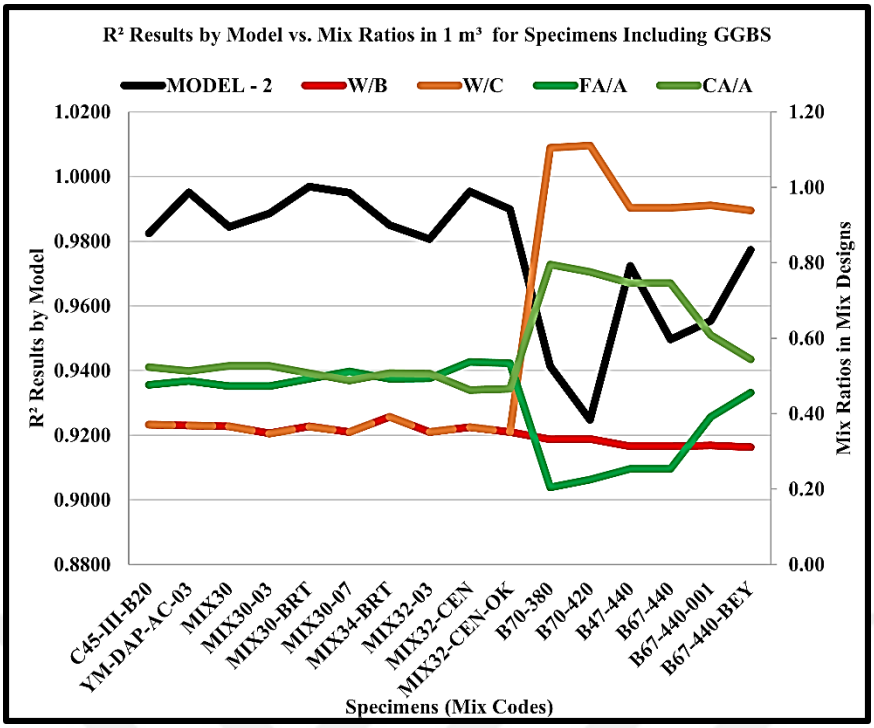

Figure 5.10: The correlations of the mixing ratios of the Model-2 in GGBS.

In the Figure 5.11, for the samples including GGBS content, the Model-2 also clarifies that [(NS) - (CS)] of the maximum R^2 result is less than [(NS) - (CS)] of the minimum R^2 result.

This result proves that the amounts of natural sand may be effective on the strength prediction. For some specimens, NO:0 Agg., NO:1 Agg., and NO:2 Agg. amounts dramatically increase the R^2 result. At the maximum R^2 value, the NO:0 Agg., NO:1 Agg., and NO:2 Agg. amounts are the highest. But, for the minimum R^2 result, the amount of crushed sand needs to be minimum. Moreover, the amount of water is the same for the maximum R^2. Also, there are again some specimens including the GGBS content for decreasing the strength prediction values of the concrete. Because GGBS was used as a combining material of the concrete matrix. In total, there is not a proof of admixture effects on the strength gaining. For the maximum R^2 result, the use of cement has positive impacts on the strength development. For the maximum R^2, NO:0 Agg. is 0.00 kg/m^3. NO:1 Agg. is 909.00 kg/m^3, and NO:2 Agg. is also 0.00 kg/m^3. At the minimum R^2, the GGBS subsequent is 294.00 kg/m^3. For the highest R^2 result, CEMIII 32.5 type cement; for the lowest R^2 result, CEMI 52.5N type cement are come out. Except these, there is not enough clue for the model computation in encountering purposes. As the remaining results are improper for any confrontation.

In the Model-2, for both contents, the results are shown in the boxplot which is in the Figure 5.12. It is for sure clear that FA + MS subsequent support the higher compressive strength prediction results than GGBS existence does. Except day-14, and day-28, for all ages, the specimen strengths including FA + MS are close and/or above the median strength values. Except day-14, and day-28, for all ages, the specimen strengths including GGBS theme are close and/or above the median strength values. And the strength estimations for the specimens including FA + MS are not that much coherent. To sum up, the whiskers of the specimens including GGBS content are reliable than the specimens including FA + MS substance. In the Table 5.5 and the Table 5.6, the numerical results of the boxplots are also shown. Also, in the Table 5.8, the model reveals the strength developments of the concrete samples.

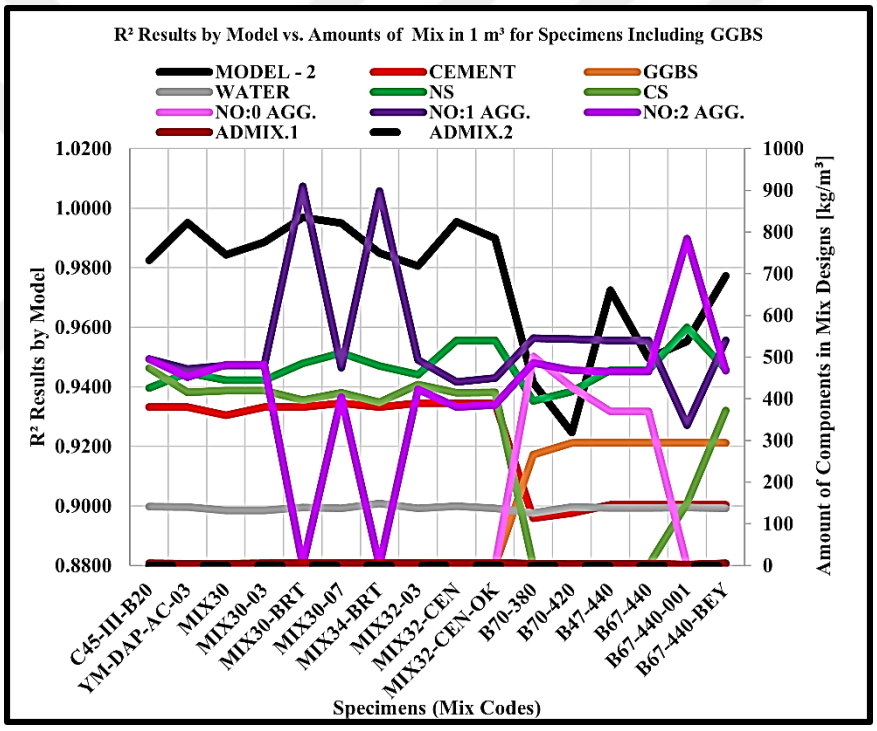

Figure 5.11: The correlations of the mixing amounts of the Model-2 in GGBS.

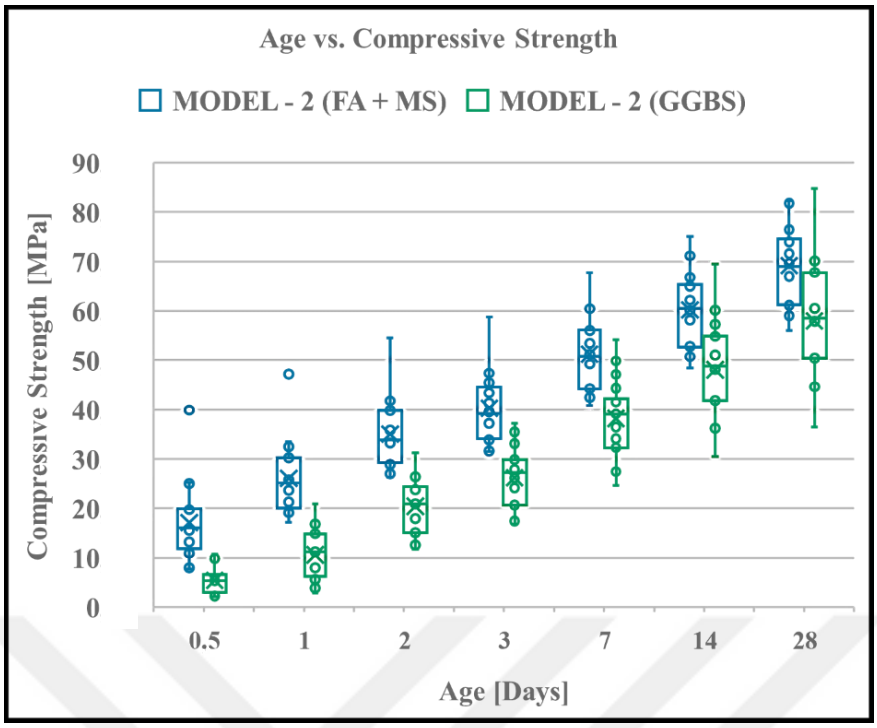

Figure 5.12: The age and the compressive strength relationship for the Model-2.

Table 5.5: The age dependent CS results in FA + MS content for the Model-2.

Model-2 [MPa]	0.5-Day	1-Day	2-Day	3-Day	7-Day	14-Day	28-Day
Minimum Value	7.68	17.11	26.27	31.44	40.77	48.39	56.01
1st-Quartile-Value	11.75	20.06	29.27	34.08	44.21	52.64	61.27
Median Value	16.10	25.09	33.85	39.18	50.82	60.44	68.95
3rd-Quartile-Value	19.95	30.27	39.84	44.55	56.20	65.30	74.55
Maximum Value	39.90	47.21	54.52	58.79	67.72	75.03	82.33
Mean Value	17.13	26.09	35.04	40.28	51.23	60.18	69.14
Range	32.22	30.10	28.24	27.34	26.95	26.64	26.32

Table 5.6: The age dependent CS results in GGBS content for the Model-2.

Model-2 [MPa]	0.5-Day	1-Day	2-Day	3-Day	7-Day	14-Day	28-Day
Minimum Value	2.07	2.89	11.63	16.75	24.62	30.54	36.47
1st-Quartile-Value	3.00	6.24	15.02	20.60	32.28	41.83	50.41
Median Value	5.36	11.17	20.94	27.28	39.13	48.83	58.53
3rd-Quartile-Value	6.57	14.86	24.36	29.91	42.21	54.84	67.77
Maximum Value	10.63	20.93	31.23	37.26	54.16	69.45	84.74
Mean Value	5.40	10.56	20.41	26.17	38.21	48.06	57.91
Range	8.56	18.04	19.60	20.50	29.53	38.90	48.27

Table 5.7: The results of the regression Model-2.

Model-2					
Mixing Codes	**Logarithmic Regression**	**R^2**	**R^2_{adj}**	**SSE**	**RMSE**
C45-III-B20	$f'_c = 11.23 + 22.06ln(t)$	0.9825	0.9790	107.820	4.644
YM-SEG-03	$f'_c = 33.51 + 11.91ln(t)$	0.9667	0.9600	60.711	3.485
YM-SEG-03-FSTC	$f'_c = 32.44 + 10.75ln(t)$	0.9834	0.9800	24.239	2.202
MIX-15A-04	$f'_c = 25.78 + 12.52ln(t)$	0.9578	0.9472	70.977	4.212
YM-SEG-05	$f'_c = 27 + 14.92ln(t)$	0.9648	0.9578	100.749	4.489
YM-SEG-08	$f'_c = 30.22 + 13.86ln(t)$	0.9744	0.9693	62.684	3.541
MIX-15E-03	$f'_c = 20.29 + 12.31ln(t)$	0.9681	0.9618	61.907	3.519
MIX-15-AC-04	$f'_c = 26.4 + 13.56ln(t)$	0.9702	0.9643	69.971	3.741
YM-SEG-10	$f'_c = 23.68 + 13.79ln(t)$	0.9996	0.9995	0.594	0.385
DURABET PLUS AIR-AC-03	$f'_c = 15.18 + 13.89ln(t)$	0.9695	0.9634	75.401	3.883
YM-SEG-10A	$f'_c = 24.39 + 12.77ln(t)$	0.9997	0.9996	0.497	0.353
YM-SEG-10E	$f'_c = 21.29 + 11.72ln(t)$	0.9847	0.9808	16.750	2.046
YM-DAP-AC-03	$f'_c = 11.91 + 13.99ln(t)$	0.9951	0.9941	11.997	1.549
MIX-15-AC-03	$f'_c = 19.17 + 11.96ln(t)$	0.9441	0.9329	105.122	4.585
MIX-30	$f'_c = 6.238 + 11.52ln(t)$	0.9844	0.9813	26.087	2.284
MIX-30-03	$f'_c = 16.79 + 10.09ln(t)$	0.9886	0.9863	14.632	1.711
MIX-30-BRT	$f'_c = 14.86 + 16.58ln(t)$	0.9969	0.9962	10.739	1.466

Table 5.7 (continued): The results of the regression Model-2.

Model-2					
Mixing Codes	**Logarithmic Regression**	**R^2**	**R^2_{adj}**	**SSE**	**RMSE**
MIX-30-07	$f'_c = 11.17 + 11.79ln(t)$	0.9950	0.9940	8.691	1.318
MIX-34-BRT	$f'_c = 15.41 + 12.76ln(t)$	0.9849	0.9834	30.827	2.776
MIX-32-03	$f'_c = 20.93 + 14.86ln(t)$	0.9806	0.9768	54.127	3.290
MIX-32-CEN	$f'_c = 7.994 + 8.545ln(t)$	0.9954	0.9944	4.233	0.920
MIX32-CEN-OK	$f'_c = 14.86 + 13.7ln(t)$	0.9899	0.9878	23.854	2.184
B70-380	$f'_c = 3.821 + 12.56ln(t)$	0.9413	0.9296	122.083	4.941
B70-420	$f'_c = 2.887 + 12.62ln(t)$	0.9247	0.9097	160.930	5.673
B47-440	$f'_c = 7.994 + 18.68ln(t)$	0.9724	0.9669	122.963	4.959
B67-440	$f'_c = 5.626 + 18.65ln(t)$	0.9497	0.9396	228.641	6.762
B67-440-001	$f'_c = 5.465 + 13.78ln(t)$	0.9554	0.9464	110.101	4.693
C45-B25-425	$f'_c = 17.11 + 13.22ln(t)$	0.9486	0.9357	74.152	4.306
B67-440-BEY	$f'_c = 7.163 + 15.51ln(t)$	0.9773	0.9728	69.379	3.725
C45-B26-475	$f'_c = 30.42 + 15.43ln(t)$	0.8772	0.8527	413.240	9.091
C45-B25-400	$f'_c = 19.09 + 16.46ln(t)$	0.9627	0.9552	130.310	5.105
C50-B22-460	$f'_c = 47.21 + 10.54ln(t)$	0.9587	0.9505	59.359	3.446
YM-SEG-11	$f'_c = 19.36 + 11ln(t)$	0.9938	0.9922	5.950	1.220

Table 5.8: The compressive strength developments of samples for the Model-2.

Model-2	Strength Development of Actual Data [Day/Day]							Strength Development of Predicted Data [Day/Day]						
Mixing Codes	**0.5/28**	**1/28**	**2/28**	**3/28**	**7/28**	**14/28**	**28/28**	**0.5/28**	**1/28**	**2/28**	**3/28**	**7/28**	**14/28**	**28/28**
C45-III-B20	0.0233	0.1105	0.2791	0.3547	0.5930	0.8663	1.0000	-0.0479	0.1325	0.3130	0.4185	0.6391	0.8196	1.0000
YM-SEG-03	0.2797	0.5105	0.6014	0.6923	0.8252	0.8741	1.0000	0.3450	0.4578	0.5706	0.6366	0.7744	0.8872	1.0000
YM-SEG-03-FSTC	0.3212	0.5255	0.5985	0.6350	0.7737	0.8759	1.0000	0.3661	0.4752	0.5844	0.6482	0.7817	0.8908	1.0000
MIX-15A-04	0.1797	0.4219	0.6016	0.6641	0.7969	-	1.0000	0.2534	0.3819	0.5105	0.5857	0.7429	0.8714	1.0000
YM-SEG-05	0.1293	0.4218	0.5714	0.5714	0.7687	0.9048	1.0000	0.2171	0.3519	0.4868	0.5656	0.7304	0.8652	1.0000
YM-SEG-08	0.2053	0.4570	0.5298	0.6291	0.7881	0.8477	1.0000	0.2698	0.3955	0.5213	0.5948	0.7485	0.8743	1.0000
MIX-15E-03	0.1017	0.3983	0.5339	0.6102	0.7627	0.8814	1.0000	0.1918	0.3309	0.4701	0.5515	0.7217	0.8608	1.0000
MIX-15-AC-04	0.1655	0.3957	0.5755	0.6403	0.7770	0.8633	1.0000	0.2375	0.3688	0.5001	0.5769	0.7374	0.8687	1.0000
YM-SEG-10	-	0.3381	0.4820	0.5612	0.7194	0.8705	1.0000	0.2028	0.3401	0.4774	0.5577	0.7255	0.8627	1.0000
DURABET PLUS AIR-AC-03	0.1181	0.2913	0.3543	0.4173	0.5906	0.8740	1.0000	0.0903	0.2470	0.4036	0.4952	0.6867	0.8434	1.0000
YM-SEG-10A	0.2331	-	0.4962	0.5789	0.7444	0.8797	1.0000	0.2321	0.3643	0.4966	0.5739	0.7355	0.8678	1.0000
YM-SEG-10E	-	0.3884	0.4793	0.5124	0.7273	0.8843	1.0000	0.2182	0.3528	0.4874	0.5662	0.7308	0.8654	1.0000
YM-DAP-AC-03	0.0504	0.2185	0.3613	0.4202	0.6303	0.8403	1.0000	0.0378	0.2035	0.3692	0.4661	0.6686	0.8343	1.0000
MIX-15-AC-03	0.0741	0.4167	0.5463	0.6574	0.8333	0.9537	1.0000	0.1843	0.3248	0.4652	0.5474	0.7191	0.8595	1.0000
MIX-30	0.0323	0.1183	0.2688	0.3441	0.6237	0.7849	1.0000	-0.0391	0.1398	0.3187	0.4234	0.6421	0.8211	1.0000
MIX-30-03	0.1500	0.3900	0.4900	0.5500	0.7100	0.8800	1.0000	0.1943	0.3331	0.4718	0.5529	0.7225	0.8613	1.0000
MIX-30-BRT	0.0500	0.2357	0.3643	0.4500	0.6571	0.8643	1.0000	0.0480	0.2120	0.3759	0.4718	0.6722	0.8361	1.0000

Table 5.8 (continued): The compressive strength developments of samples for the Model-2.

Model-2	Strength Development of Actual Data [Day/Day]							Strength Development of Predicted Data [Day/Day]						
Mixing Codes	**0.5/28**	**1/28**	**2/28**	**3/28**	**7/28**	**14/28**	**28/28**	**0.5/28**	**1/28**	**2/28**	**3/28**	**7/28**	**14/28**	**28/28**
MIX-30-07	0.0594	0.2475	0.3762	0.4554	0.6436	0.8713	1.0000	0.0594	0.2214	0.3833	0.4781	0.6761	0.8380	1.0000
MIX-34-BRT	0.0678	0.3136	0.4407	-	0.6271	0.8305	1.0000	0.1133	0.2660	0.4187	0.5080	0.6946	0.8473	1.0000
MIX-32-03	0.0845	0.3592	0.4648	0.5423	0.6690	0.8310	1.0000	0.1509	0.2971	0.4433	0.5288	0.7076	0.8538	1.0000
MIX-32-CEN	0.0548	0.2466	0.3836	0.4384	0.6575	0.8630	1.0000	0.0568	0.2192	0.3816	0.4766	0.6752	0.8376	1.0000
MIX-32-CEN-OK	0.0417	0.2583	0.4583	0.5250	0.6667	0.8417	1.0000	0.0886	0.2456	0.4025	0.4943	0.6861	0.8431	1.0000
B70-380	0.0300	0.0800	0.1700	0.2400	0.5000	0.7800	1.0000	-0.1070	0.0837	0.2743	0.3858	0.6188	0.8094	1.0000
B70-420	0.0208	0.0729	0.1354	0.2188	0.4896	0.8542	1.0000	-0.1304	0.0642	0.2589	0.3728	0.6107	0.8053	1.0000
B47-440	0.0207	0.1034	0.2276	0.3172	0.5724	0.8483	1.0000	-0.0705	0.1138	0.2982	0.4060	0.6313	0.8157	1.0000
B67-440	0.0138	0.0759	0.1862	0.2759	0.4828	0.8276	1.0000	-0.1077	0.0830	0.2738	0.3853	0.6185	0.8093	1.0000
B67-440-001	0.0090	0.1351	0.1982	0.2973	0.4865	0.8018	1.0000	-0.0795	0.1064	0.2922	0.4010	0.6282	0.8141	1.0000
C45-B25-425	-	0.2261	0.4348	0.6435	0.8087	0.9043	1.0000	0.1299	0.2798	0.4296	0.5172	0.7004	0.8502	1.0000
B67-440-BEY	0.0161	0.1210	0.2500	0.3065	0.5726	0.7984	1.0000	-0.0610	0.1217	0.3044	0.4113	0.6346	0.8173	1.0000
C45-B26-475	0.0654	0.5033	0.6471	0.6667	0.8301	0.8889	1.0000	0.2410	0.3717	0.5024	0.5789	0.7386	0.8693	1.0000
C45-B25-400	0.0132	0.3158	0.4539	0.5329	0.6316	0.7632	1.0000	0.1039	0.2582	0.4125	0.5028	0.6914	0.8457	1.0000
C50-B22-460	0.4259	0.6111	0.7222	0.7531	0.8333	0.9074	1.0000	0.4847	0.5734	0.6622	0.7141	0.8225	0.9113	1.0000
YM-SEG-11	-	0.3394	0.5046	0.5780	0.7523	0.9174	1.0000	0.2095	0.3456	0.4817	0.5614	0.7278	0.8639	1.0000

5.1.3 Power Regression (Model-3)

The power regression model (the Model-3) is one of the other univariate regression analysis models depending on concrete age like in the Model-1 and Model-2. In this model, for 0.5-day, 1-day, 2-day, 3-day, 7-day, 14-day, and 28-day compressive strength predictions were studied. At the end, the R^2 (btw 0.7700 & 0.9850), and R^2_{adj} results are high; the SSE, and RMSE results are very low as much as in the Model-1 and in Model-2. However, in the Model-3, the R^2 and R^2_{adj} results are notionally less than the first two models. And the SSE and RMSE results are also higher than the first two models' results. This simple comparison says that in the Model-3, the estimation of the compressive strength has more errors from the actual data sets on the fitting planar. In this way of thinking, the strength development of the compressive strength is ranged in the Table 5.12.

In the Figure 5.13, the correlations of the actual data sets and predicted data sets are executed. The correlation no doubtly describes that the results of the Model-3 are less satisfying than the Model-1 and Model-2 set forth. In contrast with the Model-1, the Model-3 seems safe to presume the compressive strength of the concrete because of no deflection effects in the data fittings.

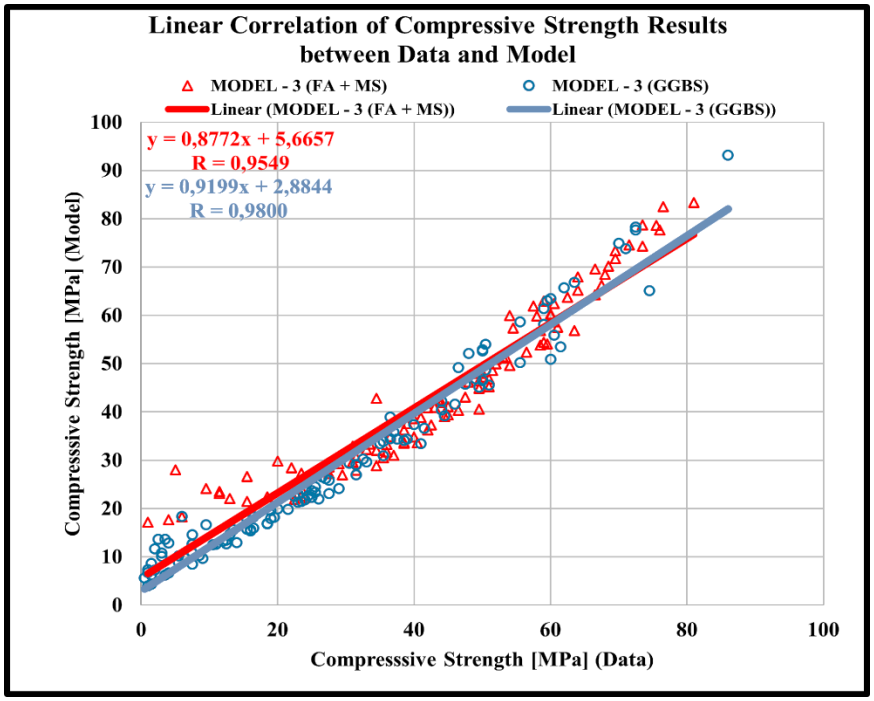

Figure 5.13: The correlations of the compressive strength of the Model-3.

In the Figure 5.14, for the samples that have FA + MS substance, the Model-3 accounts that [(W/C) - (W/B)] of the maximum R^2 result is equal to [(W/C) - (W/B)] of the minimum R^2 result. Besides, while [(CA/A) - (FA/A)] result gets higher, the R^2 result also comes close to 1.00 which means that the CA/A ratio impacts the data prediction with respect to the FA/A ratio. In this manner, the CA/A ratio is 0.61, and the FA/A ratio is 0.39 for the maximum R^2 value. But this comparison could not be accurate for all the specimens in the compressive strength estimations of the model because of the biases of the prediction results. For instance, it is not followed that when the R^2 result increases, the W/C and W/B ratios go in a straight line, or the FA/A and CA/A ratios decrease. That is why a direct relationship cannot be conducted except the ones which have the minimum and maximum R^2 values like what happens in the previous models.

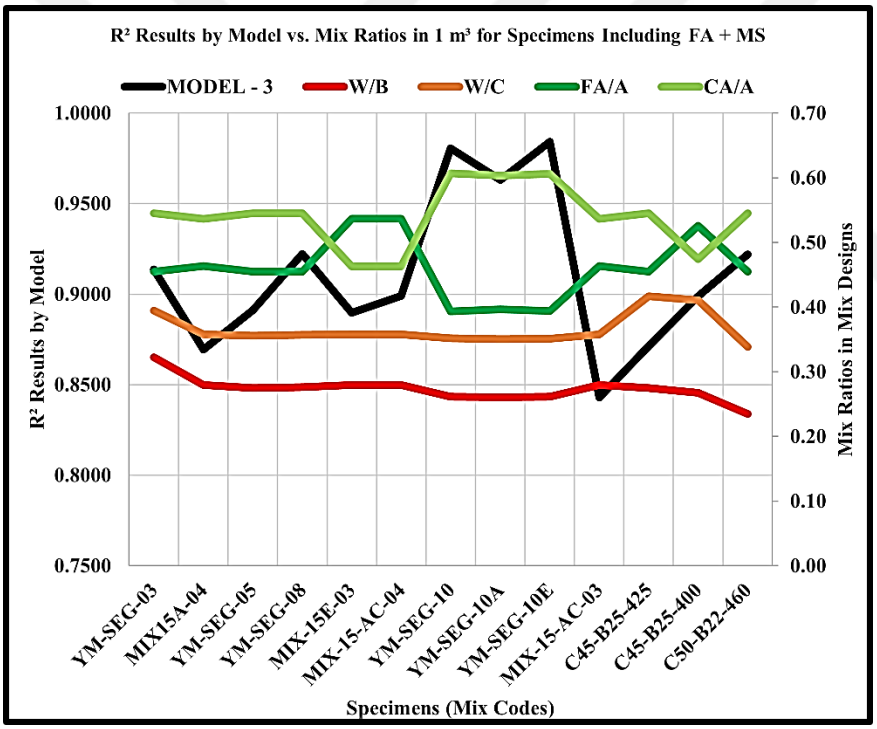

Figure 5.14: The correlations of the mixing ratios of the Model-3 in FA + MS.

In the Figure 5.15, for the samples including FA + MS content, the Model-3 predicts that [(CS) - (NS)] of the minimum R^2 is greater than [(CS) - (NS)] of the maximum R^2. And the amount of NO:1 Agg., and NO:2 Agg. are almost equal for the maximum R^2 which means there is no major effects on the maximum R^2. Also [(NO:1 Agg.) - (NO:2 Agg.)] of the minimum R^2 is greater than [(NO:1 Agg.) - (NO:2 Agg.)] of the maximum R^2 result. Moreover, the gap between FA and MS decreases the R^2 result like in the Model-2. Further, if the amounts of cement increase, the R^2 result increases

as well in this model. In addition to this, the maximum amount of MS is 50.00 kg/m^3 for the highest-level R^2 result. In contrast with the maximized amount of MS, the minimum FA ingredient is 30.00 kg/m^3, and the minimum water existence is 102.00 kg/m^3 for the lowest-level R^2 result likewise in the Model-2. Nonetheless, this is an infrequent situation in the results of the model. There is no confirmation for the effects of admixture use in the compressive strength development. At the end, the highest and the lowest R^2 results have an impact of CEMI 42.5 type of cement use. Because of the identical type of cement use, the cement effect is out of the comparison.

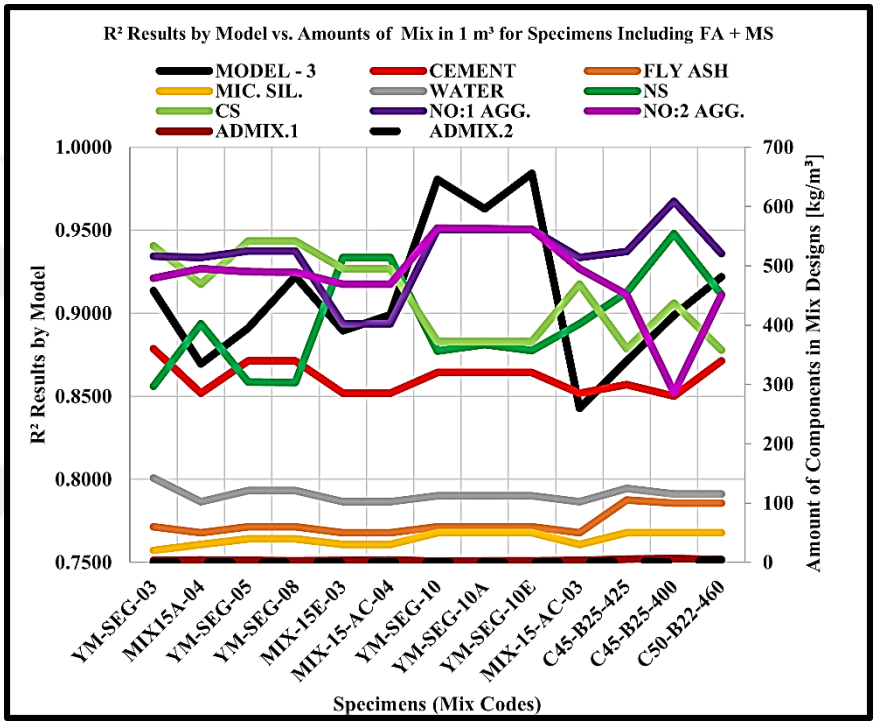

Figure 5.15: The correlations of the mixing amounts of the Model-3 in FA + MS.

In the Figure 5.16, for the samples including GGBS substance, the Model-3 forecasts that [(W/C) – (W/B)] of the minimum R^2 is less than [(W/C) – (W/B)] of the maximum R^2. Onto this, the W/C ratio is equal to the W/B ratio for only the minimum R^2 result. Because the GGBS substance could not be accepted as an influencer on the compressive strength development, even though it is a binding material. Moreover, while [(CA/A) - (FA/A)] result gets higher, the R^2 result decreases which means the CA/A ratio is more operative on the data prediction with respect to the FA/A ratio. The figure also points that the FA/A ratio is 0.80 for the maximum R^2 result, and the CA/A ratio is 0.20 for the maximum R^2 result.

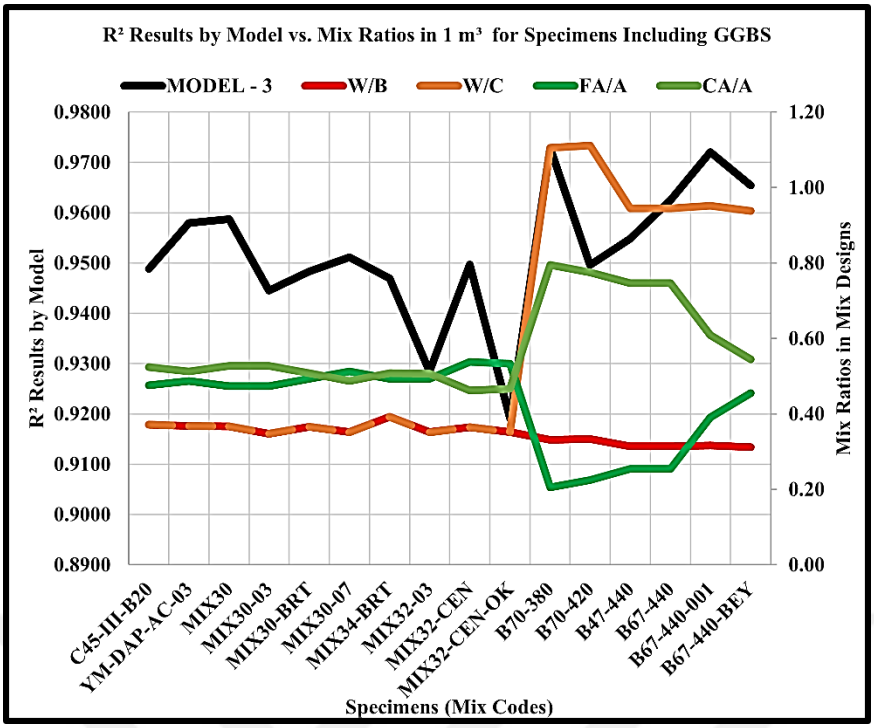

Figure 5.16: The correlations of the mixing ratios of the Model-3 in GGBS.

In the Figure 5.17, for the samples that have GGBS content, the Model-3 clearly estimates that [(NS) - (CS)] of the maximum R^2 result is greater than [(NS) - (CS)] of the minimum R^2 value. This result proves that the amounts of natural sand may be penetrating on the strength estimation. At the maximum R^2 value, NO:0 Agg., NO:1 Agg., and NO:2 Agg. amounts are the nearest.

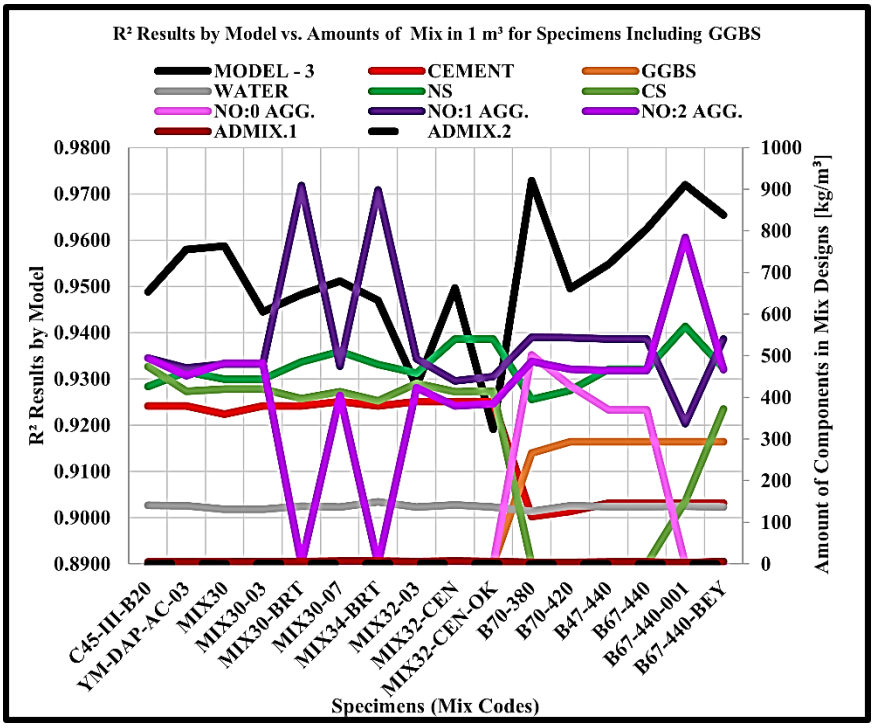

Figure 5.17: The correlations of the mixing amounts of the Model-3 in GGBS.

On the other hand, for some specimen R^2 values, NO:0 Agg., NO:1 Agg., and NO:2 Agg. amounts get much more. Yet, for the minimum R^2 result, the crushed sand needs to be minimum (0.00 kg/m^3). Besides, the amount of water for the maximum R^2 result is greater than for the minimum R^2 result. This case is the same for the cement contents. Additionally, there are anew some specimens including the GGBS content in decrease of the strength prediction values of the concrete. Again, there is not a demonstration of the admixture effects on the strength development like in the previous models. For the maximum R^2, NS is also 0.00 kg/m^3, cement is 114.00 kg/m^3. NO:0 Agg. is maximized as 486.00 kg/m^3 for the maximum R^2 value. At the maximum R^2 result, the GGBS content is measured 266.00 kg/m^3. For the lowest R^2 result (MIX-32-CEN-OK), CEMIII 32.5 type cement, and for the highest R^2 result (B370-80), CEMI 52.5N type cement are put forth. Except these, there is not enough indicator for the model computation to class with. Inasmuch as the other results are indecent to set against. For the Model-3, for both subsequent, the results are shown in the boxplot which is in the Figure 5.18.

In the Table 5.9 and Table 5.10, the numerical results of the tests are shared with both FA + MS and GGBS contents. In the Figure 5.18, it is expressly clear that FA + MS ingredient support the higher compressive strength prediction results than GGBS ingredient exposes.

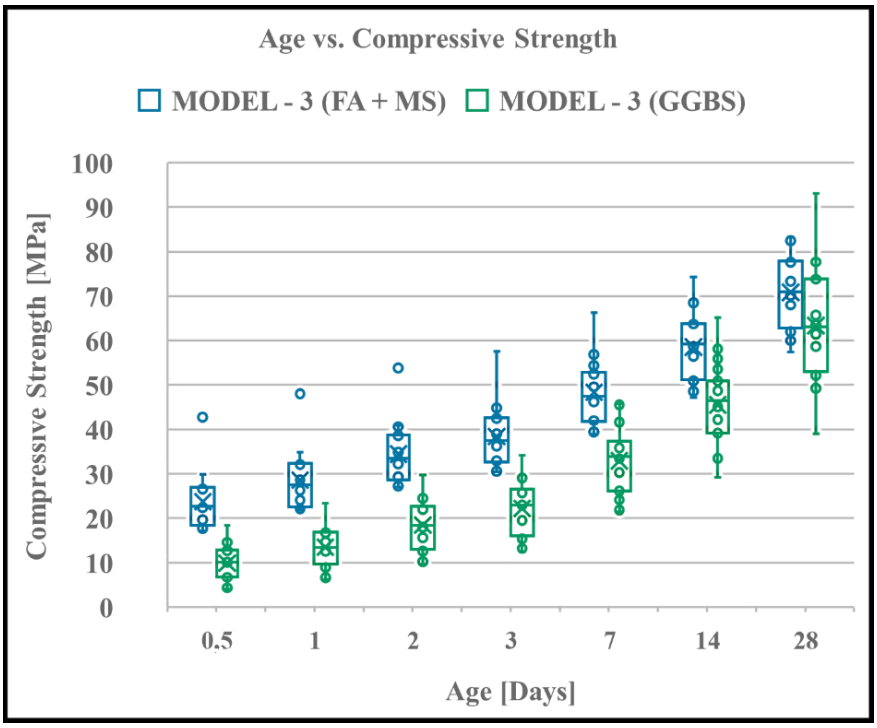

Figure 5.18: The age and the compressive strength relationship for the Model-3.

Table 5.9: The age dependent CS results in FA + MS content for the Model-3.

Model-3 [MPa]	0.5-Day	1-Day	2-Day	3-Day	7-Day	14-Day	28-Day
Minimum Value	17.16	21.84	26.94	30.47	38.81	47.19	57.39
1st-Quartile-Value	18.38	22.54	28.63	32.59	41.74	51.11	62.84
Median Value	22.69	27.54	33.41	37.42	47.41	59.26	70.93
3rd-Quartile-Value	26.92	32.33	38.66	42.64	52.82	63.83	77.87
Maximum Value	42.78	47.98	53.82	57.55	66.22	74.28	83.31
Mean Value	23.69	28.53	34.40	38.40	48.37	58.49	70.80
Range	25.62	26.14	26.87	27.09	27.41	27.08	25.92

Table 5.10: The age dependent CS results in GGBS content for the Model-3.

Model-3 [MPa]	0.5-Day	1-Day	2-Day	3-Day	7-Day	14-Day	28-Day
Minimum Value	3.96	6.17	9.62	12.47	21.45	29.16	38.96
1st-Quartile-Value	6.69	9.67	12.92	15.96	26.15	39.15	52.91
Median Value	10.07	13.44	18.39	22.97	33.83	46.53	63.05
3rd-Quartile-Value	12.83	16.88	22.69	26.57	37.34	50.92	73.81
Maximum Value	18.37	23.34	29.66	34.12	45.72	65.12	93.13
Mean Value	9.89	13.49	18.45	22.21	32.88	45.53	63.33
Range	14.41	17.17	20.03	21.64	24.26	35.96	54.17

Except day-14, for all ages, the strengths of the specimens including FA + MS are close and/or above the median strength values. Except day-0.5, and day-28, for all ages, the specimen strengths including GGBS substance are close and/or above the median strength values. It is described that the strength predictions for the specimens including FA + MS theme are not consistent. Hence, the whiskers of the specimens including GGBS ingredient are more reasonable than the specimens including FA + MS content. In the Table 5.12, the strength developments by the regression model for the concrete specimens are exposed.

5.2 Univariate Regression Analysis for Splitting Tensile Strength

In this section of the thesis, the Table 5.15, the Table 5.19, and the Table 5.23 publish the regression models with their statistical results in the study.

5.2.1 Power Regression (Model-1)

The power regression model (the Model-1) is one of the other univariate regression analysis models depending on compressive strength of concrete. In this model, for 0.5-day, 1-day, 2-day, 3-day, 7-day, 14-day, and 28-day splitting tensile strength predictions were exposed. At the end, R^2 (btw 0.8345 & 0.9977), and R^2_{adj} results are very high; SSE, and RMSE results are very low. This basic comparison shows that presuming of the splitting tensile strength has less errors from the actual data sets on

Table 5.11: The results of the regression Model-3.

Model-3					
Mixing Codes	**Power Regression**	**R^2**	**R^2_{adj}**	**SSE**	**RMSE**
C45-III-B20	$f'_c = 16.67t^{0.5163}$	0.9488	0.9385	314.795	7.935
YM-SEG-03	$f'_c = 34.9t^{0.228}$	0.9137	0.8965	157.208	5.607
YM-SEG-03-FSTC	$f'_c = 33.22t^{0.2243}$	0.9587	0.9504	60.230	3.471
MIX-15A-04	$f'_c = 27.79t^{0.2684}$	0.8694	0.8368	219.615	7.410
YM-SEG-05	$f'_c = 29.59t^{0.2936}$	0.8911	0.8693	311.743	7.896
YM-SEG-08	$f'_c = 32.03t^{0.2694}$	0.9221	0.9066	190.575	6.174
MIX-15E-03	$f'_c = 22.58t^{0.3078}$	0.8896	0.8676	214.365	6.548
MIX-15-AC-04	$f'_c = 28.62t^{0.2824}$	0.8991	0.8789	237.253	6.888
YM-SEG-10	$f'_c = 27.28t^{0.2901}$	0.9806	0.9757	28.940	2.690
DURABET PLUS AIR-AC-03	$f'_c = 16.88t^{0.4128}$	0.9722	0.9666	68.714	3.707
YM-SEG-10A	$f'_c = 26.28t^{0.2923}$	0.9630	0.9537	63.255	3.977
YM-SEG-10E	$f'_c = 24t^{0.287}$	0.9842	0.9802	17.284	2.079
YM-DAP-AC-03	$f'_c = 14.63t^{0.4384}$	0.9580	0.9495	102.655	4.531
MIX-15-AC-03	$f'_c = 21.84t^{0.303}$	0.8428	0.8114	295.416	7.687
MIX-30	$f'_c = 8.886t^{0.5135}$	0.9587	0.9505	69.014	3.715
MIX-30-03	$f'_c = 18.19t^{0.3188}$	0.9445	0.9334	70.964	3.767
MIX-30-BRT	$f'_c = 18.24t^{0.4241}$	0.9483	0.9379	177.006	5.950

Table 5.11 (continued): The results of the regression Model-3.

Model-3					
Mixing Codes	**Power Regression**	**R^2**	**R^2_{adj}**	**SSE**	**RMSE**
MIX-30-07	$f'_c = 13.44t^{0.4171}$	0.9511	0.9413	84.815	4.119
MIX-34-BRT	$f'_c = 16.8t^{0.3888}$	0.9469	0.9334	108.496	5.208
MIX-32-03	$f'_c = 23.34t^{0.3455}$	0.9285	0.9142	199.965	6.324
MIX-32-CEN	$f'_c = 9.667t^{0.4183}$	0.9497	0.9396	45.812	3.027
MIX32-CEN-OK	$f'_c = 17.73t^{0.3828}$	0.9192	0.9030	190.087	6.166
B70-380	$f'_c = 6.67t^{0.6215}$	0.9729	0.9675	56.429	3.359
B70-420	$f'_c = 6.173t^{0.6402}$	0.9496	0.9395	107.836	4.644
B47-440	$f'_c = 12.57t^{0.5488}$	0.9548	0.9458	201.098	6.342
B67-440	$f'_c = 10.21t^{0.6089}$	0.9625	0.9550	170.549	5.840
B67-440-001	$f'_c = 8.419t^{0.5824}$	0.9720	0.9664	69.036	3.716
C45-B25-425	$f'_c = 22.05^{t0.31}$	0.8713	0.8391	185.646	6.813
B67-440-BEY	$f'_c = 10.74t^{0.5437}$	0.9655	0.9586	105.516	4.594
C45-B26-475	$f'_c = 33.68t^{0.2687}$	0.7792	0.7350	743.397	12.193
C45-B25-400	$f'_c = 22.25t^{0.375}$	0.8988	0.8786	353.187	8.405
C50-B22-460	$f'_c = 47.98t^{0.1656}$	0.9220	0.9064	112.220	4.738
YM-SEG-11	$f'_c = 22.41t^{0.2822}$	0.9609	0.9512	37.270	3.052

Table 5.12: The compressive strength developments of samples for the Model-3.

Model-3	Strength Development of Actual Data [Day/Day]							Strength Development of Predicted Data [Day/Day]						
Mixing Codes	**0.5/28**	**1/28**	**2/28**	**3/28**	**7/28**	**14/28**	**28/28**	**0.5/28**	**1/28**	**2/28**	**3/28**	**7/28**	**14/28**	**28/28**
C45-III-B20	0.0233	0.1105	0.2791	0.3547	0.5930	0.8663	1.0000	0.1251	0.1790	0.2560	0.3156	0.4888	0.6992	1.0000
YM-SEG-03	0.2797	0.5105	0.6014	0.6923	0.8252	0.8741	1.0000	0.3994	0.4678	0.5479	0.6009	0.7290	0.8538	1.0000
YM-SEG-03-FSTC	0.3212	0.5255	0.5985	0.6350	0.7737	0.8759	1.0000	0.4054	0.4736	0.5533	0.6059	0.7328	0.8560	1.0000
MIX-15A-04	0.1797	0.4219	0.6016	0.6641	0.7969	-	1.0000	0.3395	0.4089	0.4925	0.5491	0.6893	0.8302	1.0000
YM-SEG-05	0.1293	0.4218	0.5714	0.5714	0.7687	0.9048	1.0000	0.3067	0.3759	0.4608	0.5190	0.6656	0.8159	1.0000
YM-SEG-08	0.2053	0.4570	0.5298	0.6291	0.7881	0.8477	1.0000	0.3381	0.4075	0.4912	0.5479	0.6883	0.8297	1.0000
MIX-15E-03	0.1017	0.3983	0.5339	0.6102	0.7627	0.8814	1.0000	0.2897	0.3586	0.4438	0.5028	0.6527	0.8079	1.0000
MIX-15-AC-04	0.1655	0.3957	0.5755	0.6403	0.7770	0.8633	1.0000	0.3209	0.3902	0.4746	0.5322	0.6760	0.8222	1.0000
YM-SEG-10	-	0.3381	0.4820	0.5612	0.7194	0.8705	1.0000	0.3111	0.3803	0.4651	0.5231	0.6689	0.8178	1.0000
DURABET PLUS AIR-AC-03	0.1181	0.2913	0.3543	0.4173	0.5906	0.8740	1.0000	0.1898	0.2527	0.3364	0.3977	0.5642	0.7512	1.0000
YM-SEG-10A	0.2331	-	0.4962	0.5789	0.7444	0.8797	1.0000	0.3083	0.3776	0.4624	0.5205	0.6668	0.8166	1.0000
YM-SEG-10E	-	0.3884	0.4793	0.5124	0.7273	0.8843	1.0000	0.3150	0.3843	0.4689	0.5267	0.6718	0.8196	1.0000
YM-DAP-AC-03	0.0504	0.2185	0.3613	0.4202	0.6303	0.8403	1.0000	0.1712	0.2320	0.3144	0.3756	0.5446	0.7380	1.0000
MIX-15-AC-03	0.0741	0.4167	0.5463	0.6574	0.8333	0.9537	1.0000	0.2953	0.3643	0.4495	0.5083	0.6570	0.8106	1.0000
MIX-30	0.0323	0.1183	0.2688	0.3441	0.6237	0.7849	1.0000	0.1266	0.1807	0.2579	0.3176	0.4907	0.7005	1.0000
MIX-30-03	0.1500	0.3900	0.4900	0.5500	0.7100	0.8800	1.0000	0.2771	0.3457	0.4311	0.4906	0.6428	0.8017	1.0000
MIX-30-BRT	0.0500	0.2357	0.3643	0.4500	0.6571	0.8643	1.0000	0.1814	0.2434	0.3265	0.3878	0.5555	0.7453	1.0000

Table 5.12 (continued): The compressive strength developments of samples for the Model-3.

Model-3	Strength Development of Actual Data [Day/Day]							Strength Development of Predicted Data [Day/Day]						
Mixing Codes	**0.5/28**	**1/28**	**2/28**	**3/28**	**7/28**	**14/28**	**28/28**	**0.5/28**	**1/28**	**2/28**	**3/28**	**7/28**	**14/28**	**28/28**
MIX-30-07	0.0594	0.2475	0.3762	0.4554	0.6436	0.8713	1.0000	0.1866	0.2491	0.3326	0.3939	0.5609	0.7489	1.0000
MIX-34-BRT	0.0678	0.3136	0.4407	-	0.6271	0.8305	1.0000	0.2091	0.2737	0.3584	0.4196	0.5833	0.7638	1.0000
MIX-32-03	0.0845	0.3592	0.4648	0.5423	0.6690	0.8310	1.0000	0.2489	0.3162	0.4018	0.4622	0.6194	0.7870	1.0000
MIX-32-CEN	0.0548	0.2466	0.3836	0.4384	0.6575	0.8630	1.0000	0.1857	0.2481	0.3316	0.3929	0.5600	0.7483	1.0000
MIX-32-CEN-OK	0.0417	0.2583	0.4583	0.5250	0.6667	0.8417	1.0000	0.2142	0.2793	0.3641	0.4253	0.5882	0.7669	1.0000
B70-380	0.0300	0.0800	0.1700	0.2400	0.5000	0.7800	1.0000	0.0819	0.1261	0.1939	0.2495	0.4225	0.6500	1.0000
B70-420	0.0208	0.0729	0.1354	0.2188	0.4896	0.8542	1.0000	0.0760	0.1184	0.1846	0.2393	0.4117	0.6416	1.0000
B47-440	0.0207	0.1034	0.2276	0.3172	0.5724	0.8483	1.0000	0.1098	0.1606	0.2350	0.2935	0.4673	0.6836	1.0000
B67-440	0.0138	0.0759	0.1862	0.2759	0.4828	0.8276	1.0000	0.0862	0.1315	0.2005	0.2567	0.4299	0.6557	1.0000
B67-440-001	0.0090	0.1351	0.1982	0.2973	0.4865	0.8018	1.0000	0.0959	0.1436	0.2150	0.2723	0.4460	0.6679	1.0000
C45-B25-425	-	0.2261	0.4348	0.6435	0.8087	0.9043	1.0000	0.2871	0.3559	0.4413	0.5004	0.6507	0.8066	1.0000
B67-440-BEY	0.0161	0.1210	0.2500	0.3065	0.5726	0.7984	1.0000	0.1121	0.1634	0.2381	0.2969	0.4706	0.6860	1.0000
C45-B26-475	0.0654	0.5033	0.6471	0.6667	0.8301	0.8889	1.0000	0.3390	0.4085	0.4921	0.5487	0.6890	0.8301	1.0000
C45-B25-400	0.0132	0.3158	0.4539	0.5329	0.6316	0.7632	1.0000	0.2210	0.2866	0.3717	0.4327	0.5946	0.7711	1.0000
C50-B22-460	0.4259	0.6111	0.7222	0.7531	0.8333	0.9074	1.0000	0.5135	0.5759	0.6460	0.6908	0.7949	0.8916	1.0000
YM-SEG-11	-	0.3394	0.5046	0.5780	0.7523	0.9174	1.0000	0.3211	0.3905	0.4749	0.5324	0.6762	0.8223	1.0000

the fitting planar. In this way of the results, the strength development of the splitting tensile strength is settled in the Table 5.16.

In the Figure 5.19, the correlations of the actual data sets, and the predicted data sets are exhibited. The correlation plainly demonstrates that the results of the model are satisfying, and the model outwards safe to predict the splitting tensile strength of the concrete because of no negative deflection effects in the data fittings.

In the Figure 5.20, for the samples that have FA + MS content, the Model-1 shows up that [(W/C) - (W/B)] of the maximum R^2 result is equal to [(W/C) - (W/B)] of the minimum R^2 result. On the side, while [(CA/A) - (FA/A)] result gets higher, the R^2 result also increases which means that the CA/A ratio has potency on the data estimation according to the FA/A ratio.

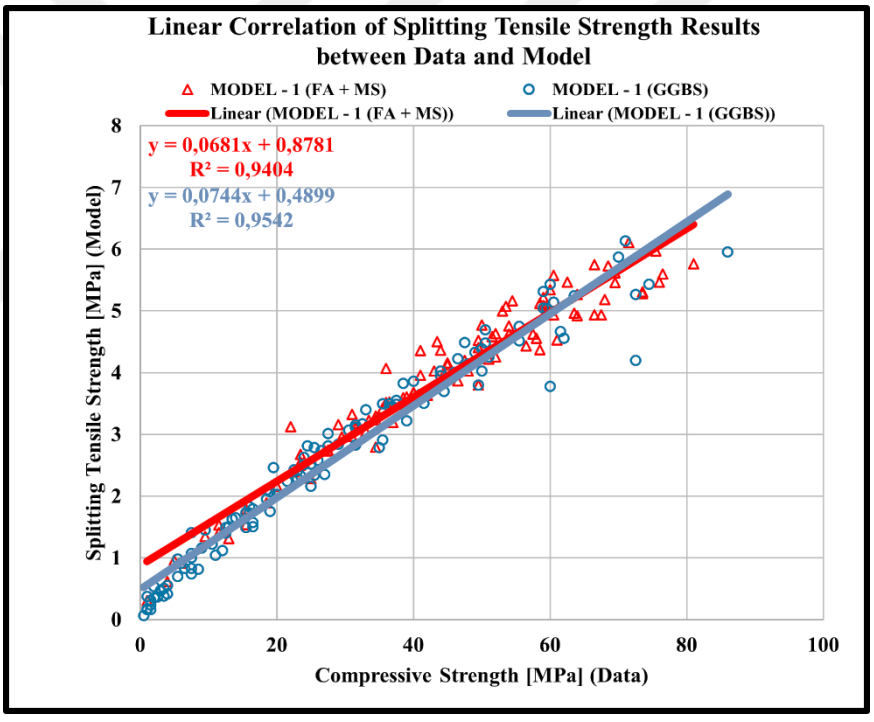

Figure 5.19: The correlations of the splitting tensile strength of the Model-1.

In the Figure 5.21, for the samples including FA + MS material, the Model-1 represents that [(NS) - (CS)] of the minimum R^2 is less than [(NS) - (CS)] of the maximum R^2. Also, [(NO:1 Agg.) - (NO:2 Agg.)] of the minimum R^2 result is less than [(NO:1 Agg.) - (NO:2 Agg.)] of the maximum R^2 result, too. In addition to this, [(FA) - (MS)] result of the minimum and maximum R^2 values are the same. At that time, the amount of cement and water are also the same for both, as well.

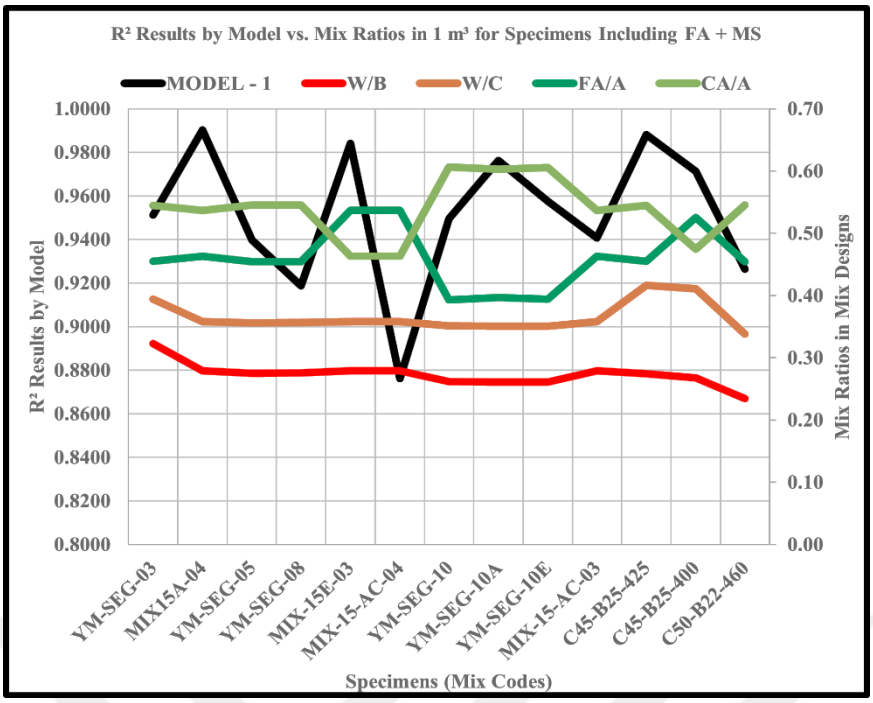

Figure 5.20: The correlations of the mixing ratios of the Model-1 in FA + MS.

Moreover, there is no proof for the effects of admixture use in the splitting tensile strength development. To sum up, the highest and the lowest R^2 values have an effect of CEMI 42.5 type of cement use. That is why, the type of cement could not be evaluated in this manner.

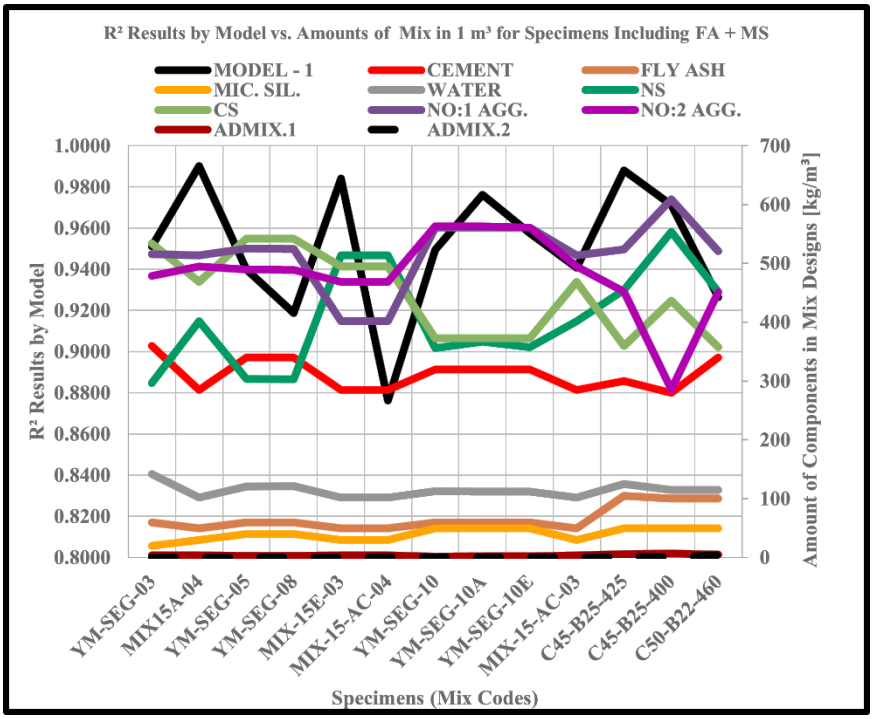

Figure 5.21: The correlations of the mixing amounts of the Model-1 in FA + MS.

In the Figure 5.22 for the samples including GGBS content, the Model-1 presumes that [(W/C) – (W/B)] of the minimum R^2 is less than [(W/C) – (W/B)] of the maximum R^2. Continuously, the maximum W/B ratio is found 0.31 for the maximum R^2 result, and there is no evidence of GGBS effects on the splitting tensile strength estimation. Also, while [(CA/A) - (FA/A)] result gets higher, the R^2 result increases which means the CA/A ratio is accurate on the data prediction due to the FA/A ratio.

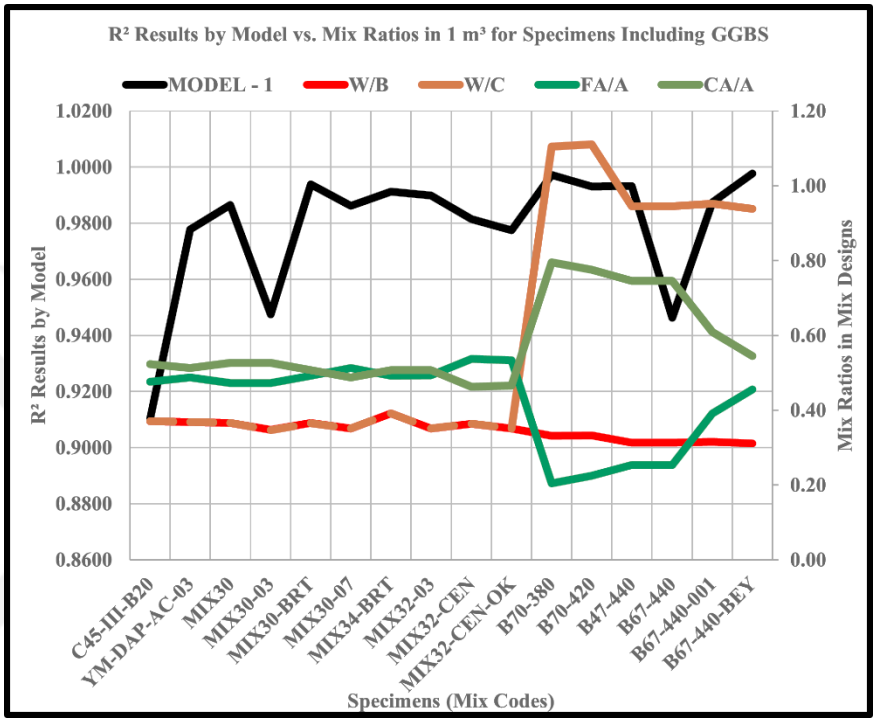

Figure 5.22: The correlations of the mixing ratios of the Model-1 in GGBS.

In the Figure 5.23, for the samples including GGBS content, the Model-1 also explains that [(NS) - (CS)] of the maximum R^2 result is greater than [(NS) - (CS)] of the minimum R^2 value. This result proves that the amounts of natural sand force the strength prediction. For some specimens, NO:0 Agg., NO:1 Agg., and NO:2 Agg. amounts continuously increase the R^2 result. Further, the amount of water and cement of the minimum R^2 are greater than the maximum R^2 has. Onto this, there are again some specimens including the GGBS content for decreasing the strength prediction values of the concrete. For the highest R^2 value, CEMI 52.5N type cement, and for the lowest R^2 result, CEMIII BS type cement are come out. Except these, there are not enough satisfying results for the model calculation in comparing purposes. Because the rest of the results are not suitable for any confrontation. In the Model-1, for both contents, the results are shown in the boxplot which is in the Figure 5.24.

Followingly, in the Table 5.13 and the Table 5.14, the numerical results of the tests are listed for both FA + MS and GGBS materials. In the Figure 5.24, it is exactly clear that FA + MS material leads the higher splitting tensile strength prediction results than GGBS content has. Except day-1, and day-2, for all ages, the strengths of the specimens including FA + MS are close and/or above the median strength values. Except day-1, day-2, and day-7, for all ages, the specimen strengths having GGBS theme are close and/or above the median strength values. It is studied that the strength estimations for the specimens including FA + MS are less coherent. Hence, the whiskers of the specimens including GGBS substance are more regular than the specimens including FA + MS ingredient. In Table 5.16, the strength developments by the model of the concrete specimens are enlisted.

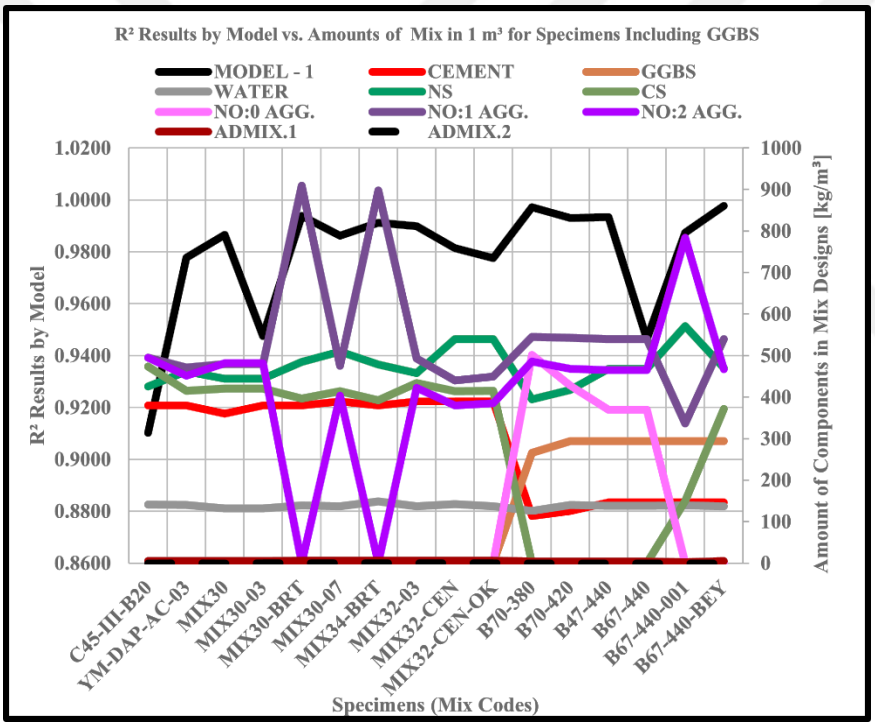

Figure 5.23: The correlations of the mixing amounts of the Model-1 in GGBS.

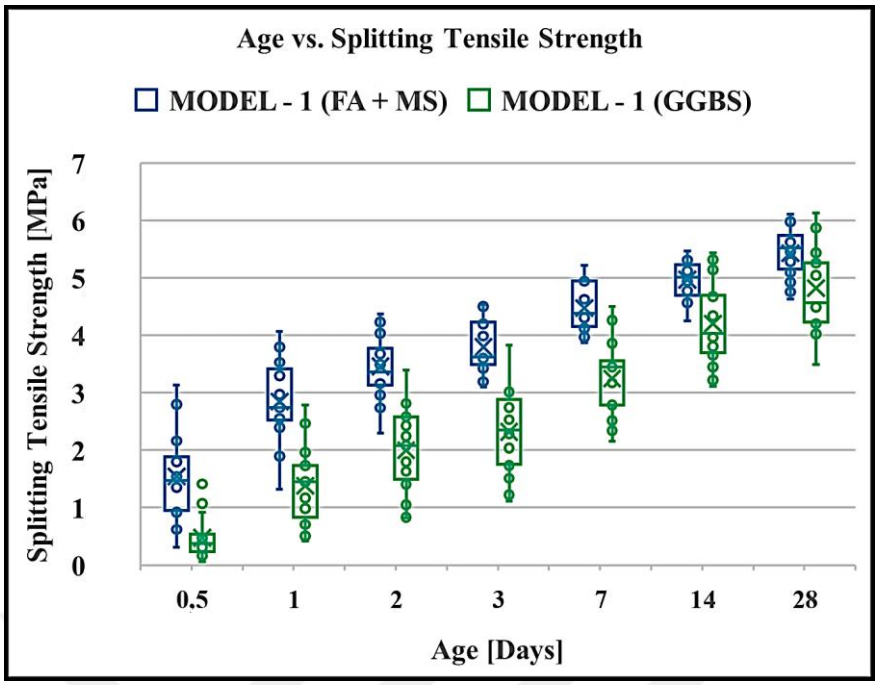

Figure 5.24: The age and the splitting tensile strength relationship for the Model-1.

Table 5.13: The CS dependent STS results in FA + MS content for the Model-1.

Model-1 [MPa]	0.5-Day	1-Day	2-Day	3-Day	7-Day	14-Day	28-Day
Minimum Value	0.31	1.32	2.29	3.10	3.87	4.25	4.63
1st-Quartile-Value	0.95	2.52	3.13	3.49	3.49	4.70	5.15
Median Value	1.47	2.74	3.36	3.62	3.62	5.01	5.52
3rd-Quartile-Value	1.88	3.41	3.77	4.23	4.23	5.23	5.74
Maximum Value	3.13	4.07	4.37	4.53	4.53	5.47	6.10
Mean Value	1.54	2.84	3.46	3.79	3.79	4.96	5.43
Range	2.82	2.75	2.08	1.43	0.66	1.22	1.48

Table 5.14: The CS dependent STS results in GGBS content for the Model-1.

Model-1 [MPa]	0.5-Day	1-Day	2-Day	3-Day	7-Day	14-Day	28-Day
Minimum Value	0.06	0.42	0.82	1.12	2.16	3.11	3.49
1st-Quartile-Value	0.24	0.83	1.49	1.75	2.79	3.70	4.23
Median Value	0.38	1.45	2.08	2.35	3.45	4.03	4.56
3rd-Quartile-Value	0.54	1.73	2.58	2.88	3.55	4.70	5.26
Maximum Value	1.41	2.79	3.40	3.83	4.50	5.43	6.13
Mean Value	0.47	1.38	2.00	2.32	3.25	4.20	4.82
Range	1.35	2.37	2.58	2.71	2.34	2.32	2.64

Table 5.15: The results of the regression Model-1.

Model-1					
Mixing Codes	**Power Regression**	**R^2**	**R^2_{adj}**	**SSE**	**RMSE**
C45-III-B20	$f'_t = 0.3438 f_c^{0.6403}$	0.9102	0.8922	2.530	0.711
YM-SEG-03	$f'_t = 0.1876 f_c^{0.8156}$	0.9512	0.9414	0.586	0.342
YM-SEG-03-FSTC	$f'_t = 0.6025 f_c^{0.5329}$	0.8345	0.7931	0.396	0.315
MIX-15A-04	$f'_t = 0.294 f_c^{0.6776}$	0.9903	0.9879	0.071	0.134
YM-SEG-05	$f'_t = 0.3003 f_c^{0.6672}$	0.9398	0.9248	0.657	0.405
YM-SEG-08	$f'_t = 0.2233 f_c^{0.76}$	0.9187	0.9025	0.998	0.447
MIX-15E-03	$f'_t = 0.2388 f_c^{0.7504}$	0.9841	0.9809	0.191	0.196
MIX-15-AC-04	$f'_t = 0.2152 f_c^{0.769}$	0.8762	0.8515	1.767	0.595
YM-SEG-10	$f'_t = 0.2595 f_c^{0.7181}$	0.9496	0.9370	0.322	0.284
DURABET PLUS AIR-AC-03	$f'_t = 0.2394 f_c^{0.744}$	0.9904	0.9884	0.131	0.162
YM-SEG-10A	$f'_t = 0.1312 f_c^{0.9006}$	0.9763	0.9704	0.281	0.265
YM-SEG-10E	$f'_t = 0.2339 f_c^{0.7731}$	0.9575	0.9469	0.307	0.277
YM-DAP-AC-03	$f'_t = 0.1956 f_c^{0.7951}$	0.9778	0.9733	0.354	0.266
MIX-15-AC-03	$f'_t = 0.2089 f_c^{0.7834}$	0.9407	0.9288	0.814	0.403
MIX-30	$f'_t = 0.1689 f_c^{0.8386}$	0.9865	0.9838	0.180	0.190
MIX-30-03	$f'_t = 0.436 f_c^{0.5831}$	0.9476	0.9371	0.334	0.258
MIX-30-BRT	$f'_t = 0.1221 f_c^{0.9116}$	0.9939	0.9926	0.139	0.167

Table 5.15 (continued): The results of the regression Model-1.

Model-1					
Mixing Codes	**Power Regression**	**R^2**	**R^2_{adj}**	**SSE**	**RMSE**
MIX-30-07	$f'_t = 0.2028 f_c^{0.7898}$	0.9862	0.9835	0.174	0.186
MIX-34-BRT	$f'_t = 0.1803 f_c^{0.8171}$	0.9912	0.9890	0.115	0.169
MIX-32-03	$f'_t = 0.2296 f_c^{0.7706}$	0.9899	0.9879	0.189	0.194
MIX-32-CEN	$f'_t = 0.2085 f_c^{0.7836}$	0.9814	0.9777	0.144	0.170
MIX32-CEN-OK	$f'_t = 0.1718 f_c^{0.8435}$	0.9776	0.9731	0.411	0.287
B70-380	$f'_t = 0.1199 f_c^{0.8981}$	0.9972	0.9967	0.036	0.085
B70-420	$f'_t = 0.1855 f_c^{0.8023}$	0.9930	0.9916	0.104	0.144
B47-440	$f'_t = 0.2336 f_c^{0.7272}$	0.9933	0.9920	0.145	0.170
B67-440	$f'_t = 0.3755 f_c^{0.5637}$	0.9464	0.9356	0.749	0.387
B67-440-001	$f'_t = 0.1197 f_c^{0.9038}$	0.9874	0.9849	0.200	0.200
C45-B25-425	$f'_t = 0.1514 f_c^{0.8441}$	0.9881	0.9851	0.092	0.152
B67-440-BEY	$f'_t = 0.1632 f_c^{0.807}$	0.9977	0.9973	0.035	0.084
C45-B26-475	$f'_t = 0.3423 f_c^{0.6442}$	0.8998	0.8798	1.447	0.538
C45-B25-400	$f'_t = 0.3086 f_c^{0.6636}$	0.9713	0.9655	0.495	0.315
C50-B22-460	$f'_t = 0.1393 f_c^{0.8471}$	0.9265	0.9118	0.469	0.306
YM-SEG-11	$f'_t = 0.1256 f_c^{0.9296}$	0.9406	0.9257	0.485	0.348

Table 5.16: The splitting tensile strength developments of samples for the Model-1.

Model-1	Strength Development of Actual Data [Day/Day]							Strength Development of Predicted Data [Day/Day]						
Mixing Codes	**0.5/28**	**1/28**	**2/28**	**3/28**	**7/28**	**14/28**	**28/28**	**0.5/28**	**1/28**	**2/28**	**3/28**	**7/28**	**14/28**	**28/28**
C45-III-B20	0.0382	0.1832	0.4122	0.4962	0.7557	0.6412	1.0000	0.0900	0.2440	0.4417	0.5149	0.7156	0.9122	1.0000
YM-SEG-03	0.2821	0.6581	0.7521	0.7521	0.8974	0.9487	1.0000	0.3538	0.5779	0.6605	0.7409	0.8549	0.8961	1.0000
YM-SEG-03-FSTC	-	0.7345	0.7611	0.8142	0.8053	1.0177	1.0000	0.5459	0.7098	0.7607	0.7851	0.8722	0.9318	1.0000
MIX-15A-04	0.2813	0.5938	0.7396	0.7917	0.8854	-	1.0000	0.3125	0.5572	0.7087	0.7578	0.8574	-	1.0000
YM-SEG-05	0.2525	0.5051	0.7778	0.8687	-	1.0202	1.0000	0.2554	0.5621	0.6884	0.6884	0.8390	0.9354	1.0000
YM-SEG-08	0.3203	0.4375	0.6094	0.7188	0.7344	0.7500	1.0000	0.3002	0.5514	0.6171	0.7031	0.8344	0.8820	1.0000
MIX-15E-03	0.1810	0.4571	0.6190	0.6952	0.8095	0.8190	1.0000	0.1799	0.5012	0.6244	0.6902	0.8161	0.9096	1.0000
MIX-15-AC-04	0.2203	0.4407	0.7119	0.7542	0.6017	0.8559	1.0000	0.2507	0.4902	0.6539	0.7097	0.8236	0.8931	1.0000
YM-SEG-10	-	0.4906	0.5660	0.7170	0.7642	1.0000	1.0000	-	0.4590	0.5921	0.6604	0.7894	0.9052	1.0000
DURABET PLUS AIR-AC-03	0.1667	0.3981	0.4722	0.5278	0.6389	0.8426	1.0000	0.2041	0.3995	0.4621	0.5220	0.6758	0.9047	1.0000
YM-SEG-10A	0.2793	-	0.5766	0.5676	0.8288	0.9640	1.0000	0.2694	-	0.5320	0.6113	0.7665	0.8910	1.0000
YM-SEG-10E	-	0.4434	0.6038	0.6509	0.8774	0.9811	1.0000	-	0.4814	0.5664	0.5963	0.7818	0.9093	1.0000
YM-DAP-AC-03	0.1068	0.2233	0.4466	0.5340	0.7184	0.7864	1.0000	0.0930	0.2984	0.4451	0.5019	0.6928	0.8708	1.0000
MIX-15-AC-03	0.1068	0.3981	0.6408	0.7282	0.7670	0.7864	1.0000	0.1302	0.5037	0.6227	0.7199	0.8669	0.9635	1.0000
MIX-30	0.0494	0.1728	0.3333	0.4321	0.6667	0.9383	1.0000	0.0561	0.1669	0.3323	0.4087	0.6730	0.8162	1.0000
MIX-30-03	0.2750	0.6375	0.6875	0.8125	0.9500	0.9750	1.0000	0.3308	0.5775	0.6597	0.7057	0.8190	0.9282	1.0000
MIX-30-BRT	0.0661	0.2810	0.4132	0.4380	0.6446	0.8264	1.0000	0.0652	0.2678	0.3983	0.4829	0.6820	0.8755	1.0000

Table 5.16 (continued): The splitting tensile strength developments of samples for the Model-1.

Model-1	Strength Development of Actual Data [Day/Day]							Strength Development of Predicted Data [Day/Day]						
Mixing Codes	**0.5/28**	**1/28**	**2/28**	**3/28**	**7/28**	**14/28**	**28/28**	**0.5/28**	**1/28**	**2/28**	**3/28**	**7/28**	**14/28**	**28/28**
MIX-30-07	0.0920	0.2874	0.4713	0.5977	0.7816	0.9195	1.0000	0.1075	0.3320	0.4621	0.5373	0.7060	0.8969	1.0000
MIX-34-BRT	0.1238	0.3905	0.4952	-	0.6286	0.7905	1.0000	0.1109	0.3877	0.5119	-	0.6830	0.8592	1.0000
MIX-32-03	0.1186	0.4831	0.5508	0.6610	0.7966	0.9237	1.0000	0.1490	0.4543	0.5541	0.6240	0.7336	0.8670	1.0000
MIX-32-CEN	0.0909	0.2879	0.5000	0.5909	0.8182	0.9697	1.0000	0.1027	0.3338	0.4719	0.5240	0.7200	0.8910	1.0000
MIX-32-CEN-OK	0.0545	0.3455	0.5364	0.5818	0.6000	0.8909	1.0000	0.0685	0.3193	0.5179	0.5807	0.7103	0.8647	1.0000
B70-380	0.0375	0.1125	0.2000	0.2500	0.5750	0.8000	1.0000	0.0429	0.1035	0.2036	0.2776	0.5366	0.8000	1.0000
B70-420	0.0353	0.0941	0.2000	0.3412	0.5176	0.8353	1.0000	0.0448	0.1224	0.2011	0.2954	0.5638	0.8812	1.0000
B47-440	0.0196	0.1961	0.3627	0.4608	0.6667	0.9608	1.0000	0.0596	0.1921	0.3408	0.4339	0.6665	0.8872	1.0000
B67-440	0.0267	0.1867	0.4533	0.5067	0.8933	1.0667	1.0000	0.0894	0.2337	0.3877	0.4839	0.6633	0.8988	1.0000
B67-440-001	0.0213	0.1489	0.2128	0.3298	0.5426	0.7128	1.0000	0.0142	0.1638	0.2316	0.3341	0.5214	0.8190	1.0000
C45-B25-425	-	0.3158	0.4632	0.6421	0.8316	0.8737	1.0000	-	0.2851	0.4951	0.6893	0.8359	0.9186	1.0000
B67-440-BEY	0.0323	0.2043	0.3118	0.3763	0.6237	0.7957	1.0000	0.0358	0.1819	0.3267	0.3850	0.6376	0.8338	1.0000
C45-B26-475	0.2063	0.5238	0.6349	0.7698	0.7222	0.7460	1.0000	0.1725	0.6425	0.7555	0.7701	0.8869	0.9269	1.0000
C45-B25-400	0.0348	0.4609	0.6348	0.6087	0.6435	0.7391	1.0000	0.0565	0.4654	0.5921	0.6586	0.7372	0.8358	1.0000
C50-B22-460	0.5045	0.6667	0.7117	0.8829	0.9459	0.9640	1.0000	0.4853	0.6589	0.7591	0.7865	0.8569	0.9210	1.0000
YM-SEG-11	-	0.3571	0.4732	0.5714	0.7054	0.7589	1.0000	-	0.3663	0.5295	0.6007	0.7675	0.9230	1.0000

5.2.2 Logarithmic Regression (Model-2)

The logarithmic regression model (the Model-2) is one of the other univariate regression analysis models depending on compressive strength of concrete like in the Model-1. In this model, for 0.5-day, 1-day, 2-day, 3-day, 7-day, 14-day, and 28-day splitting tensile strength predictions were exposed. At the end, R^2 (btw 0.8309 & 0.9993), and R^2_{adj} results are very high; SSE, and RMSE results are very low. This principal comparison indicates that forecasting of the splitting tensile strength has less errors from the actual data sets on the fitting planar. In this way of the results, the strength development of the splitting tensile strength is settled in the Table 5.20.

In the Figure 5.25, the correlations of the actual and predicted data sets are revealed. The correlation precisely shows that the results of the model are satisfying, and the model comes out safe to predict the splitting tensile strength of the concrete because of no negative deflection effects in the data fittings.

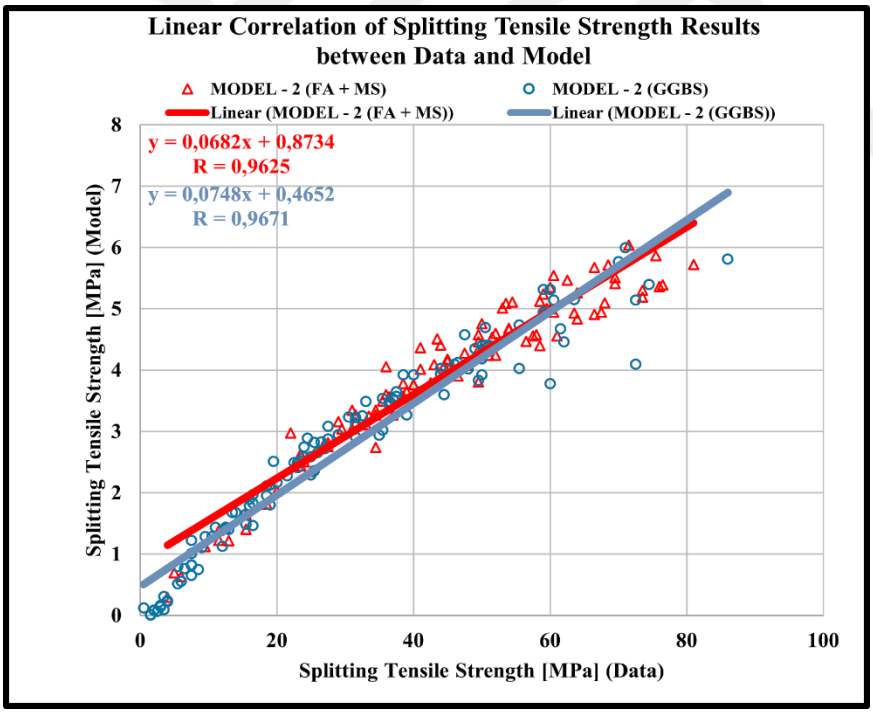

Figure 5.25: The correlations of the splitting tensile strength of the Model-2.

In the Figure 5.26, for the samples including FA + MS theme, the Model-2 comes forward that [(W/C) - (W/B)] of the maximum R^2 result is equal to [(W/C) - (W/B)] of the minimum R^2 result as well in the Model-1. Moreover, while [(CA/A) - (FA/A)] result gets higher, the R^2 result also increases which means that the CA/A ratio is more efficient on the data prediction with respect to the FA/A ratio.

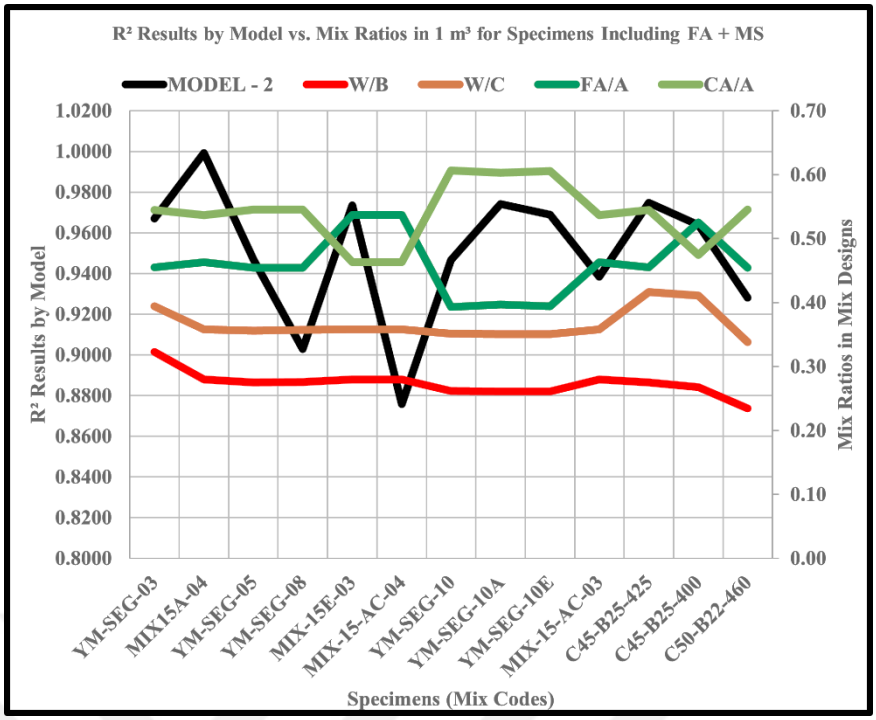

Figure 5.26: The correlations of the mixing ratios of the Model-2 in FA + MS.

In the Figure 5.27, for the samples including FA + MS material, the Model-2 explains that [(NS) - (CS)] of the minimum R^2 is greater than [(NS) - (CS)] of the maximum R^2. And [(NO:1 Agg.) - (NO:2 Agg.)] of the minimum R^2 is less than [(NO:1 Agg.) - (NO:2 Agg.)] of the maximum R^2 result, too. Additionally, [(FA) - (MS)] result and the amount of cement and water of the minimum and maximum R^2 are the same.

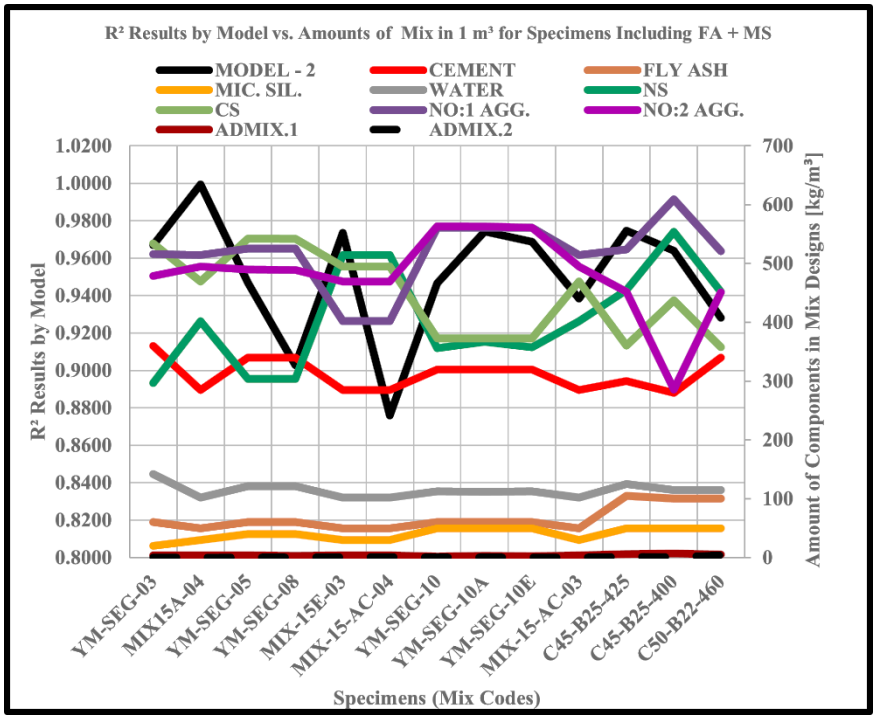

Figure 5.27: The correlations of the mixing amount of the Model-2 in FA + MS.

The minimum amount of NO:1 Agg. is 402.00 kg/m^3 for the minimum R^2 result. Except this, there is no sign of use of an exact amount of GGBS for low and/or high prediction on the splitting tensile strength. And there is no effect of admixture use in the model. Besides, the cement types are CEMI 42.5N for both lowest and highest R^2 values which means that the cement type is not a concern for the strength prediction in this model.

In the Figure 5.28, for the samples composed of GGBS content, the Model-2 also describes that [(W/C) – (W/B)] of the minimum R^2 is less than [(W/C) – (W/B)] of the maximum R^2. Followingly, there is no open sign of GGBS effects on the splitting tensile strength prediction. And, while [(CA/A) - (FA/A)] result gets higher, the R^2 result decreases which means that the CA/A ratio is accurate on the data forecasting because of the FA/A ratio.

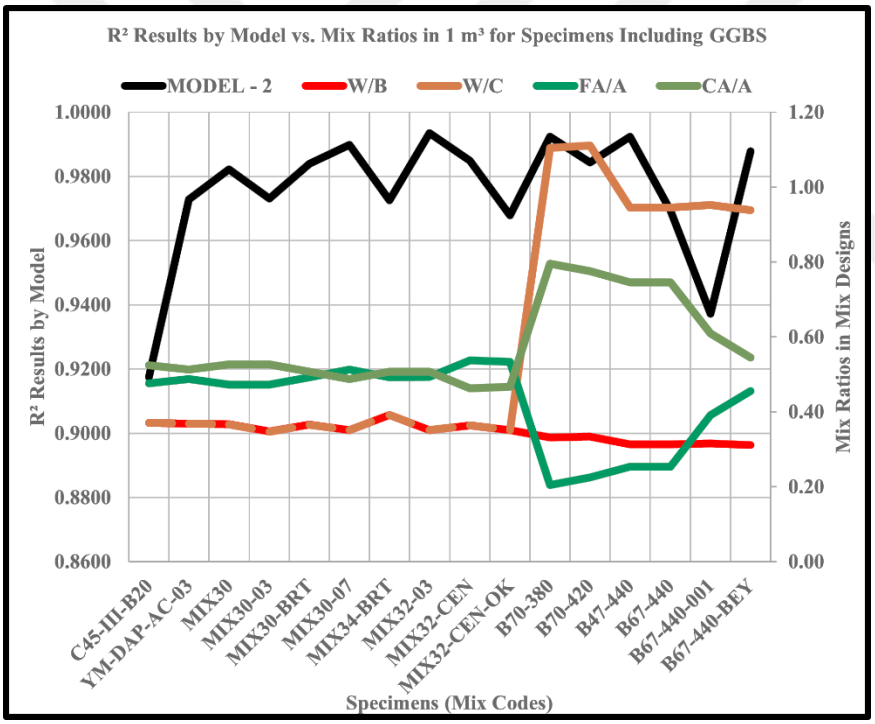

Figure 5.28: The correlations of the mixing ratios of the Model-2 in GGBS.

In the Figure 5.29, for the samples made of GGBS substance that [(NS) - (CS)] of the maximum R^2 result is greater than [(NS) - (CS)] of the minimum R^2 value. This result shows that the amounts of natural sand imply the strength prediction. For some specimens, NO:0 Agg., NO:1 Agg., and NO:2 Agg. amounts effectively increase the R^2 value. Furthermore, the amount of water and cement of the minimum R^2 are opposite to each other. When the amount of cement is increased, the prediction is resulted well. However, the amount of water in increasing causes worse predictions.

Addition to this, there are again some specimens compounded of the GGBS substance for decreasing the strength estimation results of the concrete. For the highest R^2 result, CEMIII 32.5 type cement, and for the lowest R^2 value, CEMIII BS type cement are figured out. Except these, there are no satisfying results for the model calculation in further comparing purposes. Because the remain results are not appropriate for any complex competition. In the Model-2, for both contents, the results are shown in the boxplot which is in the Figure 5.30.

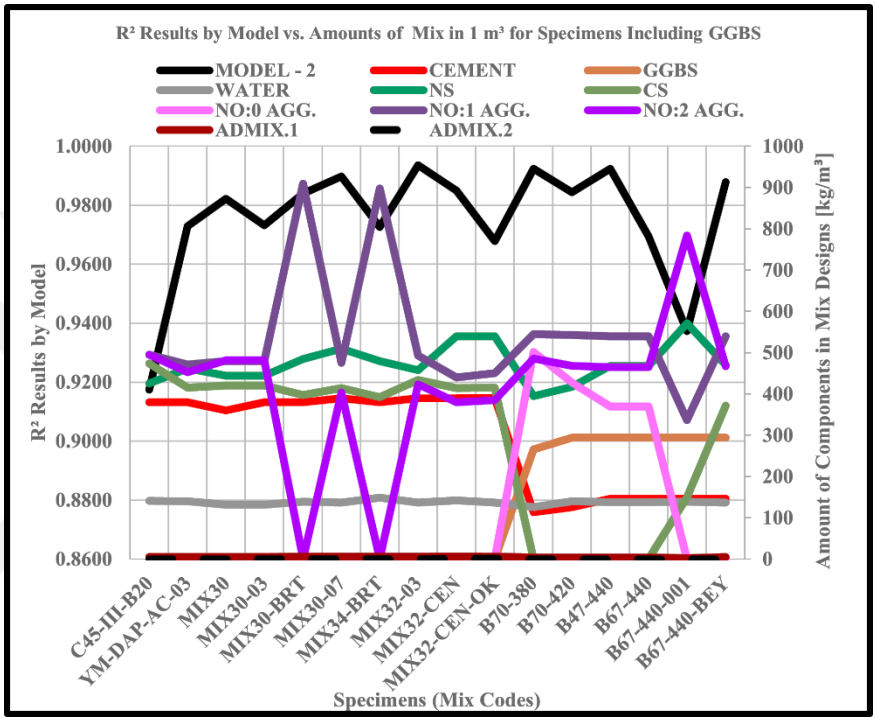

Figure 5.29: The correlations of the mixing amounts of the Model-2 in GGBS.

In the Figure 5.30, it is certain that FA + MS substance affects the higher splitting tensile strength prediction results than GGBS theme has. Except day-14, and day-28, for all ages, the strengths of the specimens including FA + MS are close and/or above the median strength values. Except day-1, day-7, and day-28, for all ages, the specimen strengths having GGBS theme are close and/or above the median strength values. It is understood that the strength predictions for the specimens including FA + MS are less logical. Thus, the whiskers of the specimens including GGBS substance are more consistent than the specimens including FA + MS ingredient. In the Table 5.17 and the Table 5.18, the numerical results of the boxplots are also given.

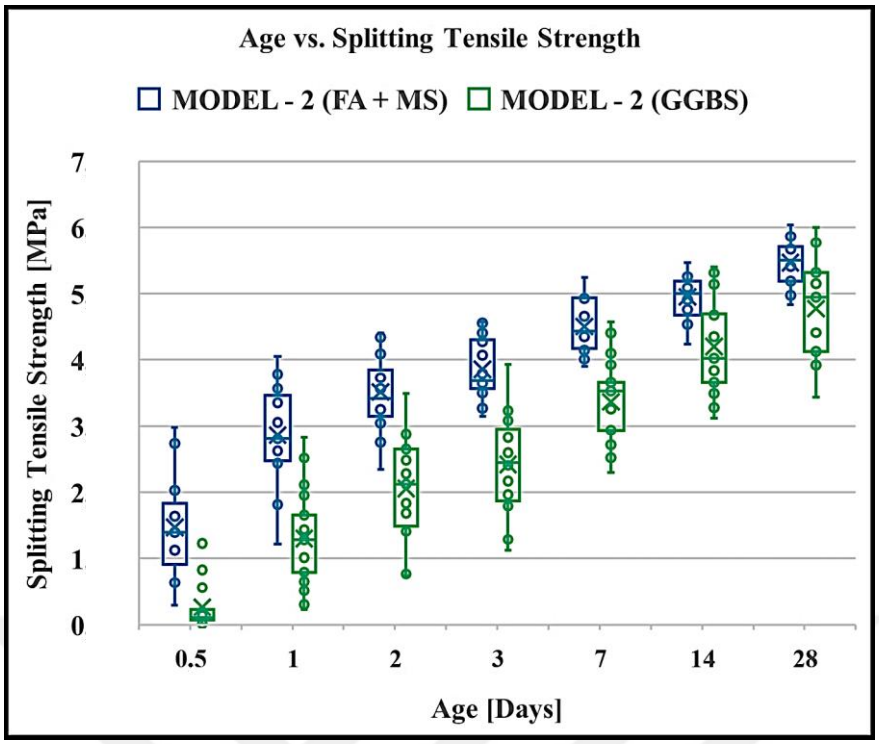

Figure 5.30: The age and the splitting tensile strength relationship for the Model-2.

Table 5.17: The CS dependent STS results in FA + MS content for the Model-2.

Model-2 [MPa]	0.5-Day	1-Day	2-Day	3-Day	7-Day	14-Day	28-Day
Minimum Value	0.30	1.22	2.34	3.15	3.90	4.24	4.56
1st-Quartile-Value	0.91	2.48	3.15	3.57	4.18	4.68	5.08
Median Value	1.39	2.81	3.42	3.69	4.44	5.00	5.41
3rd-Quartile-Value	1.84	3.46	3.85	4.31	4.94	5.19	5.68
Maximum Value	2.98	4.05	4.40	4.58	5.24	5.47	6.04
Mean Value	1.47	2.86	3.51	3.85	4.50	4.95	5.35
Range	2.68	2.84	2.06	1.43	1.34	1.23	1.48

Table 5.18: The CS dependent STS results in GGBS content for the Model-2.

Model-2 [MPa]	0.5-Day	1-Day	2-Day	3-Day	7-Day	14-Day	28-Day
Minimum Value	0.01	0.23	0.75	1.13	2.29	3.12	3.43
1st-Quartile-Value	0.07	0.79	1.49	1.87	2.94	3.66	4.09
Median Value	0.11	1.29	2.12	2.45	3.53	4.03	4.46
3rd-Quartile-Value	0.23	1.65	2.66	2.95	3.66	4.69	5.15
Maximum Value	1.23	2.83	3.49	3.93	4.58	5.40	6.00
Mean Value	0.26	1.30	2.06	2.42	3.37	4.20	4.69
Range	1.22	2.60	2.74	2.80	2.28	2.28	2.57

Table 5.19: The results of the regression Model-2.

Model-2					
Mixing Codes	**Logarithmic Regression**	**R^2**	**R^2_{adj}**	**SSE**	**RMSE**
C45-III-B20	$f'_t = 0.2139ln(f'_c)^{2.21}$	0.9175	0.9010	2.324	0.682
YM-SEG-03	$f'_t = 0.06975ln(f'_c)^{3.073}$	0.9670	0.9604	0.396	0.282
YM-SEG-03-FSTC	$f'_t = 0.2838ln(f'_c)^{2.083}$	0.8309	0.7886	0.405	0.318
MIX-15A-04	$f'_t = 0.1733ln(f'_c)^{2.335}$	0.9993	0.9991	0.005	0.036
YM-SEG-05	$f'_t = 0.1641ln(f'_c)^{2.369}$	0.9468	0.9335	0.581	0.381
YM-SEG-08	$f'_t = 0.09805ln(f'_c)^{2.794}$	0.9027	0.8833	1.194	0.489
MIX-15E-03	$f'_t = 0.1481ln(f'_c)^{2.50}$	0.9734	0.9681	0.320	0.253
MIX-15-AC-04	$f'_t = 0.1078ln(f'_c)^{2.722}$	0.8759	0.8510	1.772	0.595
YM-SEG-10	$f'_t = 0.1093ln(f'_c)^{2.701}$	0.9467	0.9333	0.340	0.292
DURABET PLUS AIR-AC-03	$f'_t = 0.1404ln(f'_c)^{2.531}$	0.9890	0.9868	0.150	0.173
YM-SEG-10A	$f'_t = 0.05118ln(f'_c)^{3.282}$	0.9742	0.9678	0.306	0.277
YM-SEG-10E	$f'_t = 0.0992ln(f'_c)^{2.851}$	0.9688	0.9611	0.225	0.237
YM-DAP-AC-03	$f'_t = 0.1099ln(f'_c)^{2.705}$	0.9728	0.9674	0.433	0.294
MIX-15-AC-03	$f'_t = 0.1263ln(f'_c)^{2.611}$	0.9384	0.9261	0.845	0.411
MIX-30	$f'_t = 0.1312ln(f'_c)^{2.563}$	0.9822	0.9786	0.237	0.218
MIX-30-03	$f'_t = 0.3368ln(f'_c)^{1.848}$	0.9731	0.9678	0.171	0.185
MIX-30-BRT	$f'_t = 0.0494ln(f'_c)^{3.291}$	0.9840	0.9807	0.365	0.270

Table 5.19 (continued): The results of the regression Model-2.

Model-2					
Mixing Codes	**Logarithmic Regression**	**R^2**	**R^2_{adj}**	**SSE**	**RMSE**
MIX-30-07	$f'_t = 0.1356ln(f'_c)^{2.548}$	0.9898	0.9877	0.129	0.161
MIX-34-BRT	$f'_t = 0.1004ln(f'_c)^{2.773}$	0.9726	0.9658	0.358	0.299
MIX-32-03	$f'_t = 0.1136ln(f'_c)^{2.736}$	0.9935	0.9922	0.122	0.156
MIX-32-CEN	$f'_t = 0.1827ln(f'_c)^{2.291}$	0.9849	0.9819	0.117	0.153
MIX32-CEN-OK	$f'_t = 0.08785ln(f'_c)^{2.911}$	0.9679	0.9614	0.589	0.343
B70-380	$f'_t = 0.09205ln(f'_c)^{2.751}$	0.9924	0.9908	0.101	0.142
B70-420	$f'_t = 0.1827ln(f'_c)^{2.284}$	0.9843	0.9812	0.234	0.216
B47-440	$f'_t = 0.149ln(f'_c)^{2.434}$	0.9924	0.9909	0.164	0.181
B67-440	$f'_t = 0.3068ln(f'_c)^{1.781}$	0.9694	0.9633	0.427	0.292
B67-440-001	$f'_t = 0.25ln(f'_c)^{2.00}$	0.9373	0.9247	0.999	0.447
C45-B25-425	$f'_t = 0.07993ln(f'_c)^{2.89}$	0.9748	0.9684	0.196	0.221
B67-440-BEY	$f'_t = 0.09983ln(f'_c)^{2.68}$	0.9879	0.9854	0.185	0.193
C45-B26-475	$f'_t = 0.2597ln(f'_c)^{2.068}$	0.8598	0.8318	2.024	0.636
C45-B25-400	$f'_t = 0.146ln(f'_c)^{2.459}$	0.9639	0.9567	0.621	0.352
C50-B22-460	$f'_t = 0.0368ln(f'_c)^{3.409}$	0.9281	0.9138	0.458	0.303
YM-SEG-11	$f'_t = 0.05387ln(f'_c)^{3.285}$	0.9327	0.9159	0.549	0.371

Table 5.20: The splitting tensile strength developments of samples for the Model-2.

Model-2	Strength Development of Actual Data [Day/Day]							Strength Development of Predicted Data [Day/Day]						
Mixing Codes	**0.5/28**	**1/28**	**2/28**	**3/28**	**7/28**	**14/28**	**28/28**	**0.5/28**	**1/28**	**2/28**	**3/28**	**7/28**	**14/28**	**28/28**
C45-III-B20	0.0382	0.1832	0.4122	0.4962	0.7557	0.6412	1.0000	0.0164	0.2213	0.4742	0.5569	0.7590	0.9302	1.0000
YM-SEG-03	0.2821	0.6581	0.7521	0.7521	0.8974	0.9487	1.0000	0.3366	0.5906	0.6773	0.7582	0.8680	0.9063	1.0000
YM-SEG-03-FSTC	-	0.7345	0.7611	0.8142	0.8053	1.0177	1.0000	0.5211	0.7090	0.7636	0.7892	0.8777	0.9358	1.0000
MIX-15A-04	0.2813	0.5938	0.7396	0.7917	0.8854	-	1.0000	0.2885	0.5810	0.7376	0.7851	0.8771	-	1.0000
YM-SEG-05	0.2525	0.5051	0.7778	0.8687	-	1.0202	1.0000	0.2162	0.5879	0.7185	0.7185	0.8610	0.9457	1.0000
YM-SEG-08	0.3203	0.4375	0.6094	0.7188	0.7344	0.7500	1.0000	0.2797	0.5722	0.6415	0.7285	0.8536	0.8968	1.0000
MIX-15E-03	0.1810	0.4571	0.6190	0.6952	0.8095	0.8190	1.0000	0.1280	0.5275	0.6585	0.7241	0.8421	0.9244	1.0000
MIX-15-AC-04	0.2203	0.4407	0.7119	0.7542	0.6017	0.8559	1.0000	0.2226	0.5110	0.6840	0.7391	0.8462	0.9085	1.0000
YM-SEG-10	-	0.4906	0.5660	0.7170	0.7642	1.0000	1.0000	-	0.4505	0.6005	0.6733	0.8039	0.9141	1.0000
DURABET PLUS AIR-AC-03	0.1667	0.3981	0.4722	0.5278	0.6389	0.8426	1.0000	0.1605	0.4097	0.4829	0.5497	0.7093	0.9199	1.0000
YM-SEG-10A	0.2793	-	0.5766	0.5676	0.8288	0.9640	1.0000	0.2469	-	0.5491	0.6326	0.7871	0.9032	1.0000
YM-SEG-10E	-	0.4434	0.6038	0.6509	0.8774	0.9811	1.0000	-	0.4738	0.5694	0.6022	0.7942	0.9169	1.0000
YM-DAP-AC-03	0.1068	0.2233	0.4466	0.5340	0.7184	0.7864	1.0000	0.0286	0.2838	0.4607	0.5245	0.7230	0.8890	1.0000
MIX-15-AC-03	0.1068	0.3981	0.6408	0.7282	0.7670	0.7864	1.0000	0.0633	0.5236	0.6511	0.7482	0.8850	0.9693	1.0000
MIX-30	0.0494	0.1728	0.3333	0.4321	0.6667	0.9383	1.0000	0.0031	0.1248	0.3418	0.4341	0.7144	0.8462	1.0000
MIX-30-03	0.2750	0.6375	0.6875	0.8125	0.9500	0.9750	1.0000	0.2934	0.6012	0.6893	0.7360	0.8442	0.9405	1.0000
MIX-30-BRT	0.0661	0.2810	0.4132	0.4380	0.6446	0.8264	1.0000	0.0180	0.2546	0.4094	0.5040	0.7100	0.8914	1.0000

Table 5.20 (continued): The splitting tensile strength developments of samples for the Model-2.

Model-2	Strength Development of Actual Data [Day/Day]							Strength Development of Predicted Data [Day/Day]						
Mixing Codes	**0.5/28**	**1/28**	**2/28**	**3/28**	**7/28**	**14/28**	**28/28**	**0.5/28**	**1/28**	**2/28**	**3/28**	**7/28**	**14/28**	**28/28**
MIX-30-07	0.0920	0.2874	0.4713	0.5977	0.7816	0.9195	1.0000	0.0391	0.3259	0.4817	0.5654	0.7381	0.9129	1.0000
MIX-34-BRT	0.1238	0.3905	0.4952	-	0.6286	0.7905	1.0000	0.0502	0.3953	0.5368	-	0.7139	0.8787	1.0000
MIX-32-03	0.1186	0.4831	0.5508	0.6610	0.7966	0.9237	1.0000	0.0934	0.4716	0.5815	0.6544	0.7626	0.8856	1.0000
MIX-32-CEN	0.0909	0.2879	0.5000	0.5909	0.8182	0.9697	1.0000	0.0230	0.3232	0.4918	0.5507	0.7528	0.9086	1.0000
MIX-32-CEN-OK	0.0545	0.3455	0.5364	0.5818	0.6000	0.8909	1.0000	0.0128	0.3109	0.5404	0.6075	0.7382	0.8823	1.0000
B70-380	0.0375	0.1125	0.2000	0.2500	0.5750	0.8000	1.0000	0.0020	0.0576	0.1902	0.2869	0.5848	0.8348	1.0000
B70-420	0.0353	0.0941	0.2000	0.3412	0.5176	0.8353	1.0000	0.0000	0.0760	0.1902	0.3202	0.6276	0.9094	1.0000
B47-440	0.0196	0.1961	0.3627	0.4608	0.6667	0.9608	1.0000	0.0032	0.1595	0.3563	0.4679	0.7120	0.9091	1.0000
B67-440	0.0267	0.1867	0.4533	0.5067	0.8933	1.0667	1.0000	0.0000	0.1938	0.4117	0.5289	0.7176	0.9227	1.0000
B67-440-001	0.0213	0.1489	0.2128	0.3298	0.5426	0.7128	1.0000	0.0298	0.2517	0.3564	0.4872	0.6734	0.8930	1.0000
C45-B25-425	-	0.3158	0.4632	0.6421	0.8316	0.8737	1.0000	-	0.2668	0.5142	0.7168	0.8559	0.9300	1.0000
B67-440-BEY	0.0323	0.2043	0.3118	0.3763	0.6237	0.7957	1.0000	0.0000	0.1464	0.3339	0.4046	0.6777	0.8604	1.0000
C45-B26-475	0.2063	0.5238	0.6349	0.7698	0.7222	0.7460	1.0000	0.1287	0.7002	0.8035	0.8163	0.9132	0.9447	1.0000
C45-B25-400	0.0348	0.4609	0.6348	0.6087	0.6435	0.7391	1.0000	0.0000	0.4672	0.6095	0.6796	0.7589	0.8534	1.0000
C50-B22-460	0.5045	0.6667	0.7117	0.8829	0.9459	0.9640	1.0000	0.4790	0.6668	0.7693	0.7966	0.8655	0.9266	1.0000
YM-SEG-11	-	0.3571	0.4732	0.5714	0.7054	0.7589	1.0000	-	0.3553	0.5399	0.6160	0.7846	0.9309	1.0000

5.2.3 Fraction Regression (Model-3)

The fraction regression model (the Model-3) is one of the other univariate regression analysis models depending on compressive strength of concrete like in the Model-1 and Model-2. In this model, for 0.5-day, 1-day, 2-day, 3-day, 7-day, 14-day, and 28-day splitting tensile strength predictions were revealed. At the end, R^2 (btw 0.8276 & 0.9990), and R^2_{adj} results are very high; SSE, and RMSE results are very low. This elementary comparison focuses that the presuming of the splitting tensile strength has less errors from the actual data sets on the fitting planar. In this thinking, the strength development of the splitting tensile strength is shown in the Table 5.24.

In the Figure 5.31, the correlations of the actual data sets and the estimated data sets are shared. The correlation exactly shows that the results of the model are satisfying, and the model sets forth safe to predict the splitting tensile strength of the concrete because of the absences of negative deflection effects in the data fittings.

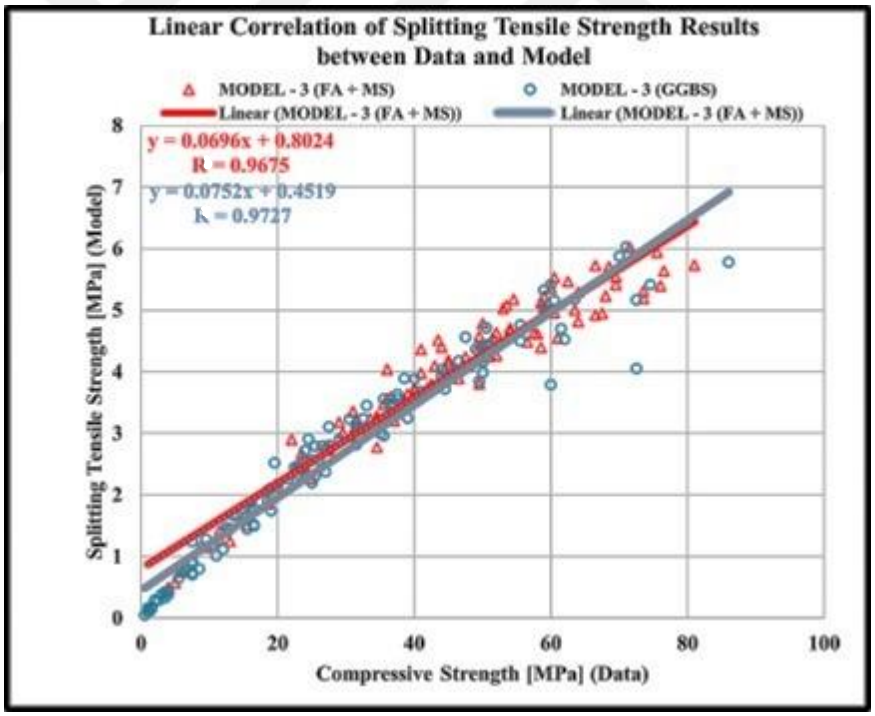

Figure 5.31: The correlations of the splitting tensile strength of the Model-3.

In the Figure 5.32, for the samples including FA + MS substance, the Model-3 evinces that [(W/C) - (W/B)] of the maximum R^2 result is equal to [(W/C) - (W/B)] of the minimum R^2 result as well in the Model-1 and the Model-2. Moreover, while [(CA/A) - (FA/A)] result gets higher, the R^2 result also increases that the CA/A ratio is effective

on the data estimation with respect to the FA/A ratio. Also, the minimum CA/A ratio is 0.46, and the maximum FAA ratio is 0.54 for the minimum R^2 value.

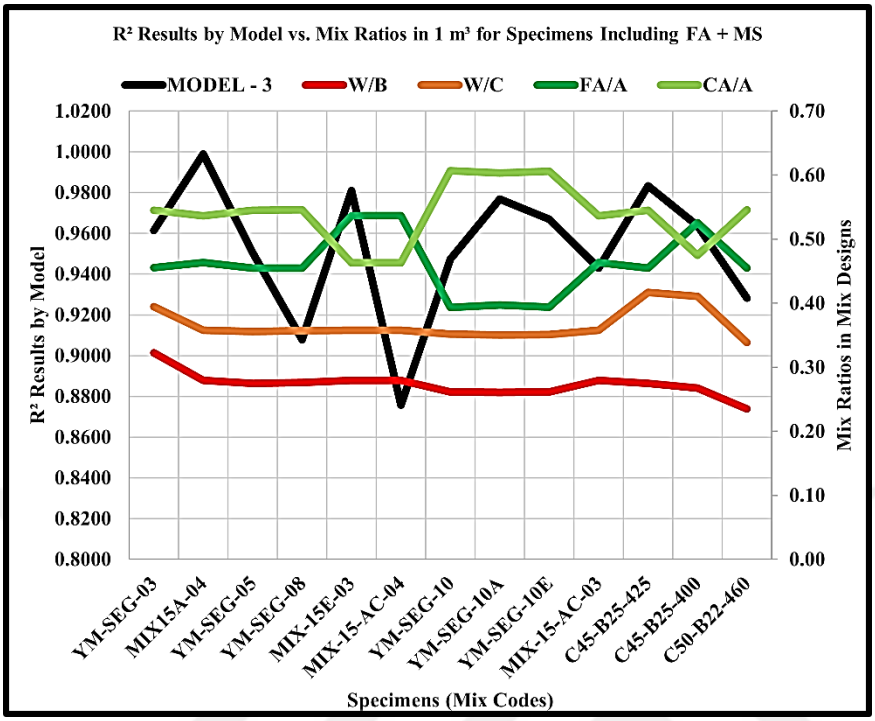

Figure 5.32: The correlations of the mixing ratios of the Model-3 in FA + MS.

In the Figure 5.33, for the samples including FA + MS content, the Model-3 argues that [(NS) - (CS)] of the minimum R^2 is greater than [(NS) - (CS)] of the maximum R^2.

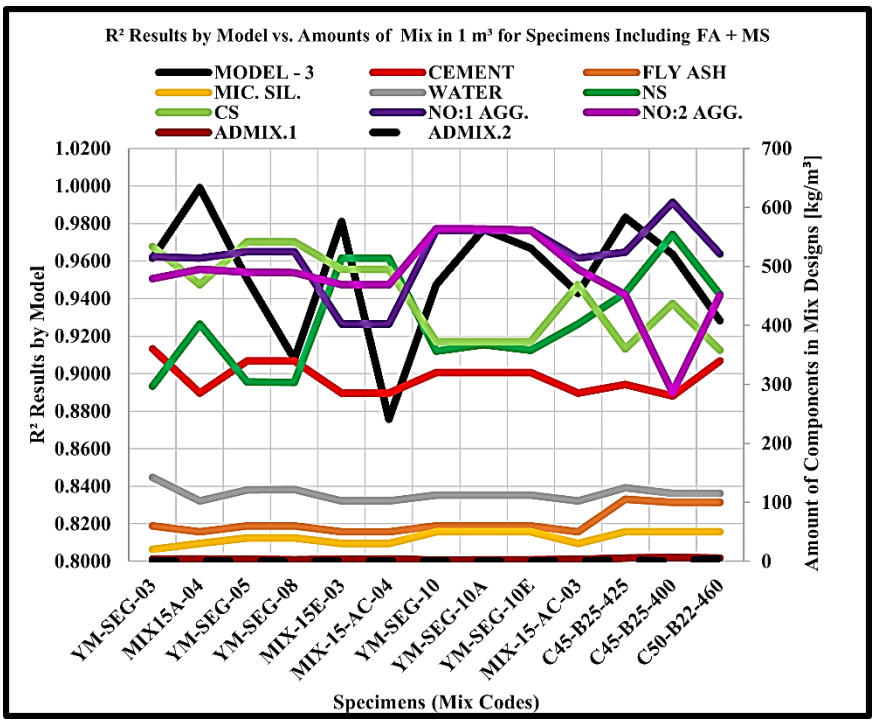

Figure 5.33: The correlations of the mixing amounts of the Model-3 in FA + MS.

And [(NO:1 Agg.) - (NO:2 Agg.)] of the minimum R^2 is less than [(NO:1 Agg.) - (NO:2 Agg.)] of the maximum R^2 result, as well in the previous models.

Further, [(FA) - (MS)] result, and the amount of cement and water of the minimum R^2 is less than the maximum R^2 has. Yet, the use of admixtures and water seem like inefficient on the data forecasting. The minimum amount of NO:1 Agg. is 402.00 kg/m^3 for the minimum R^2 result. Onto this, there is no sign of use of specific amount of FA + MS for low and/or high prediction on the splitting tensile strength. Also, there is no efficient way of admixture use in this model, as well. Moreover, the cement types are CEMI 42.5N for both the lowest and highest R^2 results which means that the cement type is out of any comparison for the strength prediction in this model.

In the Figure 5.34, for the samples in form of GGBS theme, the Model-3 also discloses that [(W/C) – (W/B)] of the minimum R^2 is less than [(W/C) – (W/B)] of the maximum R^2, as well in the last models. Continuously, there is no overt sign of GGBS effects on the splitting tensile strength prediction, even though it is a binder substance like the cement. While [(CA/A) - (FA/A)] result gets higher, the R^2 result is increased which means that the CA/A ratio effect is acceptable on the data presuming in use of the FA/A ratio. The minimum FA/A ratio (0.20), and the maximum CA/A ratio (0.80) are found out for the highest R^2 results. The cement types attract the attention for in B70-380 (CEMI 52.5N), and C45-III-B20 (CEMIII BS) mixing codes.

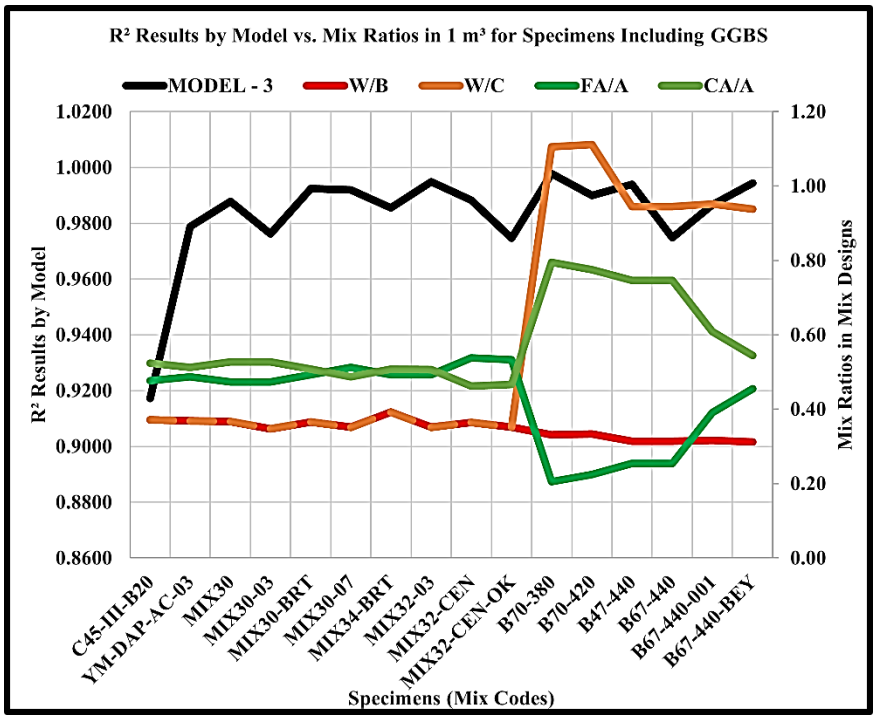

Figure 5.34: The correlations of the mixing ratios of the Model-3 in GGBS.

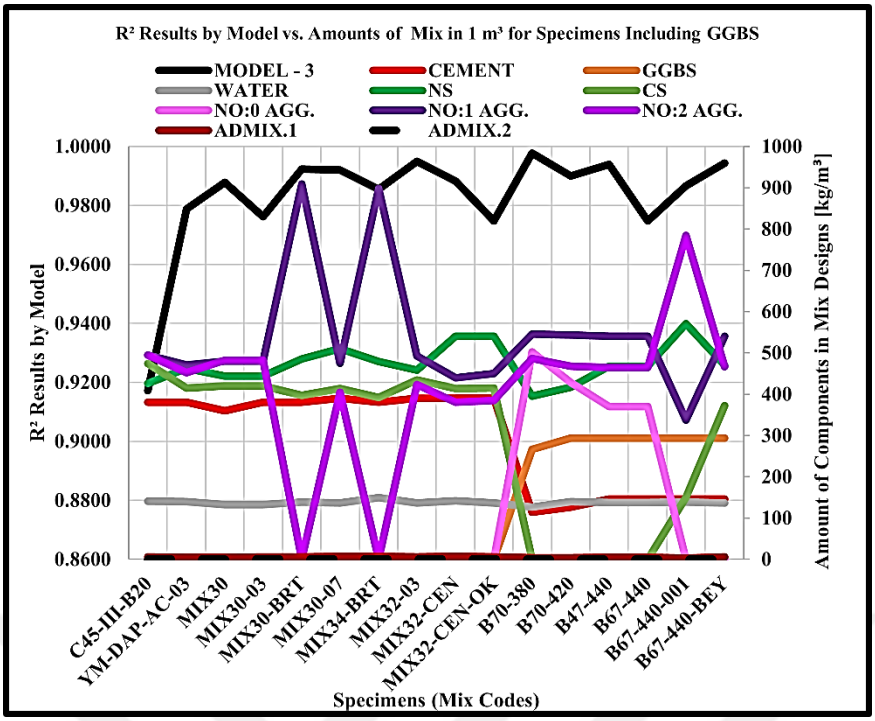

Figure 5.35: The correlations of the mixing amounts of the Model-3 in GGBS.

In the Figure 5.36, for the samples GGBS resultants, [(NS) - (CS)] of the maximum R^2 result is greater than [(NS) - (CS)] of the minimum R^2 result like in the previous models. This result shows that the amounts of natural sand impose the strength prediction. For some specimens, NO:0 Agg., NO:1 Agg., and NO:2 Agg. amounts effectively increase the R^2 value. The amounts of water and cement of the minimum R^2 result are greater than the maximum R^2 result owns. When the amount of cement is increased, the prediction is worsened. Like the amount of cement, the amount of water in increasing results worse predictions. Else, there are some specimens compounded of the GGBS substance for decreasing the strength results of the concrete in forecasting. For the maximum R^2 result, the minimum cement content is 114.00 kg/m^3, and the maximum amount of NO:0 Agg. is 486.00 kg/m^3. Meanwhile, the minimum amount of CS content is 0.00 kg/m^3, and the minimum amount of NS content is 395.00 kg/m^3. Beyond these, there are no satisfying results for the model calculation in comparing purposes. As the remaining results are not liable for any cross check. In the Model-3, for both contents, the results are exposed by the boxplot in the Figure 5.36.

In the Figure 5.36, it is certain that FA + MS material is more impactful on the higher splitting tensile strength prediction results than GGBS material is. Except day-0.5, day-14, and day-28, for all ages, the strengths of the specimens made of FA + MS are close and/or above the median strength values. Except day-2, day-3, and day-7, for all ages,

the specimen strengths having GGBS content are close and/or above the median strength values. It is seen that the strength estimations for the specimens including FA + MS are less appreciated. That is why, the whiskers of the specimens including GGBS subsequent are more dependable than the specimens including FA + MS ingredient. In the Table 5.21 and the Table 5.22, the numerical results of the boxplots are also given.

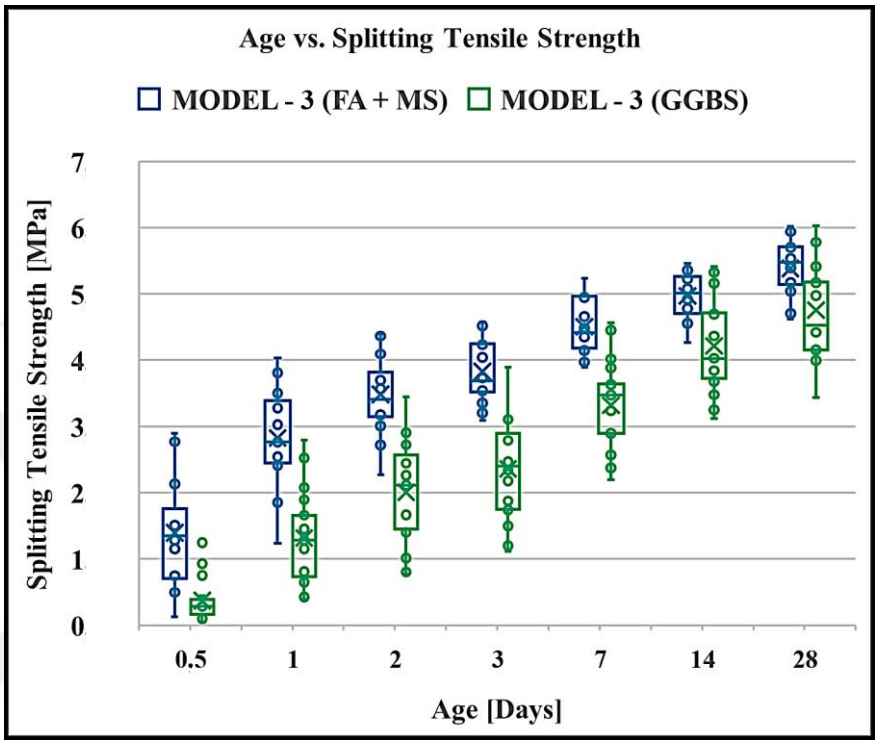

Figure 5.36: The age and the splitting tensile strength relationship for the Model-3.

Table 5.21: The CS dependent STS results in FA + MS content for the Model-3.

Model-3 [MPa]	0.5-Day	1-Day	2-Day	3-Day	7-Day	14-Day	28-Day
Minimum Value	0.13	1.24	2.27	3.10	3.89	4.26	4.62
1st-Quartile-Value	0.70	2.45	3.15	3.52	3.52	4.71	5.14
Median Value	1.35	2.77	3.41	3.69	3.69	5.02	5.47
3rd-Quartile-Value	1.75	3.39	3.82	4.25	4.25	5.26	5.71
Maximum Value	2.90	4.03	4.39	4.58	4.58	5.46	6.02
Mean Value	1.39	2.83	3.48	3.83	3.83	4.97	5.39
Range	2.77	2.79	2.12	1.48	0.69	1.20	1.40

Table 5.22: The CS dependent STS results in GGBS content for the Model-3.

Model-3 [MPa]	0.5-Day	1-Day	2-Day	3-Day	7-Day	14-Day	28-Day
Minimum Value	0.05	0.39	0.77	1.12	2.20	3.12	3.44
1st-Quartile-Value	0.17	0.74	1.45	1.74	2.90	3.72	4.15
Median Value	0.28	1.28	2.11	2.40	3.47	4.03	4.53
3rd-Quartile-Value	0.39	1.66	2.57	2.89	3.64	4.72	5.18
Maximum Value	1.24	2.79	3.45	3.89	4.56	5.42	6.03
Mean Value	0.37	1.32	2.01	2.36	3.32	4.22	4.75
Range	1.20	2.41	2.68	2.78	2.36	2.30	2.59

Table 5.23: The results of the regression Model-3.

Model-3					
Mixing Codes	**Fraction Regression**	**R^2**	**R^2_{adj}**	**SSE**	**RMSE**
C45-III-B20	$f'_t = 10.22 f'_c / (66.07 + f'_c)$	0.9172	0.9007	2.332	0.683
YM-SEG-03	$f'_t = 20.67 f'_c / (174.10 + f'_c)$	0.9615	0.9537	0.463	0.304
YM-SEG-03-FSTC	$f'_t = 10.53 f'_c / (57.96 + f'_c)$	0.8276	0.7844	0.413	0.321
MIX-15A-04	$f'_t = 10.21 f'_c / (71.77 + f'_c)$	0.9990	0.9987	0.008	0.043
YM-SEG-05	$f'_t = 10.84 f'_c / (80.04 + f'_c)$	0.9504	0.9380	0.541	0.368
YM-SEG-08	$f'_t = 18.77 f'_c / (163.10 + f'_c)$	0.9077	0.8893	1.133	0.476
MIX-15E-03	$f'_t = 14.35 f'_c / (109.10 + f'_c)$	0.9809	0.9771	0.230	0.214
MIX-15-AC-04	$f'_t = 16.09 f'_c / (132.50 + f'_c)$	0.8757	0.8509	1.775	0.596
YM-SEG-10	$f'_t = 14.51 f'_c / (116.70 + f'_c)$	0.9474	0.9342	0.336	0.259
DURABET PLUS AIR-AC-03	$f'_t = 13.44 f'_c / (101.20 + f'_c)$	0.9892	0.9871	0.146	0.171
YM-SEG-10A	$f'_t = 38.37 f'_c / (379.30 + f'_c)$	0.9768	0.9710	0.276	0.263
YM-SEG-10E	$f'_t = 7.44 f'_c / (130.30 + f'_c)$	0.9669	0.9586	0.239	0.244
YM-DAP-AC-03	$f'_t = 15.57 f'_c / (126.70 + f'_c)$	0.9787	0.9745	0.339	0.260
MIX-15-AC-03	$f'_t = 14.69 f'_c / (114.60 + f'_c)$	0.9428	0.9314	0.784	0.396
MIX-30	$f'_t = 15.42 f'_c / (125.03 + f'_c)$	0.9877	0.9853	0.163	0.181
MIX-30-03	$f'_t = 7.078 f'_c / (35.20 + f'_c)$	0.9762	0.9715	0.152	0.174
MIX-30-BRT	$f'_t = 51.77 f'_c / (546.70 + f'_c)$	0.9923	0.9908	0.174	0.187

Table 5.23 (continued): The results of the regression Model-3.

Model-3					
Mixing Codes	**Fraction Regression**	**R^2**	**R^2_{adj}**	**SSE**	**RMSE**
MIX-30-07	$f'_t = 13.02\, f'_c\ /\ (98.25 + f'_c)$	0.9920	0.9904	0.101	0.142
MIX-34-BRT	$f'_t = 20.93\, f'_c\ /\ (186.00 + f'_c)$	0.9855	0.9819	0.189	0.217
MIX-32-03	$f'_t = 17.17\, f'_c\ /\ (131.30 + f'_c)$	0.9949	0.9938	0.097	0.139
MIX-32-CEN	$f'_t = 9.823\, f'_c\ /\ (67.83 + f'_c)$	0.9883	0.9859	0.091	0.135
MIX32-CEN-OK	$f'_t = 25.49\, f'_c\ /\ (222.50 + f'_c)$	0.9747	0.9697	0.464	0.304
B70-380	$f'_t = 21.50\, f'_c\ /\ (219.30 + f'_c)$	0.9977	0.9973	0.030	0.077
B70-420	$f'_t = 12.65\, f'_c\ /\ (100.10 + f'_c)$	0.9899	0.9879	0.150	0.173
B47-440	$f'_t = 11.78\, f'_c\ /\ (92.78 + f'_c)$	0.9939	0.9927	0.131	0.162
B67-440	$f'_t = 6.023\, f'_c\ /\ (35.35 + f'_c)$	0.9747	0.9697	0.353	0.266
B67-440-001	$f'_t = 29.62\, f'_c\ /\ (309.70 + f'_c)$	0.9866	0.9839	0.214	0.207
C45-B25-425	$f'_t = 22.74\, f'_c\ /\ (225.40 + f'_c)$	0.9833	0.9791	0.130	0.180
B67-440-BEY	$f'_t = 15.50\, f'_c\ /\ (150.20 + f'_c)$	0.9943	0.9932	0.086	0.132
C45-B26-475	$f'_t = 14.73\, f'_c\ /\ (123.60 + f'_c)$	0.8726	0.8471	1.840	0.607
C45-B25-400	$f'_t = 11.98\, f'_c\ /\ (92.79 + f'_c)$	0.9637	0.9564	0.625	0.354
C50-B22-460	$f'_t = 27.79\, f'_c\ /\ (311.60 + f'_c)$	0.9281	0.9138	0.459	0.303
YM-SEG-11	$f'_t = 64.00\, f'_c\ /\ (619.70 + f'_c)$	0.9390	0.9238	0.498	0.353

Table 5.24: The splitting tensile strength developments of samples for the Model-3.

Model-3	Strength Development of Actual Data [Day/Day]							Strength Development of Predicted Data [Day/Day]						
Mixing Codes	**0.5/28**	**1/28**	**2/28**	**3/28**	**7/28**	**14/28**	**28/28**	**0.5/28**	**1/28**	**2/28**	**3/28**	**7/28**	**14/28**	**28/28**
C45-III-B20	0.0382	0.1832	0.4122	0.4962	0.7557	0.6412	1.0000	0.0520	0.2223	0.4712	0.5585	0.7703	0.9371	1.0000
YM-SEG-03	0.2821	0.6581	0.7521	0.7521	0.8974	0.9487	1.0000	0.3539	0.5953	0.6803	0.7604	0.8694	0.9074	1.0000
YM-SEG-03-FSTC	-	0.7345	0.7611	0.8142	0.8053	1.0177	1.0000	0.5079	0.7073	0.7649	0.7915	0.8818	0.9390	1.0000
MIX-15A-04	0.2813	0.5938	0.7396	0.7917	0.8854	-	1.0000	0.2930	0.5799	0.7407	0.7890	0.8813	-	1.0000
YM-SEG-05	0.2525	0.5051	0.7778	0.8687	-	1.0202	1.0000	0.2216	0.5832	0.7189	0.7189	0.8644	0.9480	1.0000
YM-SEG-08	0.3203	0.4375	0.6094	0.7188	0.7344	0.7500	1.0000	0.2743	0.5518	0.6224	0.7128	0.8447	0.8906	1.0000
MIX-15E-03	0.1810	0.4571	0.6190	0.6952	0.8095	0.8190	1.0000	0.1485	0.5049	0.6383	0.7069	0.8320	0.9197	1.0000
MIX-15-AC-04	0.2203	0.4407	0.7119	0.7542	0.6017	0.8559	1.0000	0.2321	0.4996	0.6740	0.7307	0.8416	0.9059	1.0000
YM-SEG-10	-	0.4906	0.5660	0.7170	0.7642	1.0000	1.0000	-	0.4491	0.5975	0.6711	0.8036	0.9147	1.0000
DURABET PLUS AIR-AC-03	0.1667	0.3981	0.4722	0.5278	0.6389	0.8426	1.0000	0.1790	0.4009	0.4718	0.5382	0.7013	0.9186	1.0000
YM-SEG-10A	0.2793	-	0.5766	0.5676	0.8288	0.9640	1.0000	0.2632	-	0.5366	0.6177	0.7739	0.8958	1.0000
YM-SEG-10E	-	0.4434	0.6038	0.6509	0.8774	0.9811	1.0000	-	0.4819	0.5741	0.6061	0.7961	0.9180	1.0000
YM-DAP-AC-03	0.1068	0.2233	0.4466	0.5340	0.7184	0.7864	1.0000	0.0724	0.2912	0.4540	0.5157	0.7147	0.8855	1.0000
MIX-15-AC-03	0.1068	0.3981	0.6408	0.7282	0.7670	0.7864	1.0000	0.1053	0.5124	0.6392	0.7384	0.8803	0.9681	1.0000
MIX-30	0.0494	0.1728	0.3333	0.4321	0.6667	0.9383	1.0000	0.0437	0.1554	0.3351	0.4184	0.6944	0.8335	1.0000
MIX-30-03	0.2750	0.6375	0.6875	0.8125	0.9500	0.9750	1.0000	0.2993	0.6075	0.6993	0.7474	0.8556	0.9467	1.0000
MIX-30-BRT	0.0661	0.2810	0.4132	0.4380	0.6446	0.8264	1.0000	0.0560	0.2581	0.3926	0.4800	0.6838	0.8778	1.0000

Table 5.24 (continued): The splitting tensile strength developments of samples for the Model-3.

Model-3	Strength Development of Actual Data [Day/Day]							Strength Development of Predicted Data [Day/Day]						
Mixing Codes	**0.5/28**	**1/28**	**2/28**	**3/28**	**7/28**	**14/28**	**28/28**	**0.5/28**	**1/28**	**2/28**	**3/28**	**7/28**	**14/28**	**28/28**
MIX-30-07	0.0920	0.2874	0.4713	0.5977	0.7816	0.9195	1.0000	0.0873	0.3325	0.4773	0.5587	0.7322	0.9111	1.0000
MIX-34-BRT	0.1238	0.3905	0.4952	-	0.6286	0.7905	1.0000	0.0874	0.3757	0.5093	-	0.6890	0.8658	1.0000
MIX-32-03	0.1186	0.4831	0.5508	0.6610	0.7966	0.9237	1.0000	0.1245	0.4634	0.5723	0.6460	0.7569	0.8834	1.0000
MIX-32-CEN	0.0909	0.2879	0.5000	0.5909	0.8182	0.9697	1.0000	0.0819	0.3348	0.4890	0.5456	0.7470	0.9065	1.0000
MIX-32-CEN-OK	0.0545	0.3455	0.5364	0.5818	0.6000	0.8909	1.0000	0.0523	0.3066	0.5179	0.5839	0.7175	0.8710	1.0000
B70-380	0.0375	0.1125	0.2000	0.2500	0.5750	0.8000	1.0000	0.0366	0.0965	0.2010	0.2794		0.8132	1.0000
B70-420	0.0353	0.0941	0.2000	0.3412	0.5176	0.8353	1.0000	0.0305	0.1042	0.1881	0.2929		0.8965	1.0000
B47-440	0.0196	0.1961	0.3627	0.4608	0.6667	0.9608	1.0000	0.0363	0.1705	0.3442	0.4529	0.7046	0.9088	1.0000
B67-440	0.0267	0.1867	0.4533	0.5067	0.8933	1.0667	1.0000	0.0409	0.2003	0.4111	0.5375	0.7401	0.9361	1.0000
B67-440-001	0.0213	0.1489	0.2128	0.3298	0.5426	0.7128	1.0000	0.0106	0.1556	0.2257	0.3328		0.8267	1.0000
C45-B25-425	-	0.3158	0.4632	0.6421	0.8316	0.8737	1.0000	-	0.2683	0.4912	0.6938	0.8414	0.9223	1.0000
B67-440-BEY	0.0323	0.2043	0.3118	0.3763	0.6237	0.7957	1.0000	0.0226	0.1628	0.3202	0.3843		0.8484	1.0000
C45-B26-475	0.2063	0.5238	0.6349	0.7698	0.7222	0.7460	1.0000	0.1017	0.6212	0.7480	0.7640	0.8877	0.9283	1.0000
C45-B25-400	0.0348	0.4609	0.6348	0.6087	0.6435	0.7391	1.0000	0.0237	0.4564	0.6019	0.6748	0.7572	0.8543	1.0000
C50-B22-460	0.5045	0.6667	0.7117	0.8829	0.9459	0.9640	1.0000	0.4832	0.6644	0.7661	0.7935	0.8630	0.9251	1.0000
YM-SEG-11	-	0.3571	0.4732	0.5714	0.7054	0.7589	1.0000	-	0.3586	0.5256	0.5984	0.7677	0.9236	1.0000

5.3 Univariate Regression Analysis for Modulus of Elasticity

In this section of the thesis, the Table 5.27, and the Table 5.31 share the regression models with their statistical results in the study.

5.3.1 Power Regression (Model-1)

The power regression model (the Model-1) is one of the other univariate regression analysis models depending on compressive strength of concrete like the splitting tensile strength. In this model, for 0.5-day, 1-day, 2-day, 3-day, 7-day, 14-day, and 28-day modulus of elasticity estimations were represented. At the end, although R^2 (btw 0.7209 & 0.9921), and R^2_{adj} results are very high; SSE, and RMSE results are very high, as well. However, it does not mean that very high results are very off the data estimation. Because the elastic modulus test results that are used in the regression model are in four and five digits. This principal comparison indicates that presuming the modulus of elasticity has less errors from the actual data sets on the fitting planar. In this way of thinking, the development of the modulus of elasticity is settled in the Table 5.28.

In the Figure 5.37, the correlations of the actual data sets, and the predicted data sets are drawn. The correlation absolutely shows that the results of the model are satisfying. Nevertheless, FA + MS included sample results are respectively less than GGBS included sample results. Yet the model comes out safe to predict the modulus of elasticity of the concrete because of no negative deflection effects in the data fittings.

In the Figure 5.38, for the samples made of FA + MS material, the Model-1 sets forth that [(W/C) - (W/B)] of the maximum R^2 result is equal to [(W/C) - (W/B)] of the minimum R^2 result as well in the splitting tensile strength predictions. While [(CA/A) - (FA/A)] result gets higher, the R^2 result decreases which means that the FA/A ratio is more efficient on the data prediction with respect to the CA/A ratio.

In the Figure 5.39, for the samples composed of FA + MS material, the Model-1 shows that [(NS) - (CS)] of the minimum R^2 is less than [(NS) - (CS)] of the maximum R^2. Also, [(NO:1 Agg.) - (NO:2 Agg.)] of the minimum R^2 result is greater than [(NO:1 Agg.) - (NO:2 Agg.)] of the maximum R^2 result. Furthermore, [(FA) - (MS)] result of the minimum R^2 result is less than the maximum R^2 result.

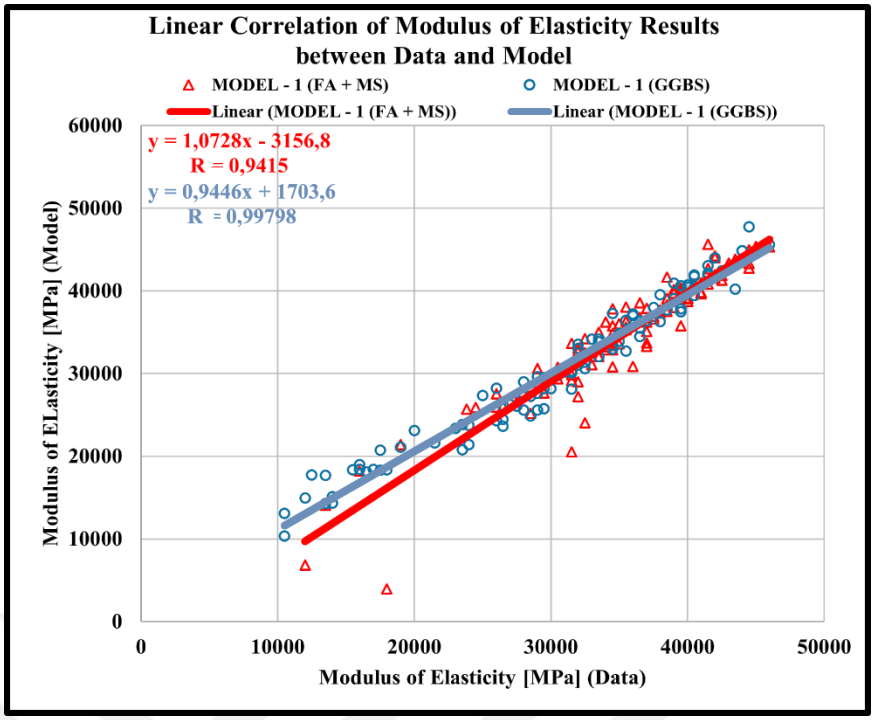

Figure 5.37: The correlations of the modulus of elasticity of the Model-1.

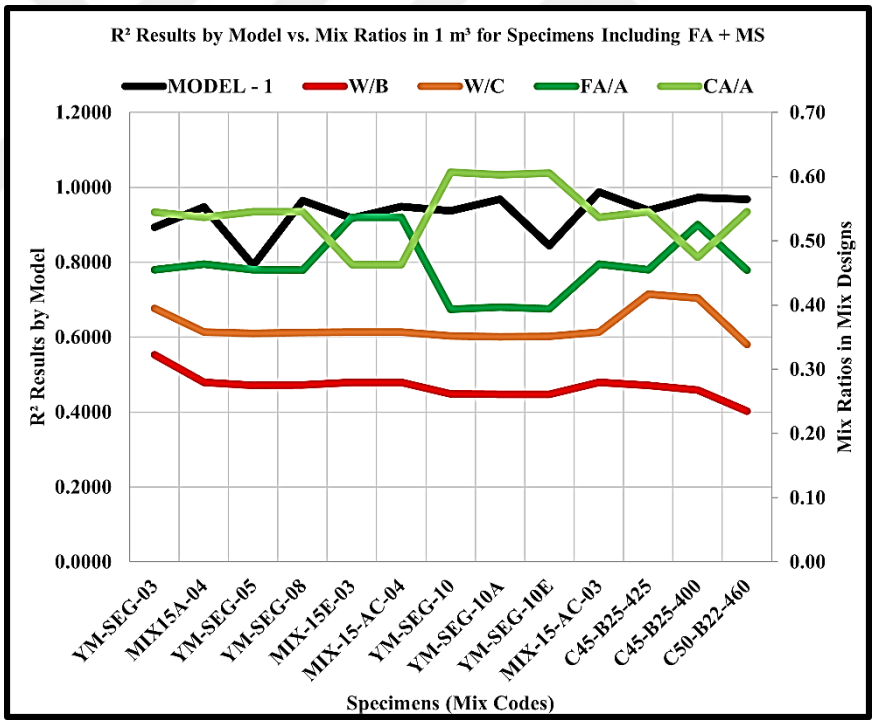

Figure 5.38: The correlations of the mixing ratios of the Model-1 in FA + MS.

Besides, the amount of water and cement for the minimum R^2 result are greater than the maximum R^2 owns. When the amount of cement is in increasing, the prediction is in decreasing. And it is inactive to use admixture in this model. On the other side, the cement types are CEMI 42.5N for both the lowest and highest R^2 results which means that the cement type is not a choice for the elastic modulus development in this model.

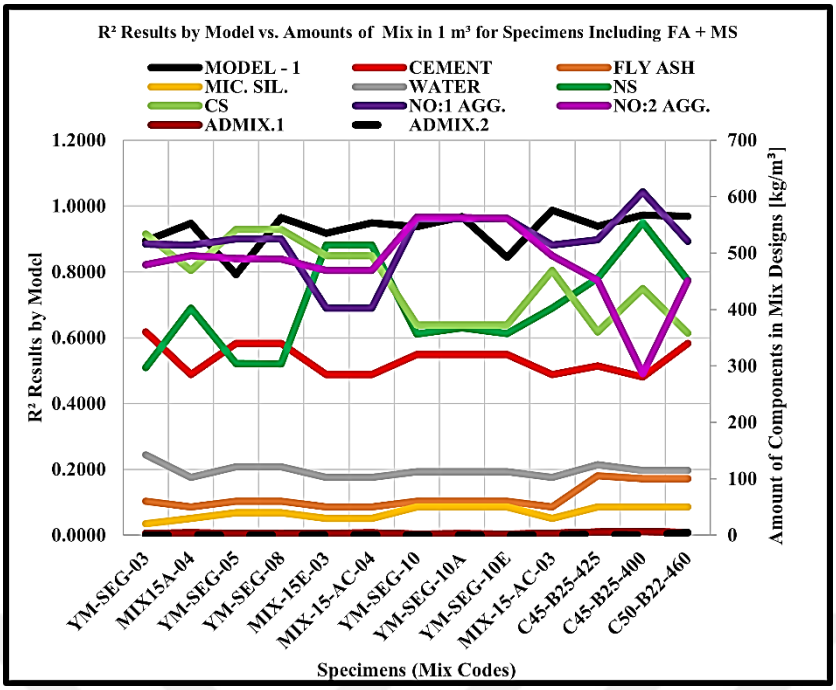

Figure 5.39: The correlations of the mixing amounts of the Model-1 in FA + MS.

In the Figure 5.40, for the samples composed of GGBS additive, the Model-1 portraits that [(W/C) – (W/B)] of the minimum R^2 is equal to [(W/C) – (W/B)] of the maximum R^2. There is also inexactness for GGBS use on the elastic modulus presuming. And while [(FA/A) - (CA/A)] result gets higher, the R^2 result increases that the FA/A ratio is more raid on the data forecasting because of the CA/A ratio.

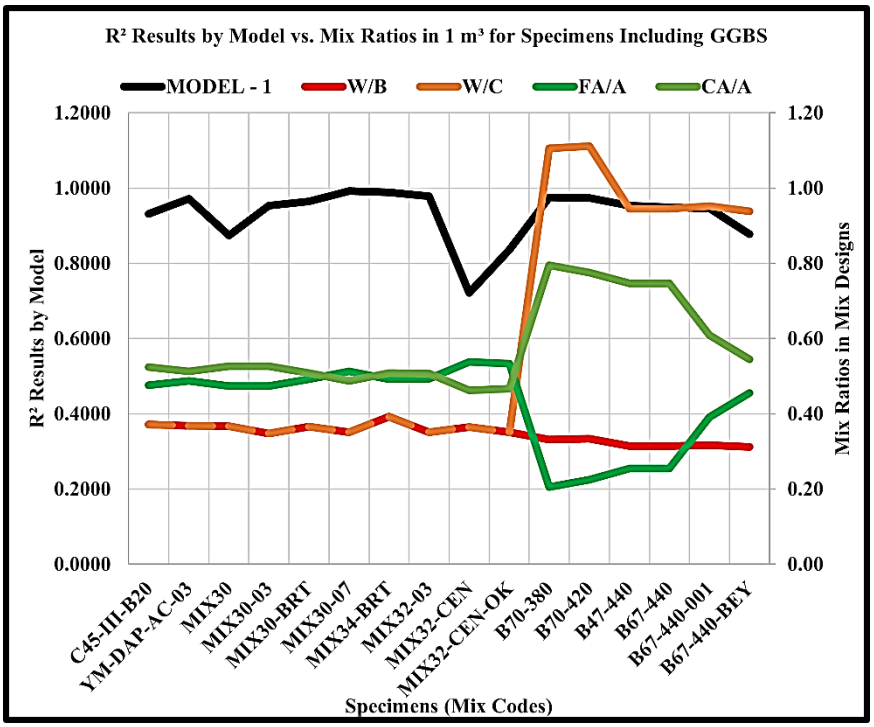

Figure 5.40: The correlations of the mixing ratios of the Model-1 in GGBS.

For the minimum R^2 result, the minimum FA/A ratio is 0.54, and the minimum CA/A ratio is 0.46. In the Figure 5.41, for the samples made of GGBS material that [(NS) - (CS)] of the maximum R^2 result is less than [(NS) - (CS)] of the minimum R^2 result. This result imposes that the amounts of natural sand imply the elastic modulus prediction. For some specimens, NO:0 Agg., NO:1 Agg., and NO:2 Agg. amounts dramatically increase the R^2 result as in the previous mechanical property models.

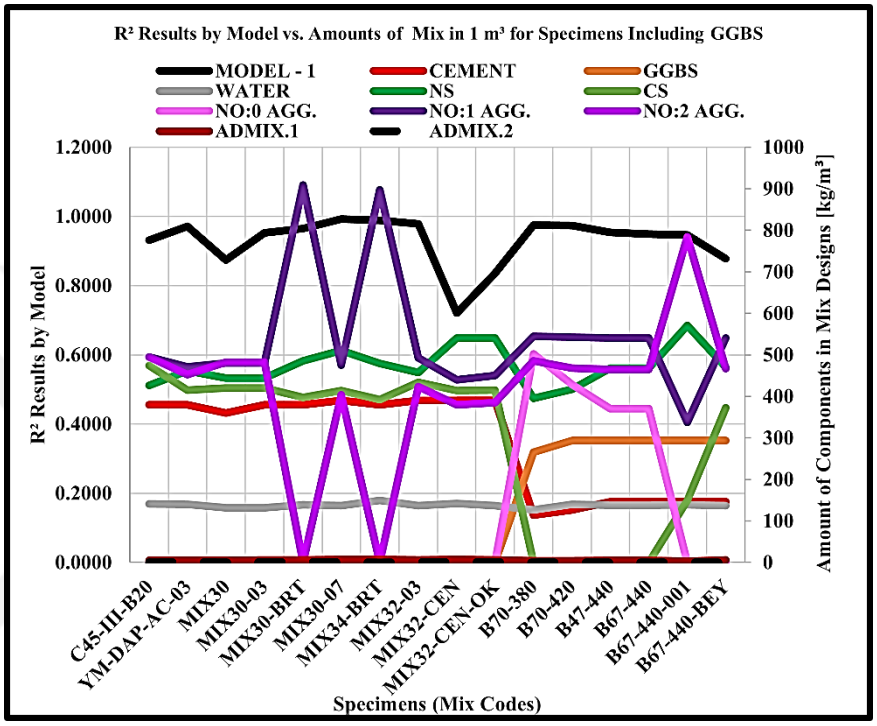

Figure 5.41: The correlations of the mixing amounts of the Model-1 in GGBS.

At the same time, the amount of water in increasing leads well predictions. Moreover, there are again some specimens composed of the GGBS theme for decreasing the elastic modulus prediction results of the concrete. For the highest R^2 result, CEMIII BS type cement is for both lowest and highest R^2 results. Out of these, there are no well represented results for the model calculation in comparing goals. Because the other results are unsuitable for any further complex comparison. In the Model-1, for both materials, the results are dictated in the boxplot which is in the Figure 5.42.

In the Figure 5.42, it is certain that FA + MS substance affects the higher modulus of elasticity estimation results than GGBS theme does. Except, day-1, day-14, and day-28, for all ages, the elastic modulus of the specimens composed of FA + MS are close and/or above the median values. Except day-14, and day-28, for all ages, the specimen elastic modulus made of GGBS subsequent is close and/or above the median values. It is seen that the elastic modulus forecasting for the specimens including FA + MS

are less appropriate. Hence, the whiskers of the specimens including GGBS substance are more descent than the specimens including FA + MS content. In the Table 5.25 and the Table 5.26, the numerical results of the boxplots are also given.

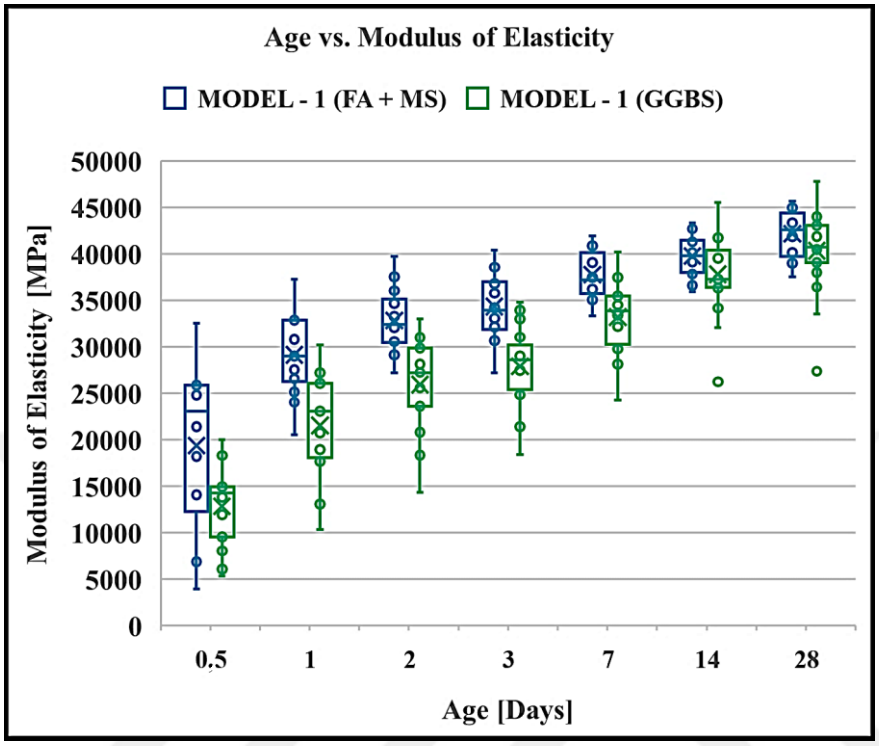

Figure 5.42: The age and the modulus of elasticity relationship for the Model-1.

Table 5.25: The CS dependent ME results in FA + MS content for the Model-1.

Model-1 [MPa]	0.5-Day	1-Day	2-Day	3-Day	7-Day	14-Day	28-Day
Minimum Value	3920	20505	27171	27171	33288	35938	37514
1st-Quartile-Value	12274	26286	30428	31855	31855	37960	39700
Median Value	23091	29001	32359	33933	33933	39813	42596
3rd-Quartile-Value	25875	32868	35117	37016	37016	41437	44387
Maximum Value	32505	37278	39717	40353	40353	43311	45640
Mean Value	19371	29122	32812	34319	34319	39736	42144
Range	28584	16772	12547	13182	7066	7373	8127

Table 5.26: The CS dependent ME results in GGBS content for the Model-1.

Model-1 [MPa]	0.5-Day	1-Day	2-Day	3-Day	7-Day	14-Day	28-Day
Minimum Value	5358	10345	14320	18422	24263	26225	27354
1st-Quartile-Value	9547	18086	23606	25386	30271	36380	39035
Median Value	14275	23081	27219	28612	33827	37244	40687
3rd-Quartile-Value	14955	26042	29832	30178	35475	40362	43035
Maximum Value	19973	30187	33006	34816	40188	45542	47751
Mean Value	12833	21534	25919	27901	33187	37781	40301
Range	14615	19841	18686	16394	15925	19317	20397

Table 5.27: The results of the regression Model-1.

Model-1					
Mixing Codes	**Power Regression**	**R^2**	**R^2_{adj}**	**SSE**	**RMSE**
C45-III-B20	$E'_c = 10980 f'^{0.33}_c$	0.9315	0.9143	33762304	2905.267
YM-SEG-03	$E'_c = 6909 f'^{0.4406}_c$	0.8939	0.8727	31016962	2490.661
YM-SEG-03-FSTC	$E'_c = 6623 f'^{0.4469}_c$	0.9466	0.9332	4870934	1103.510
MIX-15A-04	$E'_c = 11920 f'^{0.3141}_c$	0.9470	0.9338	12138774	1742.037
YM-SEG-05	$E'_c = 850.5 f'^{0.9268}_c$	0.7914	0.7393	133442880	5775.874
YM-SEG-08	$E'_c = 9452 f'^{0.3521}_c$	0.9650	0.9534	1703889	753.633
MIX-15E-03	$E'_c = 9864 f'^{0.3416}_c$	0.9175	0.9010	29761364	2439.728
MIX-15-AC-04	$E'_c = 7688 f'^{0.4186}_c$	0.9484	0.9381	22541233	2123.263
YM-SEG-10	$E'_c = 11220 f'^{0.3043}_c$	0.9371	0.9214	6004683	1225.223
DURABET PLUS AIR-AC-03	$E'_c = 8491 f'^{0.3841}_c$	0.9849	0.9819	6194402	1113.050
YM-SEG-10A	$E'_c = 10510 f'^{0.3293}_c$	0.9678	0.9598	5464025	1168.763
YM-SEG-10E	$E'_c = 8147 f'^{0.3857}_c$	0.8443	0.8054	21598383	2323.703
YM-DAP-AC-03	$E'_c = 10180 f'^{0.3314}_c$	0.9717	0.9646	5039702	1122.464
MIX-15-AC-03	$E'_c = 8159 f'^{0.3921}_c$	0.9872	0.9846	5865875	1083.132
MIX-30	$E'_c = 13210 f'^{0.2641}_c$	0.8736	0.8420	26198341	2559.216
MIX-30-03	$E'_c = 10090 f'^{0.3389}_c$	0.9527	0.9369	2379055	890.516
MIX-30-BRT	$E'_c = 9526 f'^{0.36}_c$	0.9651	0.9581	23146583	2151.585

Table 5.27 (continued): The results of the regression Model-1.

Model-1					
Mixing Codes	**Power Regression**	**R^2**	**R^2_{adj}**	**SSE**	**RMSE**
MIX-30-07	$E'_c = 9651 f'_c{}^{0.3563}$	0.9921	0.9905	3521552	839.232
MIX-34-BRT	$E'_c = 8863 f'_c{}^{0.3841}$	0.9892	0.9864	5492279	1171.781
MIX-32-03	$E'_c = 9834 f'_c{}^{0.3463}$	0.9785	0.9741	8937454	1336.971
MIX-32-CEN	$E'_c = 9777 f'_c{}^{0.286}$	0.7209	0.6512	24475018	2473.612
MIX32-CEN-OK	$E'_c = 11220 f'_c{}^{0.2674}$	0.8359	0.7949	13245223	1819.699
B70-380	$E'_c = 7025 f'_c{}^{0.4484}$	0.9753	0.9691	15291880	1955.242
B70-420	$E'_c = 5358 f'_c{}^{0.5252}$	0.9739	0.9673	21773412	2333.099
B47-440	$E'_c = 8817 f'_c{}^{0.3797}$	0.9533	0.9417	25562988	2527.993
B67-440	$E'_c = 9547 f_c^{0.3612}$	0.9482	0.9353	31731996	2816.558
B67-440-001	$E'_c = 8044 f'_c{}^{0.4021}$	0.9465	0.9332	23081486	2402.160
C45-B25-425	$E'_c = 13840 f'_c{}^{0.2461}$	0.9382	0.9228	6138540	1238.804
B67-440-BEY	$E'_c = 8046 f'_c{}^{0.3927}$	0.8775	0.8469	57766035	3800.199
C45-B26-475	$E'_c = 938.8 f'_c{}^{0.8881}$	0.8002	0.7503	74273902	4309.115
C45-B25-400	$E'_c = 6943 f'_c{}^{0.4049}$	0.9722	0.9630	2130363	842.687
C50-B22-460	$E'_c = 8479 f'_c{}^{0.3795}$	0.9682	0.9618	3373835	821.442
YM-SEG-11	$E'_c = 9362 f'_c{}^{0.3573}$	0.9544	0.9430	5279843	1148.895

Table 5.28: The elastic modulus developments of samples for the Model-1.

Model-1	Elastic Modulus Development of Actual Data [Day/Day]							Elastic Modulus Development of Predicted Data [Day/Day]						
Mixing Codes	**0.5/28**	**1/28**	**2/28**	**3/28**	**7/28**	**14/28**	**28/28**	**0.5/28**	**1/28**	**2/28**	**3/28**	**7/28**	**14/28**	**28/28**
C45-III-B20	-	0.4772	0.6547	0.7473	0.8915	0.9610	1.0000	0.3657	0.6081	0.7059	0.7556	0.8547	0.9521	1.0000
YM-SEG-03	0.6014	0.7545	0.8645	0.9087	0.9651	0.9881	1.0000	0.3557	0.6405	0.7300	-	0.8359	0.9312	1.0000
YM-SEG-03-FSTC	-	0.7616	0.8690	0.9119	0.9664	0.9885	1.0000	0.4250	0.7014	0.7670	0.8090	0.8701	0.9379	1.0000
MIX-15A-04	0.6073	0.7591	0.8674	0.9108	0.9659	-	1.0000	-	0.6700	0.7603	0.7899	0.8870	0.9587	1.0000
YM-SEG-05	0.4102	0.5863	-	0.8211	0.9273	0.9745	1.0000	-	0.6963	0.8117	0.8417	0.8972	0.9550	1.0000
YM-SEG-08	-	0.8106	-	0.9327	0.9747	0.9914	1.0000	-	0.3222	0.4518	0.5273	0.7329	0.8946	1.0000
MIX-15E-03	0.5344	0.7004	0.8292	0.8834	0.9546	0.9844	1.0000	-	0.2528	0.3499	0.4501	0.6872	0.9205	1.0000
MIX-15-AC-04	0.5101	0.6796	0.8150	0.8730	0.9502	0.9828	1.0000	-	0.4226	0.5700	0.6467	0.8091	0.9394	1.0000
YM-SEG-10	-	0.7216	0.8434	0.8936	0.9589	0.9859	1.0000	-	0.3940	0.5449	0.6280	0.7687	0.9339	1.0000
DURABET PLUS AIR-AC-03	0.4424	0.6177	0.7704	0.8396	0.9357	0.9776	1.0000	-	0.4472	0.5216	0.6140	0.7485	0.9150	1.0000
YM-SEG-10A	0.6187	-	0.8729	0.9146	0.9675	0.9889	1.0000	-	0.6936	0.8147	0.8972	0.9491	0.9756	1.0000
YM-SEG-10E	-	0.6644	0.8043	0.8651	0.9469	0.9816	1.0000	-	0.4363	0.5802	0.6285	0.8033	0.9154	1.0000
YM-DAP-AC-03	-	0.5952	0.7533	0.8265	0.9297	0.9754	1.0000	0.5435	0.6794	-	0.6976	0.8475	0.9007	1.0000
MIX-15-AC-03	0.4492	0.6243	0.7753	0.8433	0.9373	0.9782	1.0000	-	0.7263	0.7750	0.8302	0.8963	-	1.0000
MIX-30	-	0.5633	0.7282	0.8069	0.9207	0.9721	1.0000	0.9257	0.7505	0.8607	0.9170	0.9317	0.9682	1.0000
MIX-30-03	-	0.7763	-	0.9183	0.9690	0.9894	1.0000	-	0.6797	0.7832	0.8221	0.9033	0.9697	1.0000
MIX-30-BRT	0.3832	0.5586	0.7244	0.8039	0.9193	0.9716	1.0000	0.3657	0.6081	0.7059	0.7556	0.8547	0.9521	1.0000

Table 5.28 (continued): The elastic modulus developments of samples for the Model-1.

Model-1	Elastic Modulus Development of Actual Data [Day/Day]							Elastic Modulus Development of Predicted Data [Day/Day]						
Mixing Codes	**0.5/28**	**1/28**	**2/28**	**3/28**	**7/28**	**14/28**	**28/28**	**0.5/28**	**1/28**	**2/28**	**3/28**	**7/28**	**14/28**	**28/28**
MIX-30-07	0.3982	0.5741	0.7368	0.8137	0.9239	0.9733	1.0000	-	0.4834	0.6563	0.7103	0.8416	0.9537	1.0000
MIX-34-BRT	0.4267	0.6026	0.7590	-	0.9317	0.9762	1.0000	0.5705	0.7436	0.7993	0.8504	0.9188	0.9424	1.0000
MIX-32-03	0.4822	0.6548	0.7976	0.8601	0.9447	0.9808	1.0000	-	0.7501	0.7950	0.8163	0.8917	0.9425	1.0000
MIX-32-CEN	-	0.6366	0.7844	0.8502	0.9404	0.9793	1.0000	0.5832	0.7626	0.8525	0.8793	0.9312	-	1.0000
MIX-32-CEN-OK	-	0.6991	0.8283	0.8827	0.9544	0.9843	1.0000	0.5953	0.4493	-	0.6281	0.7837	0.9114	1.0000
B70-380	-	0.2905	0.4595	0.5702	0.7865	0.9170	1.0000	-	0.7996	-	0.8495	0.9196	0.9435	1.0000
B70-420	-	0.2133	0.3603	0.4677	0.7093	0.8798	1.0000	0.4580	0.7302	0.8070	0.8447	0.9116	0.9578	1.0000
B47-440	-	0.4017	0.5823	0.6850	0.8580	0.9477	1.0000	0.4709	0.6783	0.7935	0.8298	0.8998	0.9403	1.0000
B67-440	-	0.3754	0.5552	0.6607	0.8440	0.9419	1.0000	-	0.7190	0.8009	0.8388	0.9047	0.9587	1.0000
B67-440-001	-	0.3842	0.5644	0.6690	0.8488	0.9440	1.0000	0.4402	0.6227	0.6713	0.7149	0.8168	0.9496	1.0000
C45-B25-425	-	0.6882	0.8209	0.8773	0.9521	0.9835	1.0000	0.6190	-	0.7939	0.8353	0.9074	0.9587	1.0000
B67-440-BEY	-	0.4146	0.5953	0.6965	0.8644	0.9503	1.0000	-	0.6944	0.7531	0.7727	0.8844	0.9537	1.0000
C45-B26-475	0.5192	0.6875	-	0.8770	0.9519	0.9834	1.0000	-	0.6041	0.7137	0.7502	0.8581	0.9440	1.0000
C45-B25-400	-	0.7099	0.8356	0.8880	0.9566	-	1.0000	0.3604	0.7094	0.7889	0.8483	0.9310	0.9816	1.0000
C50-B22-460	0.7414	0.8538	0.9238	0.9498	0.9813	0.9937	1.0000	-	0.5691	0.7068	0.7545	0.8828	0.9381	1.0000
YM-SEG-11	-	0.6738	0.8109	0.8700	0.9489	0.9824	1.0000	-	0.7852	-	0.8166	0.8904	0.9576	1.0000

5.3.2 Fraction Power Regression (Model-2)

The power regression model (the Model-2) is the other univariate regression analysis model depending on compressive strength of concrete like the Model-1. In this model, for 0.5-day, 1-day, 2-day, 3-day, 7-day, 14-day, and 28-day modulus of elasticity presuming was studied. At the end, R^2 (btw 0.3942 & 0.9955), and R^2_{adj} results are high, and seen for some specimens, the results are under the expectations. Why SSE and RMSE results are very high is because of the elastic modulus test results used in the regression model in four, and five digits. This indicates that presuming of the modulus of elasticity has less errors from the actual data sets on the fitting planar. By this way, the modulus of elasticity development is shown in the Table 5.32.

In the Figure 5.43, the correlations of the actual data sets and predicted data sets are showed off. The correlation shows that the results of the model are satisfying, and safe for data presuming without negative deflections in data fitting planar, though FA + MS contented sample results are respectively lower in contrast with the first model.

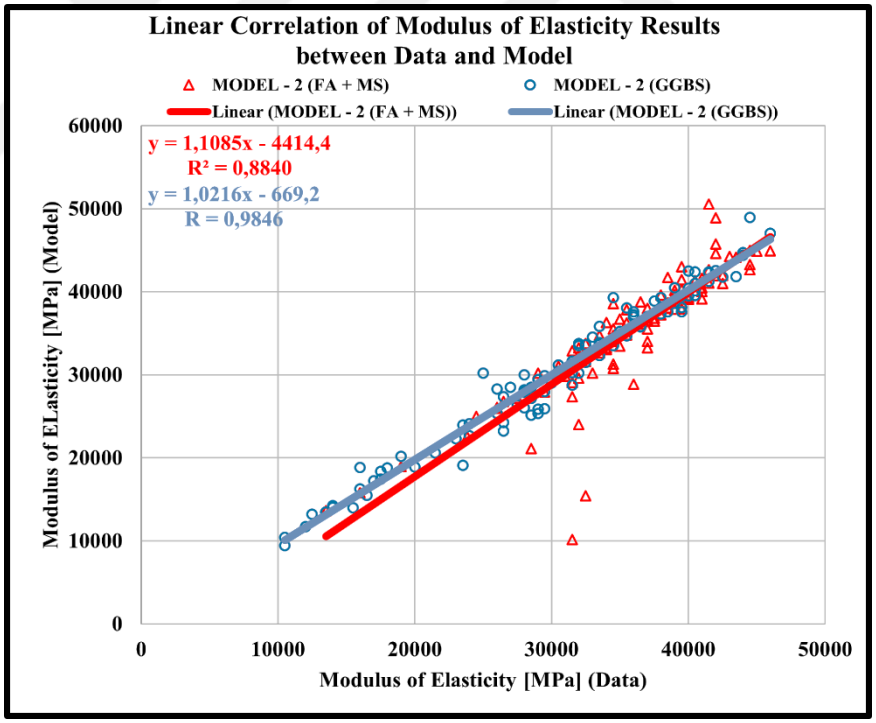

Figure 5.43: The correlations of the modulus of elasticity of the Model-2.

In the Figure 5.44, for the samples made of FA + MS material, the Model-2 is showed up that [(W/C) - (W/B)] of the maximum R^2 result is equal to [(W/C) - (W/B)] of the minimum R^2 result. While [(CA/A) - (FA/A)] result gets higher, the R^2 result also decreases which means that the CA/A ratio is operative on the data prediction than the FA/A ratio.

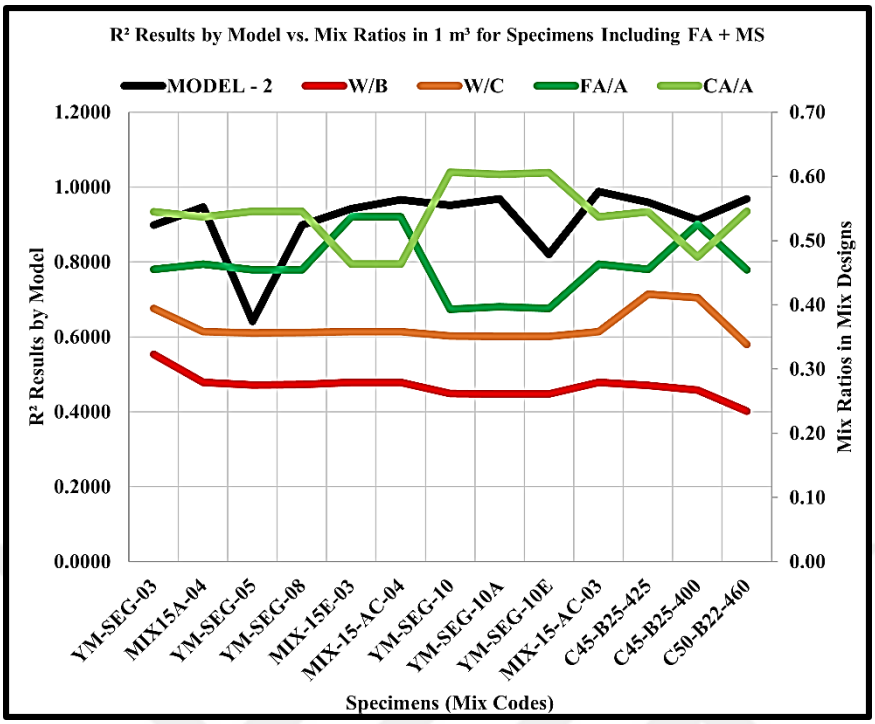

Figure 5.44: The correlations of the mixing ratios of the Model-2 in FA + MS.

In the Figure 5.45, the amounts of water and cement for the minimum R^2 result are greater than the maximum R^2 water and cement contents. When the amount of cement is in increasing, the prediction is in decreasing. And it is impression for using admixture in this model. On the side, the cement types are CEMI 42.5N for both the lowest and highest R^2 results which means that the cement type could not be interpreted for the elastic modulus development in this model. Moreover, [(NS) - (CS)] of the maximum R^2 result is greater than [(NS) - (CS)] of the minimum R^2 result. In an opposite case, [(NO:1 Agg.) - (NO:2 Agg.)] of the maximum R^2 result is less than [(NO:1 Agg.) - (NO:2 Agg.)] of the minimum R^2 result. The minimum NS is 304.00 kg/m^3, and the maximum CS material is 542.00 kg/m^3 for the minimum R^2 result. The minimum water content is 102.00 kg/m^3, the minimum FA substance is 50.00 kg/m^3, and the minimum MS ingredient is 30.00 kg/m^3 for the maximum R^2 result in this model results.

In the Figure 5.46, for the samples made of GGBS material, the Model-2 describes that [(W/C) – (W/B)] of the minimum R^2 result is less than [(W/C) – (W/B)] of the maximum R^2 result. And there are no effects of GGBS use on the modulus of elasticity estimation, even though GGBS is a combining material. While [(CA/A) - (FA/A)]

result gets higher, the R^2 result also increases which means that the CA/A ratio is more incursive on the data prediction because of the FA/A ratio.

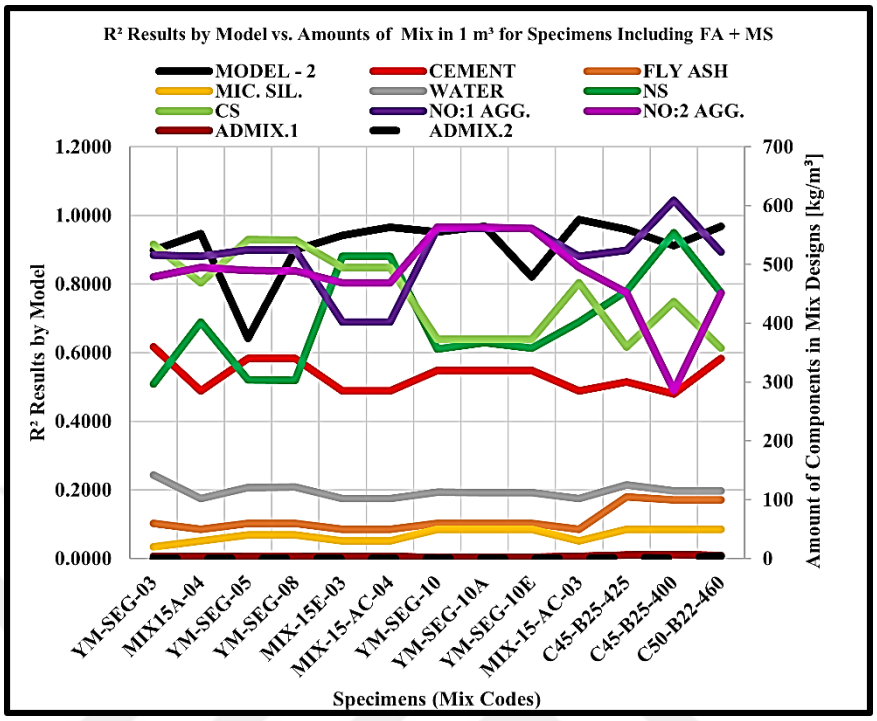

Figure 5.45: The correlations of the mixing amounts of the Model-2 in FA + MS.

For the minimum R^2 result, the maximum FA/A ratio is 0.54, and the minimum CA/A ratio is 0.46. For the maximum R^2 result FA/A ratio is 0.20, and the minimum CA/A ratio is 0.80.

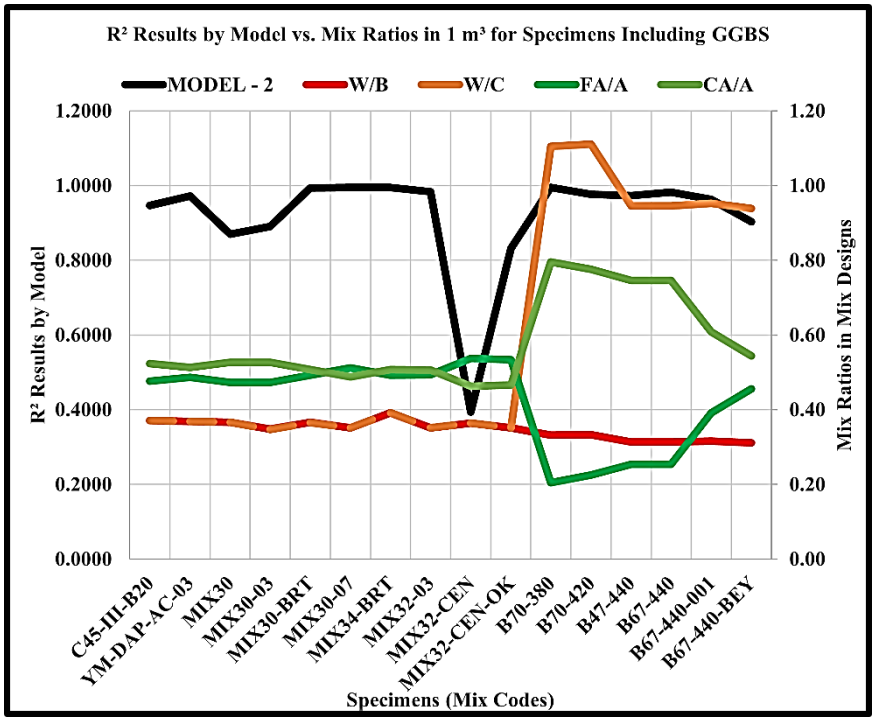

Figure 5.46: The correlations of the mixing ratios of the Model-2 in GGBS.

In the Figure 5.47, for the samples compound of GGBS content that [(NS) - (CS)] of the maximum R^2 result is greater than [(NS) - (CS)] of the minimum R^2 result. This describes that the amounts of natural sand impose the elastic modulus prediction. For some specimens, NO:0 Agg., NO:1 Agg., and NO:2 Agg. amounts dramatically increase the R^2 result. Meanwhile, the amount of water in increasing causes worse results. Also, there are some specimens composed of the GGBS substance for decreasing the elastic modulus estimation results of the concrete. For the highest R^2 result, CEMI 52.5N type cement, and for the lowest R^2 result, CEMIII 32.5 type cement are decisive. Onto these results, the maximum R^2 result has the minimum cement (114.00 kg/m^3), minimum CS (0.00 kg/m^3), minimum NS (395.00 kg/m^3), maximum NO:0 Agg. (486.00 kg/m^3) contents with GGBS (266.00 kg/m^3) substance. There are no other well-presented results for the model calculation for any other comparative issues. As the other results are inappropriate for any comparison. In the Model-2, for both materials, the results are followed in the boxplot which is in the Figure 5.48**.**

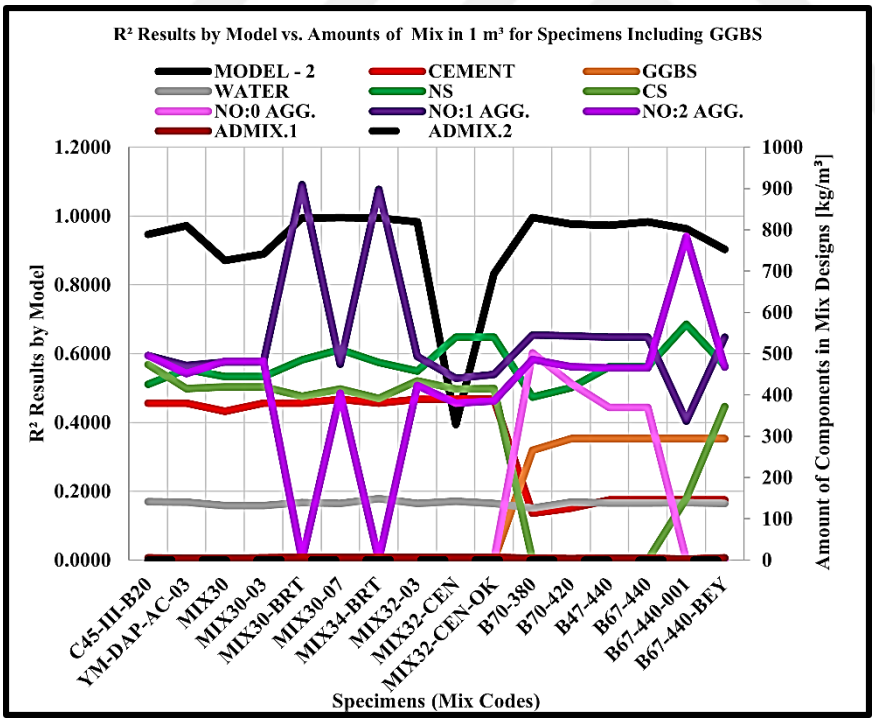

Figure 5.47: The correlations of the mixing amounts of the Model-2 in GGBS.

In the Figure 5.48, it is certain that FA + MS content influences the higher modulus of elasticity prediction results than GGBS content does. Except, day-0.5, day-1, and day-28, for all ages, the elastic modulus of the specimens composed of FA + MS content are close and/or above the median values. Except day-0.5, day-2, and day-3, for all

ages, the specimen elastic modulus composed of GGBS content are close and/or above the median values. It is understood that the elastic modulus presuming for the specimens including FA + MS are less suitable. That is why, the whiskers of the specimens including GGBS content are more ascendent than the specimens including FA + MS content as shown in the Table 5.29 and the Table 5.30.

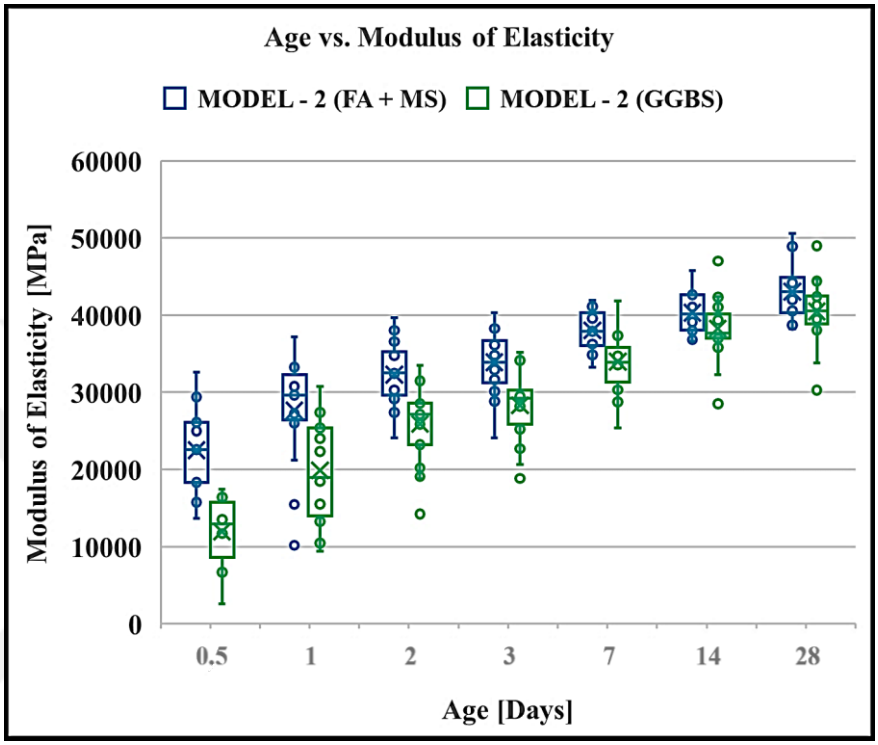

Figure 5.48: The age and the modulus of elasticity relationship for the Model-2.

Table 5.29: The CS dependent ME results in FA + MS content for the Model-2.

Model-1 [MPa]	0.5-Day	1-Day	2-Day	3-Day	7-Day	14-Day	28-Day
Minimum Value	13636	10173	24061	24061	33232	36596	38253
1st-Quartile-Value	18327	26397	29650	31273	36069	38023	40277
Median Value	22572	29602	32517	33885	37930	40152	43065
3rd-Quartile-Value	26077	32260	35212	36655	40283	42666	44868
Maximum Value	32606	37206	39642	40286	41902	45737	50566
Mean Value	22483	27624	32260	33872	38033	40322	43017
Range	18970	27033	15581	16225	8670	9141	12313

Table 5.30: The CS dependent ME results in GGBS content for the Model-2.

Model-1 [MPa]	0.5-Day	1-Day	2-Day	3-Day	7-Day	14-Day	28-Day
Minimum Value	2552	9417	14238	18845	25352	28533	30260
1st-Quartile-Value	8591	13961	23215	25823	31344	36977	38887
Median Value	12979	18949	27140	29217	33860	37660	40541
3rd-Quartile-Value	15776	25349	28550	30245	35807	40138	42497
Maximum Value	17425	30749	33492	35191	41802	47016	48996
Mean Value	11951	19879	25904	28302	33964	38272	40485
Range	14873	21333	19254	16346	16450	18483	18736

Table 5.31: The results of the regression Model-2.

Model-2					
Mixing Codes	**Fraction Power Regression**	**R^2**	**R^2_{adj}**	**SSE**	**RMSE**
C45-III-B20	$E'_c = 1175000 f'_c{}^{0.01118} - 1186000$	0.9466	0.9111	26287816	2960.170
YM-SEG-03	$E'_c = 80820 f'_c{}^{0.1236} - 92070$	0.8985	0.8478	29679019	2723.923
YM-SEG-03-FSTC	$E'_c = 64.52 f'_c{}^{1.343} + 25300$	0.9539	0.9232	4200531	1183.291
MIX-15A-04	$E'_c = 582500 f'_c{}^{0.02061} - 590000$	0.9472	0.9119	12110048	2009.150
YM-SEG-05	$E'_c = 421300 f'_c{}^{0.08114} - 546500$	0.6420	0.2840	198568796	9964.156
YM-SEG-08	$E'_c = 84450 f'_c{}^{0.1246} - 100500$	0.8991	0.7981	4915156	1567.666
MIX-15E-03	$E'_c = 476400 f'_c{}^{0.02022} - 478200$	0.9417	0.8834	21038506	2648.176
MIX-15-AC-04	$E'_c = 304500 f'_c{}^{0.04114} - 317700$	0.9660	0.9490	14860082	1927.439
YM-SEG-10	$E'_c = 229 f'_c{}^{1.016} + 24300$	0.9517	0.9195	4611561	1239.833
DURABET PLUS AIR-AC-03	$E'_c = 39100 f'_c{}^{0.1694} - 37710$	0.9902	0.9854	4000113	1000.014
YM-SEG-10A	$E'_c = 5441 f'_c{}^{0.4357} + 8117$	0.9684	0.9473	5367424	1337.588
YM-SEG-10E	$E'_c = 174500 f'_c{}^{0.06871} - 190800$	0.8211	0.7018	24820154	2876.349
YM-DAP-AC-03	$E'_c = 5049 f'_c{}^{0.4478} + 8103$	0.9722	0.9537	4946689	1284.094
MIX-15-AC-03	$E'_c = 13650 f'_c{}^{0.304} - 7169$	0.9882	0.9823	5399619	1161.854
MIX-30	$E'_c = 1108000 f'_c{}^{0.008112} - 1105000$	0.8704	0.7840	26855239	2991.947
MIX-30-03	$E'_c = 163300 f'_c{}^{0.06934} - 175300$	0.8900	0.7800	5533560	1663.364
MIX-30-BRT	$E'_c = 415500 f'_c{}^{0.02326} - 416100$	0.9941	0.9911	3922215	990.229

Table 5.31 (continued): The results of the regression Model-2.

Model-2					
Mixing Codes	**Fraction Power Regression**	**R^2**	**R^2_{adj}**	**SSE**	**RMSE**
MIX-30-07	$E'_c = 20430\, f'^{\,0.2365}_c - 13020$	0.9951	0.9926	2196318	740.999
MIX-34-BRT	$E'_c = 28100\, f'^{\,0.2063}_c - 23380$	0.9945	0.9908	2808252	967.514
MIX-32-03	$E'_c = 34620\, f'^{\,0.1721}_c - 29700$	0.9832	0.9748	6957106	1318.816
MIX-32-CEN	$E'_c = 988900\, f'^{\,0.01139}_c - 1000000$	0.3942	-0.0097	53135832	4208.556
MIX32-CEN-OK	$E'_c = 290600\, f'^{\,0.02656}_c - 290200$	0.8324	0.7206	13528744	2123.577
B70-380	$E'_c = 239100\, f'^{\,0.04288}_c - 243300$	0.9955	0.9924	2818646	969.303
B70-420	$E'_c = 11130\, f'^{\,0.3835}_c - 8578$	0.9762	0.9603	19845420	2571.991
B47-440	$E'_c = 537500\, f'^{\,0.02155}_c - 545100$	0.9727	0.9545	14956485	2232.822
B67-440	$E'_c = 975100\, f'^{\,0.012}_c - 981800$	0.9824	0.9706	10804253	1897.740
B67-440-001	$E'_c = 594200\, f'^{\,0.01974}_c - 602800$	0.9627	0.9378	16119846	2318.034
C45-B25-425	$E'_c = 208.2\, f'^{\,1.047}_c + 23770$	0.9597	0.9328	4003876	1155.260
B67-440-BEY	$E'_c = 1142000\, f'^{\,0.0117}_c - 1156000$	0.9034	0.8389	45570109	3897.440
C45-B26-475	$E'_c = 253800\, f'^{\,0.1192}_c - 376700$	0.6067	0.3446	146223833	6981.495
C45-B25-400	$E'_c = 307700\, f'^{\,0.04779}_c - 337000$	0.9119	0.8238	6757250	1838.104
C50-B22-460	$E'_c = 3656\, f'^{\,0.514}_c + 10040$	0.9685	0.9528	3338754	913.613
YM-SEG-11	$E'_c = 291.7\, f'^{\,1.035}_c + 21250$	0.9654	0.9424	4000384	1154.756

Table 5.32: The elastic modulus developments of samples for the Model-2.

Model-2	Elastic Modulus Development of Actual Data [Day/Day]							Elastic Modulus Development of Predicted Data [Day/Day]						
Mixing Codes	**0.5/28**	**1/28**	**2/28**	**3/28**	**7/28**	**14/28**	**28/28**	**0.5/28**	**1/28**	**2/28**	**3/28**	**7/28**	**14/28**	**28/28**
C45-III-B20	-	0.4772	0.6547	0.7473	0.8915	0.9610	1.0000	-	0.3868	0.6429	0.7096	0.8532	0.9596	1.0000
YM-SEG-03	0.6014	0.7545	0.8645	0.9087	0.9651	0.9881	1.0000	0.5557	0.7568	0.8142	0.8645	0.9284	0.9497	1.0000
YM-SEG-03-FSTC	-	0.7616	0.8690	0.9119	0.9664	0.9885	1.0000	-	0.7531	0.7874	0.8051	0.8756	0.9304	1.0000
MIX-15A-04	0.6073	0.7591	0.8674	0.9108	0.9659	-	1.0000	0.5057	0.7493	0.8518	0.8805	0.9336	-	1.0000
YM-SEG-05	0.4102	0.5863	-	0.8211	0.9273	0.9745	1.0000	-	-	-	-	-	-	-
YM-SEG-08	-	0.8106	-	0.9327	0.9747	0.9914	1.0000	-	0.7510	-	0.8164	0.9043	0.9333	1.0000
MIX-15E-03	0.5344	0.7004	0.8292	0.8834	0.9546	0.9844	1.0000	0.4030	0.7563	0.8334	0.8686	0.9278	0.9663	1.0000
MIX-15-AC-04	0.5101	0.6796	0.8150	0.8730	0.9502	0.9828	1.0000	0.4233	0.6975	0.8183	0.8531	0.9165	0.9513	1.0000
YM-SEG-10	-	0.7216	0.8434	0.8936	0.9589	0.9859	1.0000	-	0.7249	0.7842	0.8170	0.8828	0.9458	1.0000
DURABET PLUS AIR-AC-03	0.4424	0.6177	0.7704	0.8396	0.9357	0.9776	1.0000	0.4190	0.6392	0.6916	0.7367	0.8367	0.9568	1.0000
YM-SEG-10A	0.6187	-	0.8729	0.9146	0.9675	0.9889	1.0000	0.6210	-	0.7878	0.8291	0.9026	0.9562	1.0000
YM-SEG-10E	-	0.6644	0.8043	0.8651	0.9469	0.9816	1.0000	-	0.6409	0.7187	0.7437	0.8765	0.9520	1.0000
YM-DAP-AC-03	-	0.5952	0.7533	0.8265	0.9297	0.9754	1.0000	-	0.6072	0.7089	0.7441	0.8515	0.9404	1.0000
MIX-15-AC-03	0.4492	0.6243	0.7753	0.8433	0.9373	0.9782	1.0000	0.3521	0.7231	0.8010	0.8581	0.9361	0.9830	1.0000
MIX-30	-	0.5633	0.7282	0.8069	0.9207	0.9721	1.0000	-	0.4843	0.6816	0.7412	0.8852	0.9411	1.0000
MIX-30-03	-	0.7763	-	0.9183	0.9690	0.9894	1.0000	-	0.7342	-	0.7763	0.8707	0.9514	1.0000
MIX-30-BRT	0.3832	0.5586	0.7244	0.8039	0.9193	0.9716	1.0000	0.2746	0.6437	0.7498	0.8017	0.8953	0.9635	1.0000

Table 5.32 (continued): The elastic modulus developments of samples for the Model-2.

Model-2	Elastic Modulus Development of Actual Data [Day/Day]							Elastic Modulus Development of Predicted Data [Day/Day]						
Mixing Codes	**0.5/28**	**1/28**	**2/28**	**3/28**	**7/28**	**14/28**	**28/28**	**0.5/28**	**1/28**	**2/28**	**3/28**	**7/28**	**14/28**	**28/28**
MIX-30-07	0.3982	0.5741	0.7368	0.8137	0.9239	0.9733	1.0000	0.3487	0.6240	0.7240	0.7731	0.8677	0.9571	1.0000
MIX-34-BRT	0.4267	0.6026	0.7590	-	0.9317	0.9762	1.0000	0.3356	0.6682	0.7574	-	0.8569	0.9414	1.0000
MIX-32-03	0.4822	0.6548	0.7976	0.8601	0.9447	0.9808	1.0000	0.4110	0.7252	0.7899	0.8300	0.8863	0.9467	1.0000
MIX-32-CEN	-	0.6366	0.7844	0.8502	0.9404	0.9793	1.0000	-	0.4614	0.6304	0.6817	0.8378	0.9429	1.0000
MIX-32-CEN-OK	-	0.6991	0.8283	0.8827	0.9544	0.9843	1.0000	-	0.6614	0.8033	0.8373	0.8973	0.9562	1.0000
B70-380	-	0.2905	0.4595	0.5702	0.7865	0.9170	1.0000	-	0.2646	0.4758	0.5747	0.7902	0.9241	1.0000
B70-420	-	0.2133	0.3603	0.4677	0.7093	0.8798	1.0000	-	0.2323	0.3512	0.4648	0.7097	0.9289	1.0000
B47-440	-	0.4017	0.5823	0.6850	0.8580	0.9477	1.0000	-	0.3662	0.5830	0.6754	0.8413	0.9530	1.0000
B67-440	-	0.3754	0.5552	0.6607	0.8440	0.9419	1.0000	-	0.3007	0.5418	0.6481	0.8003	0.9479	1.0000
B67-440-001	-	0.3842	0.5644	0.6690	0.8488	0.9440	1.0000	-	0.3836	0.4997	0.6235	0.7753	0.9308	1.0000
C45-B25-425	-	0.6882	0.8209	0.8773	0.9521	0.9835	1.0000	-	0.7012	0.7797	0.8600	0.9245	0.9622	1.0000
B67-440-BEY	-	0.4146	0.5953	0.6965	0.8644	0.9503	1.0000	-	0.3116	0.5463	0.6124	0.8166	0.9258	1.0000
C45-B26-475	0.5192	0.6875	-	0.8770	0.9519	0.9834	1.0000	0.3163	0.5601	-	0.5895	0.8090	0.8787	1.0000
C45-B25-400	-	0.7099	0.8356	0.8880	0.9566	-	1.0000	-	0.6618	0.7295	0.8017	0.8828	-	1.0000
C50-B22-460	0.7414	0.8538	0.9238	0.9498	0.9813	0.9937	1.0000	0.9567	0.7525	0.8587	0.9149	0.9298	0.9671	1.0000
YM-SEG-11	-	0.6738	0.8109	0.8700	0.9489	0.9824	1.0000	-	0.6887	0.7653	0.7997	0.8820	0.9605	1.0000

5.4 Multivariate Regression Analysis for Compressive Strength

In this section of the thesis, the Table 5.33, the Table 5.34, the Table 5.35, the Table 5.39, the Table 5.40, and the Table 5.41 publish the regression models with their statistical results.

5.4.1 Linear Regression (Model-1)

The linear regression model (the Model-1) is one of the multivariate regression analysis models depending on many variables such as W/C ratio, fly ash, coarse aggregate, and cement contents of concrete mixture design. In this model, for 0.5-day, 1-day, 2-day, 3-day, 7-day, 14-day, and 28-day compressive strength predictions were showed off. At the end, for the FA + MS content included samples, R^2 (btw 0.4471 & 0.9145), and R^2_{adj} results are scattered in the concrete ages; SSE, and RMSE results are also diverted at each concrete ages. For the GGBS included samples, R^2 (btw 0.1498 & 0.5590), and R^2_{adj} results are come out in the concrete ages; SSE, and RMSE results are varied in a large numeric scale for each concrete age. On the side, all data predictions are applied on these solutions, and the results are come out well in the results of R^2 except the samples in MIX-30 (R^2 = 0.1888), and MIX-CEN-32 (R^2 = 0.1693) mixing codes, which are under the expectations with respect to the other sample results. In this way of the results, the strength development of the compressive strength is settled in the Table 5.38.

In the Figure 5.49, the correlations of the actual data sets and the estimated data sets are trendlined. The correlations easily demonstrate that the results of the model are satisfying, and the model steps forward safe to predict the compressive strength of the concrete because of no negative deflection effects in the data fittings.

In the Figure 5.50, there is another correlation for material effect in the compressive strength prediction in terms of FA + MS material by using the coefficients of the model equation. In this way, it is seen that the more R^2 result is decreased, the more equation coefficient that intersects the *y* axis (the predicted data axis) is decreased for all ages, except the day-1, and day-2. For the day-1, day-2, day-14, and day-28, the W/C ratio coefficient operates the model opposite to the R^2 value which means that higher effects of the W/C ratio decrease the data prediction potential. For the FA, CA, and C content, the results of the models seem parallel to the each. And the effects of these contents

are antipoles of R^2 values at days 0.5, 14, and 28 which means that for day-0.5, day-14, and day-28, the compressive strength estimation get worse results.

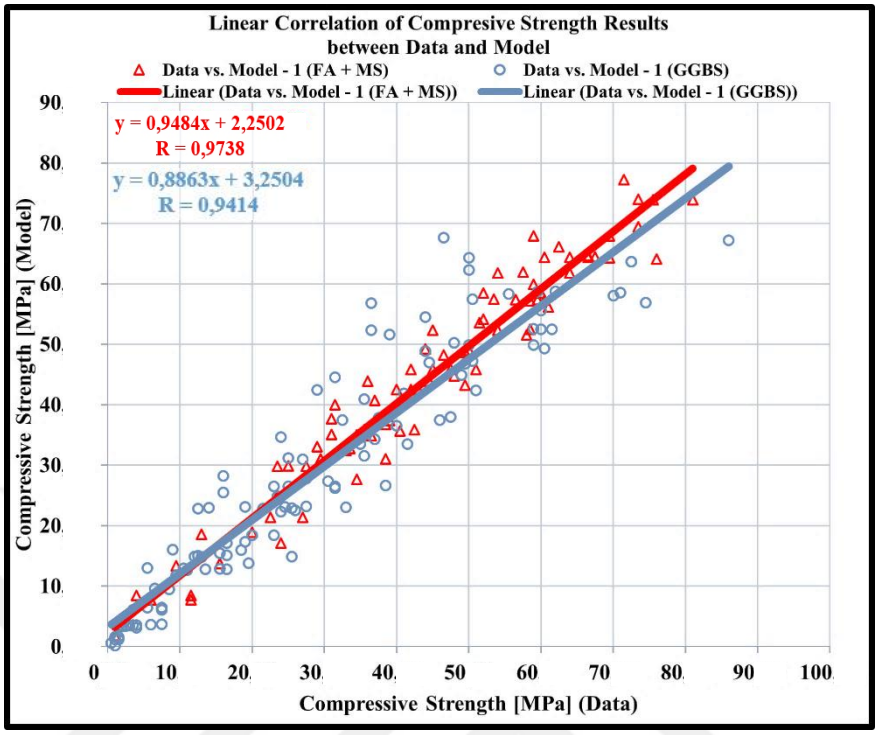

Figure 5.49: The correlations of the compressive strength of the Model-1.

Table 5.33: The MRA results for CS in FA + MS content for the Model-1.

Age	Linear Regression	R^2	R^2_{adj}	SSE	RMSE
0.5-Day	$f'_c = 520.6498 - 85.0946(w/c) - 0.2586FA - 0.2532CA - 0.0039C$	0.9145	0.8461	69.6246	3.7316
1-Day	$f'_c = 135.4715 - 186.8535(w/c) - 0.0287FA - 0.0895CA + 0.2388C$	0.7629	0.6274	217.9290	6.6020
2-Day	$f'_c = 199.8592 - 181.0989(w/c) - 0.0496FA - 0.1145CA + 0.1992C$	0.6997	0.5496	261.7889	7.2359
3-Day	$f'_c = 229.4816 - 105.5039(w/c) - 0.0757FA - 0.1336CA + 0.1573C$	0.6656	0.4985	234.5830	6.8496
7-Day	$f'_c = 149.4673 - 98.8345(w/c) - 0.0409FA - 0.0883CA + 0.1982C$	0.7590	0.6385	142.0112	5.3294
14-Day	$f'_c = 113.7616 - 94.5868(w/c) - 0.0237FA - 0.0593CA + 0.1896C$	0.6820	0.5003	156.1472	5.5883
28-Day	$f'_c = -10.4308 - 33.4529(w/c) - 0.0328FA - 0.0118CA + 0.2372C$	0.4471	0.1707	439.6684	9.3773

Table 5.34: The MRA results for CS in GGBS content for the Model-1.

Age	Linear Regression	R^2	R^2_{adj}	SSE	RMSE
0.5-Day	$f'_c = 4.7885 - 2.5613(w/c) - 0.0041FA - 0.0002CA + 0.0089C$	0.4399	0.2363	30.8652	2.4846
1-Day	$f'_c = 57.2416 - 5.4939(w/c) - 0.0341FA - 0.0338CA + 0.0436C$	0.5225	0.3489	287.9023	7.5882
2-Day	$f'_c = 41.0881 - 19.1937(w/c) - 0.0052FA - 0.0051CA - 0.0053C$	0.5590	0.3986	381.8806	8.7393
3-Day	$f'_c = 47.6756 - 42.7535(w/c) + 0.0081FA + 0.0119CA - 0.0618C$	0.4527	0.2338	496.0881	9.9608
7-Day	$f'_c = 29.2402 - 76.7295(w/c) + 0.0478FA + 0.0553CA - 0.1475C$	0.3042	0.0512	742.5425	12.1864
14-Day	$f'_c = 31.2864 - 101.9699(w/c) + 0.0671FA + 0.0855CA - 0.2145C$	0.1498	-0.1593	1574.8985	17.7477
28-Day	$f'_c = 46.8856 - 129.5414(w/c) + 0.0859FA + 0.1031CA - 0.2918C$	0.1679	-0.1347	1994.5251	19.9726

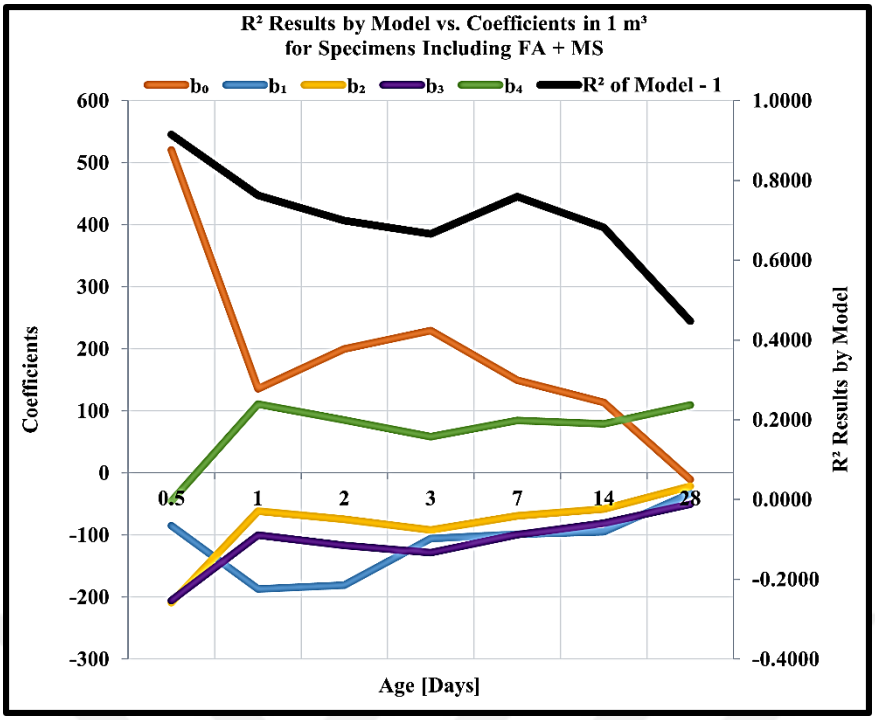

Figure 5.50: The relations of the compressive strength of the Model-1 in FA + MS.

In the Figure 5.51, there is the correlation for material effect in the compressive strength prediction for the existence of GGBS substance by using the coefficients of the model equation. In this way, it is drawn that the equation coefficient does not behave how the R^2 value behaves. Between the day-1, and day-3; day-7, and day-14, the health of the compressive strength estimation is not good. Moreover, except the day-2, and day-28, the W/C impacts are parallel to the prediction results that the W/C ratio works well for less amount of cement content. For the FA, and CA contents, except day-2, and day-28, the data forecasting is resulted in decreasing. But for the day-28, the result could be ignored because of the very high expectations. In the binder content, the cement material affects the results. The more it is used, the more the results get better. In the Table 5.35, for both substances, the R^2 values are shared with the mixing codes together.

In addition, in the Figure 5.52, it is absolute that FA + MS content influences the higher compressive strength prediction results than GGBS content does. For all ages, the compressive strength specimens made of FA + MS content are close and/or above the median values. Only for day-7, day-14, and day-28, the compressive strength of the specimens composed of GGBS content are close and/or above the median values. It is appeared that the compressive strength estimation for the specimens including FA + MS are proper. However, the whiskers of the specimens including FA + MS content

are not eligible than the specimens including GGBS content. In the Table 5.36 and the Table 5.37, the numerical results of the boxplots are also shared.

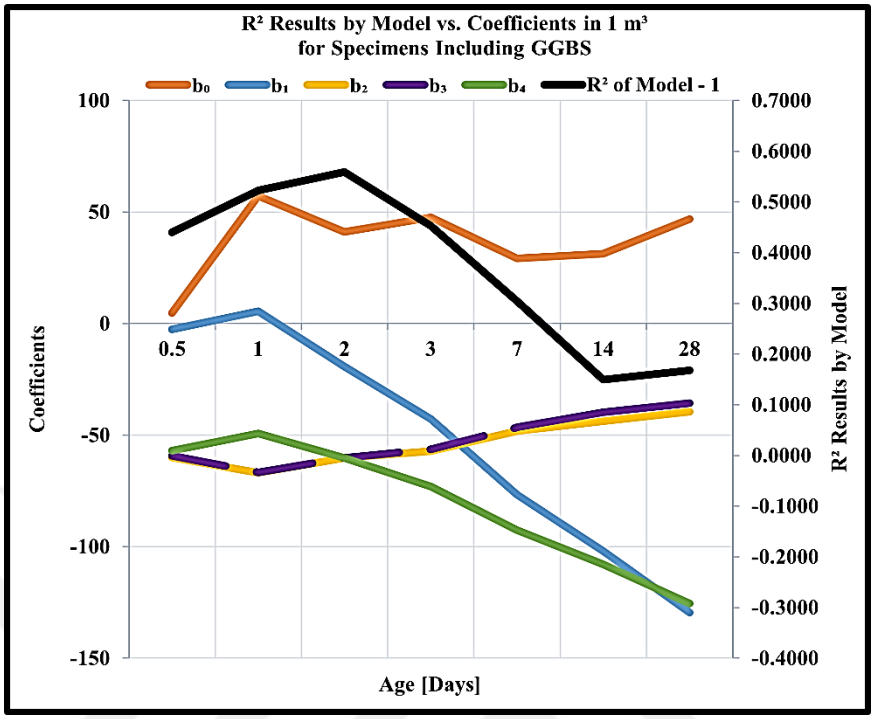

Figure 5.51: The relations of the compressive strength of the Model-1 in GGBS.

Table 5.35: The MRA results of CS in FA + MS & GGBS contents in the Model-1.

Mixing Codes (FA + MS)	R^2	Mixing Codes (GGBS)	R^2
YM-SEG-03	0.9720	**C45-III-B20**	0.8769
MIX-15A-04	0.8985	**YM-DAP-AC-03**	0.9966
YM-SEG-05	0.9818	**MIX-30**	0.1888
YM-SEG-08	0.9922	**MIX-30-03**	0.6919
MIX-15E-03	0.8180	**MIX-30-BRT**	0.8903
MIX-15AC-04	0.9883	**MIX-30-07**	0.9234
YM-SEG-10	0.9714	**MIX-34-BRT**	0.9588
YM-SEG-10A	0.9929	**MIX-32-03**	0.7547
YM-SEG-10E	0.8886	**MIX-32-CEN**	0.1693
MIX-15-AC-03	0.9524	**MIX-32-CEN-OK**	0.9618
C45-B25-425	0.9337	**B70-380**	0.8276
C45-B25-400	0.9106	**B70-420**	0.9859
C50-B22-460	0.8790	**B47-440**	0.9418
-	-	**B67-440**	0.9690
-	-	**B67-440-001**	0.9860
-	-	**B67-440-BEY**	0.9850

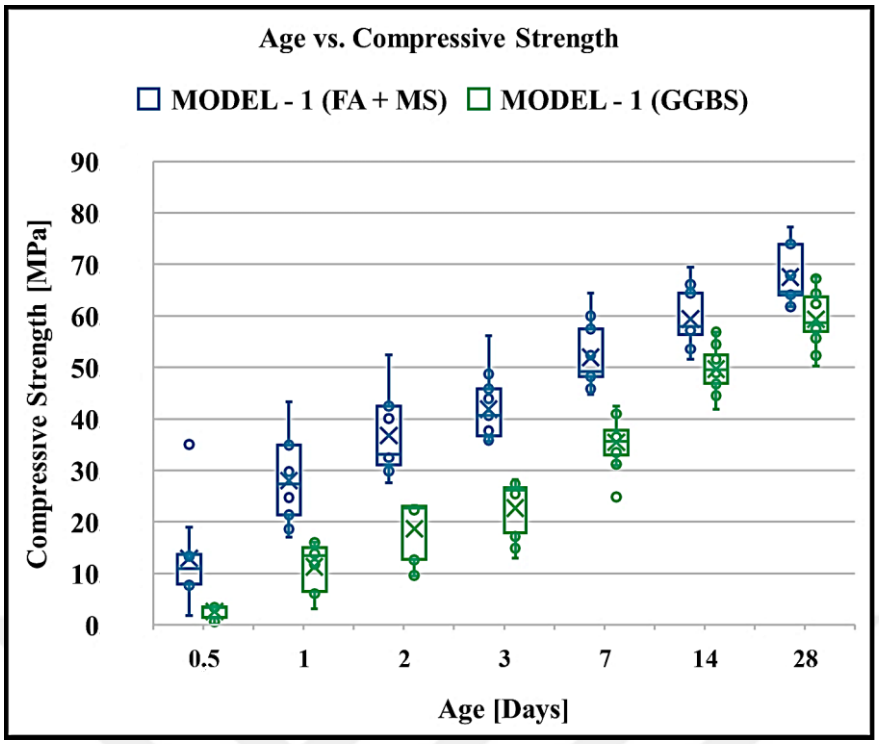

Figure 5.52: The age and the compressive strength relationship for the Model-1.

Table 5.36: The CS results from the MRA in FA + MS content for the Model-1.

Model-1 [MPa]	0.5-Day	1-Day	2-Day	3-Day	7-Day	14-Day	28-Day
Minimum Value	1.82	17.11	27.65	35.68	44.77	51.54	61.79
1st-Quartile-Value	7.90	21.41	31.08	36.75	48.20	56.41	64.11
Median Value	10.91	27.39	33.08	40.71	49.22	57.98	64.69
3rd-Quartile-Value	13.75	34.91	42.45	45.86	57.42	64.39	73.93
Maximum Value	35.05	43.27	52.46	56.18	64.43	69.48	77.21
Mean Value	12.90	28.00	36.77	41.88	51.96	59.38	67.54
Range	33.23	26.17	24.81	20.50	19.66	17.95	15.42

Table 5.37: The CS results from the MRA in GGBS content for the Model-1.

Model-1 [MPa]	0.5-Day	1-Day	2-Day	3-Day	7-Day	14-Day	28-Day
Minimum Value	1.82	17.11	27.65	35.68	44.77	51.54	61.79
1st-Quartile-Value	7.90	21.41	31.08	36.75	48.20	56.41	64.11
Median Value	10.91	27.39	33.08	40.71	49.22	57.98	64.69
3rd-Quartile-Value	13.75	34.91	42.45	45.86	57.42	64.39	73.93
Maximum Value	35.05	43.27	52.46	56.18	64.43	69.48	77.21
Mean Value	12.90	28.00	36.77	41.88	51.96	59.38	67.54
Range	33.23	26.17	24.81	20.50	19.66	17.95	15.42

Table 5.38: The compressive strength developments of samples for the Model-1.

Model-1	Strength Development of Actual Data [Day/Day]							Strength Development of Predicted Data [Day/Day]						
Mixing Codes	**0.5/28**	**1/28**	**2/28**	**3/28**	**7/28**	**14/28**	**28/28**	**0.5/28**	**1/28**	**2/28**	**3/28**	**7/28**	**14/28**	**28/28**
YM-SEG-03	0.2797	0.5105	0.6014	0.6923	0.8252	0.8741	1.0000	0.2453	0.4518	0.5498	0.6312	0.7764	0.8560	1.0000
MIX-15A-04	0.1797	0.4219	0.6016	0.6641	0.7969	-	1.0000	0.1370	0.3465	0.5029	0.5810	0.7416	-	1.0000
YM-SEG-05	0.1293	0.4218	0.5714	0.5714	0.7687	0.9048	1.0000	0.1805	0.4742	0.5750	0.6196	0.7758	0.8703	1.0000
YM-SEG-08	0.2053	0.4570	0.5298	0.6291	0.7881	0.8477	1.0000	0.1855	0.4730	0.5746	0.6209	0.7764	0.8705	1.0000
MIX-15E-03	0.1017	0.3983	0.5339	0.6102	0.7627	0.8814	1.0000	0.1136	0.4387	0.5893	0.6460	0.7708	0.8608	1.0000
MIX-15AC-04	0.1655	0.3957	0.5755	0.6403	0.7770	0.8633	1.0000	0.1136	0.4387	0.5893	0.6460	0.7708	0.8608	1.0000
YM-SEG-10	-	0.3381	0.4820	0.5612	0.7194	0.8705	1.0000	-	0.3840	0.5096	0.5818	0.7622	0.8913	1.0000
YM-SEG-10A	0.2331	-	0.4962	0.5789	0.7444	0.8797	1.0000	0.2126	-	0.5016	0.5681	0.7528	0.8838	1.0000
YM-SEG-10E	-	0.3884	0.4793	0.5124	0.7273	0.8843	1.0000	-	0.3879	0.5138	0.5853	0.7644	0.8926	1.0000
MIX-15-AC-03	0.0741	0.4167	0.5463	0.6574	0.8333	0.9537	1.0000	0.1370	0.3465	0.5029	0.5810	0.7416	0.8668	1.0000
C45-B25-425	-	0.2261	0.4348	0.6435	0.8087	0.9043	1.0000	-	0.2997	0.4822	0.6572	0.7781	0.8738	1.0000
C45-B25-400	0.0132	0.3158	0.4539	0.5329	0.6316	0.7632	1.0000	0.0284	0.2668	0.4313	0.5566	0.6984	0.8039	1.0000
C50-B22-460	0.4259	0.6111	0.7222	0.7531	0.8333	0.9074	1.0000	0.4741	0.5853	0.7096	0.7599	0.8715	0.9398	1.0000

Table 5.38 (continued): The compressive strength developments of samples for the Model-1.

Model-1	Strength Development of Actual Data [Day/Day]							Strength Development of Predicted Data [Day/Day]						
Mixing Codes	**0.5/28**	**1/28**	**2/28**	**3/28**	**7/28**	**14/28**	**28/28**	**0.5/28**	**1/28**	**2/28**	**3/28**	**7/28**	**14/28**	**28/28**
C45-III-B20	0.0233	0.1105	0.2791	0.3547	0.5930	0.8663	1.0000	0.0514	0.1750	0.3320	0.4076	0.6308	0.8461	1.0000
YM-DAP-AC-03	0.0504	0.2185	0.3613	0.4202	0.6303	0.8403	1.0000	0.0607	0.2520	0.3890	0.4520	0.6442	0.8500	1.0000
MIX-30	0.0323	0.1183	0.2688	0.3441	0.6237	0.7849	1.0000	0.0508	0.1927	0.3375	0.4169	0.6271	0.8398	1.0000
MIX-30-03	0.1500	0.3900	0.4900	0.5500	0.7100	0.8800	1.0000	0.0570	0.2146	0.3592	0.4321	0.6368	0.8472	1.0000
MIX-30-BRT	0.0500	0.2357	0.3643	0.4500	0.6571	0.8643	1.0000	0.0612	0.2599	0.3951	0.4570	0.6459	0.8496	1.0000
MIX-30-07	0.0594	0.2475	0.3762	0.4554	0.6436	0.8713	1.0000	0.0611	0.2611	0.4016	0.4609	0.6516	0.8502	1.0000
MIX-34-BRT	0.0678	0.3136	0.4407	-	0.6271	0.8305	1.0000	0.0672	0.3040	0.4289	-	0.6534	0.8553	1.0000
MIX-32-03	0.0845	0.3592	0.4648	0.5423	0.6690	0.8310	1.0000	0.0621	0.2537	0.3939	0.4556	0.6485	0.8521	1.0000
MIX-32-CEN	0.0548	0.2466	0.3836	0.4384	0.6575	0.8630	1.0000	0.0643	0.3067	0.4393	0.4870	0.6622	0.8512	1.0000
MIX-32-CEN-OK	0.0417	0.2583	0.4583	0.5250	0.6667	0.8417	1.0000	0.0610	0.2776	0.4163	0.4714	0.6565	0.8485	1.0000
B70-380	0.0300	0.0800	0.1700	0.2400	0.5000	0.7800	1.0000	0.0191	0.0500	0.1516	0.2387	0.5002	0.8283	1.0000
B70-420	0.0208	0.0729	0.1354	0.2188	0.4896	0.8542	1.0000	0.0240	0.1212	0.1917	0.2574	0.4936	0.8334	1.0000
B47-440	0.0207	0.1034	0.2276	0.3172	0.5724	0.8483	1.0000	0.0253	0.1016	0.2006	0.2895	0.5257	0.8236	1.0000
B67-440	0.0138	0.0759	0.1862	0.2759	0.4828	0.8276	1.0000	0.0253	0.1016	0.2006	0.2895	0.5257	0.8236	1.0000
B67-440-001	0.0090	0.1351	0.1982	0.2973	0.4865	0.8018	1.0000	0.0103	0.1108	0.2169	0.2939	0.5315	0.8057	1.0000
B67-440-BEY	0.0161	0.1210	0.2500	0.3065	0.5726	0.7984	1.0000	0.0028	0.1036	0.2191	0.2951	0.5369	0.7960	1.0000

5.4.2 Power Regression (Model-2)

The power regression model (the Model-2) is one of the multivariate regression analysis models depending on various variables such as amount of cement and water, and air content of concrete mixture design. In this model, for 0.5-day, 1-day, 2-day, 3-day, 7-day, 14-day, and 28-day compressive strength predictions were showed off.

For the FA + MS content included samples, R^2 (btw 0.0035 & 0.0342), and R^2_{adj} results are plotted onto the concrete age; SSE, and RMSE results also diverse in each concrete age. Like these sample results, for the GGBS included samples, R^2 (btw 0.0557 & 0.3509), and R^2_{adj} results are come out at the concrete age, as well; SSE, and RMSE results are varied in a numeric scale for each concrete age, too. All the data estimations are applied on these solutions, and the results are shared with high R^2 results except the samples in C50-B22-460 (R^2 = -0.4505), and MIX-32-CEN (-0.0021) mixing codes which are resulted negative. In this way of the results, even though the strength development of the compressive strength is listed in the Table 5.44 in a courteous manner, the way that model working brings the question marks to the mind for the use of the model due to the very low results of the concrete age dependent analysis.

In the Figure 5.53, the correlations of the actual data sets, and the predicted data sets are trendlined. The correlation shows that the model results are satisfying, and there are no negative deflections in the data fitting planar which means the model is safe to be used.

In the Table 5.39 and the Table 5.40, with the statistical results for each concrete age regression analysis, the general forms of the multivariate linear regression analysis equations are enlisted for both FA + MS and GGBS materials.

In the Figure 5.54, there is another correlation for material effects in the compressive strength prediction for FA + MS material by using the coefficients of the model equation. In this way, it is presented that there is no direct correlation between the coefficient *K*, and *n* with the R^2 value (*K* and *n* are from the Table 2.6). Because the empirical coefficient *K* seems opposite to the R^2 result in the days between 0.5, and 1; and 3, and 14. Hereupon, the other empirical coefficient *n* has no effect on the data prediction. That is why another correlation is set in the Figure 5.55 to search for the material effects on the compressive strength estimation.

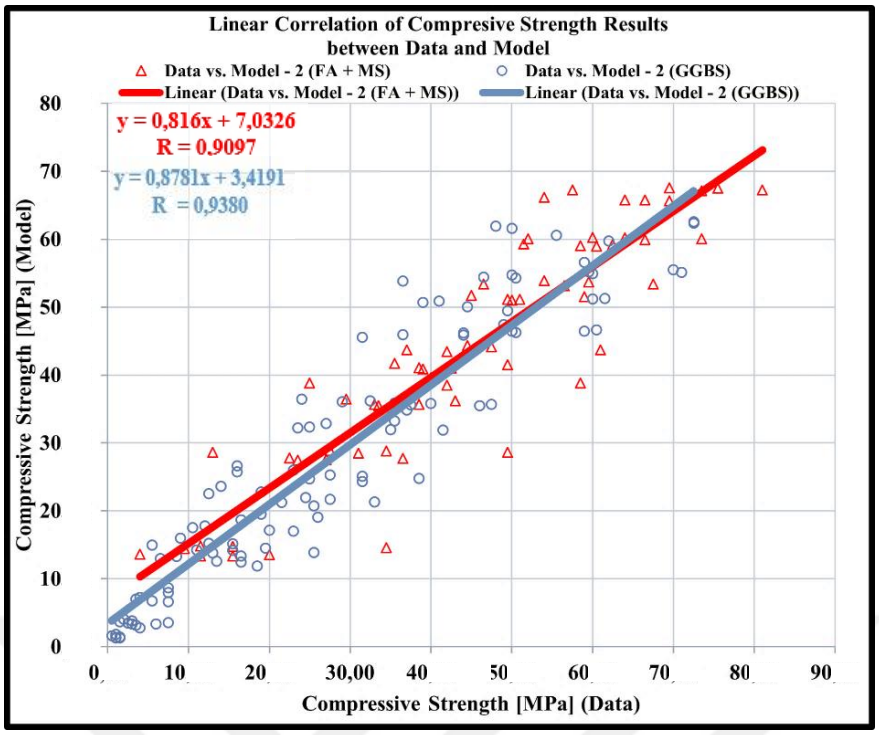

Figure 5.53: The correlations of the compressive strength of the Model-2.

Table 5.39: The MRA results for CS in FA + MS content for the Model-2.

Age	Power Regression	R^2	R^2_{adj}	SSE	RMSE
0.5-Day	$f'_c = 18.913[c/(c+w+a)]^{0.7198}$	0.0047	-0.3934	652.1313	18.0573
1-Day	$f'_c = 32.2963[c/(c+w+a)]^{0.3307}$	0.0035	-0.3287	837.1370	20.4589
2-Day	$f'_c = 49.9449[c/(c+w+a)]^{0.6945}$	0.0326	-0.2438	765.4425	19.5633
3-Day	$f'_c = 52.797[c/(c+w+a)]^{0.5201}$	0.0342	-0.2418	526.5933	16.2264
7-Day	$f'_c = 60.6492[c/(c+w+a)]^{0.3521}$	0.0287	-0.2488	438.4391	14.8061
14-Day	$f'_c = 63.2347[c/(c+w+a)]^{0.1424}$	0.0054	-0.3261	430.1576	14.6656
28-Day	$f'_c = 71.9393[c/(c+w+a)]^{0.1856}$	0.0095	-0.2734	596.1556	17.2649

Table 5.40: The MRA results for CS in GGBS content for the Model-2.

Age	Power Regression	R^2	R^2_{adj}	SSE	RMSE
0.5-Day	$f'_c = 7.8972[c/(c+w+a)]^{1.9658}$	0.3196	0.2062	37.2390	0.3196
1-Day	$f'_c = 26.9362[c/(c+w+a)]^{1.5153}$	0.3509	0.2427	389.2221	0.3509
2-Day	$f'_c = 34.4782[c/(c+w+a)]^{1.1004}$	0.3434	0.2339	548.8259	0.3434
3-Day	$f'_c = 34.7089[c/(c+w+a)]^{0.771}$	0.2443	0.1069	635.6830	0.2443
7-Day	$f'_c = 39.404[c/(c+w+a)]^{0.2278}$	0.0557	-0.1017	764.8583	0.0557
14-Day	$f'_c = 42.4802[c/(c+w+a)]^{-0.2041}$	0.0602	-0.0965	1123.7703	0.0602
28-Day	$f'_c = 49.278[c/(c+w+a)]^{-0.2577}$	0.1015	-0.0483	1472.6305	0.1015

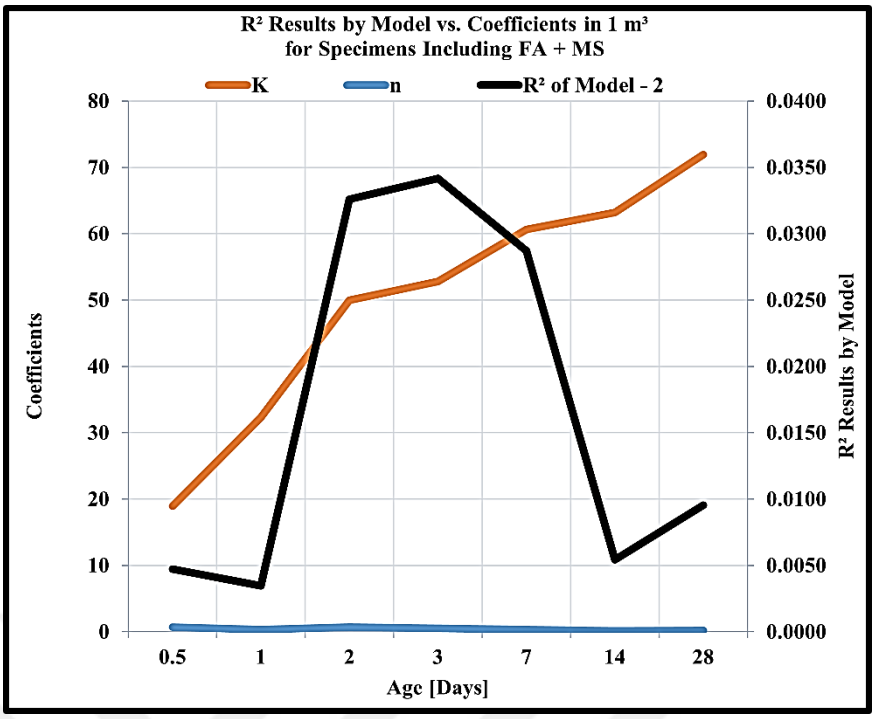

Figure 5.54: The correlations of the compressive strength of the Model-2.

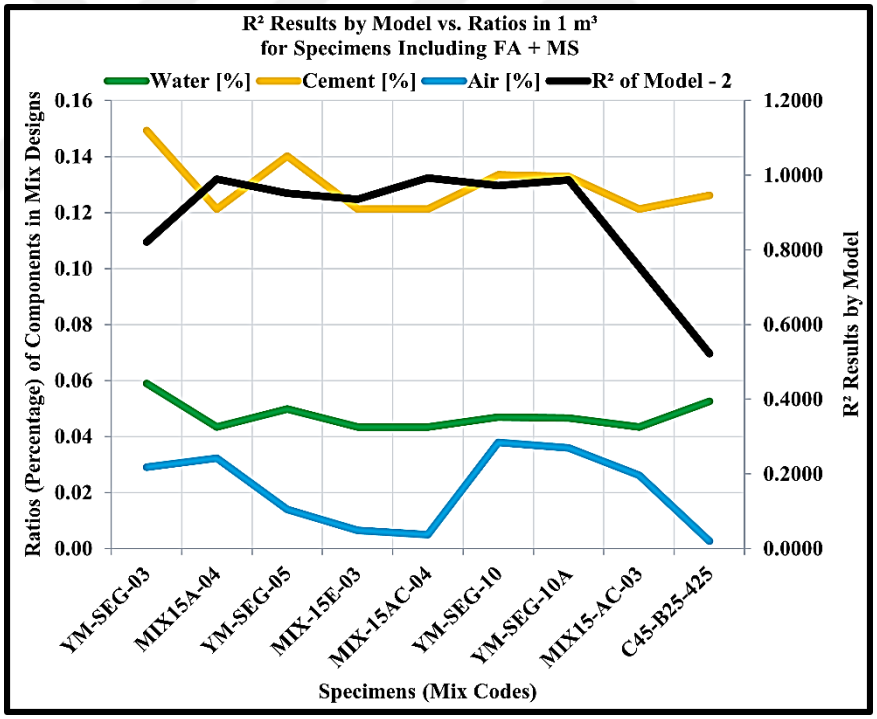

Figure 5.55: The correlations of the compressive strength of the Model-2.

In the Figure 5.55, it is exactly seen that the lowest amount of air content (0.26 %) causes the lowest well-fitting predictions (R^2 = 0.5227) on the real data set in C45-B25-425 mixing code. However, for the highest amount of air content (3.80%) does not mean the highest well-fitting estimation on the actual data values. Moreover, the minimum amount of cement content (0.12%) means the maximum R^2 (0.9927) result

for the sample in MIX-15AC-04 mixing code. Followingly, the minimum water content (0.04%) leads the highest well-fitting forecasting (R^2 = 0.9927) for the sample in MIX-15AC-04 mixing code. Like the cement content, the highest amount of water does not mean the best goodness-of-fit.

In the Figure 5.56, there is another correlation for the material effects in the compressive strength prediction for the GGBS content by using the coefficients of the model equation. In this way, it is accepted that there is no direct relation between the coefficient *K* and *n* with the R^2 value (*K* and *n* are from the Table 2.6). Because the empirical coefficient *K* seems opposite to the R^2 value at the ages between day-2, and day-7. Incidentally, the other empirical coefficient *n* seems opposite to the R^2 value at the ages between day-0.5, and day-1; and day-7, and day-28 on the data prediction. That is why another correlation is set in the Figure 5.58 to search for the material effects on the compressive strength estimation.

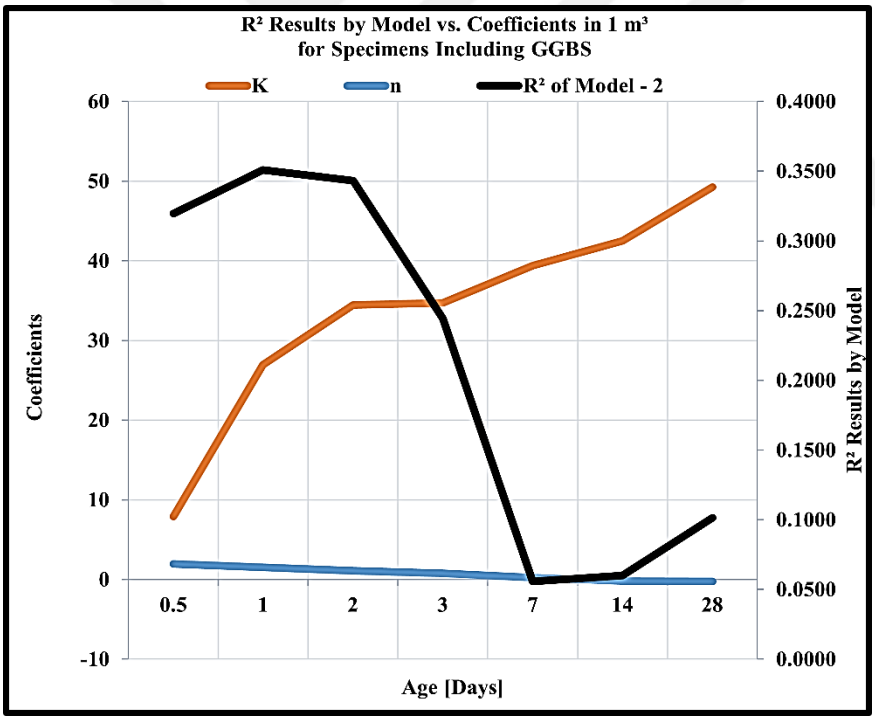

Figure 5.56: The correlations of the compressive strength of the Model-2.

In the Figure 5.57, it is unveiled that the lowest amount of air content (1.06 %) causes the best goodness-of-fit (R^2 = 0.9959) on the real data set in B67-440-BEY mixing code. Albeit, for the highest amount of air content (5.29%) does not mean the worst well-fitting presuming on the actual data values. Together with, the maximum amount of cement content (0.17%) means the minimum R^2 (0.6367) value for the sample in MIX-CEN-03 mixing code. Forbye, the use of water effect could not be understood in

this model because of it is linear behavior on the results. Followingly, in the Table 5.41, for both substances, the R^2 results are shared with the mixing codes together.

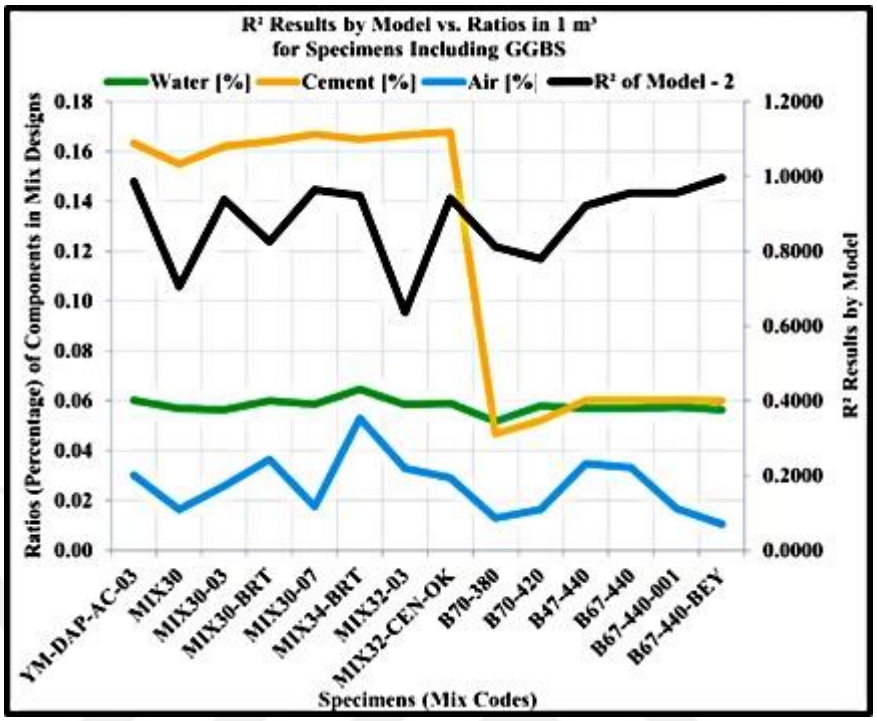

Figure 5.57: The correlations of the compressive strength of the Model-2.

Table 5.41: The MRA results of CS in FA + MS & GGBS contents in the Model-2.

Mixing Codes (FA + MS)	R^2	Mixing Codes (GGBS)	R^2
YM-SEG-03	0.8213	**YM-DAP-AC-03**	0.9855
MIX-15A-04	0.9899	**MIX-30**	0.7050
YM-SEG-05	0.9512	**MIX-30-03**	0.9376
MIX-15E-03	0.9359	**MIX-30-BRT**	0.8258
MIX-15AC-04	0.9927	**MIX-30-07**	0.9638
YM-SEG-10	0.9724	**MIX-34-BRT**	0.9482
YM-SEG-10A	0.9871	**MIX-32-03**	0.6367
MIX-15AC-03	0.7551	**MIX-32-CEN**	-0.0021
C45-B25-425	0.5227	**MIX-32-CEN-OK**	0.9410
C50-B22-460	-0.4505	**B70-380**	0.8113
-	-	**B70-420**	0.7793
-	-	**B47-440**	0.9218
-	-	**B67-440**	0.9561
-	-	**B67-440-001**	0.9564
-	-	**B67-440-BEY**	0.9959

Also. in the Figure 5.58, the FA + MS content shows the higher compressive strength prediction results than the GGBS content does. For all ages, the compressive strength specimens made of FA + MS content are close and/or above the median values. Only for day-14, day-14, and day-28, the compressive strength of the specimens made of GGBS content are close and/or above the median values. It is ended that the

compressive strength prediction for the specimens including GGBS are less proper. That is why, the whiskers of the specimens including FA + MS content are more eligible than the specimens including GGBS content. In the Table 5.42 and the Table 5.43, the numerical results of the boxplots are also shared.

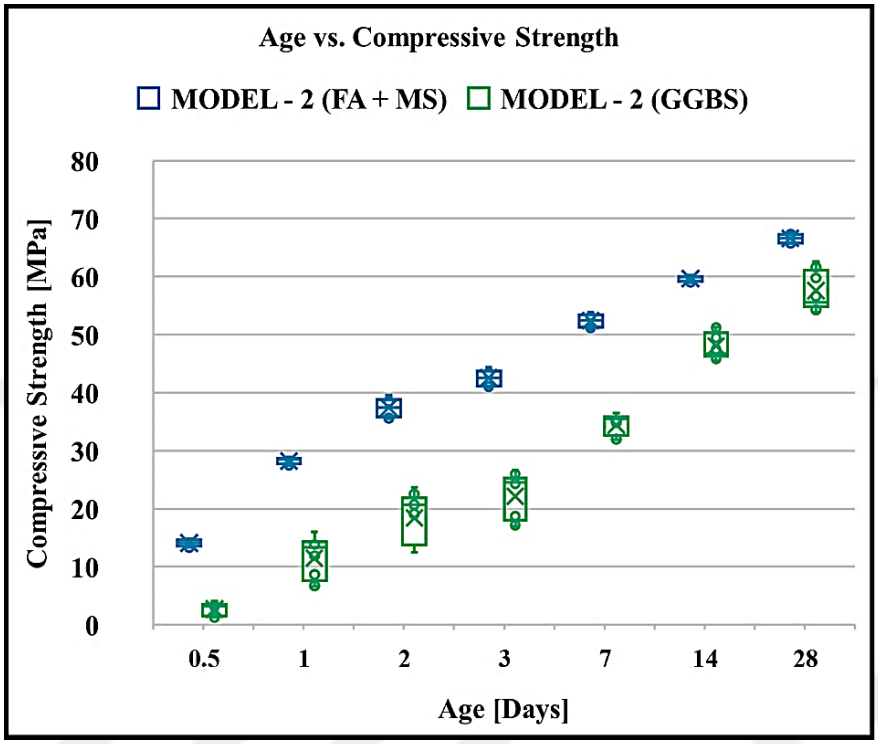

Figure 5.58: The age and the compressive strength relationship for the Model-2.

Table 5.42: The CS results from MRA in FA + MS content for the Model-2.

Model-1 [MPa]	0.5-Day	1-Day	2-Day	3-Day	7-Day	14-Day	28-Day
Minimum Value	13.34	27.45	35.48	40.87	51.00	58.95	65.66
1st-Quartile-Value	13.50	27.71	35.83	41.17	51.25	59.20	65.83
Median Value	14.04	28.52	37.46	42.57	52.42	59.94	66.61
3rd-Quartile-Value	14.61	28.65	38.82	43.72	53.38	60.05	67.26
Maximum Value	14.86	28.91	39.57	44.35	53.89	60.29	67.60
Mean Value	14.06	28.22	37.45	42.55	52.40	59.67	66.60
Range	1.52	1.46	4.08	3.47	2.90	1.33	1.94

Table 5.43: The CS results from MRA in GGBS content for the Model-2.

Model-1 [MPa]	0.5-Day	1-Day	2-Day	3-Day	7-Day	14-Day	28-Day
Minimum Value	1.28	6.63	12.46	17.02	31.92	45.56	53.83
1st-Quartile-Value	1.54	7.62	13.78	18.02	32.59	46.24	54.85
Median Value	3.18	13.36	20.72	24.51	35.46	46.69	55.52
3rd-Quartile-Value	3.49	14.35	21.82	25.25	35.84	50.36	61.10
Maximum Value	4.02	16.02	23.64	26.64	36.44	51.30	62.54
Mean Value	2.66	11.48	18.38	22.16	34.43	48.03	57.57
Range	2.74	9.38	11.18	9.63	4.52	5.74	8.70

Table 5.44: The compressive strength developments of samples for the Model-2.

Model-1	Strength Development of Actual Data [Day/Day]							Strength Development of Predicted Data [Day/Day]						
Mixing Codes	**0.5/28**	**1/28**	**2/28**	**3/28**	**7/28**	**14/28**	**28/28**	**0.5/28**	**1/28**	**2/28**	**3/28**	**7/28**	**14/28**	**28/28**
YM-SEG-03	0.2797	0.5105	0.6014	0.6923	0.8252	0.8741	1.0000	0.2053	0.4198	0.5486	0.6286	0.7805	0.8968	1.0000
MIX15A-04	0.1797	0.4219	0.6016	0.6641	0.7969	-	1.0000	0.2029	0.4184	0.5423	0.6239	0.7776	-	1.0000
YM-SEG-05	0.1293	0.4218	0.5714	0.5714	0.7687	0.9048	1.0000	0.2151	0.4251	0.5735	0.6473	0.7920	0.8934	1.0000
MIX-15E-03	0.2053	0.4570	0.5298	0.6291	0.7881	0.8477	1.0000	0.2187	0.4270	0.5825	0.6540	0.7960	0.8922	1.0000
MIX-15AC-04	0.1655	0.3957	0.5755	0.6403	0.7770	0.8633	1.0000	0.2198	0.4276	0.5853	0.6560	0.7973	0.8918	1.0000
YM-SEG-10	-	0.3381	0.4820	0.5612	0.7194	0.8705	1.0000	-	0.4180	0.5404	0.6225	0.7767	0.8979	1.0000
YM-SEG-10A	0.2331	-	0.4962	0.5789	0.7444	0.8797	1.0000	0.2031	-	0.5429	0.6244	0.7779	0.8975	1.0000
MIX15-AC-03	0.0741	0.4167	0.5463	0.6574	0.8333	0.9537	1.0000	0.2063	0.4204	0.5512	0.6306	0.7817	0.8964	1.0000
C45-B25-425	-	0.2261	0.4348	0.6435	0.8087	0.9043	1.0000	-	0.4259	0.5772	0.6500	0.7936	0.8929	1.0000
C50-B22-460	0.4259	0.6111	0.7222	0.7531	0.8333	0.9074	1.0000	0.2166	0.4259	0.5773	0.6501	0.7937	0.8929	1.0000

Table 5.44 (continued): The compressive strength developments of samples for the Model-2.

Model-1	Strength Development of Actual Data [Day/Day]							Strength Development of Predicted Data [Day/Day]						
Mixing Codes	**0.5/28**	**1/28**	**2/28**	**3/28**	**7/28**	**14/28**	**28/28**	**0.5/28**	**1/28**	**2/28**	**3/28**	**7/28**	**14/28**	**28/28**
YM-DAP-AC-03	0.0504	0.2185	0.3613	0.4202	0.6303	0.8403	1.0000	0.0602	0.2504	0.3848	0.4479	0.6458	0.8419	1.0000
MIX-30	0.0323	0.1183	0.2688	0.3441	0.6237	0.7849	1.0000	0.0678	0.2753	0.4137	0.4731	0.6627	0.8443	1.0000
MIX-30-03	0.1500	0.3900	0.4900	0.5500	0.7100	0.8800	1.0000	0.0645	0.2644	0.4011	0.4622	0.6554	0.8433	1.0000
MIX-30-BRT	0.0500	0.2357	0.3643	0.4500	0.6571	0.8643	1.0000	0.0573	0.2407	0.3733	0.4377	0.6388	0.8409	1.0000
MIX-30-07	0.0594	0.2475	0.3762	0.4554	0.6436	0.8713	1.0000	0.0695	0.2807	0.4200	0.4785	0.6663	0.8449	1.0000
MIX-34-BRT	0.0678	0.3136	0.4407	-	0.6271	0.8305	1.0000	0.0484	0.2104	0.3368	-	0.6157	0.8375	1.0000
MIX-32-03	0.0845	0.3592	0.4648	0.5423	0.6690	0.8310	1.0000	0.0606	0.2518	0.3864	0.4492	0.6467	0.8421	1.0000
MIX-32-CEN	0.0548	0.2466	0.3836	0.4384	0.6575	0.8630	1.0000	0.0748	0.2976	0.4391	0.4950	0.6770	0.8463	1.0000
MIX-32-CEN-OK	0.0417	0.2583	0.4583	0.5250	0.6667	0.8417	1.0000	0.0627	0.2587	0.3945	0.4564	0.6515	0.8428	1.0000
B70-380	0.0300	0.0800	0.1700	0.2400	0.5000	0.7800	1.0000	0.0233	0.1175	0.2155	0.2887	0.5249	0.8229	1.0000
B70-420	0.0208	0.0729	0.1354	0.2188	0.4896	0.8542	1.0000	0.0223	0.1135	0.2099	0.2830	0.5200	0.8220	1.0000
B47-440	0.0207	0.1034	0.2276	0.3172	0.5724	0.8483	1.0000	0.0205	0.1061	0.1993	0.2721	0.5104	0.8204	1.0000
B67-440	0.0138	0.0759	0.1862	0.2759	0.4828	0.8276	1.0000	0.0210	0.1080	0.2020	0.2749	0.5129	0.8208	1.0000
B67-440-001	0.0090	0.1351	0.1982	0.2973	0.4865	0.8018	1.0000	0.0270	0.1320	0.2357	0.3089	0.5419	0.8258	1.0000
B67-440-BEY	0.0161	0.1210	0.2500	0.3065	0.5726	0.7984	1.0000	0.0303	0.1449	0.2531	0.3261	0.5560	0.8281	1.0000

5.5 Multivariate Regression Analysis for Splitting Tensile Strength

In his section of the thesis, the Table 5.45, the Table 5.46, and the Table 5.47 present the regression models with their statistical results.

5.5.1 Antilogarithmic Linear Regression (Model-1)

The antilogarithmic linear regression model (the Model-1) is one of the multivariate regression analysis models depending on multitudinous variables such as water, cement, and air content of concrete mixture design. In this model, for 0.5-day, 1-day, 2-day, 3-day, 7-day, 14-day, and 28-day splitting tensile strength predictions were featured. At the end, for the FA + MS content included samples, R^2 (btw 0.1827 & 0.8828), and R^2_{adj} results are scattered on the concrete age; SSE, and RMSE results are also diverted at each concrete age. For the GGBS added samples, R^2 (btw 0.4457 & 0.8150), and R^2_{adj} results are come out on the concrete age; SSE, and RMSE results are varied in a small numeric scale for each concrete age, as well. In other respects, all the data predictions are applied on these solutions, and the results are come out in expectations. In this way of the results, the strength development of the splitting tensile strength is settled in the Table 5.50**.**

In the Figure 5.59, the correlations of the actual data sets and predicted data sets are trendlined. The correlation shows that the model results are satisfying, and there are no negative deflections in the data fitting planar which means the model is safe to be used.

In the Table 5.45 and the Table 5.46, with the statistical results for each concrete age regression analysis, the general forms of the multivariate antilogarithmic linear regression analysis equations are shared with both FA + MS and GGBS materials.

In the Figure 5.60, there is another correlation for material effects in the splitting tensile strength prediction for the FA + MS substance by using the coefficients of the model equation. In this way, it is discovered that the equation coefficient is appropriate except the ages between 0.5-day, and 1-day; and 2-day, and 3-day. Moreover, the amount of water in proportion is effective at the ages between day-0.5, and day-1; and day-7 and day-28. The cement proportion increases the R^2 value for all ages, even though for some ages, the R^2 value decreases at the same time.

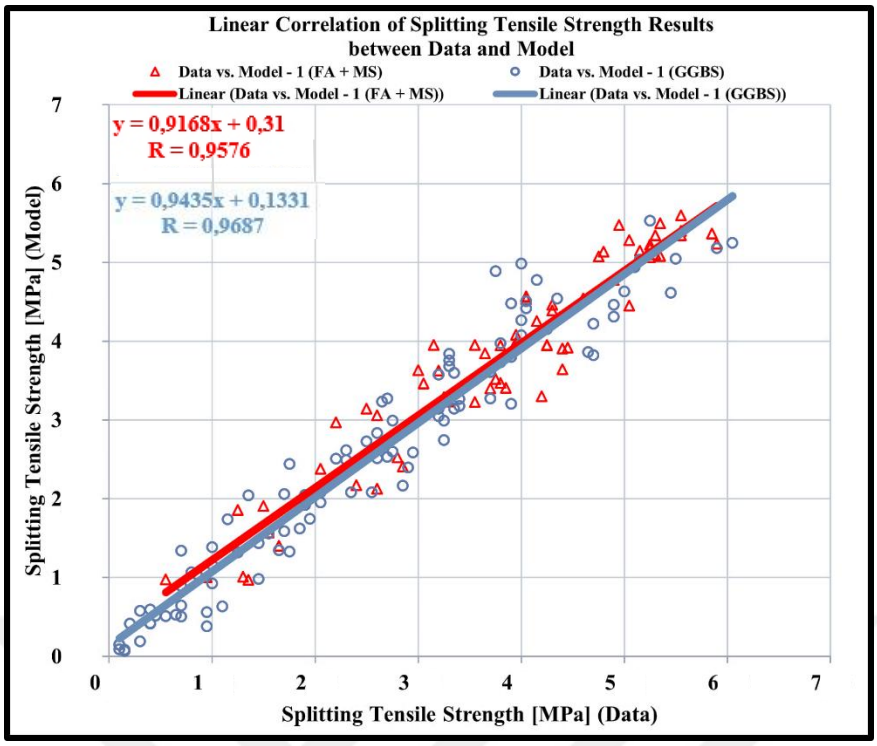

Figure 5.59: The correlations of the splitting tensile strength of the Model-1.

Table 5.45: The MRA results for STS in FA + MS content for the Model-1.

Age	Power Regression	R^2	R^2_{adj}	SSE	RMSE
0.5-Day	$f'_t = 29.8652(C^{9.201})(W^{-5.0715})(A^{-0.0228})$	0.6950	0.2883	0.9151	0.4783
1-Day	$f'_t = 104.3518(C^{3.1811})(W^{-1.0107})(A^{0.0659})$	0.6201	0.2402	1.6529	0.6428
2-Day	$f'_t = 9.9646(C^{2.089})(W^{-1.0319})(A^{-0.0126})$	0.2876	-0.2823	2.6779	0.8182
3-Day	$f'_t = 8.191(C^{2.5842})(W^{-1.3935})(A^{-0.0647})$	0.4869	0.0764	1.5887	0.6302
7-Day	$f'_t = 61.2896(C^{1.7853})(W^{-0.326})(A^{-0.0006})$	0.8828	0.7655	0.6548	0.4046
14-Day	$f'_t = 26.7237(C^{1.6027})(W^{-0.5263})(A^{0.0117})$	0.6835	0.3671	0.8473	0.4602
28-Day	$f'_t = 7.4947(C^{0.7115})(W^{-0.3468})(A^{-0.0105})$	0.1827	-0.4711	1.2155	0.5512

Table 5.46: The MRA results for STS in GGBS content for the Model-1.

Age	Power Regression	R^2	R^2_{adj}	SSE	RMSE
0.5-Day	$f'_t = 0.0001(C^{1.5952})(W^{-5.0321})(A^{0.6727})$	0.6260	0.4764	0.4317	0.3285
1-Day	$f'_t = 0.0004(C^{1.0034})(W^{-4.6289})(A^{0.7769})$	0.7315	0.6242	2.1523	0.7335
2-Day	$f'_t = 0.273(C^{0.5883})(W^{-1.7093})(A^{0.4356})$	0.8150	0.7410	1.5526	0.6230
3-Day	$f'_t = 1.7166(C^{0.4704})(W^{-0.9819})(A^{0.3861})$	0.7762	0.6767	1.9136	0.6917
7-Day	$f'_t = 0.5725(C^{0.2247})(W^{-1.1074})(A^{0.2465})$	0.6571	0.5199	2.1579	0.7345
14-Day	$f'_t = 1.3486(C^{0.1019})(W^{-0.7839})(A^{0.2376})$	0.5941	0.4317	2.7214	0.8248
28-Day	$f'_t = 4.4046(C^{0.0688})(W^{-0.3532})(A^{0.2097})$	0.4457	0.2240	5.0679	1.1256

That is why the cement effect could not be expressed well in this model. For the air content, the model seems parallel to the ages between the day 0.5, and 3; and 7, and 28. So, the model puts forth the air effect in the analysis. Because while the air content decreases, the model prediction also decreases. For the minimum R^2 value, the cement proportion is also minimum, the water proportion is maximum. However, for the maximum R^2 value, the air content is neither maximum nor minimum. In this model, there is no other correlation for the maximum R^2 value.

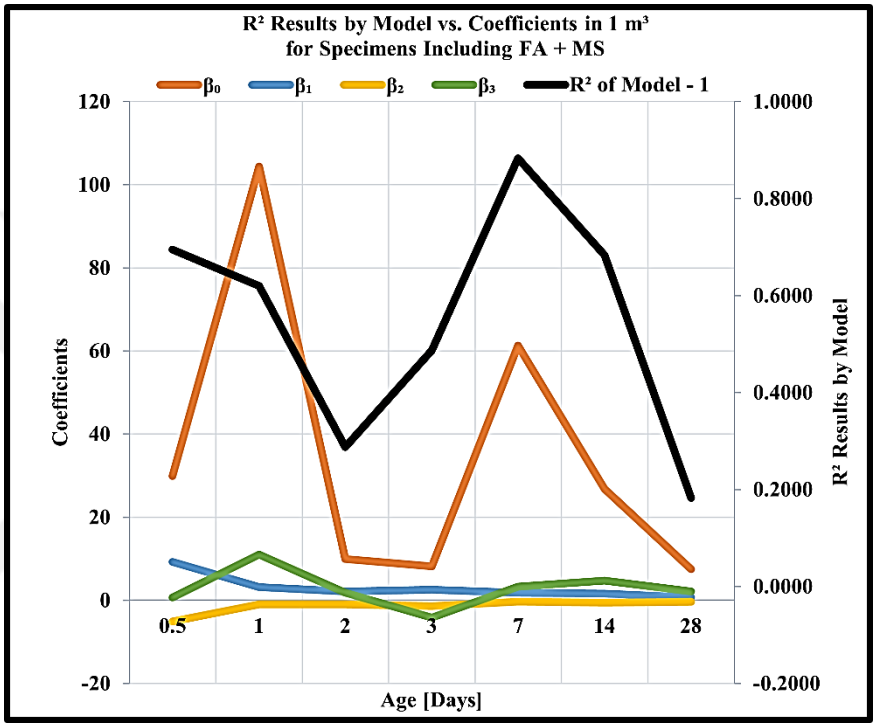

Figure 5.60: The correlations of the splitting tensile strength of the Model-1.

In the Figure 5.61, the splitting tensile strength prediction for the GGBS material by using the coefficients of the model equation is given. The equation correlation is opposite for the model results between the day 2, and 3; and 7, and 28. The water proportion results seem parallel to the equation coefficient which means that the more water the worse model results. So, the high proportion of water content is not beneficial for the concrete strength gaining. Except the age between day-1 and day-2, the air content works with the model. So, for the GGBS included concrete samples, the air proportion is effective on the data prediction. Because the less proportion of the air causes worse result of strength gaining process. Nevertheless, it is not clear that the high proportion of air leads well results of the model. In the Table 5.47, for both additive materials, the R^2 values are given with the mixing codes together.

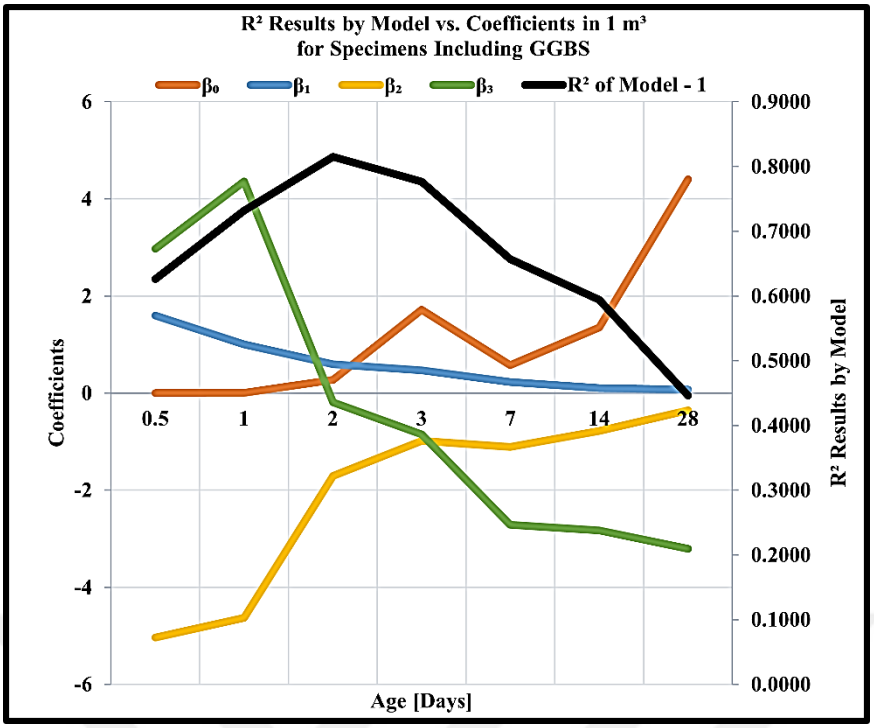

Figure 5.61: The correlations of the splitting tensile strength of the Model-1.

Table 5.47: The MRA results of STS in FA + MS & GGBS contents in the Model-1.

Mixing Codes (FA + MS)	R^2	Mixing Codes (GGBS)	R^2
YM-SEG-03	0.8896	**YM-DAP-AC-03**	0.9620
MIX-15A-04	0.8977	**MIX-30**	0.8502
YM-SEG-05	0.8990	**MIX-30-03**	0.7124
MIX-15E-03	0.9822	**MIX-30-BRT**	0.9406
MIX-15AC-04	0.8360	**MIX-30-07**	0.9945
YM-SEG-10	0.8526	**MIX-34-BRT**	0.9354
YM-SEG-10A	0.9202	**MIX-32-03**	0.8307
MIX-15-AC-03	0.9572	**MIX-32-CEN**	0.9315
C45-B25-425	0.8643	**MIX-32-CEN-OK**	0.9576
C50-B22-460	0.9600	**B70-380**	0.9635
-	-	**B70-420**	0.9897
-	-	**B47-440**	0.9744
-	-	**B67-440**	0.8931
-	-	**B67-440-001**	0.9774
-	-	**B67-440-BEY**	0.8835

Also, in the Figure 5.62, the FA + MS subsequent shows the higher splitting tensile strength prediction results than the GGBS content does. Except the day-3, day-14, and day-28, for all ages, the splitting tensile strength of the specimens made of FA + MS content are close and/or above the median values. Except the day-0.5 day-14, and day-28, the splitting tensile strength of the specimens made of GGBS content are close and/or above the median values. Whiskers of the specimens including FA + MS

content is unleashed that the splitting tensile strength prediction for the specimens including GGBS are more appropriate. That is why, they are not proper than the specimens including GGBS content. In the Table 5.48, and the Table 5.49, the numerical results of the boxplots are also shared.

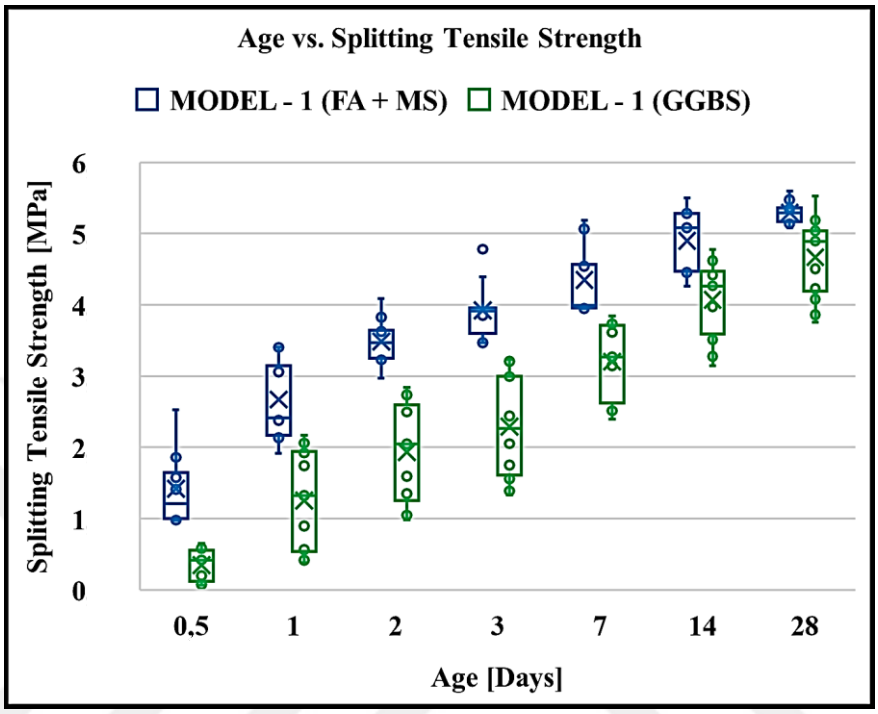

Figure 5.62: The age and the splitting tensile strength relationship for the Model-1.

Table 5.48: The STS results from MRA in FA + MS content for the Model-1.

Model-1 [MPa]	0.5-Day	1-Day	2-Day	3-Day	7-Day	14-Day	28-Day
Minimum Value	0.97	1.91	2.97	3.46	3.95	4.26	5.08
1st-Quartile-Value	1.00	2.17	3.25	3.60	3.95	4.47	5.17
Median Value	1.21	2.41	3.47	3.91	3.99	5.08	5.29
3rd-Quartile-Value	1.64	3.15	3.64	3.95	4.57	5.28	5.36
Maximum Value	2.53	3.41	4.08	4.78	5.18	5.50	5.60
Mean Value	1.42	2.67	3.48	3.92	4.35	4.90	5.30
Range	1.56	1.50	1.11	1.32	1.24	1.24	0.52

Table 5.49: The STS results from MRA in GGBS content for the Model-1.

Model-1 [MPa]	0.5-Day	1-Day	2-Day	3-Day	7-Day	14-Day	28-Day
Minimum Value	0.07	0.38	0.98	1.33	2.40	3.14	3.75
1st-Quartile-Value	0.12	0.54	1.26	1.61	2.62	3.59	4.19
Median Value	0.42	1.32	2.05	2.26	3.27	4.26	4.89
3rd-Quartile-Value	0.56	1.94	2.59	2.99	3.71	4.47	5.04
Maximum Value	0.65	2.17	2.84	3.24	3.84	4.78	5.53
Mean Value	0.34	1.25	1.93	2.29	3.20	4.07	4.67
Range	0.58	1.78	1.86	1.91	1.45	1.63	1.78

Table 5.50: The splitting tensile strength developments of samples for the Model-1.

Model-1	Strength Development of Actual Data [Day/Day]							Strength Development of Predicted Data [Day/Day]						
Mixing Codes	**0.5/28**	**1/28**	**2/28**	**3/28**	**7/28**	**14/28**	**28/28**	**0.5/28**	**1/28**	**2/28**	**3/28**	**7/28**	**14/28**	**28/28**
YM-SEG-03	0.2821	0.6581	0.7521	0.7521	0.8974	0.9487	1.0000	0.2620	0.6356	0.6789	0.7288	0.9658	1.0066	1.0000
MIX15A-04	0.2813	0.5938	0.7396	0.7917	0.8854	-	1.0000	0.1892	0.4694	0.6281	0.6754	0.7683	-	1.0000
YM-SEG-05	0.2525	0.5051	0.7778	0.8687	-	1.0202	1.0000	0.3394	0.5747	0.6985	0.8017	-	0.9649	1.0000
MIX-15E-03	0.1810	0.4571	0.6190	0.6952	0.8095	0.8190	1.0000	0.1930	0.4156	0.6303	0.7366	0.7563	0.8547	1.0000
MIX-15AC-04	0.2203	0.4407	0.7119	0.7542	0.6017	0.8559	1.0000	0.1936	0.4066	0.6306	0.7479	0.7541	0.8493	1.0000
YM-SEG-10	-	0.4906	0.5660	0.7170	0.7642	1.0000	1.0000	-	0.5720	0.6794	0.7386	0.8546	0.9545	1.0000
YM-SEG-10A	0.2793	-	0.5766	0.5676	0.8288	0.9640	1.0000	0.2940	-	0.6786	0.7401	0.8499	0.9508	1.0000
MIX-15-AC-03	0.1068	0.3981	0.6408	0.7282	0.7670	0.7864	1.0000	0.1898	0.4620	0.6284	0.6832	0.7668	0.8814	1.0000
C45-B25-425	-	0.3158	0.4632	0.6421	0.8316	0.8737	1.0000	-	0.3763	0.5849	0.6824	0.7853	0.8384	1.0000
C50-B22-460	0.5045	0.6667	0.7117	0.8829	0.9459	0.9640	1.0000	0.4515	0.6077	0.7294	0.8538	0.9042	0.9822	1.0000

Table 5.50 (continued): The splitting tensile strength developments of samples for the Model-1.

Model-1	Strength Development of Actual Data [Day/Day]							Strength Development of Predicted Data [Day/Day]						
Mixing Codes	**0.5/28**	**1/28**	**2/28**	**3/28**	**7/28**	**14/28**	**28/28**	**0.5/28**	**1/28**	**2/28**	**3/28**	**7/28**	**14/28**	**28/28**
YM-DAP-AC-03	0.1068	0.2233	0.4466	0.5340	0.7184	0.7864	1.0000	0.1019	0.3460	0.4954	0.5940	0.7169	0.8770	1.0000
MIX-30	0.0494	0.1728	0.3333	0.4321	0.6667	0.9383	1.0000	0.0928	0.2983	0.4542	0.5415	0.7261	0.8823	1.0000
MIX-30-03	0.2750	0.6375	0.6875	0.8125	0.9500	0.9750	1.0000	0.1279	0.4178	0.5212	0.6005	0.7486	0.8984	1.0000
MIX-30-BRT	0.0661	0.2810	0.4132	0.4380	0.6446	0.8264	1.0000	0.1137	0.3923	0.5205	0.6165	0.7242	0.8830	1.0000
MIX-30-07	0.0920	0.2874	0.4713	0.5977	0.7816	0.9195	1.0000	0.0926	0.2904	0.4592	0.5534	0.7193	0.8744	1.0000
MIX-34-BRT	0.1238	0.3905	0.4952	-	0.6286	0.7905	1.0000	0.0960	0.3540	0.5131	-	0.6946	0.8642	1.0000
MIX-32-03	0.1186	0.4831	0.5508	0.6610	0.7966	0.9237	1.0000	0.1247	0.4176	0.5302	0.6186	0.7370	0.8905	1.0000
MIX-32-CEN	0.0909	0.2879	0.5000	0.5909	0.8182	0.9697	1.0000	0.0515	0.1500	0.3592	0.4659	0.6748	0.8377	1.0000
MIX-32-CEN-OK	0.0545	0.3455	0.5364	0.5818	0.6000	0.8909	1.0000	0.1152	0.3803	0.5127	0.6046	0.7304	0.8848	1.0000
B70-380	0.0375	0.1125	0.2000	0.2500	0.5750	0.8000	1.0000	0.0208	0.1272	0.2623	0.3402	0.6412	0.8774	1.0000
B70-420	0.0353	0.0941	0.2000	0.3412	0.5176	0.8353	1.0000	0.0162	0.0998	0.2516	0.3456	0.6044	0.8445	1.0000
B47-440	0.0196	0.1961	0.3627	0.4608	0.6667	0.9608	1.0000	0.0308	0.1874	0.3285	0.4223	0.6435	0.8727	1.0000
B67-440	0.0267	0.1867	0.4533	0.5067	0.8933	1.0667	1.0000	0.0302	0.1828	0.3252	0.4190	0.6424	0.8717	1.0000
B67-440-001	0.0213	0.1489	0.2128	0.3298	0.5426	0.7128	1.0000	0.0212	0.1195	0.2754	0.3694	0.6226	0.8521	1.0000
B67-440-BEY	0.0323	0.2043	0.3118	0.3763	0.6237	0.7957	1.0000	0.0185	0.0994	0.2542	0.3442	0.6202	0.8477	1.0000

5.6 Multivariate Regression Analysis for Modulus of Elasticity

In this section of the thesis, the Table 5.51, the Table 5.52, and the Table 5.53 share the regression models with their statistical results.

5.6.1 Logarithmic Regression (Model-1)

The logarithmic regression model (the Model-1) is one of the multivariate regression analysis models depending on the water to cement ratio of concrete mixture design. In this model, for 0.5-day, 1-day, 2-day, 3-day, 7-day, 14-day, and 28-day, the modulus of elasticity predictions was presented. At the end, for the FA + MS content included samples R^2 (btw -0.1102 & 0.1561), and R^2_{adj} results are scattered on the concrete age; SSE, and RMSE results are also differentiated at each concrete age for very huge numeric scales. For the GGBS included samples R^2 (btw 0.0788 & 0.6413), and R^2_{adj} results are come out at the concrete age; SSE, and RMSE results are varied in huge numeric scales for each concrete age, as well in FA + MS content included sample analysis. On the side, all data predictions are applied on these solutions, and the results are come out in expectations. In this way of the results, the elastic modulus development is enlisted in the Table 5.56.

In the Figure 5.63, the correlations of the actual data sets, and the predicted data sets are trendlined. The correlation shows that the model results are partially satisfying, and there are no negative deflections in the data fitting planar which means the model is safe to be used. In the Table 5.51, and the Table 5.52, with the statistical results for each concrete age regression analysis, the general forms of the multivariate logarithmic regression analysis equations are shared with both FA + MS and GGBS materials.

In the Figure 5.64, there is another correlation for the material effects in elastic modulus prediction for the FA + MS content by using the coefficients of the model equation. In this way, it is understood that the equation coefficient is not compatible except the age between 0.5-day, and 1-day.

Furthermore, the coefficient of the W/C ratio is also not coherent at the ages between the day-1, and day-3; and day-7 and day-14, either. That is why, just because using the coefficients of the equation is not beneficial for understanding of this model, another correlation is investigated in the Figure 5.65.

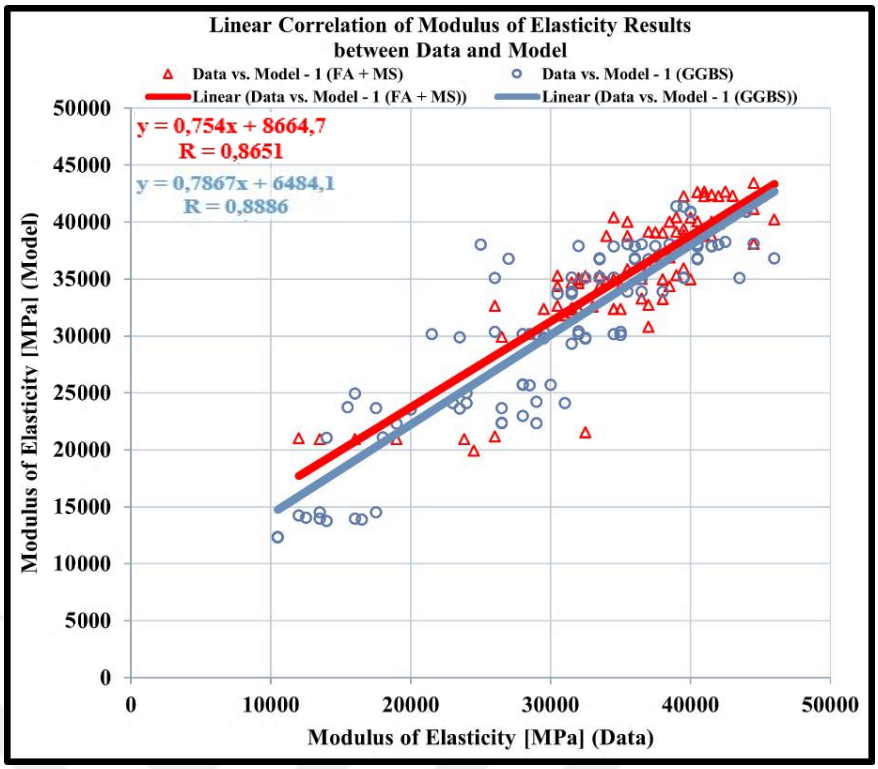

Figure 5.63: The correlations of the modulus of elasticity of the Model-1.

Table 5.51: The MRA results for ME in FA + MS content for the Model-1.

Age	Logarithmic Regression	R^2	R^2_{adj}	SSE	RMSE
0.5-Day	$E'_c = 10189.9202 - 10471.6522ln(w/c)$	0.0178	-0.3751	337617307.0311	12992.6384
1-Day	$E'_c = 15903.9507 - 16004.0346ln(w/c)$	0.1184	-0.0775	149634582.1434	8649.6989
2-Day	$E'_c = 16912.8034 - 16988.6726ln(w/c)$	0.1009	-0.1239	83820082.1366	6473.7965
3-Day	$E'_c = 17168.3024 - 17313.764ln(w/c)$	0.0576	-0.1309	113158379.5726	7521.9140
7-Day	$E'_c = 19037.639 - 19202.8744ln(w/c)$	0.1561	-0.0126	66308751.8124	5757.9837
14-Day	$E'_c = 19578.5593 - 19892.1432ln(w/c)$	-0.1102	-0.3877	118385194.5663	7693.6725
28-Day	$E'_c = 20754.3645 - 20925.1799ln(w/c)$	0.0635	-0.1238	61054049.9543	5525.1267

Table 5.52: The MRA results for ME in GGBS content for the Model-1.

Age	Logarithmic Regression	R^2	R^2_{adj}	SSE	RMSE
0.5-Day	$E'_c = 7061.7024 - 7134.843ln(w/c)$	0.0788	-1.7636	14969472.5720	2735.8246
1-Day	$E'_c = 13389.2285 - 10235.4957ln(w/c)$	0.6413	0.5862	243475525.0649	11033.4837
2-Day	$E'_c = 21897.7311 - 7912.3393ln(w/c)$	0.5119	0.4306	220073658.4568	10489.8441
3-Day	$E'_c = 25459.6284 - 4672.6015ln(w/c)$	0.2241	0.0948	285793460.8959	11953.9420
7-Day	$E'_c = 33816.0983 - 1273.6693ln(w/c)$	0.0230	-0.1273	266960662.1811	11553.3688
14-Day	$E'_c = 37934.2893 - 1126.7044ln(w/c)$	0.0179	-0.1332	269561837.0324	11609.5184
28-Day	$E'_c = 41067.1937 + 3008.9793ln(w/c)$	0.0945	-0.0448	336253286.5035	12966.3658

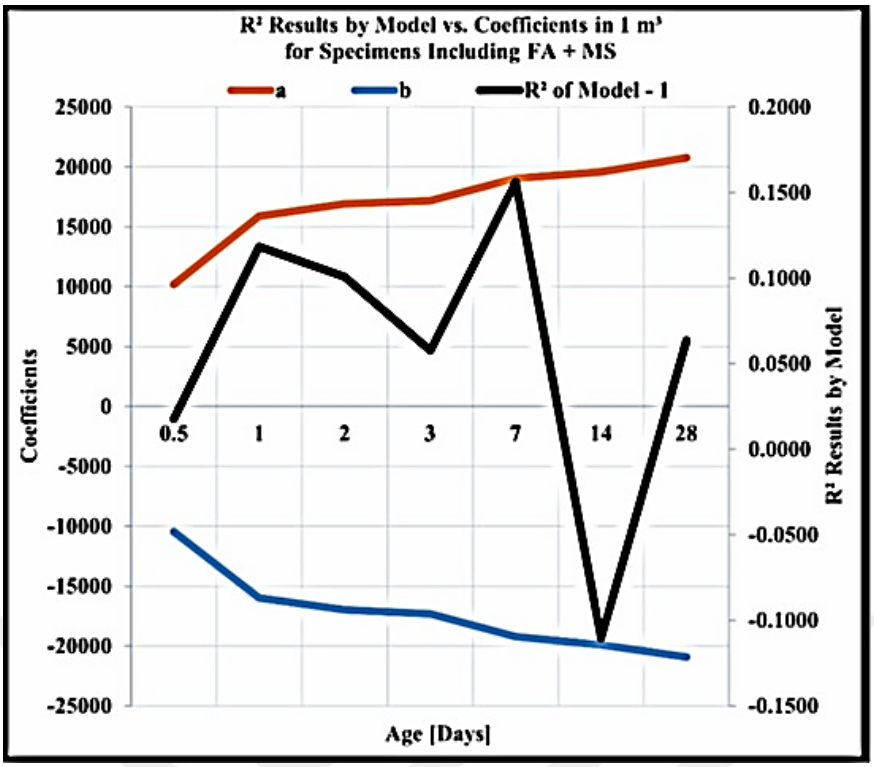

Figure 5.64: The correlations of the modulus of elasticity of the Model-1.

In the Figure 5.65, for both the minimum and maximum R^2 values of the model, the W/C ratio is neither the maximum nor the minimum. Especially for some specimens, the W/C ratio is seen almost ineffective. That is why this model is accepted as inappropriate to estimate the modulus of elasticity for the FA + MS content included concrete samples, even though the linear correlation of the model between the actual , and predicted data sets are coherent.

In the Figure 5.66, the correlation for material effects in elastic modulus prediction for GGBS content by using the coefficients of the model equation is given. In this way, it is enlightened that the equation coefficient is not compatible except the ages between 0.5-day, and 3-day; and day-14, and day-28. In addition, the coefficient of the W/C ratio is also not coherent at the ages between the day-1, and day-3; and day-14 and day-28, either. That is why, only using the coefficients of the equation is not beneficial for understanding of this model, another correlation is investigated in the Figure 5.66.

In the Figure 5.67, for the minimum R^2 value of the model, the W/C ratio is also the minimum (0.34). Especially for some specimens, the W/C ratio is seen almost ineffective. That is why this model is accepted as inappropriate to estimate the modulus of elasticity for the GGBS content included concrete samples, as well in FA + MS content included modulus of elasticity analysis.

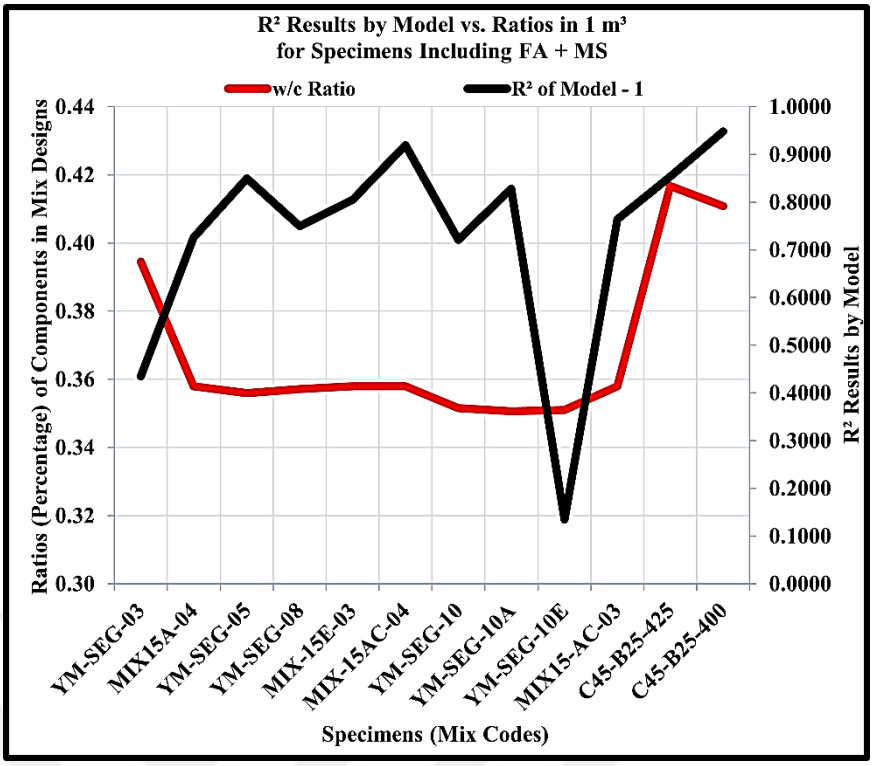

Figure 5.65: The relations of the modulus of elasticity of the Model-1 in FA + MS.

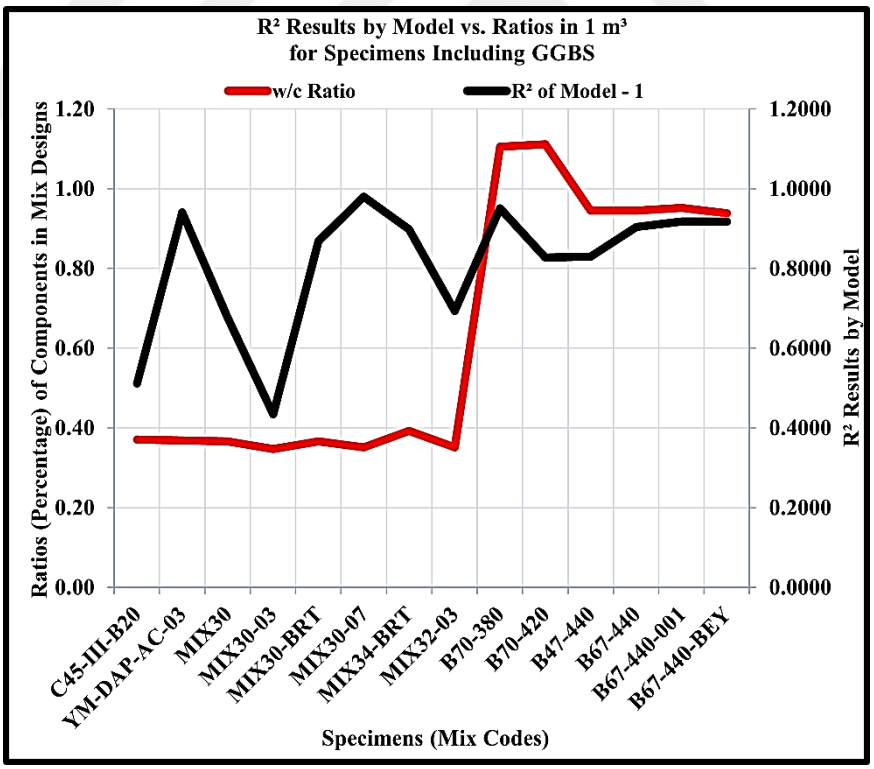

Figure 5.66: The relations of the modulus of elasticity of the Model-1 in GGBS.

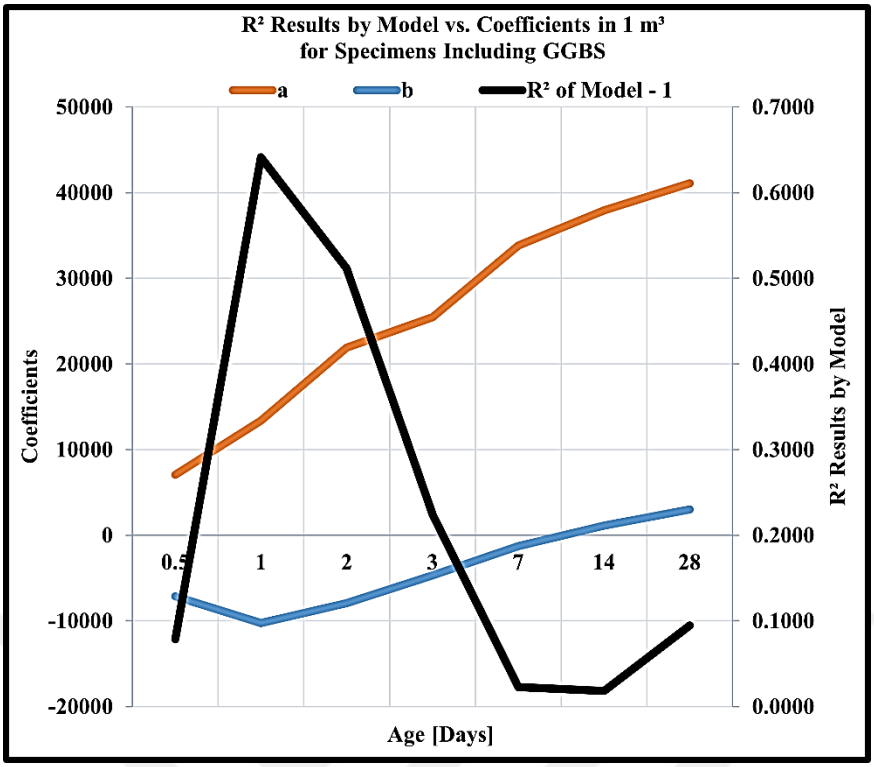

Figure 5.67: The correlations of the modulus of elasticity of the Model-1.

In the Table 5.53, for both pozzolans, the R^2 values are given with the mixing codes together. Also, in the Figure 5.68, the FA + MS content shows the higher elastic modulus prediction results than GGBS content does. Except the day-0.5, day-14, and day-28, for all ages, the modulus of elasticity for the specimens made of FA + MS content are close and/or above the median values. Except the day-3, day-7, and day-28, the elastic modulus of the specimens made of the GGBS content are close and/or above the median values. It is expresses that the modulus of elasticity prediction for the specimens including GGBS are more appropriate. However, the whiskers of the specimens including FA + MS content are more proper than the specimens including GGBS content. In the Table 5.54 and the Table 5.55, the numerical results of the boxplots are also shared.

Table 5.53: The MRA results of ME in FA + MS & GGBS contents in the Model-1.

Mixing Codes (FA + MS)	R^2	Mixing Codes (GGBS)	R^2
YM-SEG-03	0.4348	**C45-III-B20**	0.5117
MIX-15A-04	0.7256	**YM-DAP-AC-03**	0.9411
YM-SEG-05	0.8499	**MIX-30**	0.6777
YM-SEG-08	0.7500	**MIX-30-03**	0.4341
MIX-15E-03	0.8051	**MIX-30-BRT**	0.8681
MIX-15AC-04	0.9193	**MIX-30-07**	0.9805
YM-SEG-10	0.7212	**MIX-34-BRT**	0.8979
YM-SEG-10A	0.8276	**MIX-32-03**	0.6933
YM-SEG-10E	0.1352	**MIX-32-CEN**	-5.0710
MIX-15-AC-03	0.7643	**MIX-32-CEN-OK**	-0.0143
C45-B25-425	0.8541	**B70-380**	0.9513
C45-B25-400	0.9485	**B70-420**	0.8268
C50-B22-460	-0.7530	**B47-440**	0.8296
-	-	**B67-440**	0.9035
-	-	**B67-440-001**	0.9177
-	-	**B67-440-BEY**	0.9176

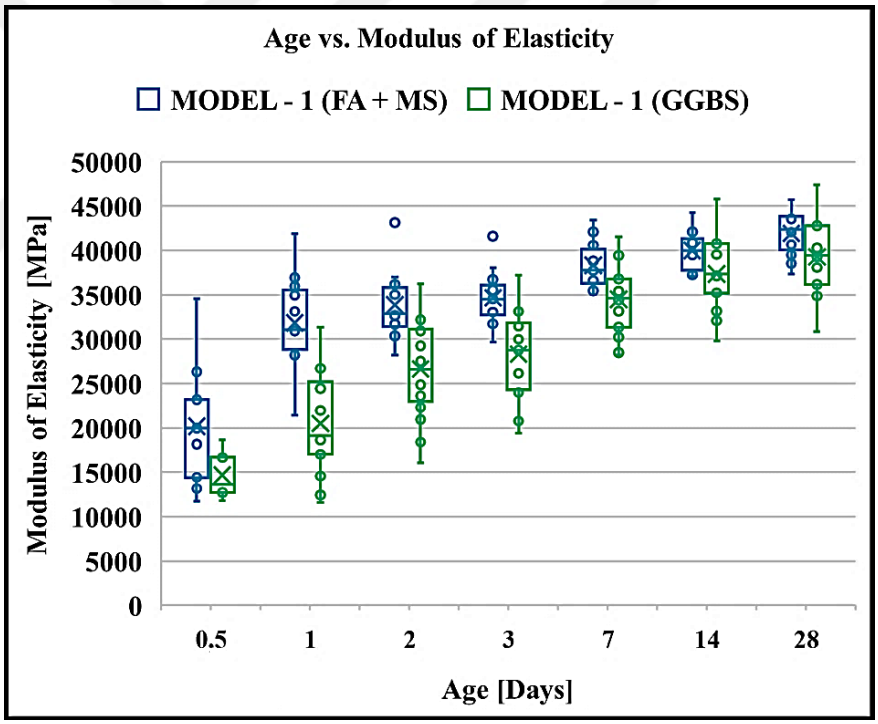

Figure 5.68: The age and the modulus of elasticity relationship for the Model-1.

Table 5.54: The ME results from MRA in FA + MS content for the Model-1.

Model-1 [MPa]	0.5-Day	1-Day	2-Day	3-Day	7-Day	14-Day	28-Day
Minimum Value	11770	21444	28214	29652	35046	37057	37340
1st-Quartile-Value	14416	28832	31415	32719	36316	37770	40087
Median Value	19958	31047	32902	34514	37731	39999	42362
3rd-Quartile-Value	23170	35498	35799	36115	40148	41310	43858
Maximum Value	34567	41845	43160	41594	43407	44270	45732
Mean Value	20162	31843	33845	34641	38311	40004	41897
Range	22797	20401	14945	11943	8361	7213	8392

Table 5.55: The ME results from MRA in GGBS content for the Model-1.

Model-1 [MPa]	0.5-Day	1-Day	2-Day	3-Day	7-Day	14-Day	28-Day
Minimum Value	11782	11618	16088	19430	28197	29791	30884
1st-Quartile-Value	12726	17007	22967	24263	31324	35209	36147
Median Value	13605	19141	26569	28756	34657	37345	39431
3rd-Quartile-Value	16662	25226	31152	31861	36788	40771	42769
Maximum Value	18629	31360	36250	37205	41539	45815	47406
Mean Value	14681	20482	26625	28307	34480	37337	39261
Range	6847	19742	20162	17775	13342	16024	16522

Table 5.56: The modulus of elasticity developments of samples for the Model-1.

Model-1	Strength Development of Actual Data [Day/Day]							Strength Development of Predicted Data [Day/Day]						
Mixing Codes	**0.5/28**	**1/28**	**2/28**	**3/28**	**7/28**	**14/28**	**28/28**	**0.5/28**	**1/28**	**2/28**	**3/28**	**7/28**	**14/28**	**28/28**
YM-SEG-03	0.5326	0.8043	0.8043	0.7935	0.8370	0.9674	1.0000	0.4956	0.7656	0.8134	0.8273	0.9175	0.9469	1.0000
MIX15A-04	0.5675	0.8333	0.9167	0.9524	0.9762	-	1.0000	0.4958	0.7655	0.8134	0.8273	0.9175	-	1.0000
YM-SEG-05	0.2892	0.7590	-	0.7711	0.9518	1.0120	1.0000	0.4958	0.7655	-	0.8273	0.9175	0.9471	1.0000
YM-SEG-08	-	0.8023	-	0.8488	0.9535	0.9419	1.0000	-	0.7655	-	0.8273	0.9175	0.9471	1.0000
MIX-15E-03	0.3902	0.7805	0.8171	0.8415	0.8293	0.8659	1.0000	0.4958	0.7655	0.8134	0.8273	0.9175	0.9471	1.0000
MIX-15AC-04	0.4222	0.7667	0.7778	0.8444	0.9222	0.9222	1.0000	0.4958	0.7655	0.8134	0.8273	0.9175	0.9471	1.0000
YM-SEG-10	-	0.7531	0.7901	0.8025	0.9259	0.9877	1.0000	-	0.7655	0.8134	0.8273	0.9175	0.9471	1.0000
YM-SEG-10A	0.6118	-	0.8000	0.7882	0.9176	0.9176	1.0000	0.4958	-	0.8133	0.8273	0.9175	0.9471	1.0000
YM-SEG-10E	-	0.6341	0.7683	0.7439	0.9024	0.8415	1.0000	-	0.7655	0.8133	0.8273	0.9175	0.9471	1.0000
MIX-15-AC-03	0.3418	0.7468	0.7722	0.8101	0.8987	0.9747	1.0000	0.4958	0.7655	0.8134	0.8273	0.9175	0.9471	1.0000
C45-B25-425	-	0.6974	0.8158	0.8289	0.9342	0.9868	1.0000	-	0.7656	0.8135	0.8273	0.9175	0.9468	1.0000
C45-B25-400	-	0.7215	0.7975	0.8354	0.9367	-	1.0000	-	0.7656	0.8135	0.8273	0.9175	-	1.0000
C50-B22-460	0.7303	0.8539	0.8764	0.8876	0.9438	1.0000	1.0000	0.4959	0.7655	0.8133	0.8273	0.9175	0.9472	1.0000
YM-SEG-03	0.5326	0.8043	0.8043	0.7935	0.8370	0.9674	1.0000	0.4956	0.7656	0.8134	0.8273	0.9175	0.9469	1.0000

Table 5.56 (continued): The modulus of elasticity developments of samples for the Model-1.

Model-1	Modulus of Elasticity Development of Actual Data [Day/Day]							Modulus of Elasticity Development of Predicted Data [Day/Day]						
Mixing Codes	**0.5/28**	**1/28**	**2/28**	**3/28**	**7/28**	**14/28**	**28/28**	**0.5/28**	**1/28**	**2/28**	**3/28**	**7/28**	**14/28**	**28/28**
C45-III-B20	-	0.4494	0.7303	0.7865	0.9775	1.0337	1.0000	-	0.6180	0.7810	0.7901	0.9211	0.9667	1.0000
YM-DAP-AC-03	-	0.5802	0.7284	0.7160	0.8272	0.8889	1.0000	-	0.6203	0.7829	0.7915	0.9218	0.9671	1.0000
MIX-30	-	0.4930	0.8310	0.7887	0.9155	0.9437	1.0000	-	0.6218	0.7842	0.7924	0.9224	0.9673	1.0000
MIX-30-03	-	0.7733	-	0.8533	0.8933	0.9867	1.0000	-	0.6391	-	0.8024	0.9281	0.9698	1.0000
MIX-30-BRT	0.2857	0.6310	0.7738	0.8214	0.9405	0.9643	1.0000	0.3743	0.6226	0.7848	0.7928	0.9226	0.9674	1.0000
MIX-30-07	0.3462	0.6154	0.7179	0.7564	0.8846	0.9231	1.0000	0.3831	0.6355	0.7958	0.8003	0.9269	0.9693	1.0000
MIX-34-BRT	0.3294	0.6588	0.7412	-	0.8588	0.8941	1.0000	0.3593	0.6006	0.7662	-	0.9153	0.9642	1.0000
MIX-32-03	0.4217	0.7470	0.7711	0.8434	0.9518	0.9759	1.0000	0.3831	0.6355	0.7958	0.8003	0.9269	0.9693	1.0000
MIX-32-CEN	-	0.6200	0.9400	0.8600	1.0400	1.0800	1.0000	-	0.6240	0.7861	0.7937	0.9231	0.9676	1.0000
MIX-32-CEN-OK	-	0.7188	0.8906	0.8125	0.9844	1.0469	1.0000	-	0.6355	0.7958	0.8003	0.9269	0.9693	1.0000
B70-380	-	0.2658	0.4557	0.6076	0.7722	0.9241	1.0000	-	0.2989	0.5102	0.6041		0.9197	1.0000
B70-420	-	0.2692	0.3590	0.4103	0.8077	0.9872	1.0000	-	0.2975	0.5090	0.6033		0.9195	1.0000
B47-440	-	0.3636	0.6591	0.6364	0.8636	0.9432	1.0000	-	0.3415	0.5463	0.6290	0.8286	0.9260	1.0000
B67-440	-	0.3068	0.6023	0.6818	0.8295	0.9205	1.0000	-	0.3415	0.5463	0.6290	0.8286	0.9260	1.0000
B67-440-001	-	0.4125	0.4750	0.7125	0.7875	0.9000	1.0000	-	0.3395	0.5446	0.6278		0.9257	1.0000
B67-440-BEY	-	0.3125	0.6625	0.7000	0.8875	0.8625	1.0000	-	0.3435	0.5480	0.6301	0.8293	0.9263	1.0000

5.7 Machine Learning Algorithm for Mechanical Properties of Concrete

In this section, Levenberg-Marquardt algorithm is studied for the compressive strength, splitting tensile strength and modulus of elasticity. In the input data sets, with all variables given in the Table 3.2 for the concrete mixture designs, the air content is either included or not included for the algorithm computations. Because it is aimed to see how the algorithm is accurate in unreal-like and real-like conditions.

5.7.1 Levenberg-Marquardt (LM) Algorithm

In the Table 5.57, for both FA + MS and GGBS contents, the algorithm is shared with the matrix designs and statistical results. The term of the target represents the actual test result. The training, validation, test, and all mean the algorithm results revealed by the software for the algorithm trials. In the Table 5.58, the Table 5.59, the Table 5.60, and the Table 5.61 with the actual data set, the predicted results are also enlisted for the compressive strength with the R^2 values for the accuracy checks.

Table 5.57: The LM Algorithm for the compressive strength prediction.

Content	Input	Target	Output	Air [%]	≈ Output	Linear Model	R	MSE
FA + MS	[ ]13 X 10	[ ]13 X 7	[ ]13 X 7	0.00	**Training**	1 X Target + 0.33	0.993	6.82664
					Validation	0.98 X Target - 0.49	0.92518	66.22872
					Test	0.24 X Target + 39	0.095505	3127.51988
					All	0.86 X Target + 7.8	0.62771	-
	[ ]13 X 10	[ ]13 X 7	[ ]13 X 7	> 0.00	**Training**	0.95 X Target + 3.3	0.95211	41.76505
					Validation	1.3 X Target - 20	0.85387	239.54692
					Test	0.87 X Target + 11	0.96703	63.08069
					All	0.94 X Target + 3.6	0.9156	-
GGBS	[ ]16 X 10	[ ]13 X 7	[ ]13 X 7	0.00	**Training**	1 X Target + 0.84	0.99232	9.77084
					Validation	1 X Target - 0.78	0.97444	29.87086
					Test	1.3 X Target + 2.7	0.98349	177.29129
					All	1 X Target + 1.5	0.97383	-
	[ ]16 X 10	[ ]13 X 7	[ ]13 X 7	> 0.00	**Training**	0.98 X Target + 2.3	0.98433	18.67574
					Validation	0.89 X Target + 3.8	0.93338	66.64377
					Test	1.7 X Target - 5.4	0.98141	283.09677
					All	0.93 X Target + 2.9	0.93468	-

In the Table 5.57, by comparing with the R values, the predictions were revealed by the software. For the FA + MS content included samples with the air content, the

results are very appropriate. Moreover, for the MSE results, the predictions without the air content, the estimations are worse than the air content included predictions except the training results of the algorithm. In contrast with the FA + MS included results, statistically, the GGBS content included sample prediction results are better with no air content.

Due to the algorithm working manner, without the air content in the FA + MS existence, the samples in C45-B25-425, and C45-B25-400 mixing codes are resulted negative in the R^2 values. That is why, the LM algorithm does not work for these concrete samples. However, with the air content in the FA + MS existence, only the sample in C50-B22-460 mixing code R^2 value is not acceptable. So, in general, the LM algorithm works for all scenarios in the content of FA + MS. The same method is also followed for the GGBS existence in the concrete samples. Without the air content, only the sample MIX-30-03 seems unsuitable in the result of R^2. For the air effect, the samples MIX-30, and MIX-30-03 are not convenient for the R^2 results.

In this light of the results, in the Figure 5.69, the Figure 5.70, the Figure 5.71, and the Figure 5.72, the neural network (NN) frames are given constructed on the mixture design variables. In the Figure 5.73, the Figure 5.74, the Figure 5.75, and the Figure 5.76, the linear correlations from the software are also shown. Onto this, in the Figure 5.77, and the Figure 5.78, the actual and predicted results are trendlined. In these correlations, each concrete specimen strength behavior was checked for the accuracy of the algorithm in the data fitting planar to see if there was a negative deflection or not. At the end, it was seen that there was no negative deflection for both FA + MS and GGBS content included sample results. That is why the algorithm is said to be safe for the compressive strength prediction, even though for the FA + MS including without air content results are statistically under the expectations.

Table 5.58: The LM Algorithm for the compressive strength prediction in FA + MS content without air.

LM Algorithm	Actual Data [MPa]							Predicted Data [MPa]							R^2
Mixing Codes	0.5-Day	1-Day	2-Day	3-Day	7-Day	14-Day	28-Day	0.5-Day	1-Day	2-Day	3-Day	7-Day	14-Day	28-Day	
YM-SEG-03	20.00	36.50	43.00	49.50	59.00	62.50	71.50	18.81	38.19	43.24	52.46	61.69	67.67	74.21	0.9702
MIX-15A-04	11.50	27.00	38.50	42.50	51.00	-	64.00	8.94	31.95	38.38	43.49	51.83	-	66.18	0.9777
YM-SEG-05	9.50	31.00	42.00	-	56.50	66.50	73.50	10.45	29.33	42.86	-	56.88	69.46	73.78	0.9953
YM-SEG-08	15.50	34.50	40.00	-	59.50	64.00	-	7.70	21.93	37.76	-	52.01	72.62	-	0.7716
MIX-15E-03	6.00	23.50	31.50	36.00	45.00	52.00	59.00	5.30	21.70	32.77	37.19	47.21	53.54	59.37	0.9927
MIX-15AC-04	11.50	27.50	40.00	44.50	54.00	60.00	69.50	11.09	25.43	41.21	44.99	55.58	61.49	69.40	0.9954
YM-SEG-10	-	23.50	33.50	39.00	50.00	60.50	69.50	-	23.83	33.61	39.02	50.07	58.72	69.74	0.9978
YM-SEG-10A	15.50	-	33.00	38.50	49.50	58.50	66.50	15.89	-	33.29	38.44	49.46	56.49	66.57	0.9975
YM-SEG-10E	-	23.50	29.00	31.00	44.00	53.50	60.50	-	12.30	33.39	38.68	49.41	54.74	67.78	0.7370
MIX-15-AC-03	-	22.50	-	35.50	45.00	51.50	54.00	-	32.39		36.76	45.99	56.23	57.95	0.7921
C45-B25-425	-	-	25.00	-	46.50	-	-	-	-	66.72	-	91.99	-	-	-15.4833
C45-B25-400	1.00	-	34.50	40.50	48.00	-	76.00	40.10	-	79.12	70.66	97.15	-	100.93	-1.2520
C50-B22-460	34.50	49.50	58.50	-	67.50	73.50	81.00	37.48	56.45	63.99	-	64.98	73.99	79.43	0.9087

Table 5.59: The LM Algorithm for the compressive strength prediction in FA + MS content with air.

LM Algorithm	Actual Data [MPa]							Predicted Data [MPa]							R^2
Mixing Codes	0.5-Day	1-Day	2-Day	3-Day	7-Day	14-Day	28-Day	0.5-Day	1-Day	2-Day	3-Day	7-Day	14-Day	28-Day	
YM-SEG-03	20.00	36.50	43.00	49.50	59.00	62.50	71.50	18.66	40.25	45.05	47.88	63.46	64.70	73.98	0.9706
MIX-15A-04	11.50	27.00	38.50	42.50	51.00	-	64.00	9.08	26.16	38.24	41.94	46.80	-	63.81	0.9853
YM-SEG-05	9.50	31.00	42.00	-	56.50	66.50	73.50	10.98	40.58	46.44	-	60.12	72.12	74.18	0.9445
YM-SEG-08	15.50	34.50	40.00	-	59.50	64.00	-	10.91	35.00	36.63	-	60.39	95.34	-	0.3447
MIX-15E-03	6.00	23.50	31.50	36.00	45.00	52.00	59.00	12.58	29.32	41.50	42.29	51.41	56.89	67.97	0.8135
MIX-15AC-04	11.50	27.50	40.00	44.50	54.00	60.00	69.50	12.40	29.92	43.29	44.04	51.62	54.43	69.45	0.9769
YM-SEG-10	-	23.50	33.50	39.00	50.00	60.50	69.50	-	32.41	35.41	35.56	49.82	62.61	66.25	0.9263
YM-SEG-10A	15.50	-	33.00	38.50	49.50	58.50	66.50	4.41	-	35.66	35.69	49.85	61.70	66.37	0.9132
YM-SEG-10E	-	23.50	29.00	-	44.00	53.50	-	-	30.98	34.18		47.69	66.96	-	0.5098
MIX-15-AC-03	4.00	22.50	29.50	35.50	45.00	-	54.00	3.55	28.68	32.96	36.33	42.90	-	53.66	0.9640
C45-B25-425	-	13.00	25.00	37.00	46.50	52.00	57.50	-	29.80	37.64	37.75	44.41	56.31	57.18	0.6771
C45-B25-400	-	24.00	34.50	40.50	48.00	-	76.00	-	35.35	36.89	41.76	52.32	-	77.22	0.8985
C50-B22-460	34.50	49.50	58.50	-	67.50	73.50	81.00	13.62	28.17	38.00		66.51	72.59	95.09	-0.0506

Table 5.60: The LM Algorithm for the compressive strength prediction in GGBS content without air.

LM Algorithm	Actual Data [MPa]							Predicted Data [MPa]							R^2
Mixing Codes	0.5-Day	1-Day	2-Day	3-Day	7-Day	14-Day	28-Day	0.5-Day	1-Day	2-Day	3-Day	7-Day	14-Day	28-Day	
C45-III-B20	2.00	9.50	24.00	30.50	51.00	74.50	86.00	1.43	9.13	24.31	30.19	51.60	69.92	83.31	0.9953
YM-DAP-AC-03	3.00	13.00	21.50	25.00	37.50	50.00	59.50	2.19	15.72	22.84	22.99	45.90	60.76	62.98	0.9131
MIX-30	1.50	5.50	12.50	-	29.00	36.50	46.50	1.80	4.41	17.19	-	31.82	41.82	48.69	0.9608
MIX-30-03	7.50	19.50	24.50	27.50	35.50	44.00	50.00	4.77	25.42	34.57	37.98	54.93	61.21	72.86	-0.1337
MIX-30-BRT	3.50	16.50	25.50	31.50	46.00	60.50	70.00	3.24	18.03	28.18	31.12	48.49	64.06	78.64	0.9698
MIX-30-07	3.00	12.50	19.00	-	32.50	44.00	50.50	2.58	14.76	26.27	-	36.71	54.40	56.04	0.8754
MIX-34-BRT	4.00	18.50	26.00	-	37.00	49.00	59.00	3.95	20.20	28.87	-	39.87	52.29	62.28	0.9800
MIX-32-03	6.00	25.50	33.00	38.50	47.50	59.00	71.00	5.11	24.61	33.38	36.39	48.18	55.96	66.99	0.9886
MIX-32-CEN	2.00	9.00	14.00	-	24.00	31.50	36.50	2.75	10.34	17.48	-	26.90	39.14	43.34	0.8577
MIX-32-CEN-OK	2.50	15.50	27.50	31.50	40.00	50.50	60.00	3.58	17.48	29.96	32.18	42.66	58.64	69.14	0.9284
B70-380	1.50	4.00	8.50	12.00	25.00	39.00	50.00	1.58	9.84	19.49	26.56	38.29	52.93	67.17	0.5039
B70-420	1.00	3.50	6.50	10.50	23.50	41.00	48.00	0.72	3.13	6.66	11.58	24.99	42.53	49.02	0.9967
B47-440	1.50	-	16.50	23.00	41.50	61.50	72.50	1.22	-	15.39	27.16	34.89	52.50	76.44	0.9538
B67-440	1.00	5.50	13.50	20.00	35.00	60.00	72.50	0.29	5.43	13.83	20.46	35.07	60.32	70.79	0.9991
B67-440-001	0.50	7.50	11.00	16.50	27.00	44.50	55.50	0.77	4.83	12.34	18.26	27.02	46.51	57.16	0.9923
B67-440-BEY	1.00	7.50	15.50	19.00	35.50	49.50	62.00	1.27	7.42	16.74	19.74	35.84	51.28	63.99	0.9969

Table 5.61: The LM Algorithm for the compressive strength prediction in GGBS content with air.

LM Algorithm	Actual Data [MPa]							Predicted Data [MPa]							R^2
Mixing Codes	**0.5-Day**	**1-Day**	**2-Day**	**3-Day**	**7-Day**	**14-Day**	**28-Day**	**0.5-Day**	**1-Day**	**2-Day**	**3-Day**	**7-Day**	**14-Day**	**28-Day**	
C45-III-B20	2.00	9.50	24.00	30.50	51.00	74.50	86.00	2.44	11.74	24.85	33.64	48.21	63.84	77.45	0.9658
YM-DAP-AC-03	3.00	13.00	21.50	25.00	37.50	50.00	59.50	3.01	14.03	24.66	25.87	35.75	38.17	45.55	0.8569
MIX-30	1.50	5.50	12.50	16.00	29.00	36.50	46.50	1.91	8.05	17.01	20.60	38.13	68.05	80.51	-0.3658
MIX-30-03	7.50	19.50	24.50	27.50	35.50	44.00	50.00	4.62	24.00	31.58	38.39	50.29	64.33	79.16	-0.3132
MIX-30-BRT	3.50	16.50	25.50	31.50	46.00	60.50	70.00	2.59	16.54	24.56	25.76	41.87	52.34	60.81	0.9408
MIX-30-07	3.00	12.50	19.00	23.00	32.50	44.00	50.50	2.87	14.08	19.87	24.18	32.69	44.51	53.91	0.9904
MIX-34-BRT	4.00	18.50	26.00	-	37.00	49.00	59.00	4.33	18.67	24.44	-	34.32	44.29	55.23	0.9774
MIX-32-03	6.00	25.50	33.00	38.50	47.50	59.00	71.00	5.14	26.31	35.38	41.61	47.27	50.17	63.22	0.9444
MIX-32-CEN	2.00	9.00	14.00	16.00	24.00	31.50	36.50	1.46	12.19	14.16	18.31	26.86	36.31	46.14	0.8460
MIX-32-CEN-OK	2.50	15.50	27.50	31.50	40.00	50.50	60.00	2.54	15.98	26.30	34.87	37.33	46.66	59.52	0.9851
B70-380	1.50	4.00	8.50	12.00	25.00	39.00	50.00	1.79	3.76	9.65	12.03	24.27	39.65	48.44	0.9977
B70-420	1.00	3.50	6.50	10.50	23.50	41.00	48.00	0.95	2.39	6.95	12.01	24.04	40.85	47.99	0.9981
B47-440	1.50	7.50	-	23.00	41.50	61.50	72.50	3.06	20.35	-	23.60	42.33	54.35	54.97	0.8737
B67-440	1.00	5.50	13.50	20.00	35.00	60.00	72.50	1.01	7.34	13.94	20.23	33.30	61.35	72.12	0.9981
B67-440-001	-	-	11.00	-	27.00	44.50	55.50	-	-	20.68	-	34.17	49.55	66.26	0.7508
B67-440-BEY	1.00	7.50	15.50	19.00	35.50	49.50	62.00	2.35	11.59	16.01	17.48	29.90	37.34	48.42	0.8741

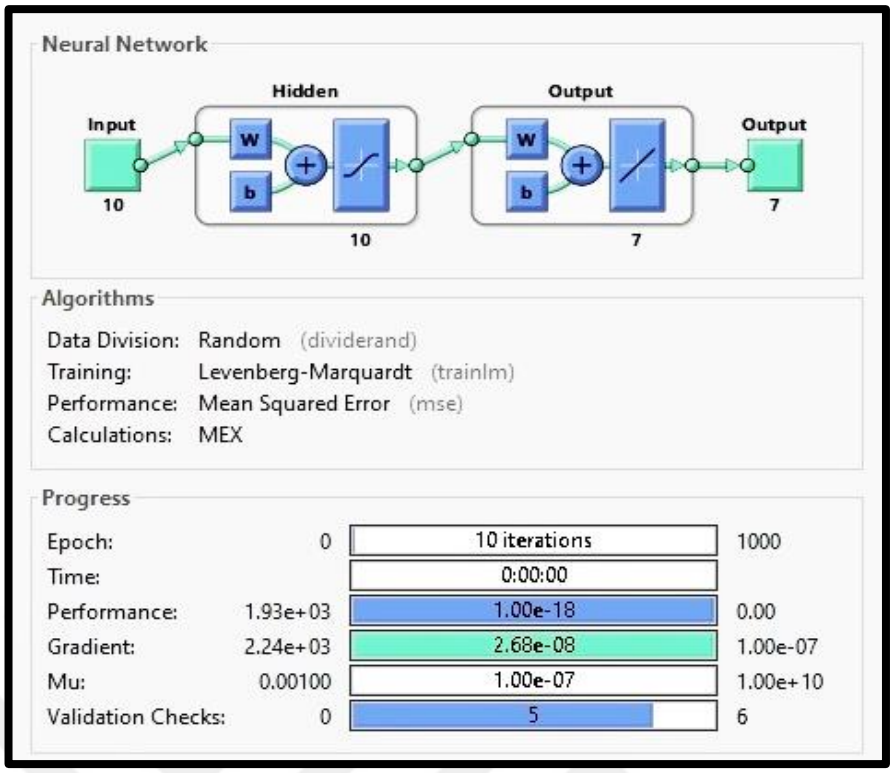

Figure 5.69: Without air content, FA + MS added NN in LM for CS.

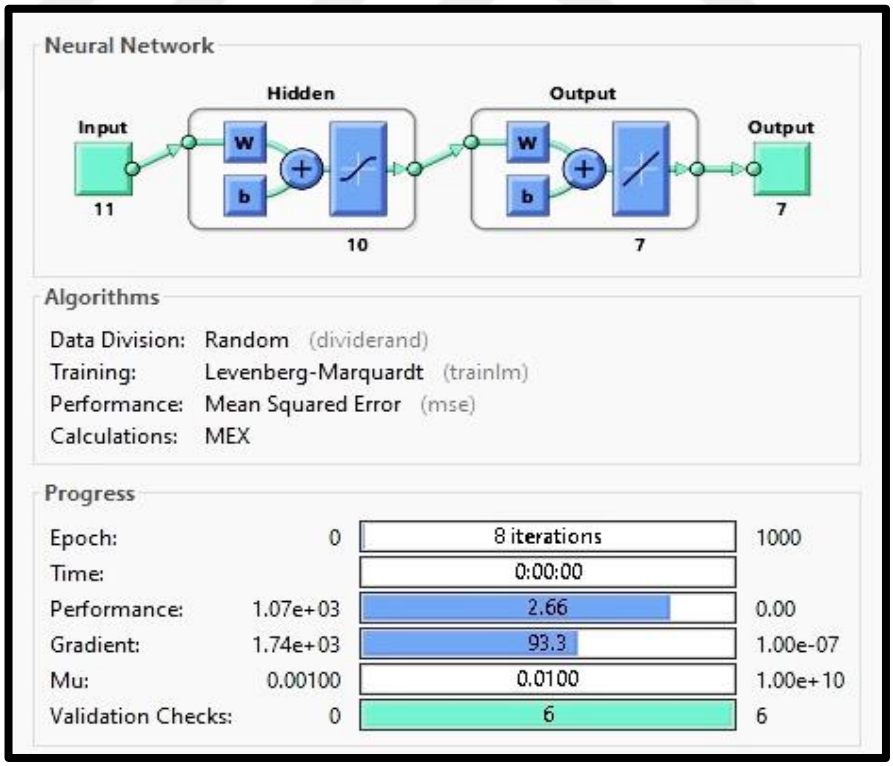

Figure 5.70: With air content, FA + MS added NN in LM for CS.

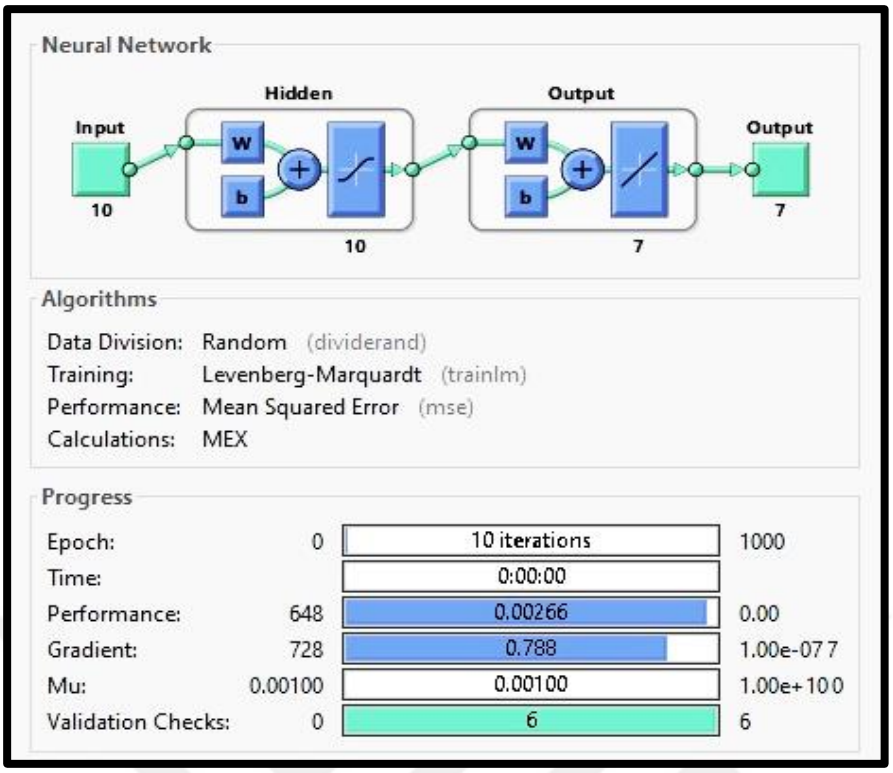

Figure 5.71: Without air content, GGBS added NN in LM for CS.

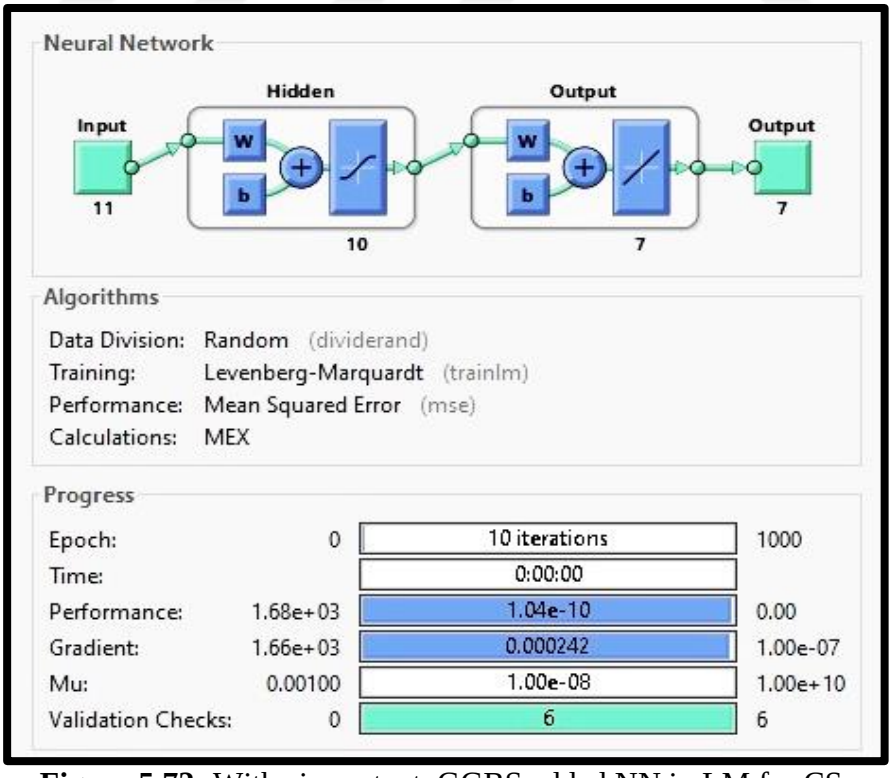

Figure 5.72: With air content, GGBS added NN in LM for CS.

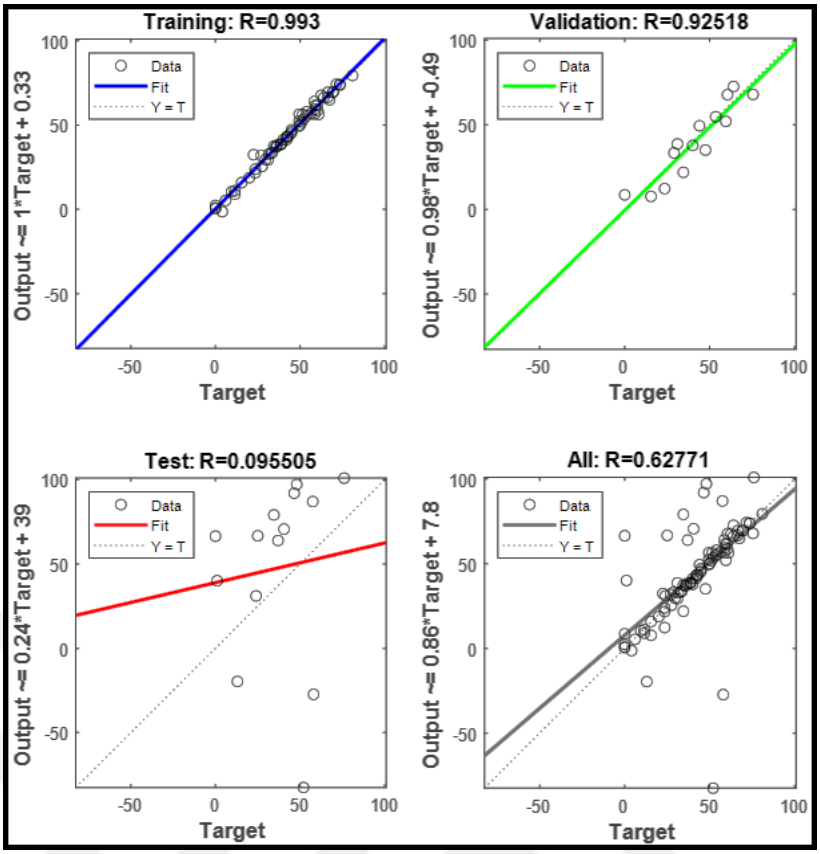

Figure 5.73: Without air content, FA + MS added results in LM for CS.

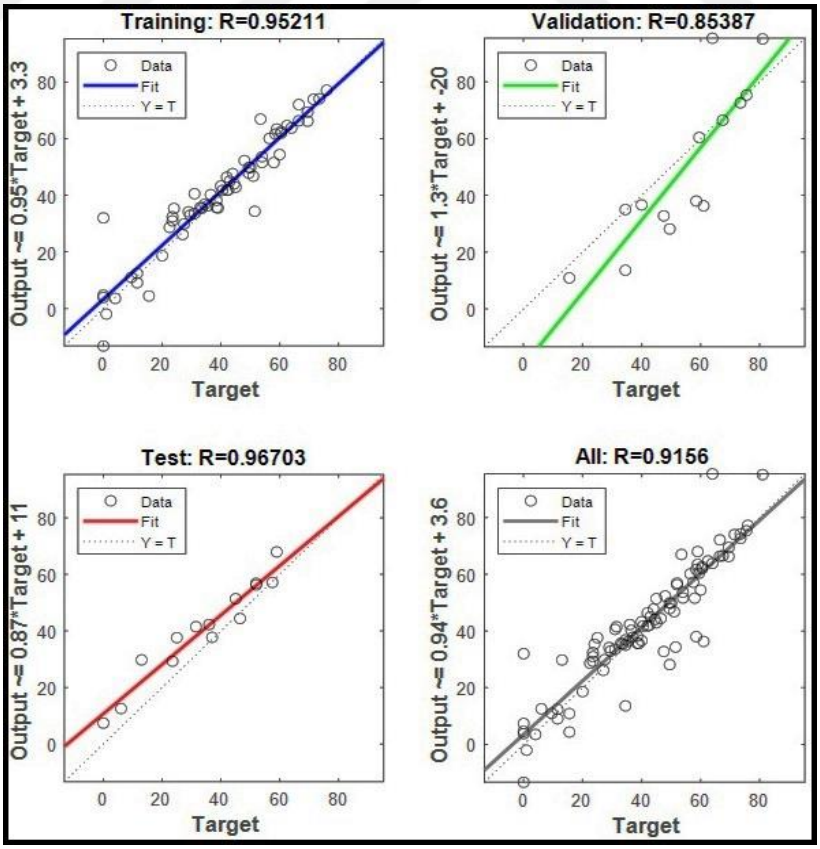

Figure 5.74: With air content, FA + MS added results in LM for CS.

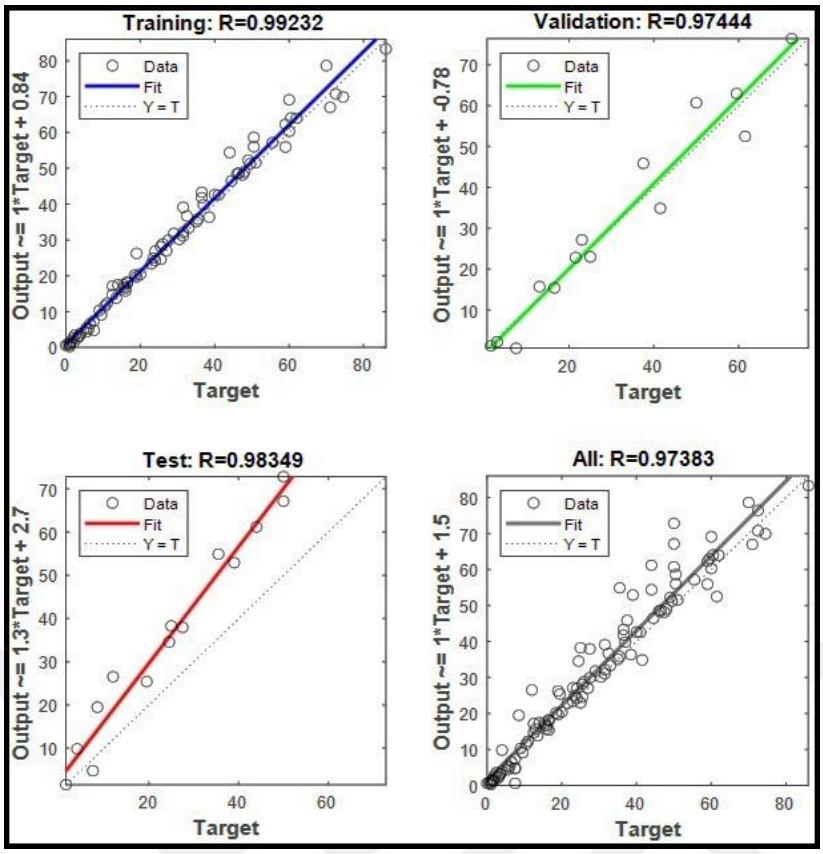

Figure 5.75: Without air content, GGBS added results in LM for CS.

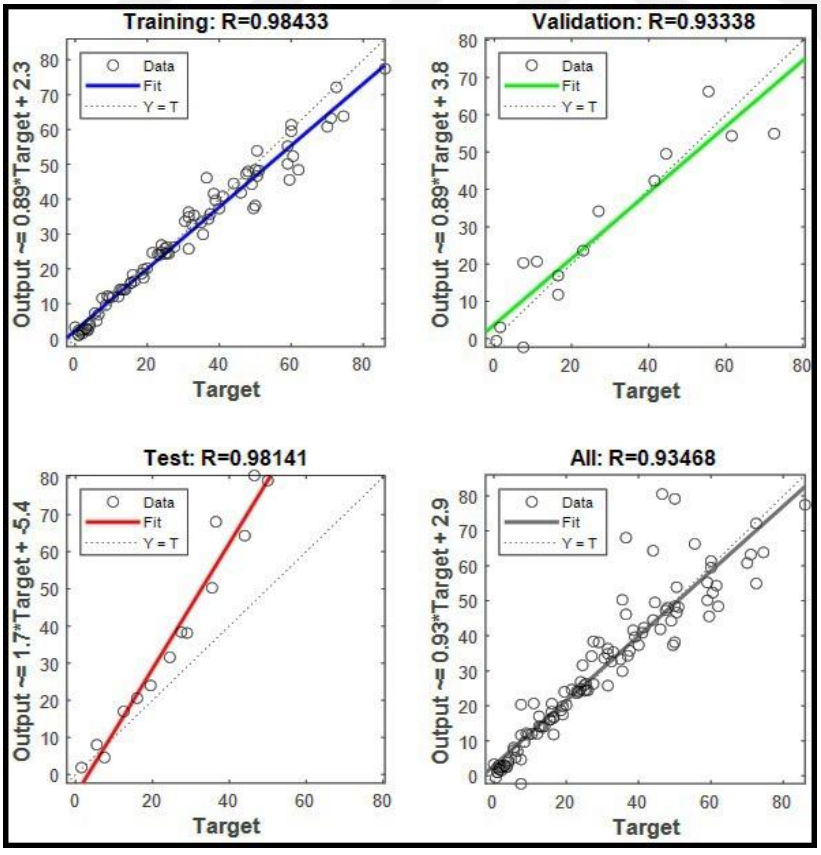

Figure 5.76: With air content, GGBS added results in LM for CS.

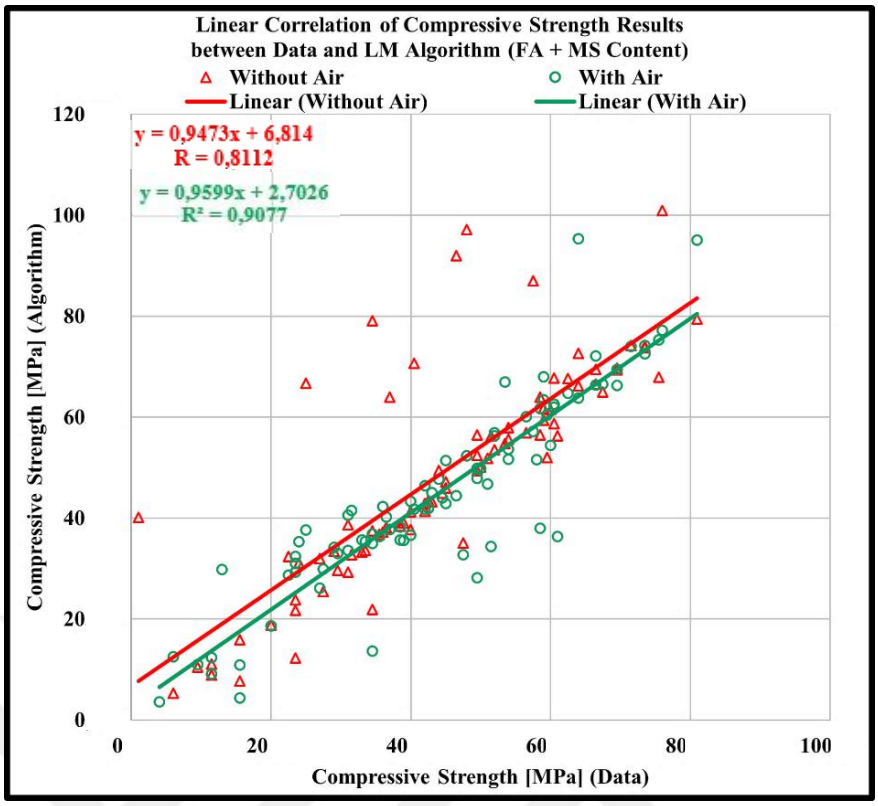

Figure 5.77: For air effect, FA + MS added results in LM for CS.

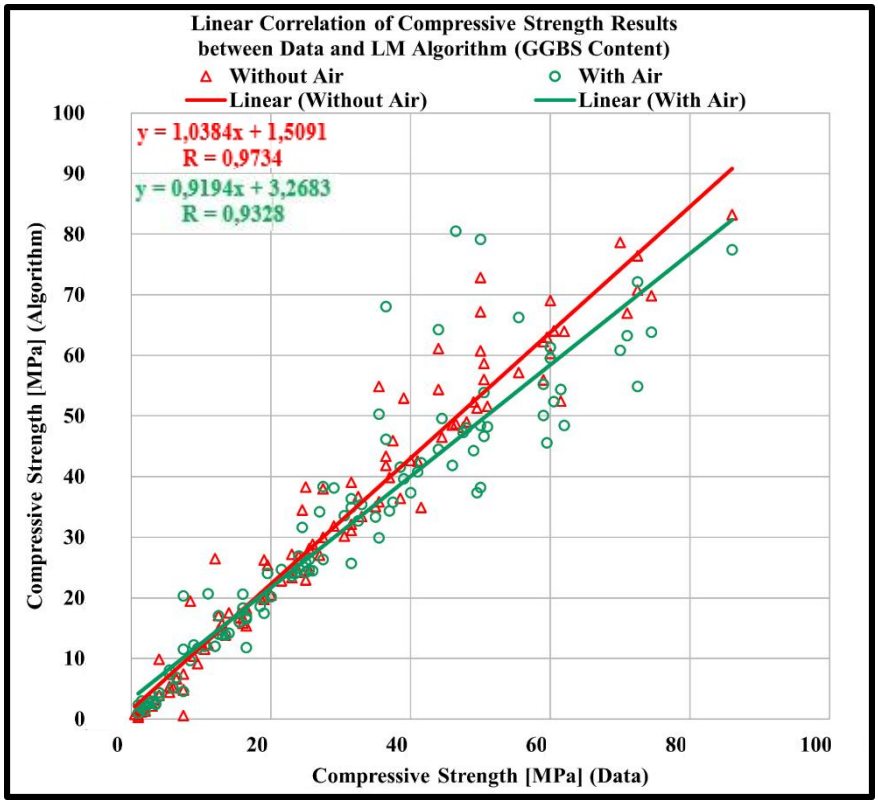

Figure 5.78: For air effect, GGBS added results in LM for CS.

In the Table 5.62, for the splitting tensile strength, in both FA + MS and GGBS contents, the algorithm is shared with the matrix designs and statistical results. The term of the target represents the actual test result as well in the compressive strength results of the LM algorithm. The training, validation, test, and all mean the algorithm results revealed by the software for the model trials. In the Table 5.63, the Table 5.64, the Table 5.65, and the Table 5.66, with the actual data set, the predicted results are also enlisted for the splitting tensile strength with the R^2 values for the accuracy.

Table 5.62: The LM Algorithm for the splitting tensile strength prediction.

Content	Input	Target	Output	Air [%]	≈ Output	Linear Model	R	MSE
FA + MS	[ ]13 x 10	[ ]13 x 7	[ ]13 x 7	0.00	**Training**	1 X Target - 0.11	0.98656	0.0791627
					Validation	0.7 X Target + 0.69	0.82299	1.24976
					Test	0.87 X Target - 0.054	0.93592	0.574912
					All	0.96 X Target - 0.01	0.96401	-
	[ ]13 x 10	[ ]13 x 7	[ ]13 x 7	> 0.00	**Training**	0.98 X Target + 0.0076	0.99399	0.0320651
					Validation	0.76 X Target + 1.1	0.84768	1.11238
					Test	0.97 X Target + 0.3	0.97957	0.164248
					All	0.96 X Target + 0.15	0.97547	-
GGBS	[ ]16 x 10	[ ]13 x 7	[ ]13 x 7	0.00	**Training**	0.92 X Target + 0.019	0.96562	0.221248
					Validation	1.3 X Target - 0.36	0.90111	0.7912
					Test	0.9 X Target - 0.08	0.94213	0.522575
					All	0.93 X Target + 0.013	0.94247	-
	[ ]16 x 10	[ ]13 x 7	[ ]13 x 7	> 0.00	**Training**	0.96 X Target + 0.19	0.97286	0.16207
					Validation	1.1 X Target - 0.2	0.93022	0.316239
					Test	1.2 X Target + 0.15	0.9206	1.35463
					All	1 X Target + 0.17	0.94707	-

In the Table 5.62, by comparing with the R values revealed by the software, for the FA + MS content included samples with and without the air content, the results are very appropriate. Moreover, for the MSE results, the predictions with and without the air content, are also in the expectations. On the contrary, the GGBS content included sample prediction results are worse than the FA + MS content included results, even though the results are not deniable.

Due to the algorithm forecasting, without the air content in the FA + MS existence, the sample in YM-SEG-10A mixing code is lower resulted among the other R^2 values. With the air content in the FA + MS existence, the same sample is lower among the

R^2 values, as well. However, this time, it is better resulted. So, in general, the LM algorithm works for all scenarios in the FA + MS content for the splitting tensile strength predictions. The same method is also followed for the GGBS existence in the concrete samples. Without the air content, the samples C45-III-B20, and MIX-30-03 seem inappropriate in the results of R^2. For the air effect, the samples in MIX-30, MIX-30-03, MIX-32-03, MIX-32-CEN, and B67-440 mixing codes are inconvenient for the R^2 values. Especially the sample MIX-32-CEN is almost zero which is inacceptable for the algorithm accuracy. In the air content included results, the sample in YM-DAP-AC-03 is under zero for the R^2 value. This shows that the algorithm does not work for this sample. At the same time, again, the samples in MIX-30-03, and MIX-32-CEN mixing codes are lower among the other R^2 results. But this time, these sample results are higher than the not air content included analysis results.

In this light of the results, in the Figure 5.79, the Figure 5.80, the Figure 5.81, and the Figure 5.82, the NN frames are given constructed on the mixture design variables. The Figure 5.83, the Figure 5.84, the Figure 5.85, and the Figure 5.86 are the linear correlations from the software. Onto this, in the Figure 5.87, and the Figure 5.88, the actual, and predicted results are trendlined. In this correlation, each concrete specimen strength behavior was checked for the accuracy of the algorithm in the data fitting planar to see if there was a negative deflection or not. At the end, without air content in the FA + MS existence, the samples in YM-SEG-10, C45-B25-425, and C45-B25-400 mixing codes were seen in negative deflections in the fitting planar. With the air content, the samples in YM-SEG-10E, MIX-15-AC-03, YM-SEG-08, and C45-B25-400 mixing codes were seen in negative deflections in the FA + MS content. For the GGBS content with the absence of the air, only the sample in MIX-30-03 mixing code was deflected in the fitting planar in negative way, which was not expected. With the air content in the GGBS existence, the samples in MIX-30-03, MIX-34-BRT, MIX-32-03, and B67-440 mixing codes were deflected in negative way, as well. That is why the algorithm is said to be less safe for the splitting tensile strength prediction in the GGBS content with air. Because of that the FA + MS content included algorithm results were more valid.

Table 5.63: The LM Algorithm for the splitting tensile strength prediction in FA + MS content without air.

LM Algorithm	Actual Data [MPa]							Predicted Data [MPa]							R^2
Mixing Codes	0.5-Day	1-Day	2-Day	3-Day	7-Day	14-Day	28-Day	0.5-Day	1-Day	2-Day	3-Day	7-Day	14-Day	28-Day	
YM-SEG-03	1.65	3.85	4.40	4.40	5.25	5.55	5.85	1.70	3.64	4.32	4.40	5.22	5.35	6.00	0.9905
MIX15A-04	1.35	2.85	3.55	3.80	4.25	-	4.80	1.19	2.35	3.38	3.68	4.10	-	4.82	0.9543
YM-SEG-05	1.25	2.50	3.85	4.30	-	5.05	4.95	1.22	2.05	3.75	4.19	-	4.60	5.17	0.9571
YM-SEG-08	2.05	2.80	3.90	4.60	4.70	-	6.40	1.72	2.65	3.87	4.37	4.80	-	6.32	0.9829
MIX-15E-03	0.95	2.40	3.25	3.65	4.25	-	5.25	0.88	2.07	3.15	3.58	3.96	-	5.23	0.9813
MIX-15AC-04	1.30	2.60	4.20	4.45	3.55	-	5.90	0.90	2.11	3.14	3.61	4.06	-	5.27	0.7722
YM-SEG-10	-	2.60	3.00	3.80	4.05	5.30	5.30	-	2.02	3.01	3.63	4.52	4.57	5.64	0.8045
YM-SEG-10A	1.55	-	3.20	3.15	-	5.35	5.55	0.02	-	2.88	3.61	-	4.42	5.31	0.6848
YM-SEG-10E	-	2.35	3.20	3.45	4.65	5.20	5.30	-	1.75	3.00	3.45	4.77	4.96	5.69	0.9147
MIX15-AC-03	0.55	2.05	3.30	3.75	3.95	-	5.15	0.59	1.60	3.15	3.70	4.03	-	5.04	0.9808
C45-B25-425	-	1.50	2.20	3.05	3.95	4.15	4.75	-	1.77	2.74	3.08	3.70	3.90	5.21	0.9089
C45-B25-400	0.20	2.65	3.65	3.50	3.70	4.25	5.75	0.34	2.16	2.99	3.34	4.09	4.10	5.25	0.9337
C50-B22-460	2.80	3.70	3.95	4.90	5.25	5.35	5.55	2.95	3.97	4.09	5.00	5.08	5.26	5.58	0.9749

Table 5.64: The LM Algorithm for the splitting tensile strength prediction in FA + MS content with air.

LM Algorithm	Actual Data [MPa]							Predicted Data [MPa]							R^2
Mixing Codes	0.5-Day	1-Day	2-Day	3-Day	7-Day	14-Day	28-Day	0.5-Day	1-Day	2-Day	3-Day	7-Day	14-Day	28-Day	
YM-SEG-03	1.65	3.85	4.40	4.40	5.25	5.55	5.85	1.79	3.17	4.32	4.35	4.58	5.39	5.72	0.9188
MIX15A-04	1.35	2.85	3.55	3.80	4.25	-	4.80	1.32	2.85	3.58	3.75	4.24	-	4.79	0.9995
YM-SEG-05	1.25	2.50	3.85	4.30	-	5.05	4.95	1.32	2.13	3.82	4.29	-	5.11	-	0.9730
YM-SEG-08	2.05	2.80	3.90	4.60	4.70	-	6.40	2.19	2.44	3.97	4.56	4.67	4.97	6.07	0.9658
MIX-15E-03	0.95	2.40	3.25	3.65	4.25	-	5.25	0.90	2.47	3.19	3.78	4.32	-	5.41	0.9946
MIX-15AC-04	1.30	2.60	4.20	4.45	3.55	-	5.90	1.32	2.68	4.22	4.40	-	4.91	5.91	0.9767
YM-SEG-10	-	2.60	3.00	3.80	4.05	5.30	5.30	-	2.58	3.02	3.80	4.07	5.30	-	0.9617
YM-SEG-10A	1.55	-	3.20	3.15	-	5.35	5.55	0.45	-	3.40	4.06	4.12	5.61	5.65	0.7998
YM-SEG-10E	-	2.35	3.20	3.45	4.65	5.20	5.30	-	2.38	3.38	4.05	4.11	5.68	-	0.8273
MIX15-AC-03	0.55	2.05	3.30	3.75	3.95	-	5.15	0.57	2.06	3.21	3.75	3.83	4.00	5.32	0.9636
C45-B25-425	-	1.50	2.20	3.05	3.95	4.15	4.75	-	1.86	2.29	2.95	3.38	3.87	4.54	0.8859
C45-B25-400	0.20	2.65	3.65	3.50	3.70	4.25	5.75	0.13	2.90	3.62	-	-	4.09	5.73	0.9946
C50-B22-460	2.80	3.70	3.95	4.90	5.25	5.35	5.55	2.81	3.53	3.90	4.91	5.07	5.32	5.56	0.9897

Table 5.65: The LM Algorithm for the splitting tensile strength prediction in GGBS content without air.

LM Algorithm	Actual Data [MPa]							Predicted Data [MPa]							R^2
Mixing Codes	0.5-Day	1-Day	2-Day	3-Day	7-Day	14-Day	28-Day	0.5-Day	1-Day	2-Day	3-Day	7-Day	14-Day	28-Day	
C45-III-B20	0.25	1.20	2.70	3.25	4.95	4.20	6.55	0.48	0.77	2.00	2.73	3.43	4.43	4.97	0.7924
YM-DAP-AC-03	0.55	1.15	2.30	2.75	3.70	4.05	5.15	0.55	0.90	2.15	2.32	3.31	4.31	4.92	0.9662
MIX-30	0.20	0.70	1.35	1.75	2.70	3.80	4.05	0.39	0.93	1.51	1.92	2.86	3.84	4.15	0.9864
MIX-30-03	1.10	2.55	2.75	3.25	3.80	3.90	4.00	0.66	1.42	2.10	2.24	3.33	4.37	4.40	0.4469
MIX-30-BRT	0.40	1.70	2.50	-	3.90	5.00	6.05	0.59	1.41	2.43	-	3.56	5.01	5.64	0.9819
MIX-30-07	0.40	1.25	2.05	2.60	3.40	4.00	4.35	0.33	1.14	1.75	2.09	3.01	3.95	4.17	0.9558
MIX-34-BRT	0.65	2.05	2.60	-	3.30	4.15	5.25	0.46	1.79	2.11	-	3.14	3.87	5.07	0.9633
MIX-32-03	0.70	2.85	3.25	3.90	4.70	5.45	5.90	0.56	1.41	2.09	2.61	3.54	4.58	4.99	0.5707
MIX-32-CEN	0.30	0.95	1.65	-	2.70	3.20	3.30	0.37	0.79	2.25	-	3.07	4.71	5.47	0.0294
MIX-32-CEN-OK	0.30	1.90	2.95	-	3.30	4.90	5.50	0.43	0.99	2.19	-	3.13	4.56	4.96	0.8993
B70-380	0.15	0.45	0.80	1.00	2.30	3.20	4.00	0.21	0.67	1.27	1.53	2.23	3.47	4.06	0.9515
B70-420	0.15	0.40	0.85	1.45	2.20	3.55	4.25	0.22	0.50	1.28	1.63	2.64	3.63	4.43	0.9688
B47-440	0.10	1.00	1.85	2.35	3.40	4.90	-	0.18	0.72	1.42	2.21	2.96	4.96	-	0.9673
B67-440	-	0.70	-	1.90	3.35	4.00	3.75	-	0.90	-	1.24	2.73	3.99	5.09	0.6632
B67-440-001	-	-	1.00	1.55	2.55	3.35	4.70	-	-	1.01	1.34	2.36	3.57	5.48	0.9144
B67-440-BEY	-	0.95	1.45	1.75	2.90	3.70	4.65	-	0.90	1.47	1.68	2.92	3.70	4.59	0.9988

Table 5.66: The LM Algorithm for the splitting tensile strength prediction in GGBS content with air.

LM Algorithm	Actual Data [MPa]							Predicted Data [MPa]							R^2
Mixing Codes	0.5-Day	1-Day	2-Day	3-Day	7-Day	14-Day	28-Day	0.5-Day	1-Day	2-Day	3-Day	7-Day	14-Day	28-Day	
C45-III-B20	0.25	1.20	2.70	-	4.95	-	6.55	0.46	1.78	2.70	-	5.10	-	6.78	0.9833
YM-DAP-AC-03	0.55	1.15	2.30	-	3.70	4.05	5.15	0.73	3.63	4.18	-	5.45	5.78	6.34	-0.0780
MIX-30	0.20	0.70	1.35	-	2.70	3.80	-	0.03	1.00	1.89	-	2.17	3.91	-	0.9198
MIX-30-03	1.10	2.55	2.75	3.25	3.80	3.90	-	0.20	2.04	2.68	3.51	3.52	5.14	-	0.4798
MIX-30-BRT	0.40	1.70	2.50	2.65	3.90	5.00	6.05	0.49	2.04	2.66	3.13	3.59	4.86	5.67	0.9720
MIX-30-07	0.40	1.25	2.05	2.60	3.40	4.00	4.35	0.47	1.16	1.82	2.12	2.44	3.97	4.30	0.9032
MIX-34-BRT	0.65	2.05	2.60	-	-	4.15	5.25	0.69	3.07	3.07	-	-	4.21	5.41	0.8995
MIX-32-03	0.70	2.85	3.25	-	4.70	5.45	5.90	0.63	2.96	3.59	-	4.79	5.58	5.64	0.9882
MIX-32-CEN	0.30	0.95	1.65	1.95	2.70	3.20	-	0.45	1.58	2.20	2.35	3.67	4.19	-	0.5144
MIX-32-CEN-OK	0.30	1.90	2.95	-	3.30	4.90	-	0.47	2.30	3.27	-	4.37	5.37	-	0.8586
B70-380	0.15	0.45	0.80	1.00	2.30	3.20	4.00	0.25	0.47	0.72	0.83	2.37	3.22	3.74	0.9909
B70-420	0.15	-	0.85	1.45	2.20	3.55	4.25	0.01	-	0.69	0.98	3.11	3.74	4.70	0.8942
B47-440	0.10	1.00	1.85	2.35	3.40	4.90	-	0.26	1.15	1.73	2.32	4.38	5.12	-	0.9273
B67-440	0.10	0.70	1.70	1.90	3.35	4.00	3.75	0.52	1.13	1.15	1.89	3.09	4.27	4.60	0.8913
B67-440-001	0.10	0.70	1.00	1.55	2.55	3.35	4.70	0.19	0.63	1.11	1.15	2.77	3.33	4.73	0.9854
B67-440-BEY	0.15	0.95	1.45	1.75	2.90	3.70	4.65	0.16	0.79	1.41	1.86	2.61	3.65	4.65	0.9918

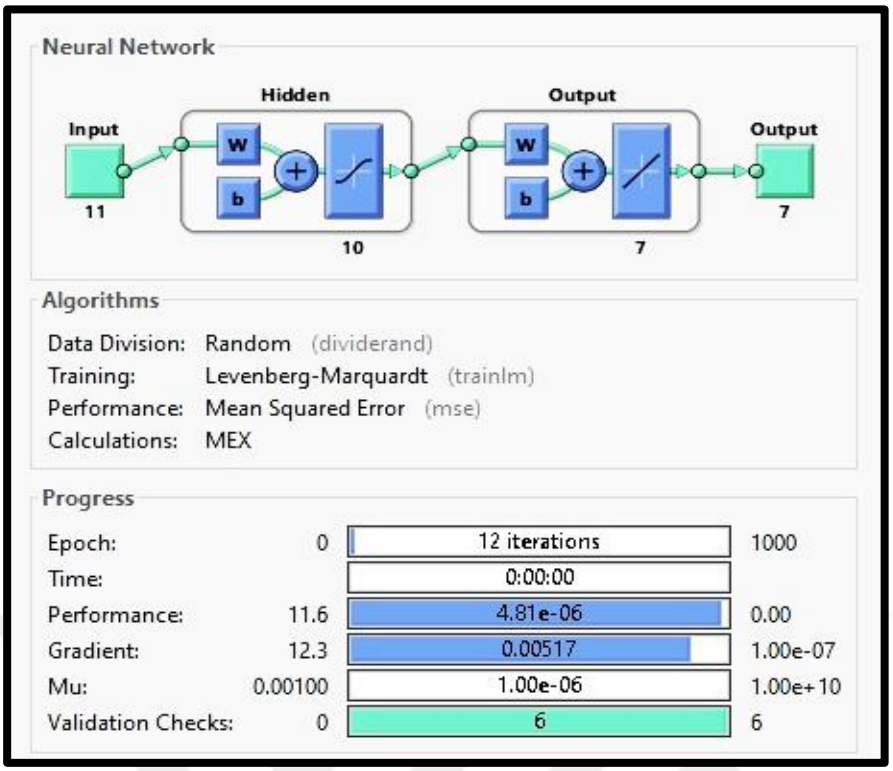

Figure 5.79: Without air content, FA + MS added NN in LM for STS.

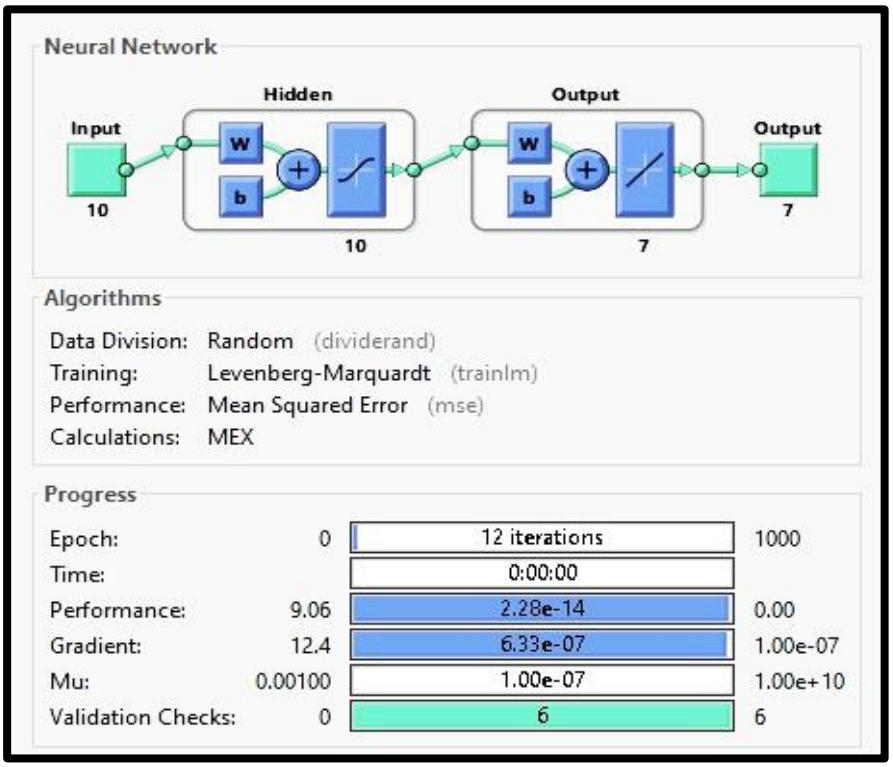

Figure 5.80: With air content, FA + MS added NN in LM for STS.

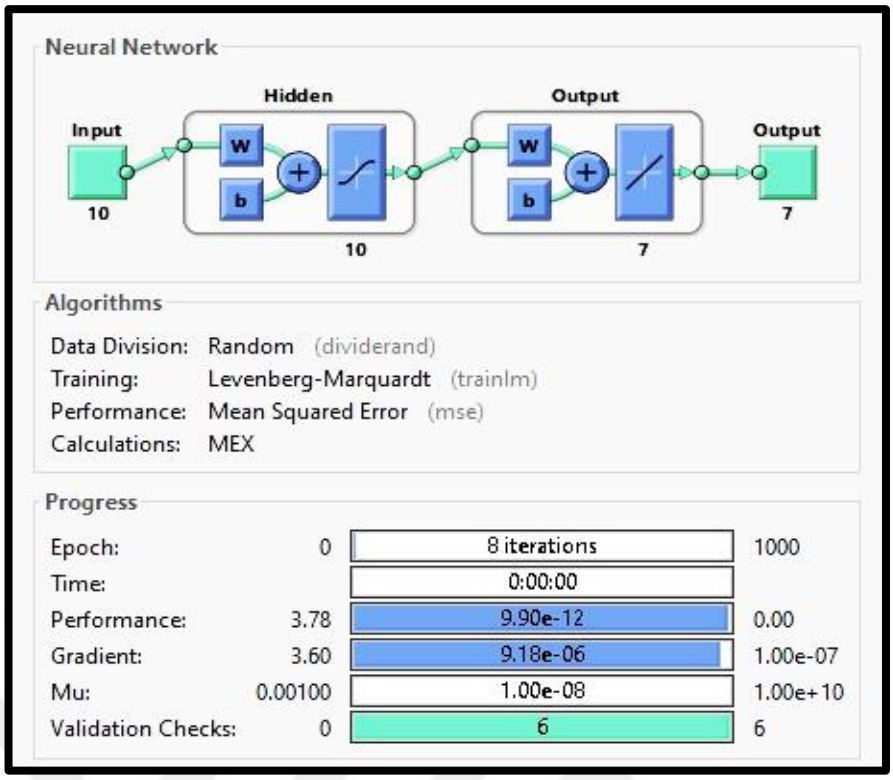

Figure 5.81: Without air content, GGBS added NN in LM for STS.

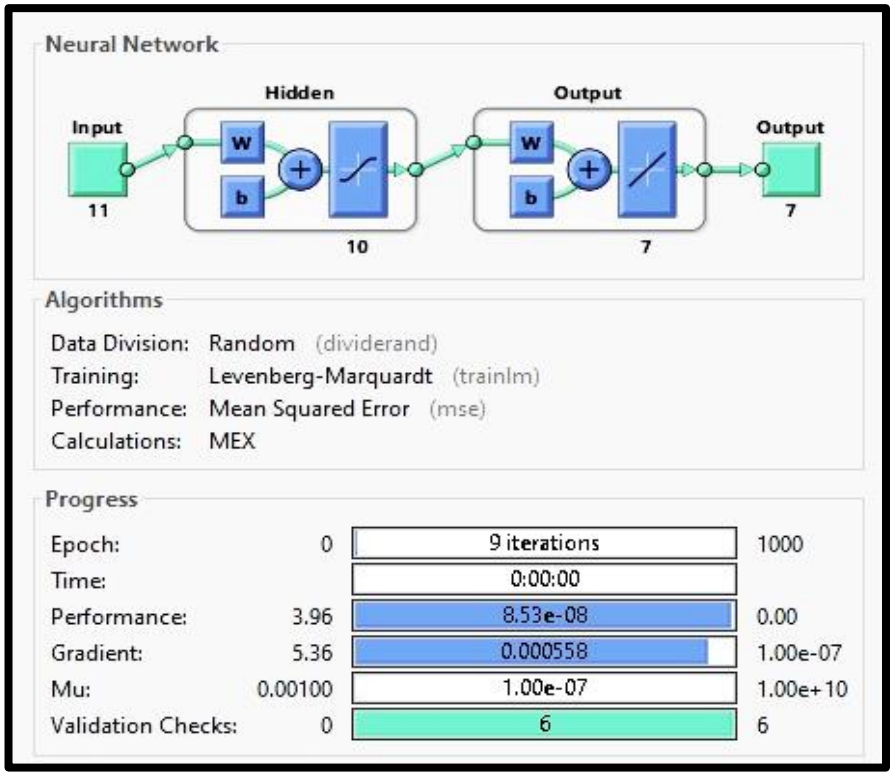

Figure 5.82: With air content, GGBS added NN in LM for STS.

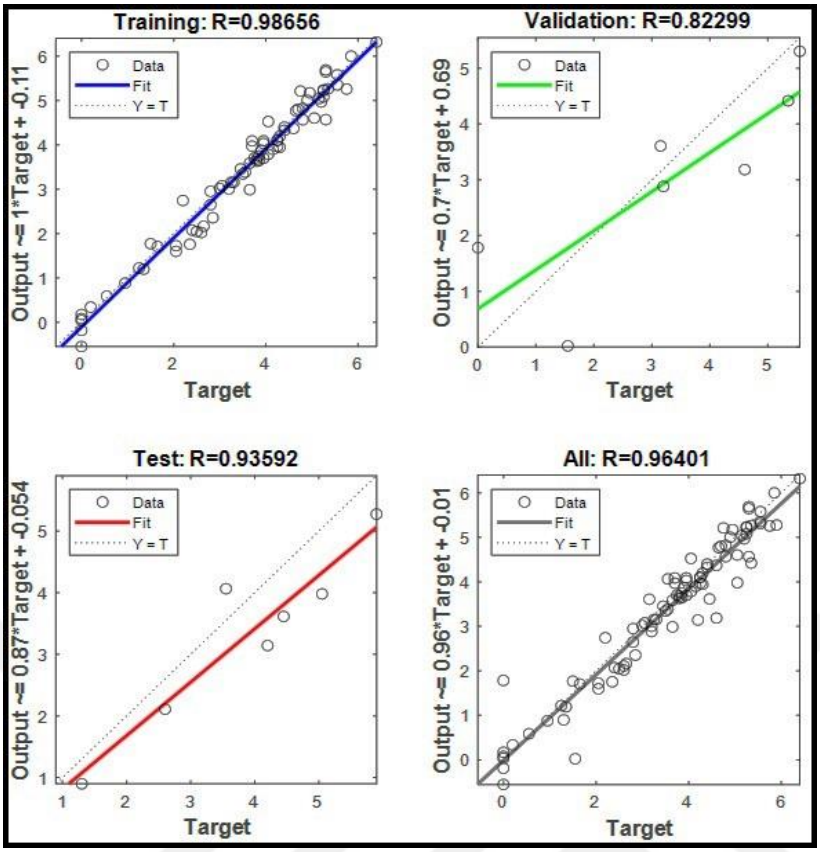

Figure 5.83: Without air content, FA + MS added results in LM for STS.

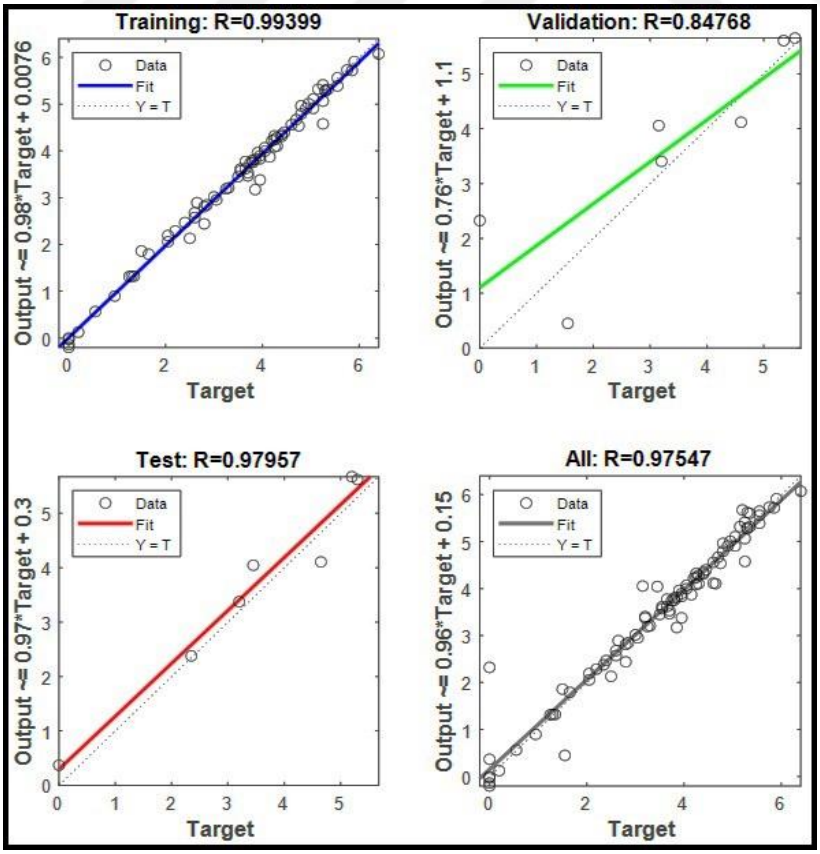

Figure 5.84: With air content, FA + MS added results in LM for STS.

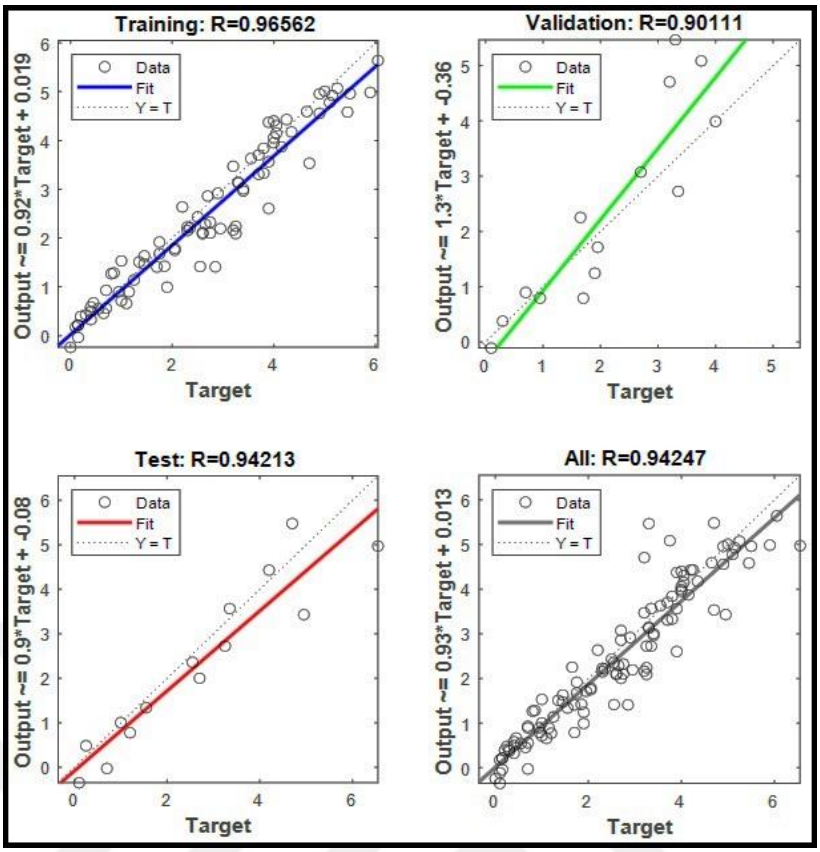

Figure 5.85: Without air content, GGBS added results in LM for STS.

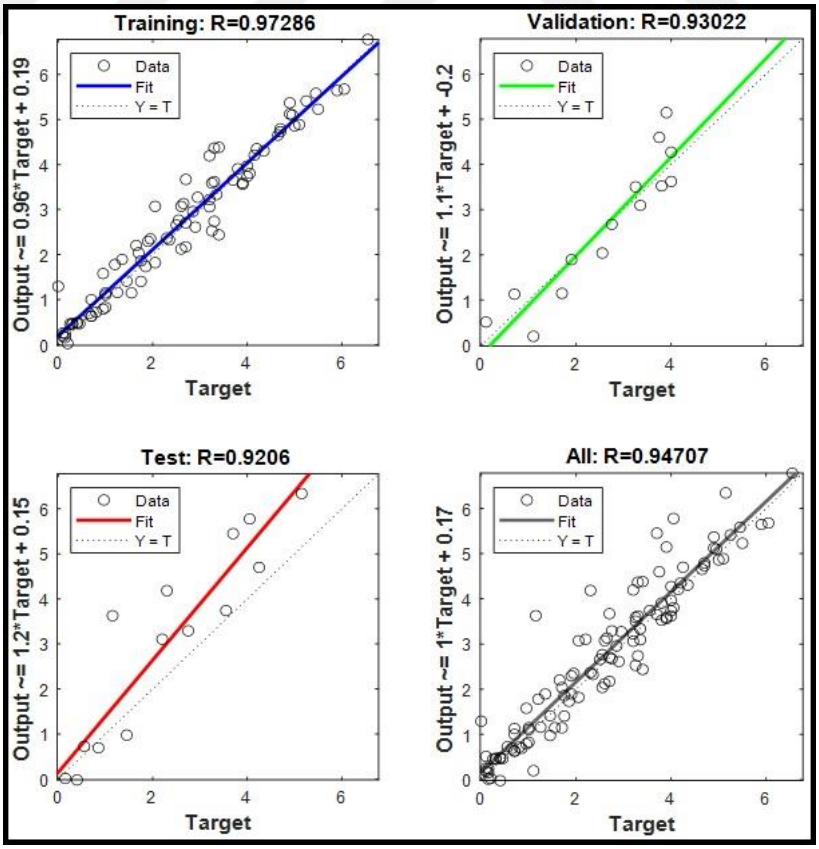

Figure 5.86: With air content, GGBS added results in LM for STS.

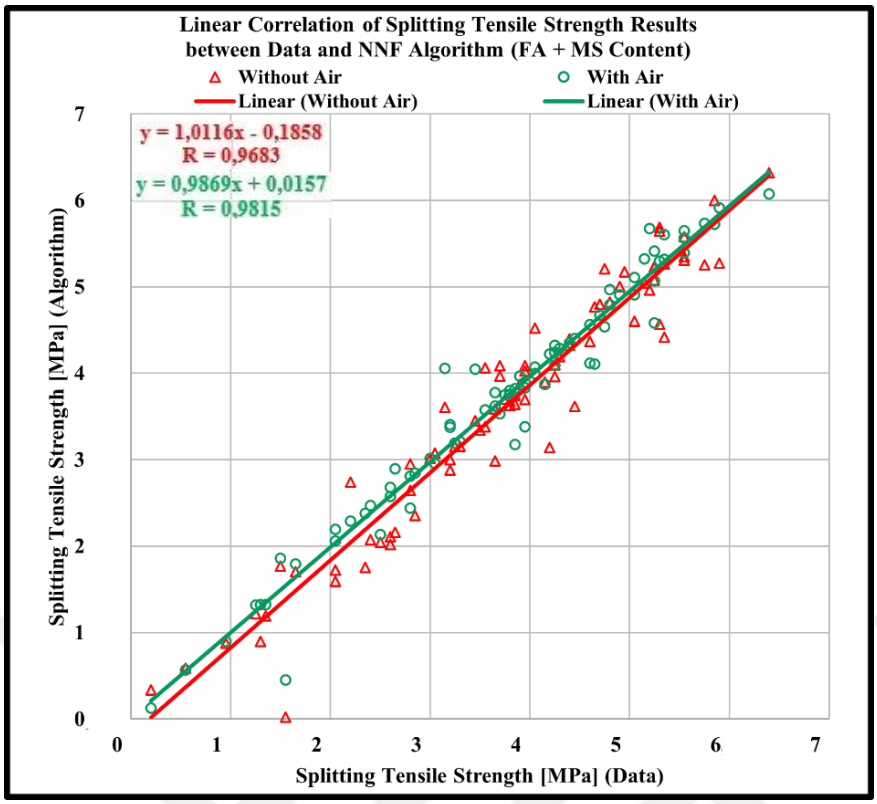

Figure 5.87: For air effect. FA + MS added results in LM for STS.

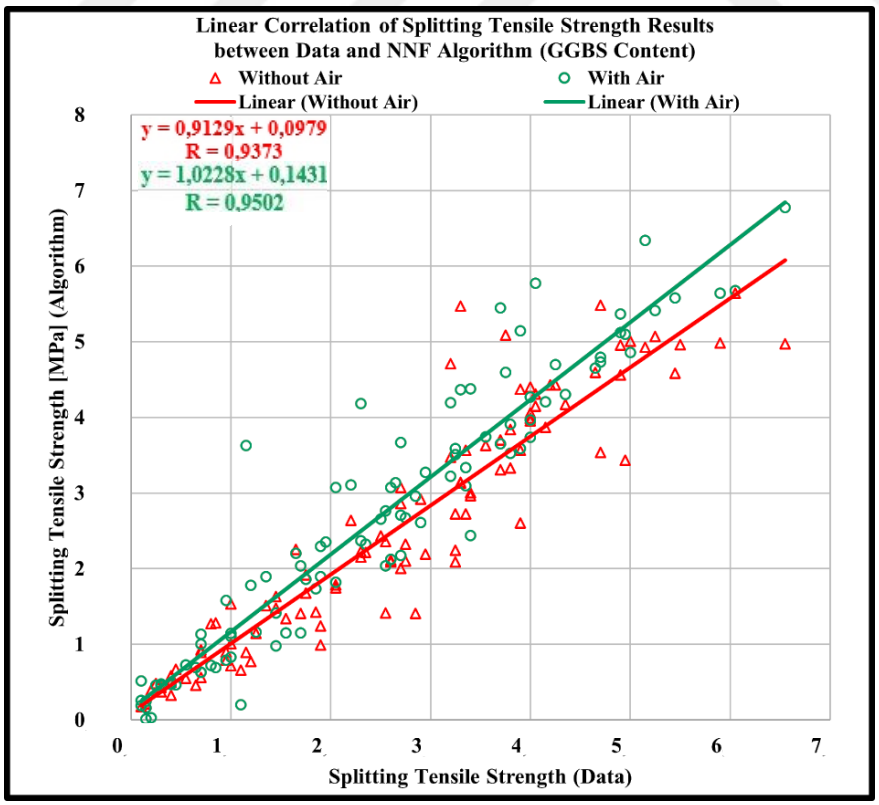

Figure 5.88: For air effect. GGBS added results in LM for STS.

In the Table 5.67, for the modulus of elasticity, in both FA + MS and GGBS contents, the algorithm is constructed with the matrix designs, and statistical results. The term of the target represents the actual test result as well in other mechanical properties of the LM algorithm. The training, validation, test, and all mean the algorithm results revealed by the software for the model trials. In the Table 5.68, the Table 5.69, the Table 5.70, and the Table 5.71, with the actual data set, the predicted results are also enlisted for the modulus of elasticity with the R^2 values for the accuracy checks.

Table 5.67: The LM Algorithm for the modulus of elasticity prediction.

Content	Input	Target	Output	Air [%]	≈ Output	Linear Model	R	MSE
FA + MS	[ ]13 x 10	[ ]13 x 7	[ ]13 x 7	0.00	Training	1 X Target - 2.1e+02	0.98783	10729719.65782
					Validation	0.86 X Target + 7.8e+03	0.92356	71376391.11623
					Test	0.94 X Target + 2.8e+03	0.86432	106008730.36134
					All	0.97 X Target + 1.5e+03	0.95937	-
	[ ]13 x 10	[ ]13 x 7	[ ]13 x 7	> 0.00	Training	1 X Target + 93	0.99514	4103059.75881
					Validation	0.95 X Target + 3.5e+03	0.92568	59510828.96048
					Test	0.97 X Target + 1.5e+03	0.91156	88512358.26314
					All	0.98 X Target + 9.1e+02	0.97026	-
GGBS	[ ]16 x 10	[ ]13 x 7	[ ]13 x 7	0.00	Training	1 X Target + 9.8e+02	0.97721	26852298.36036
					Validation	1.2 X Target - 9.7e+02	0.9696	50059972.24791
					Test	1.6 X Target - 1.4e+03	0.97797	274018353.28903
					All	1.1 X Target + 1e+03	0.95587	-
	[ ]16 x 10	[ ]13 x 7	[ ]13 x 7	> 0.00	Training	1.1 X Target + 4.8e+02	0.99413	10063692.39800
					Validation	0.95 X Target + 4.5e+03	0.97414	34672376.40111
					Test	1 X Target - 1.2e+03	0.91405	96826778.80878
					All	1 X Target + 8.7e+02	0.97808	-

In the Table 5.67, by comparing with the R values revealed by the software, for the FA + MS content included samples with and without the air content, the results are said to be very appropriate. Moreover, for the MSE results, the predictions with and without the air content are comparable to each other. On the contrary, the GGBS content included sample prediction results are better than the FA + MS content included results, except the outputs in all class for without air content.

Due to the algorithm for the estimation, without the air content in the FA + MS existence, the sample in MIX-15E-03 mixing code is lower resulted among the other R^2 values. With the air content in the FA + MS existence, the same sample is lower among the R^2 values, as well. However, this time, the same sample is better estimated.

So, in general, the LM algorithm works for all scenarios in the FA + MS content for the modulus of elasticity predictions. The same method is also followed for the GGBS existence in the concrete samples. Without the air content, the samples MIX32-CEN, B70-420, and B67-440-001 seem not to be operable in the results of R^2. For the air effect, the sample in MIX30-03 mixing code is inconvenient for the R^2 value. Especially the samples MIX32-CEN, B70-420, and B67-440-001 are in very high R^2 results currently. This shows that the algorithm may do not work for air absence model.

In this light of the results, in the Figure 5.89, the Figure 5.90, the Figure 5.91, and the Figure 5.92, the NN frames are given constructed on the mixture design variables. The Figure 5.93, the Figure 5.94, the Figure 5.95, and the Figure 5.96, the linear correlations from the software are also revealed. Onto this, in the Figure 5.97, and the Figure 5.98, the actual and predicted results are trendlined. In this correlation, each concrete specimen modulus of elasticity behavior was checked for the accuracy of the algorithm in the data fitting planar to see if there was a negative deflection or not. At the end, without the air content in the GGBS existence, the samples in MIX-30-BRT, and MIX-32-CEN-OK mixing codes were seen in negative deflections in the fitting planar. With the air content, only the sample in MIX-32-03 mixing code was seen in negative deflection in the GGBS content. For the FA + MS content, in both air content cases, the results were not deflected in negative directions. That is why the algorithm is said to be safe for the modulus of elasticity prediction in the FA + MS content with and without air content. Rather than the FA + MS content, the GGBS content included algorithm results were less valid in all types of result classes given by the software.

Table 5.68: The LM Algorithm for the modulus of elasticity prediction in FA + MS content without air.

LM Algorithm	Actual Data [MPa]							Predicted Data [MPa]							R^2
Mixing Codes	0.5-Day	1-Day	2-Day	3-Day	7-Day	14-Day	28-Day	0.5-Day	1-Day	2-Day	3-Day	7-Day	14-Day	28-Day	
YM-SEG-03	20000	36500	43000	49500	59000	62500	71500	19537	35824	42960	49762	59018	62555	71636	0.9996
MIX15A-04	11500	27000	38500	42500	51000	-	64000	8221	21696	33872	42859	50040	-	69043	0.9484
YM-SEG-05	9500	31000	42000	42000	56500	66500	-	19396	24772	35558	53100	61516	65214	-	0.8346
YM-SEG-08	15500	34500	40000	47500	59500	64000	-	8626	27763	36387	47109	58216	74716	-	0.8583
MIX-15E-03	6000	23500	31500	-	45000	52000	-	4094	25349	41672	-	54625	69074	-	0.6243
MIX-15AC-04	11500	27500	40000	-	54000	60000	69500	9504	25957	42221	-	55709	57624	67089	0.9891
YM-SEG-10	-	23500	33500	39000	50000	60500	69500	-	18634	31059	33088	51213	66307	69711	0.9330
YM-SEG-10A	15500		33000	38500	49500	58500	66500	9696	-	32087	37059	52996	54940	77670	0.8910
YM-SEG-10E	-	23500	29000	-	44000	53500	60500	-	23258	29936	-	43007	49648	61480	0.9821
MIX15-AC-03	4000	22500	29500	35500	45000	51500	-	1680	22196	30543	36101	45339	60671	-	0.9367
C45-B25-425	-	13000	25000	37000	46500	-	57500	-	11034	24055	36336	47180	-	57868	0.9953
C45-B25-400	1000	24000	34500	40500	48000	58000	76000	4318	25224	33250	40876	47452	51505	73896	0.9825
C50-B22-460	34500	49500	58500	61000	67500	73500	81000	34484	49297	58632	61385	68036	73641	80821	0.9996

Table 5.69: The LM Algorithm for the modulus of elasticity prediction in FA + MS content with air.

LM Algorithm	Actual Data [MPa]							Predicted Data [MPa]							R^2
Mixing Codes	0.5-Day	1-Day	2-Day	3-Day	7-Day	14-Day	28-Day	0.5-Day	1-Day	2-Day	3-Day	7-Day	14-Day	28-Day	
YM-SEG-03	20000	36500	43000	49500	59000	62500	71500	19720	36652	42962	49481	59637	62181	72013	0.9995
MIX15A-04	11500	27000	38500	42500	51000	-	64000	10979	27197	37301	40940	50123	-	61923	0.9945
YM-SEG-05	9500	31000	42000	42000	56500	66500	73500	18608	27077	41771	48908	61138	63055	77863	0.9310
YM-SEG-08	15500	34500	40000	47500	59500	64000	75500	15073	34511	39628	47234	58671	65932	74542	0.9977
MIX-15E-03	6000	23500	31500	36000	45000	52000	59000	7712	32832	38110	43218	51644	64011	67806	0.7674
MIX-15AC-04	11500	27500	40000	44500	54000	60000	69500	11531	26917	39902	44629	53724	61385	69785	0.9990
YM-SEG-10	-	23500	33500	39000	50000	60500	-	-	24590	26435	29609	41571	63859	-	0.7321
YM-SEG-10A	15500	-	33000	38500	49500	58500	66500	10696	-	30635	33967	48234	62291	63726	0.9574
YM-SEG-10E	-	23500	29000	31000	44000	53500	60500	-	15116	28715	32007	44925	59447	59933	0.9012
MIX15-AC-03	4000	22500	29500	35500	45000	51500	54000	3826	22124	29927	36202	45306	51571	55234	0.9987
C45-B25-425	-	13000	25000	37000	46500	52000	57500	-	11843	25385	37259	47134	52197	58050	0.9984
C45-B25-400	1000	-	34500	40500	48000	-	76000	10146	-	34074	44321	57971	-	77195	0.9316
C50-B22-460	34500	49500	58500	61000	67500	73500	81000	34497	49400	58337	60825	67518	73841	80773	0.9998

Table 5.70: The LM Algorithm for the modulus of elasticity prediction in GGBS content without air.

LM Algorithm	Actual Data [MPa]							Predicted Data [MPa]							R^2
Mixing Codes	0.5-Day	1-Day	2-Day	3-Day	7-Day	14-Day	28-Day	0.5-Day	1-Day	2-Day	3-Day	7-Day	14-Day	28-Day	
C45-III-B20	2000	9500	24000	30500	51000	74500	86000	5378	14388	23287	27136	49733	78156	81430	0.9865
YM-DAP-AC-03	3000	13000	21500	25000	37500	50000	-	3284	12040	15128	26752	40668	57313	-	0.9239
MIX-30	1500	5500	12500	-	29000	36500	46500	1370	11341	19264	-	32667	37300	52029	0.9242
MIX-30-03	7500	19500	24500	27500	35500	44000	50000	4536	18106	21289	27025	40690	50840	52220	0.9219
MIX-30-BRT	3500	16500	25500	31500	46000	60500	70000	6059	18895	25893	38450	49628	78325	79088	0.8615
MIX-30-07	3000	12500	19000	23000	32500	44000	50500	1273	14973	20948	24948	33358	49571	54478	0.9629
MIX-34-BRT	4000	18500	26000	-	37000	49000	59000	5829	18398	25980	-	41432	61123	65498	0.8962
MIX-32-03	6000	25500	33000	38500	47500	59000	-	4665	18670	24322	34105	44178	70246	-	0.8330
MIX-32-CEN	2000	9000	14000	16000	24000	31500	-	2736	14812	17837	25053	34050	48413	-	0.0635
MIX-32-CEN-OK	2500	15500	27500	31500	40000	50500	-	3147	16792	20312	34520	38062	60153	-	0.8912
B70-380	1500	4000	8500	12000	25000	39000	50000	1569	6206	9803	11215	27095	41956	56792	0.9681
B70-420	1000	3500	6500	10500	23500	41000	48000	2013	3389	12862	22859	38687	70330	80170	-0.0852
B47-440	1500	7500	16500	23000	41500	61500	72500	2649	7362	16260	23637	41486	60634	73736	0.9991
B67-440	1000	5500	13500	20000	35000	60000	72500	1127	4298	14554	19934	34315	59685	72072	0.9993
B67-440-001	-	-	11000	16500	27000	44500	55500	-	-	15640	25983	44451	59414	82152	0.0426
B67-440-BEY	1000	7500	15500	19000	35500	49500	62000	2204	4767	15500	17167	39956	46037	85060	0.8115

Table 5.71: The LM Algorithm for the modulus of elasticity prediction in GGBS content with air.

LM Algorithm	Actual Data [MPa]							Predicted Data [MPa]							R^2
Mixing Codes	0.5-Day	1-Day	2-Day	3-Day	7-Day	14-Day	28-Day	0.5-Day	1-Day	2-Day	3-Day	7-Day	14-Day	28-Day	
C45-III-B20	2000	9500	24000	30500	51000	74500	86000	2326	11396	23976	33556	50357	76137	87252	0.9971
YM-DAP-AC-03	3000	13000	21500	25000	37500	50000	59500	918	18435	26268	35881	38904	50344	70067	0.8817
MIX-30	1500	5500	12500	16000	29000	36500	46500	1778	7354	13425	19746	28400	40027	50929	0.9696
MIX-30-03	7500	19500	24500	27500	-	44000	50000	7878	21803	27172	36493	-	52653	59435	0.7926
MIX-30-BRT	3500	16500	25500	-	46000	60500	70000	2826	16709	30836	-	41502	61466	71828	0.9843
MIX-30-07	3000	12500	19000	23000	32500	44000	50500	3221	13549	19346	25323	32316	46177	52599	0.9909
MIX-34-BRT	4000	18500	26000	-	37000	49000	59000	4100	18146	26254	-	36804	49494	58892	0.9998
MIX-32-03	6000	25500	33000	38500	47500	59000	71000	6503	27185	34060	45591	46647	64981	77278	0.9534
MIX-32-CEN	2000	9000	14000	16000	24000	31500	36500	2205	9898	14274	17656	24393	33661	38577	0.9859
MIX-32-CEN-OK	2500	15500	27500	31500	-	50500	60000	2542	16826	28438	41674	-	57612	68545	0.8995
B70-380	1500	4000	8500	12000	25000	39000	50000	1466	4909	6137	14877	25481	40373	53187	0.9870
B70-420	1000	3500	6500	10500	23500	41000	48000	969	3742	6087	11554	23444	43246	48885	0.9966
B47-440	1500	7500	16500	23000	41500	61500	72500	1669	9974	14491	27672	42807	62464	75573	0.9901
B67-440	1000	5500	13500	20000	35000	60000	72500	2684	7650	16949	31226	34247	60496	65396	0.9567
B67-440-001	500	7500	11000	16500	27000	44500	55500	564	7830	12141	20416	27980	48728	59424	0.9793
B67-440-BEY	1000	7500	-	-	35500	-	62000	1464	19036	-	-	45179	-	67113	0.8924

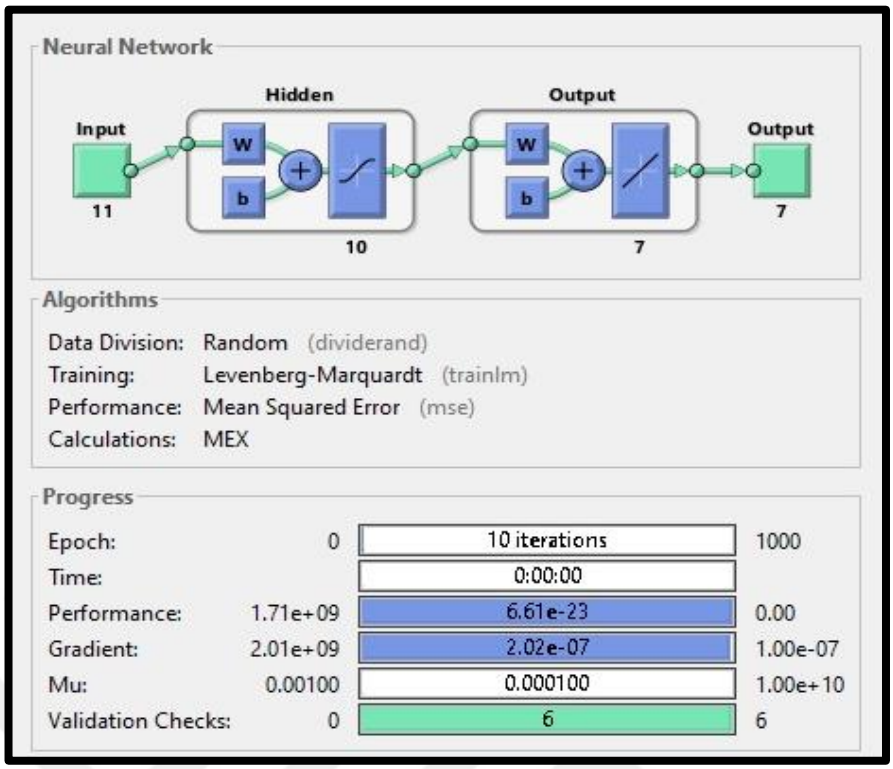

Figure 5.89: Without air content, FA + MS added NN in LM for ME.

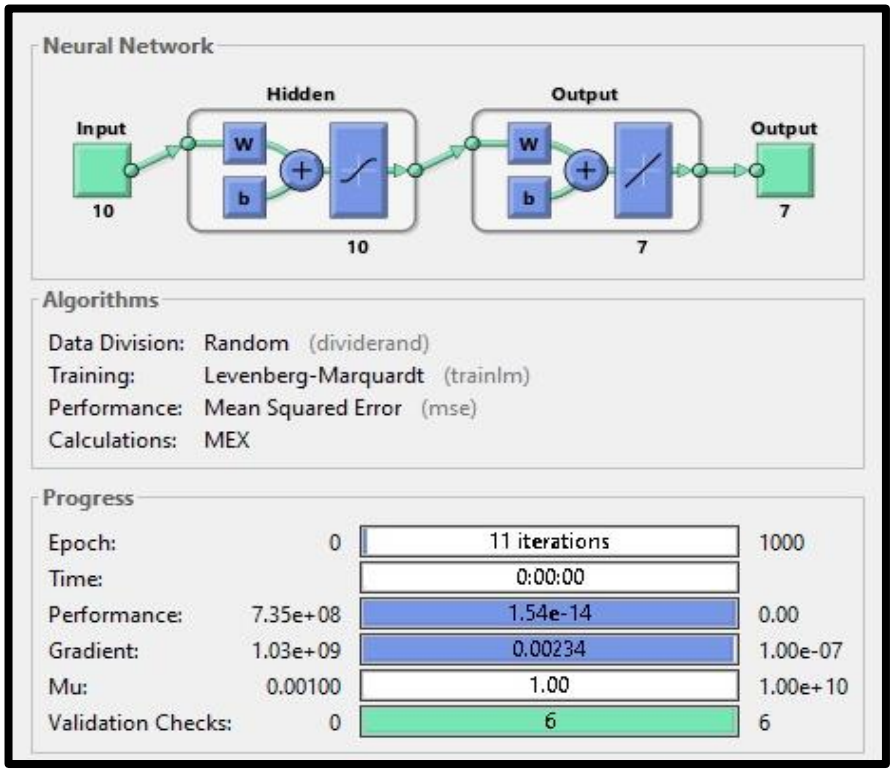

Figure 5.90: With air content, FA + MS added NN in LM for ME.

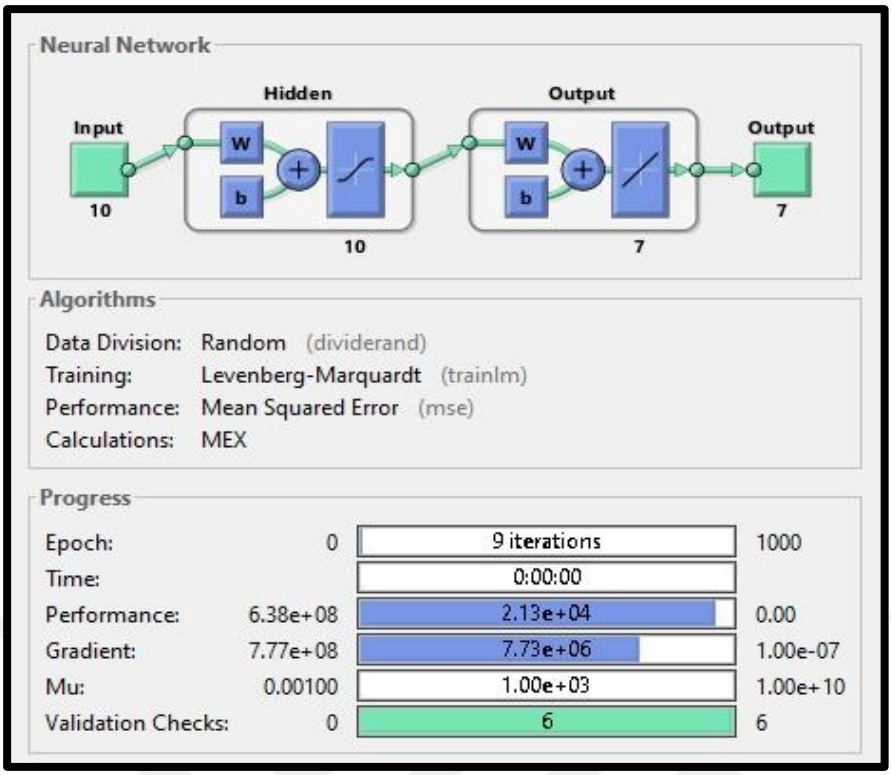

Figure 5.91: Without air content, GGBS added NN in LM for ME.

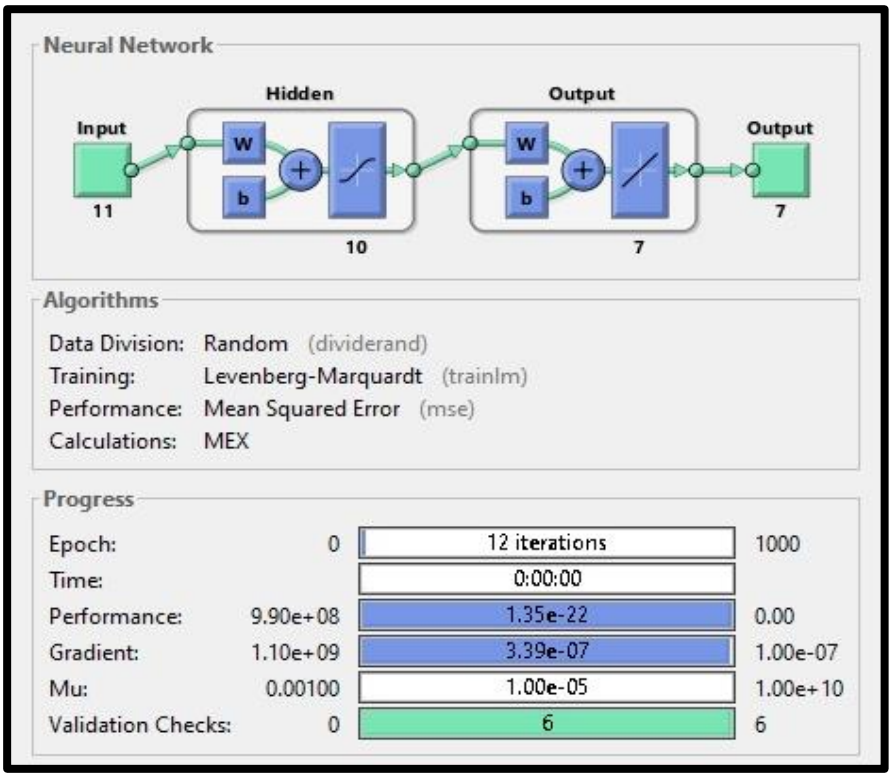

Figure 5.92 With air content, GGBS added NN in LM for ME.

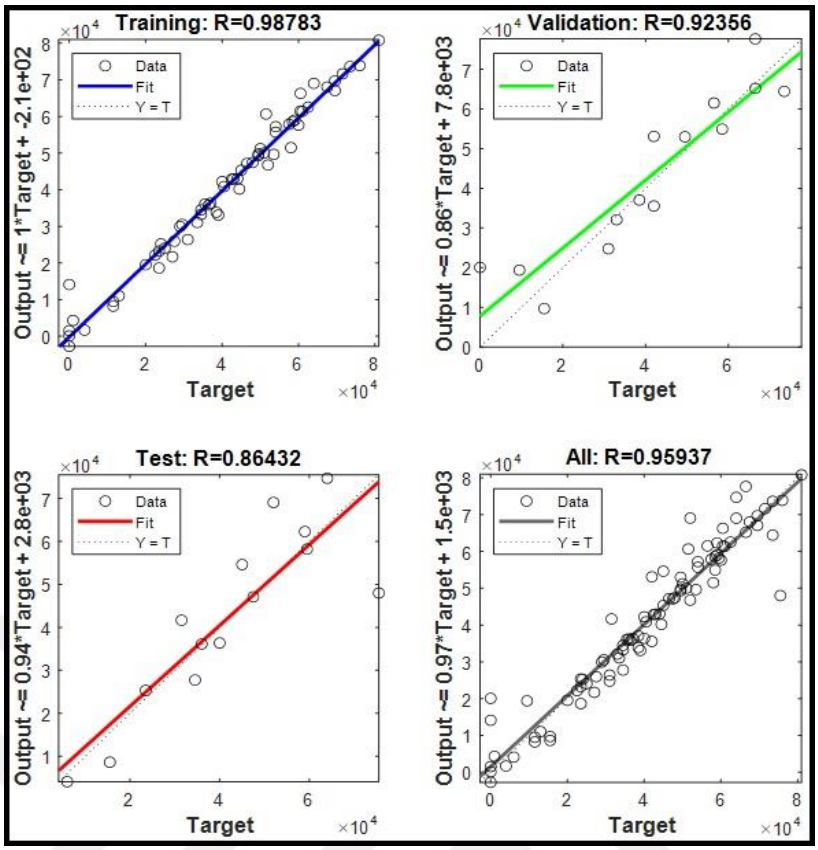

Figure 5.93: Without air content, FA + MS added results in LM for ME.

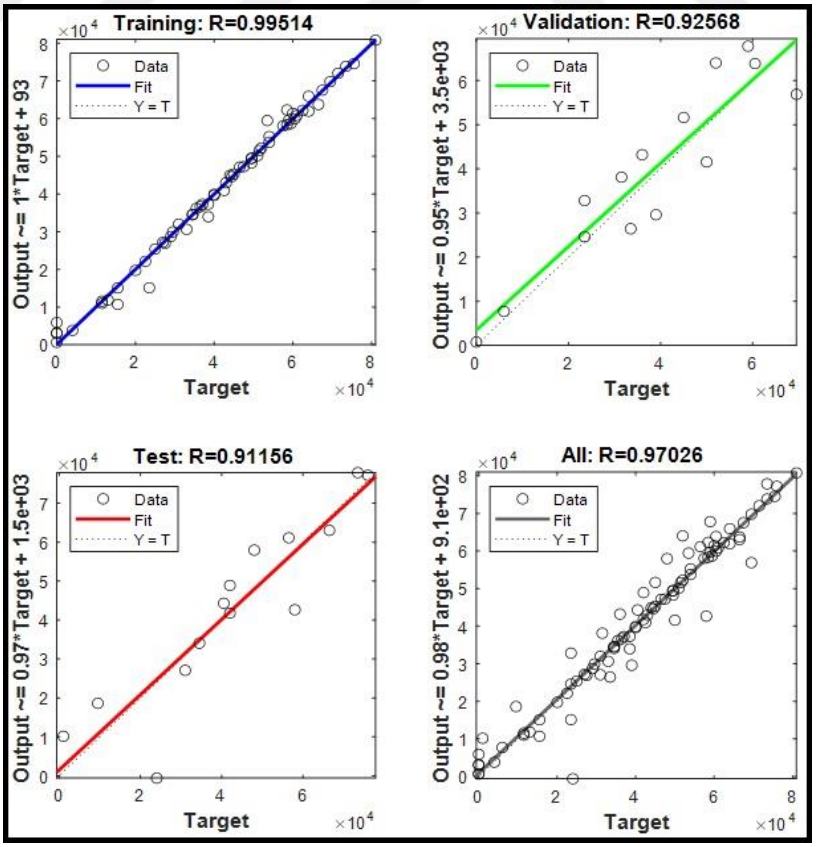

Figure 5.94: With air content, FA + MS added results in LM for ME.

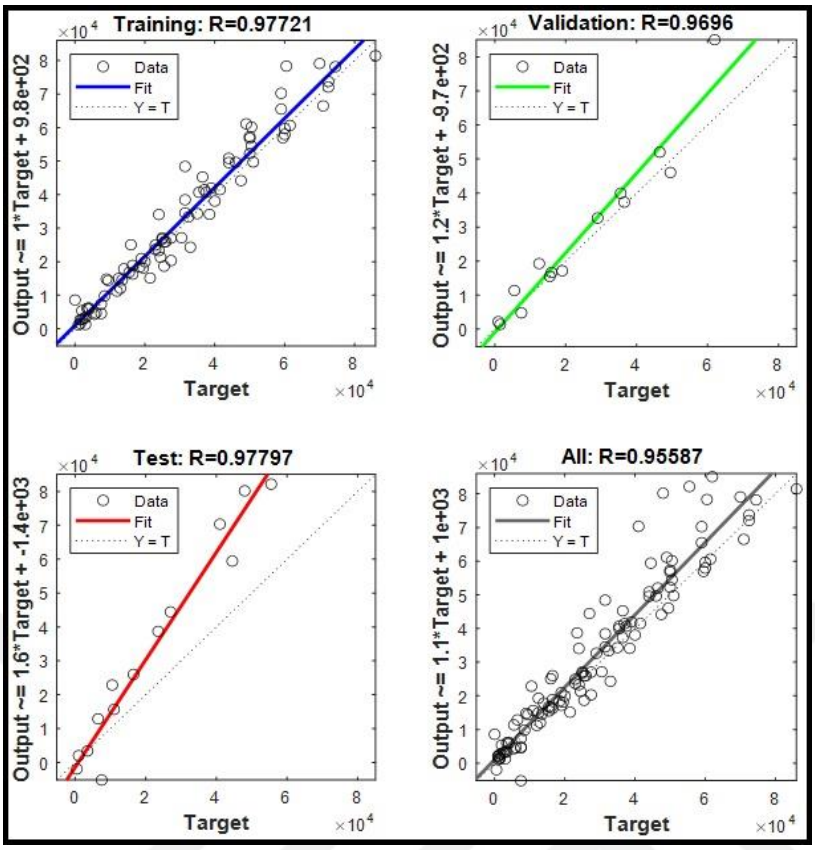

Figure 5.95: Without air content, GGBS added results in LM for ME.

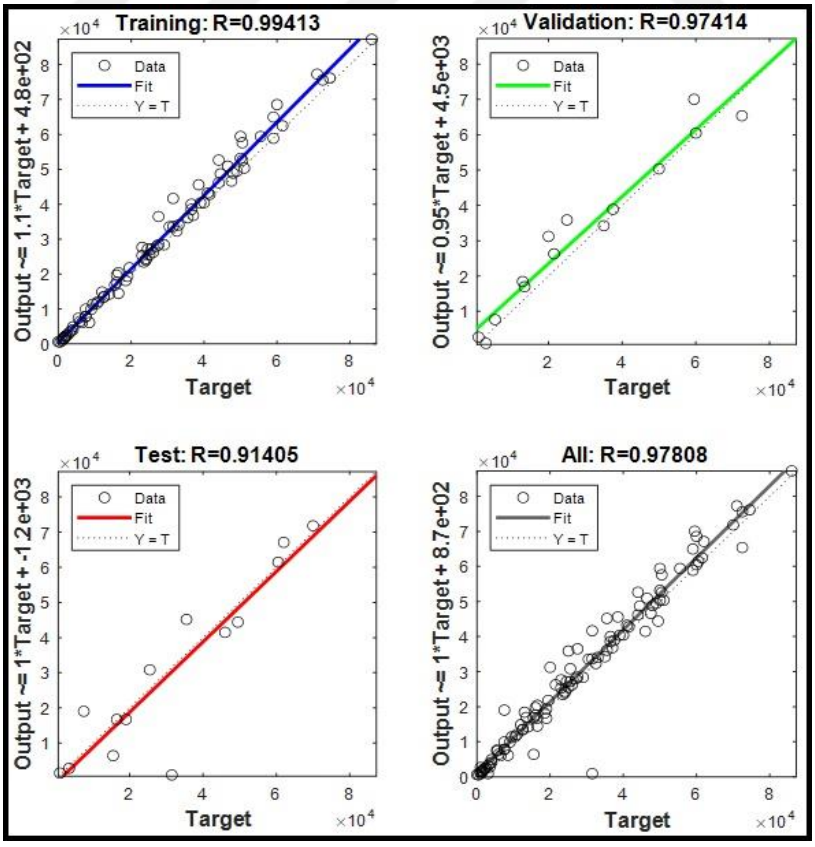

Figure 5.96: With air content, GGBS added results in LM for ME.

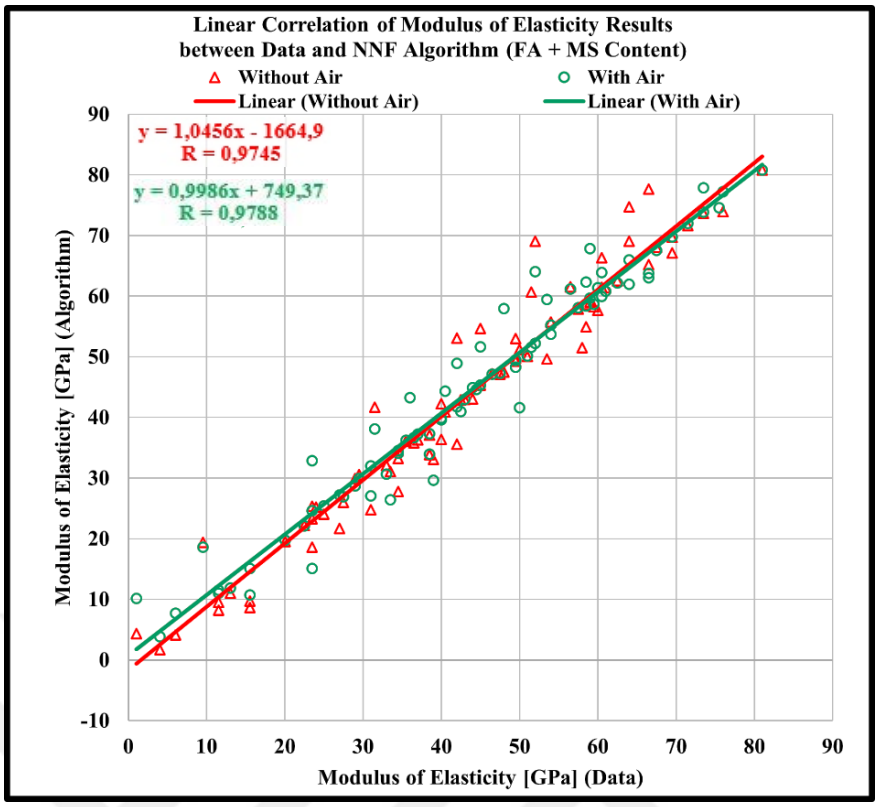

Figure 5.97: For air effect, FA + MS added results in LM for ME.

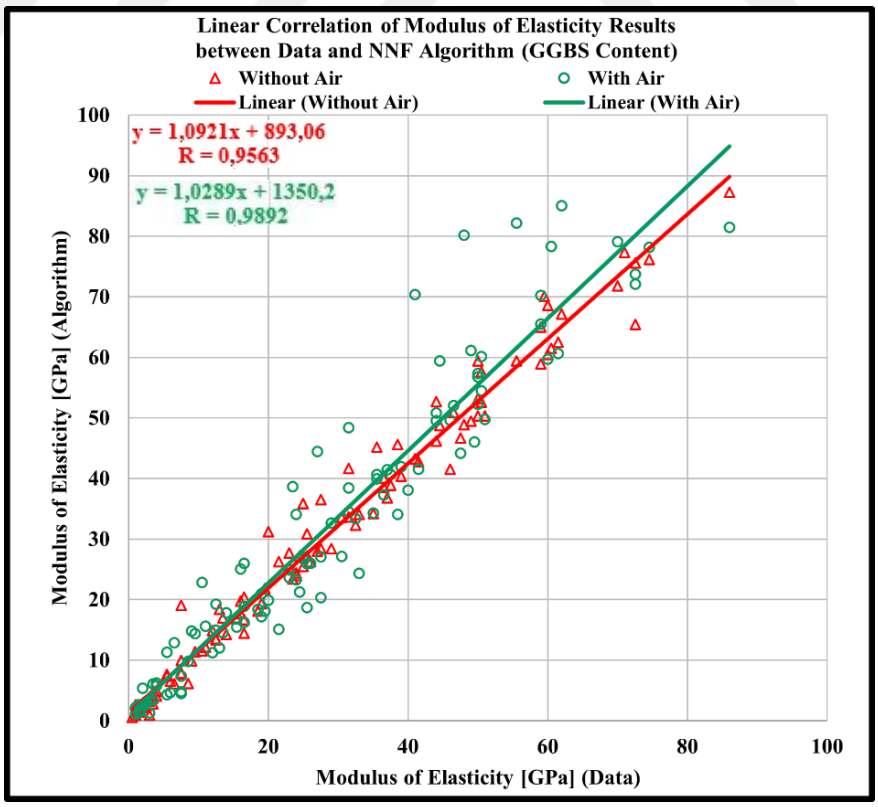

Figure 5.98: For air effect, GGBS added results in LM for ME.

6. CONCLUSIONS AND RECOMMENDATIONS

The main goal of this study is forecasting the mechanical properties of high strength concrete. Depending on the regression analysis models and machine learning algorithm, the laboratory test results were predicted and analyzed based on the concrete mixture designs. With the statistical parameters, all the estimated and analyzed results were also compared with the strength development results, the amounts of concrete mixture ingredients, and the proportions of the concrete mixture design materials for safe prediction purposes.

In this thesis, there were three main methods used for presuming the mechanical properties of the concrete such as the univariate regression analysis, the multivariate regression analysis, and the machine learning algorithm. For each method, several types of regression equations, and an algorithm were conducted with the actual test results from the laboratory tests. In the univariate regression analysis, three types of regression models were studied for the compressive and splitting tensile strengths. For the modulus of elasticity, two different regression models were computed in the univariate regression analysis. Moreover, in the multivariate regression models, for the compressive strength, two diverse models were studied. For both splitting tensile strength, and modulus of elasticity, only one model in each property was used. In the machine learning process, just only the Levenberg-Marquardt algorithm was computed for all the mechanical properties.

Besides, in the URA of the CS of the Model-1 depending on the concrete age, the regression model was spotted inappropriate for the negative deflections in the fitting planar of the actual data sets, even though the R^2 results were in between 0.9427, and 0.9999. At the same time, the strength development was also decreased between the day-7, and day-14 for the FA + MS added samples, although the GGBS included specimen estimations were suitable.

Followingly, in the URA of the CS of the Model-2 (R^2 between 0.8772 and 0.9996), and the Model-3 (R^2 between 0.7700 and 0.9850), there was not any negative deflection on the curve fitting lines. That is why these models were accepted suitable for the strength estimation, though the Model-3 was respectively less coherent.

Moreover, in the URA of the STS of the Model-1, the Model-2, and the Model-3, the data predictions were convenient depending on the concrete age without any pozzolan

classification. The R^2 results of the Model-1 were in between 0.8345 and 0.9977, the R^2 results of the Model-2 were resulted from 0.8309 to 0.9993, and lastly the R^2 results of the Model-3 were calculated in between 0.8276 and 0.9990. Because of the absence of the negative deflections for all the estimated data sets, all the three models were come out safe for prediction methods.

In addition to this, in the URA of the ME of the Model-1 and Model-2, the estimated results were satisfactory for goodness-of-fit purposes with respect to the concrete age. Because the ME results were in four and/or five digits, the errors (SSE and RMSE) also seemed in four and/or five digits, as well. Yet, this is not enough to say that predicted results are off the expectations. Differently, the second model was respectively detected incoherent for the FA + MS existence in the samples. To sum up, the first model of the ME prediction by the URA was safer than the second model.

Onto the univariate regression analysis depending on the concrete age, the multivariate regression analysis was another method for the estimation of the mechanical properties of concrete. This time, according to the model proposed, the components of the concrete mixture designs were used for advanced analyses. In this light of way, for the MRA of the CS of the Model-1 was dependent on the W/C ratio, the amounts of fine and coarse aggregates, and the cement content. Even though the model was conducted for each concrete specimen's actual test results, the model was also cumulatively investigated for the concrete ages with the pozzolan distinctions such as FA + MS, and GGBS. In this model, for the FA + MS content, the R^2 results were in between 0.4471 and 0.9145. For the GGBS substance, the R^2 results were from 0.1498 to 0.5590, which were respectively lower than the results of FA + MS content added specimens for each concrete strength calculations. Rather than the URA models, in this model, the SSE and RMSE results were largened. And, with the generalized model equations for each concrete age, for the identical concrete samples, the R^2 values were tested to find which strength development was out of the expectations. By this way, the samples in MIX-30 ($R^2 = 0.1888$), and MIX-32-CEN ($R^2 = 0.1693$) mixing codes were very under the expectations for the safe model concept.

For the MRA of the CS of the Model-2, the R^2 results of the FA + MS included specimens were from 0.0035 to 0.0342, and the R^2 results of the GGBS content included samples were in between 0.0557 and 0.3509 for each day computations. The general equations were put forth the model by using the actual data sets that each

concrete specimen was studied for an identical behavior analysis in the curve fitting planar. With respect to the Model-1, the Model-2 based on the cement, water, and air proportions was worse resulted in the data estimation. For the samples in C50-B22-460 (FA + MS added), and MIX-32-CEN (GGBS added) mixing codes were even in negative R^2 results, which were deniable. That is why, in general, although the curve fittings were seemed appropriate for the negative deflection concerns in the fitting planar, the Model-2 was enlightened inconvenient as regards the first model.

For the MRA of the STS of the Model-1, the cement, water, and air content directed the analysis. For the FA + MS content addition, the R^2 results were from 0.1827 to 0.8828, and the GGBS added specimen R^2 results were from 0.4457 and 0.8150 in each day calculations. By looking at each specimen's data estimation curves, the GGBS added samples were also appropriate for this model.

For the MRA of the ME of the Model-1, the R^2 results of the FA + MS subsequent included specimens were in between -0.1102 and 0.1561, and the GGBS additive included samples were from 0.0788 to 0.6413 for each age of the concrete. Furthermore, SSE and RMSE results were in large scale numbers. With these results, it was understood that the model was not working on the samples that have the FA + MS material rather than the GGBS addition in generalized model equations. Besides, by using these equations, even though there was not any negative deflection in the fitting planar, the model was seemed off the expectations.

Furthermore, the machine learning algorithm from Levenberg-Marquardt, the CS, STS, and ME properties were evaluated with the R values and MSE results by the software. For the correlations of the results, the training, validation, test, and all results were also revealed for further comments by the software.

By using all types of materials from the concrete mixture designs, the air content was spotted effective on the CS predictions for the FA + MS content. Also, without the air content, the estimations were worsened except the training results of the algorithm. On the contrary, statistically, the FA + MS included prediction results were also worse than the GGBS content included sample prediction results without the air content.

Following the same estimation steps, the STS predictions were revealed by using the LA algorithm R and MSE results from the software. For the FA + MS content included samples with and without the air content, the results were reached as appropriate. In

the MSE results, without thinking the air content effect in the FA + MS content included prediction results, the results were also very coherent for the expectations. The GGBS content included sample prediction results were represented worse than the FA + MS content included results, even though the results were undeniable in the fitting planar of each specimen result.

Last of all, by comparing with the R and MSE results enlisted by the LA algorithm for the ME predictions, in the FA + MS content included specimens with and without the air content, the results were understood very suitable. Addition to this, for the MSE results, presuming the results with and without the air content were comparable to each other. However, the GGBS content included sample estimation results were better than the FA + MS content included results, except the outputs in all classes without the air content.

Depending on these statistical results in this thesis, for any future investigation and/or analysis, the conclusions can followingly be illustrated:

1) By using the concrete age, the fraction power regression (Model-1) for the URA, the estimated results of the CS are not appropriate in contrast with the logarithmic regression (Model-2), and power regression (Model-3) results. Because, in each curve fitting planar for each concrete specimen, the Model-1 deflects in negative ways especially between the day-7 and day-14. And the strength development results are decreased for the same ages. Even though the SSE and RMSE results from the calculations are highly limited, and not exceeding the expectations, according to the natural behavior of the concrete for the strength development process, the compressive strength is wished to be increased as the time goes by. However, in the Model-1, this is an opposite case in between the day-7 and day-14, especially for the FA + MS content included specimens. That is why, the Model-1 is not suggested to be use for data prediction in the NWC made of FA + MS additives.

2) In the Model-1 for the URA of the CS estimations in the FA + MS existence, the W/C ratio is detected more effective than the W/B ratio. Moreover, the CA/A ratio is published very effective on data prediction than the FA/A ratio. So, for choosing an appropriate binder, the use of cement comes forward rather than the use of FA + MS ingredient. Also, the amount of fine aggregate is more

convenient than the amount of coarse aggregate. The best data prediction with respect to the R^2 results corresponds to the sample in YM-SEG-10A mixing code. The estimated result of this sample is also highly dependable for the curve fitting. That is why, depending on the concrete age, its mixture design is perfectly fine to use in real construction works. On the contrary, for the same model conditions, the worst data prediction corresponds to the sample that has FA + MS material in YM-SEG-05 mixing code. Although the estimated result of this sample is numerically suitable, in the fitting planar, it negatively deflects in between the day-7 and day-14. That is why, depending on the concrete age, the model is not safe for further investigations. For the maximum R^2 result, the amount of CS and NS are very close to each other. In this light of result, there is not exact evidence for the CS and NS use effects for the data presuming. Besides, the fine aggregate has no power on the maximum R^2 result. In following, [(CS) - (NS)] results decrease the data estimation potential for the compressive strength. Besides, when the difference in between NO:1 Agg., and NO:2 Agg. gets smaller, the R^2 result decreases in the data prediction for the compressive strength. Also, for the maximum R^2 result, the maximum amount of MS is 50.00 kg/m^3. But for only the fly ash content, there is no sign of an exact amount and/or proportion use in the mixture designs. Further, like the high amount of fly ash, the high amount of cement decreases the data forecasting success which limits the cement use for the strength gaining. And, for both minimum and maximum R^2 values, the cement type is CEMI 42.5. That is why, the cement type cannot be evaluated in these results.

3) In the Model-1 for the URA of the CS estimations in the GGBS addition, the minimum W/C ratio is 0.31 and the minimum W/B ratio is 0.35 for the maximum R^2 result. Intercalarily, [(W/C) - (W/B)] result of the maximum R^2 result is greater than the minimum R^2 result. Also, while [(CA/A) - (FA/A)] result gets higher, the R^2 result increases which means the CA/A ratio is convenient on the data prediction with respect to the FA/A ratio. Addition to this, the CA/A ratio is 0.80, and the FA/A is 0.20. Moreover, the amounts of fine aggregates seem ineffective on the maximum R^2 value. And the NS amount affects the strength prediction in a good manner. The higher amounts of NO:0 Agg., NO:1 Agg., and NO:2 Agg. make the R^2 results higher.

Especially for the NO:0 Agg., it is necessary for a well data forecasting. For the maximum R^2 value, the amount of cement [114.00 kg/m^3], No:0 Agg. [486.00 kg/m^3], CS [0.00 kg/m^3], and NS [395.00 kg/m^3], used in the mixture designs are the minimum. For the best data presuming, the amount of GGBS is measured 266.00 kg/m^3. In the highest R^2 result, CEMI 52.5N type cement, and in the lowest R^2 result, CEMIII 32.5 type cement are clearly represented. That is why the cement type is important for the strength development in this model. In general aspect of the Model-1 in the URA of the CS estimations, the FA + MS ingredient causes higher compressive strength prediction results than the GGBS presence actions with respect to the concrete age. And there is no strong sign of use of water and superplasticizer effects on the strength predictions. By following the same logic, in the Model-2 for the URA of the CS estimations, the logarithmic regression is relatively fine and safe for predicting the compressive strength except the day-0.5 for the samples that have FA + MS content in C45-III-B20, MIX-30, B70-380, B70-420, B47-440, B67-440, B67-440-001, and B67-440-BEY mixing codes.

4) In the Model-2 for the URA of the CS estimations for the FA + MS ingredient, the W/C ratio is accurate than the W/B ratio for data prediction like in the first model. Also, the CA/A ratio influences the data prediction in a satisfactory manner with respect to the FA/A ratio as in the Model-1. The best predicted result is from the same concrete sample. However, for the worst estimated results is for the specimen in MIX-15-AC-03 code. That is why MIX-15-AC-03 is to be thought to be not used in construction works depending on this model for its mixture design. Also, [(CS) - (NS)] of the minimum R^2 result is greater than [(CS) - (NS)] of the maximum R^2 result. [(NO:1 Agg.) - (NO:2 Agg.)] of the minimum R^2 is also greater than [(NO:1 Agg.) - (NO:2 Agg.)] of the maximum R^2 result. Furthermore, the gap between the FA and MS causes decreasing the R^2 value. That is why the use of the FA and MS may be close to each other in terms of the unit weight. Moreover, whether the amounts of the cement increase, the R^2 results increase as well. For the minimum R^2 result, the difference between NO:1 Agg., and NO:2 Agg. is higher when the maximum R^2 is resulted. The maximum amount of MS is 50.00 kg/m^3 for the best R^2 result. The minimum FA theme is 30.00 kg/m^3, and the minimum water

existence is 102,00 kg/m^3 for the worst R^2 result. Besides, the higher amount of cement causes increasing in the data forecasting potential that works for the cement use at the upper limit for the strength gaining. Like in the first model, the type of cement is CEMI 42.5 for both the minimum and maximum R^2 results. That is why the cement type is out of the concerns for this model.

5) In the Model-2 for the URA of the CS estimations for the GGBS ingredient, [(W/C) – (W/B)] of the minimum R^2 is higher than [(W/C) – (W/B)] of the maximum R^2 result. The maximum W/C ratio is figured 1.11 out for the minimum R^2 result. As a binder material, there is no evidence of the GGBS effects on the compressive strength estimation. The CA/A ratio is dominant on the data prediction rather than the FA/A ratio. The model also signifies that [(NS) - (CS)] of the maximum R^2 result is less than [(NS) - (CS)] of the minimum R^2 result. Additionally, the amounts of natural sand may be effective on the strength prediction. For some specimens, NO:0 Agg., NO:1 Agg., and NO:2 Agg. amounts dramatically increase the R^2 results. At the maximum R^2 result, the NO:0 Agg., NO:1 Agg., and NO:2 Agg. amounts are the highest. For the minimum R^2 value, the amount of crushed sand is the minimum. Moreover, at the maximum R^2 result, NO:0 Agg. is zero. NO:1 Agg. is 909.00 kg/m^3, and NO:2 Agg. is also zero. That is why, as coarse aggregate, only NO:1 Agg. comes forward for the best data fitting in this model. In addition to this, the GGBS content decreases the strength prediction values of the concrete for some specimens. That is why, the effects of GGBS content are not to be said exact in this model and these mixture designs. Continuously, for the maximum R^2 result, the use of cement has positive effects on the strength developments. On the other hand, at the minimum R^2 result, the GGBS is 294.00 kg/m^3. In this model, for the highest R^2 result, CEMIII 32.5 type cement, and for the lowest R^2 result, CEMI 52.5N type cement are come out. That is why type of cement is important for best data fitting purposes. Like in the first model, the FA + MS ingredient support the higher compressive strength prediction results than the GGBS content does with respect to the concrete age.

6) In the Model-3 for the URA of the CS estimations, the same methods are followed for the results from the regression analysis. In the existence of the FA + MS content of the model, the prediction of the compressive strength has more

errors from the actual data sets on the fitting planar. Besides, the results of the Model-3 are less satisfying than the Model-1 and Model-2 set forth in the FA + MS content. On the contrary, the Model-3 seems safe to predict the compressive strength of the concrete because of absence of negative deflections effects in the data fittings.

7) In the Model-3 for the URA of the CS estimations for the FA + MS ingredient, [(W/C) - (W/B)] of the maximum R^2 result is equal to [(W/C) - (W/B)] of the minimum R^2 result. Moreover, the CA/A ratio impacts the data estimation with respect to the FA/A ratio. Furthermore, the CA/A ratio is 0.61, and the FA/A ratio is 0.39 for the maximum R^2 result. Especially, when the R^2 result is in increasing, the W/C and W/B ratios do not dramatically change or neither the FA/A nor CA/A ratios are in increasing. Also, [(CS) - (NS)] of the minimum R^2 result is greater than [(CS) - (NS)] of the maximum R^2 result. And the amount of NO:1 Agg., and NO:2 Agg. are the same for the maximum R^2 result which means there is no major impacts on the maximum R^2 result. Addition to this, [(NO:1 Agg.) - (NO:2 Agg.)] of the minimum R^2 result is greater than [(NO:1 Agg.) - (NO:2 Agg.)] of the maximum R^2 result. The gap between the FA and MS materials decreases the R^2 result. Whether the amounts of cement are in increasing, the R^2 result increases as well in this model. And the maximum amount of MS is 50.00 kg/m^3 for the highest-level R^2 result. In contrast with the maximized amount of MS, the minimum FA content is 30,00 kg/m^3, and the minimum water content is 102.00 kg/m^3 for the lowest-level R^2 result. At the end, the highest, and the lowest R^2 results are included CEMI 42.5 type of cement use. Because of the identical type of cement use, the cement effect is out of the comparison.

8) In the Model-3 for the URA of the CS estimations for the GGBS ingredient, [(W/C) – (W/B)] of the minimum R^2 result is less than [(W/C) – (W/B)] of the maximum R^2 result. Also, the W/C ratio is equal to the W/B ratio in only the minimum R^2 result. Because of use of the GGBS substance, it cannot be accepted as an influencer on the compressive strength development, even though the GGBS is a binder material. While [(CA/A) - (FA/A)] result gets higher, the R^2 result decreases which means the CA/A ratio is more operative on the data estimation as regards the FA/A ratio. Also, the FA/A ratio is 0.80

and the CA/A ratio is 0.20 for the maximum R^2 result. And [(NS) - (CS)] of the maximum R^2 result is greater than [(NS) - (CS)] of the minimum R^2 result. On the other hand, the amounts of natural sand may be penetrating on the strength prediction. The crushed sand is zero for the minimum R^2. At the maximum R^2 result, NO:0 Agg., NO:1 Agg., and NO:2 Agg. amounts are the nearest. For some specimens' R^2 results, NO:0 Agg., NO:1 Agg., and NO:2 Agg. amounts get much more. However, this does not help for a general understanding of the use of the GGBS content. Also, there is not strong sign of the effects of the water and admixtures as superplasticizers. Additionally, for the maximum R^2 result, NS is 0.00 kg/m^3, cement is 114.00 kg/m^3. NO:0 Agg. is maximized with 486.00 kg/m^3. At the maximum R^2 result, the GGBS content is 266.00 kg/m^3. For the lowest R^2 result (MIX-32-CEN-OK), CEMIII 32.5 type cement, and for the highest R^2 result (B370-80), CEMI 52.5N type cement are put forth. Lastly the strength estimations for the samples including the FA + MS theme are not consistent rather than the GGBS addition.

9) In the URA of the STS estimations, the power regression (Model-1), logarithmic regression (Model-2), and fraction regression (Model-3) were studied based on the concrete age. For the FA + MS ingredient in the Model-1, predicting the splitting tensile strength has less errors from the actual data sets on the curve fittings. The model also comes out safe to predict the splitting tensile strength of the concrete because of no negative deflection effects in the strength developments.

10) In the Model-1 for the URA of the STS estimations for the FA + MS ingredient, [(W/C) - (W/B)] of the maximum R^2 result is equal to [(W/C) - (W/B)] of the minimum R^2 result. While [(CA/A) - (FA/A)] result gets higher, the R^2 result also increases that the CA/A ratio has more potential on the data prediction in contrast with the FA/A ratio. Also, [(NS) - (CS)] of the minimum R^2 result is less than [(NS) - (CS)] of the maximum R^2 result. And [(NO:1 Agg.) - (NO:2 Agg.)] of the minimum R^2 result is less than [(NO:1 Agg.) - (NO:2 Agg.)] of the maximum R^2 result, as well. Besides, [(FA) - (MS)] result of the minimum R^2 result, and [(FA) - (MS)] of the maximum R^2 result are the same. At that time, the amounts of cement and water are also the same for both. The highest and lowest R^2 values have an effect of CEMI 42.5 type of cement use. Because

of that, the type of cement cannot be evaluated for the strength prediction purposes. Moreover, the Model-1 estimates that [(W/C) – (W/B)] of the minimum R^2 result is less than [(W/C) – (W/B)] of the maximum R^2 result. Followingly, the maximum W/B ratio is found 0.31 for the maximum R^2 value, and there is not enough proof of the GGBS effects on the splitting tensile strength estimation. While [(CA/A) - (FA/A)] result gets higher, the R^2 result increases which means the CA/A ratio is dependable on the data prediction due to the FA/A ratio. Furthermore, the water and admixture contents are ineffective on the strength prediction in terms of R^2.

11) In the Model-1 for the URA of the STS estimations for the GGBS ingredient, the Model-1 expresses that [(NS) - (CS)] of the maximum R^2 result is greater than [(NS) - (CS)] of the minimum R^2 result. The results also prove that the amounts of natural sand force the prediction in the positive way of the strength development. Even though for some specimens, NO:0 Agg., NO:1 Agg., and NO:2 Agg. amounts continuously increase the R^2 results, there is mistakable evidence of the coarse aggregate use effects in the model. The amount of water, and cement of the minimum R^2 result are greater than the maximum R^2 has. In addition to this, for the highest R^2 result, CEMI 52.5N type cement, and for the lowest R^2 result, CEMIII BS type cement are figured out. In general, it is exactly clear that the FA + MS material heads the higher splitting tensile strength prediction results than the GGBS content does.

12) In the Model-2 for the URA of the STS estimations for the FA + MS ingredient, predicting the splitting tensile strength has less SSE and RMSE results from the actual data sets on the fitting planar. Also, the model results are satisfying, and the model occurs safe to predict the splitting tensile strength of the concrete because of no negative deflection effects in the strength development. Moreover, the Model-2 offers that [(W/C) - (W/B)] of the maximum R^2 result is equal to [(W/C) - (W/B)] of the minimum R^2 result as well in the Model-1. While [(CA/A) - (FA/A)] result gets higher, the R^2 result also increases which means the CA/A ratio is more accurate on the data prediction with respect to the FA/A ratio. The model also explains that [(NS) - (CS)] of the minimum R^2 result is greater than [(NS) - (CS)] of the maximum R^2 result. [(NO:1 Agg.) - (NO:2 Agg.)] of the minimum R^2 result is less than [(NO:1 Agg.) - (NO:2

Agg.)] of the maximum R^2 result. The amounts of cement and water of the minimum and maximum R^2 are the same. The minimized amount of NO:1 Agg. is 402.00 kg/m^3 for the minimum R^2 result. Besides the cement types are CEMI 42.5N for both the lowest, and the highest R^2 result which means that the cement type is not a focus for the strength prediction in this model.

13) In the Model-2 for the URA of the STS estimations for the GGBS ingredient, the Model-2 pictures that [(W/C) – (W/B)] of the minimum R^2 result is less than [(W/C) – (W/B)] of the maximum R^2 result. On the other hand, there is no open clue of the GGBS effects on the splitting tensile strength estimation. While [(CA/A) - (FA/A)] result gets higher, the R^2 result decreases which means that the CA/A ratio is impactful on the data fitting rather than the FA/A ratio. Further, [(NS) - (CS)] of the maximum R^2 result is greater than [(NS) - (CS)] of the minimum R^2 result. This inference shows that the amounts of natural sand imply the strength prediction. For some specimens, NO:0 Agg., NO:1 Agg., and NO:2 Agg. amounts highly increase the R^2 results. Moreover, the amount of water and cement of the minimum R^2 result are opposite. When the amount of cement is increased, the prediction is resulted well-predicted. Yet the amount of water in increasing causes worse estimation results. For the highest R^2 result, CEMIII 32.5 type cement, and for the lowest R^2 result, CEMIII BS type cement are figured out. That is why the cement type is important for the data estimation in this model. Finally, the GGBS substance affects the splitting tensile strength prediction results in a decreasing manner rather than the FA + MS theme does.

14) In the Model-3 for the URA of the STS estimations for the FA + MS ingredient, the errors occurred by the calculations are in the expectations. With no negative deflections in the strength development curves, the model sets forth safe to predict the splitting tensile strength of the concrete. The model also evinces that [(W/C) - (W/B)] of the maximum R^2 result is equal to [(W/C) - (W/B)] of the minimum R^2 result like in the Model-1 and Model-2. Onto this, while [(CA/A) - (FA/A)] result gets higher, the R^2 result increases that the CA/A ratio is effective on the data estimation rather than the FA/A ratio. The minimum CA/A ratio is 0.46, and the maximum FAA ratio is 0.54 for the minimum R^2 value. And the model argues that [(NS) - (CS)] of the minimum R^2 is greater

than [(NS) - (CS)] of the maximum R^2. [(NO:1 Agg.) - (NO:2 Agg.)] of the minimum R^2 result is less than [(NO:1 Agg.) - (NO:2 Agg.)] of the maximum R^2 result as well in the previous models. Besides, [(FA) - (MS)] result and the amounts of cement and water of the minimum R^2 are less than the maximum R^2 occurred. However, the use of admixtures and water seem like not influencing the data forecasting. Moreover, the minimum amount of NO:1 Agg. is 402.00 kg/m^3 for the minimum R^2 result like in the second model. There is also not the sign of use of specific amount of FA + MS for the low and/or high prediction results on the splitting tensile strength. Additionally, the cement types are CEMI 42.5N for both the lowest and highest R^2 values which means the cement type is out of any comparison for the strength prediction in this model.

15) In the Model-3 for the URA of the STS estimations for the GGBS ingredient, [(W/C) – (W/B)] of the minimum R^2 result is less than [(W/C) – (W/B)] of the maximum R^2 result, as well in the last models. Addition to this, there is no overt sign of the GGBS effects on the splitting tensile strength prediction, even though it is a binder substance like the cement. While [(CA/A) - (FA/A)] result gets higher, the R^2 result is increased which means that the CA/A ratio effect is acceptable on the data estimation in use of the FA/A ratio. Also, the minimum FA/A ratio (0.20), and the maximum CA/A ratio (0.80) are figured out for the highest R^2 value. The cement types attract the attention for in B70-380 (CEMI 52.5N), and C45-III-B20 (CEMIII BS) mixing codes. For the samples GGBS resultants, [(NS) - (CS)] of the maximum R^2 result is greater than [(NS) - (CS)] of the minimum R^2 result like in the previous models. Besides, the amounts of natural sand impose the strength prediction. For some specimens, NO:0 Agg., NO:1 Agg., and NO:2 Agg. amounts effectively increase the R^2 value. On the other side, the amounts of water and cement of the minimum R^2 result are greater than the maximum R^2 result has. When the amount of cement is increased, the prediction is worsened. Like the amount of cement, the amount of water in increasing results worse predictions. Else, there are some samples made of the GGBS subsequent for decreasing the strength results of the concrete in forecasting. For the maximum R^2 result, the minimum cement content is 114.00 kg/m^3, and the maximum amount of NO:0 Agg. is

486.00 kg/m^3. Meanwhile, the minimum amount of CS material is zero, and the minimum amount of NS content is 395.00 kg/m^3. At the end, the FA + MS addition is more effective on the higher splitting tensile strength estimation results than the GGBS material is. The model also comes out safe to predict the splitting tensile strength of the concrete because of no negative deflection effects in the strength developments.

16) In the Model-1 for the URA of the ME estimations, the power regression (Model-1) and fraction power regression (Model-2) were computed depending on the concrete age. For the FA + MS substance in the Model-1, predicting the modulus of elasticity occurs four-digit or five-digit in SSE and RMSE results, which do not mean the result are not suitable. Also, the correlation results absolutely show that the results of the model are satisfying. On the other hand, the FA + MS included sample results are respectively less than GGBS included sample results. The model also computes that [(W/C) - (W/B)] of the maximum R^2 result is equal to [(W/C) - (W/B)] of the minimum R^2 result as well in the splitting tensile strength predictions. Besides, while [(CA/A) - (FA/A)] result gets higher, the R^2 result decreases that the FA/A ratio is more efficient on the data prediction with respect to the CA/A ratio. The model additionally shows that [(NS) - (CS)] of the minimum R^2 result is less than [(NS) - (CS)] of the maximum R^2 result. Also [(NO:1 Agg.) - (NO:2 Agg.)] of the minimum R^2 result is greater than [(NO:1 Agg.) - (NO:2 Agg.)] of the maximum R^2 result. Further, [(FA) - (MS)] result of the minimum R^2 is less than the maximum R^2 result. The amounts of water and cement for the minimum R^2 result are greater than the maximum R^2 has. When the amount of cement is in increasing, the prediction is in decreasing. Also, it is ineffective to use admixtures in this model for the elastic modulus development. Furthermore, the cement types are CEMI 42,5N for both the lowest and highest R^2 values that the cement type is not a preference for the elastic modulus development in this model. Followingly, the model portraits that [(W/C) – (W/B)] of the minimum R^2 result is equal to [(W/C) – (W/B)] of the maximum R^2 result. Nevertheless, there is an inexactness of the GGBS effects on the modulus of elasticity prediction. And while [(FA/A) - (CA/A)] result gets higher, the R^2 result increases that the FA/A ratio is more raid on the data predicting because of the

CA/A ratio. For the minimum R^2 result, the minimum FA/A ratio is 0.54, and the minimum CA/A ratio is 0.46.

17) In the Model-1 for the URA of the ME estimations for the GGBS ingredient, [(NS) - (CS)] of the maximum R^2 result is less than [(NS) - (CS)] of the minimum R^2 result. This leads that the amounts of natural sand imply the elastic modulus calculations. For some specimens, NO:0 Agg., NO:1 Agg., and NO:2 Agg. amounts remarkably increase the R^2 result as in the previous mechanical property models and increase the elastic modulus prediction results of the concrete. Else, the amount of water in increasing causes well predictions. For the highest R^2 result, CEMIII BS type cement is for both lowest and highest R^2 result. According to the correlations, the MS material affects the higher modulus of elasticity estimation results than GGBS content does

18) In the Model-2 for the URA of the ME estimations for the FA + MS ingredient, although the SSE and RMSE results are very high, it does not mean that very high results are very off the data predictions. As the elastic modulus test results that are used in the regression model are in four and five digits. The correlation shows that the results of the model are satisfying, and safe for data forecasting without negative deflections in data fitting planar, even though the FA + MS contented sample results are respectively lower in contrast with the first model. The Model-2 displays that [(W/C) - (W/B)] of the maximum R^2 result is equal to [(W/C) - (W/B)] of the minimum R^2 result. While [(CA/A) - (FA/A)] result gets higher, the R^2 result also decreases which means the CA/A ratio is operative on the data prediction than the FA/A ratio. The amounts of water and cement for the minimum R^2 result are greater than the maximum R^2 water and cement contents. When the amount of cement is in increasing, the prediction is in decreasing. It is also an impression that using admixtures in this model does not dramatically change the prediction results. On the side, the cement types are CEMI 42.5N for both the lowest and highest R^2 values that the cement type could not be interpreted for the elastic modulus development in this model. Further, [(NS) - (CS)] of the maximum R^2 result is greater than [(NS) - (CS)] of the minimum R^2 result. Else, [(NO:1 Agg.) - (NO:2 Agg.)] of the maximum R^2 result is less than [(NO:1 Agg.) - (NO:2 Agg.)] of the minimum R^2 value. Moreover, the minimum NS content is 304.00 kg/m^3, and the maximum CS

material is 542.00 kg/m3 for the minimum R^2 result. The minimum water content is 102.00 kg/m^3, the minimum FA substance is 50.00 kg/m^3, and the minimum MS ingredient is 30.00 kg/m^3 for the maximum R^2 result in this model.

19) In the Model-2 for the URA of the ME estimations for the GGBS ingredient, the model describes that [(W/C) – (W/B)] of the minimum R^2 is less than [(W/C) – (W/B)] of the maximum R^2 result. There are also no effects of the GGBS use on the modulus of elasticity estimation in this model, even though GGBS is a combining material. While [(CA/A) - (FA/A)] result gets higher, the R^2 result increases which means that the CA/A ratio is more incursive on the data prediction because of the FA/A ratio. Onto this, for the minimum R^2 result, the maximum FA/A ratio is 0.54, and the minimum CA/A ratio is 0.46. For the maximum R^2 result, the FA/A ratio is 0.20, and the minimum CA/A ratio is 0.80. Addition to this, [(NS) - (CS)] of the maximum R^2 result is greater than [(NS) - (CS)] of the minimum R^2 result. The amounts of natural sand impose the elastic modulus prediction. Also, for some specimens, NO:0 Agg., NO:1 Agg., and NO:2 Agg. amounts increase the R^2 result pretty much. At the same time, the amount of water in increasing causes worse results. However, for some specimens composed of the GGBS substance decrease the elastic modulus estimation potential of the concrete. For the highest R^2 result, CEMI 52.5N type cement, and for the lowest R^2 value, CEMIII 32.5 type cement are decisive. That is why the cement type is decisive. Followingly, the maximum R^2 result has the minimum cement (114.00 kg/m^3), minimum CS (0.00 kg/m^3), minimum NS (395.00 kg/m^3) and maximum NO:0 Agg. (486.00 kg/m^3) contents with the GGBS 266.00 kg/m^3 substance. As well in the previous models, the FA + MS content influences the higher modulus of elasticity prediction results than GGBS content affects.

20) In a different manner, rather than the concrete age dependent models, the multivariate regression analysis was chosen for detailed analysis to understand how the concrete mixture ingredients were effective on the strength prediction in this study. For the compressive strength predictions, linear regression (Model-1) and power regression (Model-2) were studied depending on the amounts and proportions of the contents from the concrete mixture designs. In

this perspective, the MRA of the CS predictions for the FA + MS ingredient, the correlations clearly demonstrate that the results of the model are satisfying, and the model comes forward safe to presume the compressive strength of the concrete because of no negative deflection effects in the data fittings. The equation coefficients were also studied. In these studies, the more R^2 result is decreased, the more equation coefficient that intersects the predicted strengths is decreased for all ages, except the day-1, and day-2. Also, for the FA, CA and C contents, the results of the models seem parallel to the each. And the effects of these contents are antipoles of R^2 results at days 0.5, 14, and 28 which means the compressive strength estimation gets worsen in the results. In the day-1, day-2, day-14, and day-28, the W/C ratio coefficient also operates the model in the opposite way to the R^2 value which means higher effects of the W/C ratio decrease the data prediction potential.

21) In the Model-1 for the MRA of the CS estimations for the GGBS ingredient, the equation coefficient does not behave how the R^2 result shows. Between the day-1 and day-3; day-7,and day-14, the strength development of the compressive strength not well-estimated. Out of the day-2 and day-28, the W/C ratio impacts are parallel to the predicted results that the W/C ratio works well for the less amounts of cement content. For the FA and CA contents, except the day-2 and day-28, the predicted results are decreased. Yet for the day-28, the result can be ignored because of the very high expectations. In the binder content, the cement influences the results. The more it is used, the more the results get better. Finally, the FA + MS content heads the higher compressive strength prediction results than GGBS content does.

22) In the Model-2 for the MRA of the CS estimations for the FA + MS ingredient, the model brings the question marks to the mind for the use of itself due to the very low results of the concrete age dependent analysis in terms of R^2, R^2adj, SSE, and RMSE results. However, the linear correlation of the predicted results shows that the model results are satisfying, and there are no negative deflections in the strength development which means the model is safe to be used. Because of this contradiction, another correlation for the material impacts in the compressive strength prediction for the FA + MS content by using the coefficients of the model equation was studied. Currently, yet, no direct

correlation between the coefficient *K*, and *n* with the R^2 result is subjected (*K* and *n* are from the Table 2.6). As the empirical coefficient *K* seems reverse to the R^2 result in the days between 0.5 and 1; and 3 and 14. Hereupon, the other empirical coefficient *n* has no effect on the data prediction. The lowest amount of air content (0.26%) causes the lowest well-fitting predictions on the real data set in C45-B25-425 mixing code. For the highest amount of air content (3.80%) does not mean the highest well-fitting estimation on the actual data values, either. Also, the minimum amount of cement content (0.12%) means the maximum R^2 result for the sample in MIX-15AC-04 mixing code. And the minimum water content (0.04%) leads the highest well-fitting forecasting for the sample in MIX-15AC-04 mixing code.

23) In the Model-2 for the MRA of the CS estimations for the GGBS ingredient, the empirical coefficient *K* seems opposite to the R^2 results between the day-2 and day-7. The other empirical coefficient *n* seems opposite to the R^2 value at the ages between the day-0.5 and day-1; and day-7 and day-28 on the data estimation. The lowest amount of air content (1.06%) causes the best goodness-of-fit on the real data set in B67-440-BEY mixing code. Albeit, for the highest amount of air content (5.29%) does not mean the worst well-fitting predicted on the actual data values. Together with, the maximum amount of cement content (0.17%) means the minimum R^2 value for the sample in MIX-CEN-03 mixing code. The use of the water effect cannot be understood in this model because of it is linear behavior on the results. The higher compressive strength prediction results are from the FA + MS content.

24) For the splitting tensile strength predictions, antilogarithmic linear regression (Model-1) was studied depending on the amounts and proportions of the contents from the concrete mixture designs. In this perspective, in the Model-1, the MRA of the STS predictions for the FA + MS ingredient, all the data estimations are come out in the expectations. The linear correlation imposes that the model results are satisfactory, and there are no negative deflections in the strength development which means the model is safe to be used. And it is discovered that the equation coefficient is appropriate except the ages between the 0.5-day and 1-day; and 2-day and 3-day. Moreover, the amount of water in the proportion is effective in between day-0.5 and day-1; and day-7 and day-

28. The cement proportion increases the R^2 result for all ages, even though the R^2 result decreases at the same time for some ages. That is why the cement effect cannot be expressed well in this model. For the air content, the model seems parallel to the ages between the day 0.5 and 3; and 7 and 28. The model also puts forth the air effect in the analysis. Because while the air content decreases, the model estimation also decreases. Furthermore, for the minimum R^2 result, the cement proportion is also minimum, the water proportion is maximum. Besides, for the maximum R^2 value, the air content is neither maximum nor minimum. In this model, there is no other correlation for the maximum R^2 result.

25) In the Model-1, the MRA of the STS predictions for the GGBS ingredient, the splitting tensile strength prediction, the equation correlation is reverse for the model results between the day 2 and 3; and 7 and 28. Besides, the water proportion results seem parallel to the equation coefficient which means that the more water content the worse estimated model results. Moreover, the air proportion is effective on the data prediction in positive way. Because the less proportion of the air leads worse results of the strength gaining process. Nonetheless, it is not clear that the high proportion of air leads well results of the model. Finally, the best results in terms of strength gaining are from the FA + MS added sample results.

26) For the modulus of elasticity estimations, logarithmic regression (Model-1) was calculated depending on the amounts and proportions of the contents from the concrete mixture designs. According to this, for the Model-1, the MRA of the ME predictions for the FA + MS ingredient, the results are exposed in the expectations. Else, the linear correlation explicates that the model results are partially satisfying, and there are no negative deflections in the data fitting planar which means the model is safe to be used. For the material effects in the elastic modulus forecasting, the FA + MS content is analyzed by using the coefficients of the model equation. In this way, it is seen that the equation coefficient is not compatible except the ages in between 0.5 and 1. Continuously, the coefficient of the W/C ratio is also incoherent between the days 1 and 3; 7 and 14, either. That is why, just because using the coefficients of the equation is not beneficial for expressing this model. Both the minimum

and maximum R^2 values of the model, the W/C ratio is neither the maximum nor the minimum. For some specimens, the W/C ratio is displayed almost ineffective. That is why this model is accepted unsuitable to predict the modulus of elasticity for the FA + MS content included concrete samples, even though the linear correlation of the model between the actual and predicted data sets are coherent.

27) In the Model-1, the MRA of the ME predictions for the GGBS ingredient, it is enlightened that the equation coefficient is not compatible except the ages between 0.5-day and 3-day; day-14 and day-28. In addition to this, the coefficient of the W/C ratio is almost deniable due to the elastic modulus development between the day-1 and day-3; day-14 and day-28, either. Because of this, only using the coefficients of the equation is not useful for understanding of this model. At the end, for the minimum R^2 result of the model, the W/C ratio is also the minimum (0.34). Especially for some specimens, the W/C ratio is seen almost ineffective. That is why, this model is accepted unreliable to estimate the modulus of elasticity for the GGBS content included concrete samples, as well in FA + MS content included modulus of elasticity analysis. To sum up, in general, the FA + MS content puts forth the higher elastic modulus prediction results than GGBS content reveals.

28) As a predicting method, the Levenberg-Marquardt algorithm from the machine learning was another sub-content of this thesis. Like in the URA and MRA, LM algorithm was studied for the mechanical properties of the concrete by using the amount of the concrete mixture design ingredients with the actual test results. In the algorithm, the training, validation, test, and all are resulted by the software for the algorithm trials. Also, the R and MSE results were revealed for the error check of the forecasted results.

29) In the FA + MS content included samples computed by the LM algorithm with the air content of the CS estimations, the results are very appropriate. For the MSE results, without the air content, the predictions are worse than the air content included estimations except the training results of the algorithm. On the contrary, the, the GGBS content included sample prediction results are better with no air content. the air content in FA + MS existence, the samples in C45-B25-425, and C45-B25-400 mixing codes are resulted negative in the R^2

values. Moreover, the air content in the FA + MS ingredient, the samples in C45-B25-425 and C45-B25-400 mixing codes are negative in the R^2 results which are out of the expectations. Onto this, the air content in the FA + MS ingredient, only the sample in C50-B22-460 mixing code R^2 result is not suitable. Even though the R^2 results are not acceptable for some specimens mentioned above, in general, the LM algorithm works for all scenarios in the FA + MS content. The same method is also followed for the GGBS addition in the concrete samples. Without the air content, only the sample MIX-30-03 seems unsuitable in the result of R^2. For the air effect, the samples in MIX-30, and MIX-30-03 mixing codes are inconvenient for the R^2 results. In this light of the way, the neural network (NN) frames are given constructed on the mixture design variables. Additionally, the linear correlations from the software are also clear for understanding the results. Farther, the actual and estimated results are trendlined. In these correlations, each concrete specimen strength behavior was checked for the algorithm accuracy in the data fitting planar to see whether there was a negative deflection or not. In this perspective, it was seen that there was no negative deflection for both FA + MS and GGBS content included sample results. To sum up, why the algorithm is said to be safe for the compressive strength prediction, even though for the FA + MS including without air content results are statistically under the expectations.

30) In the FA + MS content included samples computed by the LM algorithm with the air content of the STS estimations, with and without the air content, the results are very acceptable. Furthermore, for the MSE results, the predictions with and without the air content, are also in the expectations. The GGBS content added sample estimation results are worse than the FA + MS content included results, even though the results are undeniable. Because of the algorithm predicting, without the air content in the FA + MS existence, the sample in YM-SEG-10A mixing code is lower resulted in the other R^2 results. Nonetheless, with the air content in the FA + MS existence, the same sample is lower among the R^2 results, too. Yet, this time, it is better resulted. So, the LM algorithm works for all scenarios in the FA + MS ingredient for the splitting tensile strength estimations. The same procedure was also followed for the GGBS material in the concrete samples. Without the air content, the

samples C45-III-B20 and MIX-30-03 seem unsuitable in the result of R^2. For the air effect, the samples in MIX-30, MIX-30-03, MIX-32-03, MIX-32-CEN and B67-440 mixing codes are inconvenient for the R^2 results. Especially the sample MIX-32-CEN is almost zero which is inappropriate for the algorithm accuracy check. Furthermore, in the air content included results, the sample in YM-DAP-AC-03 is at sub-zero for the R^2 result which shows that the algorithm does not work for this sample. At the same time, again, the samples in MIX-30-03 and MIX-32-CEN mixing codes are lower among the other R^2 results. But this time, these sample results are higher than the analysis results without the air content. Addition to this, the NN frames are given constructed on the mixture design variables. The actual and estimated results are trendlined, as well. In this correlation, each concrete specimen strength behavior was checked for the accuracy of the algorithm in the data fitting planar to see if there was a negative deflection or not. Without the air content in the FA + MS existence, the samples in YM-SEG-10, C45-B25-425 and C45-B25-400 mixing codes were seen in the negative deflections in the fitting planar. Besides, the air content, the samples in YM-SEG-10E, MIX-15-AC-03, YM-SEG-08 and C45-B25-400 mixing codes were seen in the negative deflections in the FA + MS content. For the GGBS content with the absence of the air, only the sample in MIX-30-03 mixing code was negatively deflected in the fitting planar, which was not expected. With the air content in the GGBS ingredient, the samples in MIX-30-03, MIX-34-BRT, MIX-32-03 and B67-440 mixing codes were also negatively deflected. Therefore, the algorithm is said to be less safe for the splitting tensile strength prediction in the GGBS content with the air. Lastly, the FA + MS content included algorithm results come forward more valid.

31) In the FA + MS content included samples computed by the LM algorithm with the air content of the ME estimations, by comparing with the R values revealed by the software, with and without the air content, the results are said to be highly accurate. Else, in the MSE results, the estimations with and without the air content are comparable to each other. In contrast with the GGBS content included sample prediction results are better than the FA + MS content included results, except the outputs in all class for without the air content. Due

to the algorithm for the forecasting, without the air content in the FA + MS existence, the sample in MIX-15E-03 mixing code is lower resulted in the R^2 results. Also, the air content in the FA + MS material, the same sample is lower among the R^2 results, as well. But in this time, it is better resulted. As a result of the LM algorithm, all the scenarios in the FA + MS content for the modulus of elasticity predictions work well. Moreover, the NN frames are constructed on the mixture design components. Onto this, in the actual and predicted results are trendlined. In this correlation, each concrete sample modulus of elasticity behavior was checked for the accuracy of the algorithm in the data fitting planar to see if there was a negative deflection or not. Without the air content in the GGBS content, the samples in MIX-30-BRT and MIX-32-CEN-OK mixing codes were seen in negative deflections in the fitting planar. Without the air content, only the sample in MIX-32-03 mixing code was seen in negative deflection in the GGBS material. The FA + MS substance, in both air content cases, the results were not deflected in negative directions. That is why the algorithm is said to be safe for the modulus of elasticity prediction in the FA + MS content with and without the air content. Rather than the FA + MS content, the GGBS content included algorithm results were less valid in all types of the result classes given by the software.

This thesis was designed to search for the mechanical properties of high strength concrete. Based on the regression analysis models and machine learning algorithm with the statistical results, the actual test results were estimated and investigated based on the concrete mixture design properties. Besides, all the predicted and analyzed results were also compared with the results of the mechanical property developments by the concrete age. Moreover, in the concrete age, the amounts of concrete mixture contents and the proportions of the concrete mixture design materials were also studied for the safe prediction goals. At the end, to success this, the URA, MRA and LM algorithm were computed in many equations for the diversities of the predicted results in the purpose of the cross checks.

Followingly, in the entire process of the analysis, it is understood that the URA is cost of time to predict the mechanical properties of concrete. Because only one independent variable was used for an estimated result. And this was either concrete age or the compressive strength from the actual laboratory tests. Besides, for all the specimens,

each model equation and statistical parameter were conducted by hand on Microsoft Office Excel 2019. And each result was graphed by hand, as well. That is why the way followed for the estimation caused so much time. However, when this was understood, MATLAB R2021a was another choice for data prediction on the curve fitting tools. And at the end, it was seen that MATLAB R2021a was easy and fast to use and estimate a data set, although a data set was huge and complicated. Besides, its results were also more convenient than Microsoft Office Excel 2019 offered, especially in the curve fitting results. That is why MATLAB R2021a came forward for a safe estimation of the mechanical properties of concrete. Moreover, even though there were unexpected results of the property developments in the estimations, the URA seemed working to predict a mechanical property. In addition to this, the URA method does not use the concrete mixture elements and/or proportions. It only uses the real test results. Because of that, deeper analysis cannot be constructed for future estimations. Further, in the real life, there may be not a wide range of time to estimate and analyze the properties of concrete due to the pace of the construction works. Even, there may be not enough number concrete sampling and/or partially or fully lack of concrete mixture design receipt due to the human based risks and problems at worksites. That is why the URA seems not flexible to be adjusted for very large-scale real life works. But it should be said that for a specific case and a narrowed range data set from the laboratory, the URA is a perfect method to see the close future of the property development of the concrete samples one-by-one.

Intercalarily, the MRA method was studied in many equations. Rather than the concrete age and the compressive strength proposed to be used in the URA, the components of the mixture designs were additionally used for the advanced analyses. The amounts and proportions of the concrete mixture designs were chosen in this direction as the models proposed. Differently, all the concrete ages were investigated from 0.5-day to 28-day. The general forms of each concrete age equations were released for goodness-of-fir purposes. In this path, dividing the data set to the concrete ages were resulted as not expected. Because of that, again for each concrete age, by using the laboratory test results and concrete mixture designs, new data sets were created to compile the estimated results. By this way, the predicted results were again conducted from 0.5-day to 28-day in the fitting planar for each concrete sample to also check whether there was any negative deflection or not for the property development.

With the new data sets created depending on each concrete age MRA analysis, the results were highly recovered with respect to the initial data set estimation results. That is why from specific age to all ages, the MRA method worked very well with these resettled data by using the laboratory test results and concrete mixture designs. Nonetheless, Microsoft Office Excel 2019 had limited tools for detailed analysis like in the URA method. It simply had only "Solver" and "Regression Analysis" tools for data prediction subjected to this thesis. The Solver tool depends on the errors occur in the calculations (SSE) and construct estimated results. And Regression Analysis tool can only solve the linear regression analysis. It is not able to solve non-linear models. That is why more complex analysis is not possible with these methods. Because of this, MATLAB R2021a comes forward rather than Microsoft Excel 2019. As it has many types of regression tools and estimating parameters. Also, it offers more reliable results in terms of R^2, R^2_{adj}, SSE, and RMSE. So, for upcoming projects and/or studied, within a big scale data set, MATLAB R2021a is better to be preferred for prediciting the mechanical properties of concrete samples for deep understanding of mechanical behavior of concrete. But it is important to point that the MRA was also cost of time like the URA.

Except the URA and MRA, as a recent trend in engineering, artificial intelligence was applied on the estimation calculations of the concrete samples. In this perspective, from MATLAB R2021a, machine learning was used for the data estimations. The LM algorithm as machine learning method was used for the deepest analysis concerns. As shown in the figures of this thesis, the results were lasted very quickly which was opposite to the time cost of the URA and MRA. Besides, the results were so rarely deflected in negative ways for the mechanical property development issues. That is why the LM algorithm proved itself for a safe use of data prediction in concrete. Moreover, the predicted results were also statistically undeniable for the consistency checks. In addition to this, the software also automatically offered prediction results either in the text or on the graphics and figures. Because of that, the method was understood noticeably clear and fast. In this frame, for civil engineers, the time can be saved, and the investigations can lead the most real-like solutions for the engineering purposes.

REFERENCES

318-99/318R-99: Building Code Requirements for Structural Concrete & Commentary. (1999). *Technical Documents*.

363R-92: Report on High-Strength Concrete (Reapproved 1997). (1992). *Technical Documents*.

Abd elaty, M. abd allah. (2014). Compressive strength prediction of Portland cement concrete with age using a new model. *HBRC Journal*, *10*(2), 145–155.

Abdelgader, H., Suleiman, R., El-Baden, A., Fahema, A., & Angelescu, N. (2013). *CONCRETE MIX PROPORTIONING USING THREE EQUATIONS METHOD (LABORATORY STUDY)*.

Abrams, L., D. (1919). Properties of Concrete. London: Pitman Publishing Ltd.

ACI 363R-10: Report on High-Strength Concrete. *Technical Documents*.

ACI Committee 318 & American Concrete Institute. (2014). *Building Code Requirements for Structural Concrete (ACI 318-14) [and] Commentary on Building Code Requirements for Structural Concrete (ACI 318R-14)*.

Akman M. S. (1990)**.** Yapi Malzemeleri, ITU Insaat Fakultesi Yayini, (1408) p.162, İstanbul.

Al-Jabri, K. S., Hisada, M., Al-Oraimi, S. K., & Al-Saidy, A. H. (2009). Copper slag as sand replacement for high performance concrete. *Cement and Concrete Composites*, *31*(7), 483–488.

Al-Jabri, K. S., Hisada, M., Al-Saidy, A. H., & Al-Oraimi, S. K. (2009). Performance of high strength concrete made with copper slag as a fine aggregate. *Construction and Building Materials*, *23*(6), 2132–2140.

Ambily, P. S., Umarani, C., Ravisankar, K., Prem, P. R., Bharatkumar, B. H., & Iyer, N. R. (2015). Studies on ultra-high-performance concrete incorporating copper slag as fine aggregate. *Construction and Building Materials*, *77*, 233–240.

American Concrete Institute, & ACI Committee 209--Creep and Shrinkage (Eds.). (2008). *Guide for modeling and calculating shrinkage and creep in hardened concrete*. American Concrete Institute.

Arioglu, E., & Arioglu, N. (2005). *Ust ve alt yapilarda beton karot deneyleri ve degerlendirilmesi*. Evrim Yayinevi.

Arioglu, E., & Koyluoglu, O., S. (1997). Mineral Katki (Ucucu Kul-Silika-Fume-Yuksek Firin Curufu) İceren Betonlarda 7-28-91 Gunluk Dayanimlar Arasinda Cikartilan Istatistiksel İliskiler, *Beton Prefabrikasyon*, 41, 5-11.

Arioglu, E., Alper, H., & Odbay, O. (1994, Nisan). Beton Dayaniminin Erken Kestirimi. *Beton Prefabrikasyon*, (30), 15-18.

Bedirhanoglu, İ. (2011). Yapi Malzemesi-Beton Tasarimi Ders Notlari. Diyarbakir: Dicle Universitesi.

Behnood, A., Verian, K. P., & Modiri Gharehveran, M. (2015). Evaluation of the splitting tensile strength in plain and steel fiber-reinforced concrete based on the compressive strength. *Construction and Building Materials*, *98*, 519–529.

Ben Chaabene, W., Flah, M., & Nehdi, M. L. (2020). Machine learning prediction of mechanical properties of concrete: Critical review. *Construction and Building Materials*, *260*, 119889.

Bendapudi, S. (2019). Correlation between Compressive Strength and Split Tensile Strength of GGBS and MK Based Geopolymer Concrete using Regression Analysis. *JOURNAL OF MECHANICS OF CONTINUA AND MATHEMATICAL SCIENCES*, *14*.

Bin Ahmed, F., Abid Ahsan, K., Shariff, T., & Rahman Meem, S. (2021). Formulation of polynomial equation predicting the splitting tensile strength of concrete. *Materials Today: Proceedings*, *38*, 3269–3278.

Bingol, A. F., Tortum, A., & Gul, R. (2013). Neural networks analysis of compressive strength of lightweight concrete after high temperatures. *Materials & Design*, *52*, 258–264.

Blick, R. L., (1973). Some Factors Influencing High-Strength Concrete. *Modern Concrete*, 36(12), 38-41.

Bourdeau, M., Zhai, X. qiang, Nefzaoui, E., Guo, X., & Chatellier, P. (2019). Modeling and forecasting building energy consumption: A review of data-driven techniques. *Sustainable Cities and Society*, *48*, 101533.

British Standards Institution. (2004). *Eurocode 2: Design of concrete structures*. British Standards Institution.

Burden, F., & Winkler, D. (2008). Bayesian regularization of neural networks. Methods in molecular biology (Clifton, N.J.), 458, 25–44.

CEB-FIP MODEL CODE 1990. (1993). Thomas Telford Publishing.

Chau, K. W., Wu, C. L., & Li, Y. S. (2005). Comparison of several flood forecasting models in Yangtze river. *Journal of Hydrologic Engineering, ASCE*, 485–491.

Chithra, S., Kumar, S. R. R. S., Chinnaraju, K., & Alfin Ashmita, F. (2016). A comparative study on the compressive strength prediction models for High Performance Concrete containing nano silica and copper slag using regression analysis and Artificial Neural Networks. *Construction and Building Materials*, *114*, 528–535.

Colak, A. (2006). A new model for the estimation of compressive strength of Portland cement concrete. *Cement and Concrete Research*, *36*, 1409–1413.

Colak, A. (2006). Estimation of Compressive Strength of Portland Cement Concrete Depending on The Water to Cement and Aggregate to Cement Ratios. Technical note, Unpublished data.

Colak, A., & Cosgun, T. (2013). Discussion of the paper titled "Design of clay/cement mixtures for extruded building products by Khelifi et al." *Materials and Structures*, *46*(3), 513–515.

Crouch, L. K., Sparkman, A., Dunn, T. R., Hewitt, R., Mittlesteadt, W., Byard, B., & Pitt, J. (n.d.). *1 Estimating Pervious PCC Pavement Design Inputs with Compressive Strength and Effective Void Content*.

Cui, Y., Gao, K., & Zhang, P. (2020). Experimental and Statistical Study on Mechanical Characteristics of Geopolymer Concrete. *Materials (Basel, Switzerland)*, *13*(7), 1651. PubMed.

Dao, D. V., Ly, H.-B., Trinh, S. H., Le, T.-T., & Pham, B. T. (2019). Artificial Intelligence Approaches for Prediction of Compressive Strength of Geopolymer Concrete. *Materials*, *12*(6).

DeRousseau, M. A., Kasprzyk, J. R., & Srubar, W. V. (2018). Computational design optimization of concrete mixtures: A review. *Cement and Concrete Research*, *109*, 42–53.

Diaz-Loya, E., Allouche, E., & Vaidya, S. (2011). Mechanical Properties of Fly-Ash-Based Geopolymer Concrete. *ACI Materials Journal*, *108*, 300–306.

Fadaei, N., Yan, W.-M., Mahdi Tafarroj, M., & Kasaeian, A. (2018). The application of artificial neural networks to predict the performance of solar chimney filled with phase change materials. *Energy Conversion and Management*, *171*, 1255–1262

***fib Model Code for Concrete Structures 2010*. (n.d.).** 436.

Ghafoori, N., & Dutta, S. (1995). Pavement Thickness Design for No-Fines Concrete Parking Lots. *Journal of Transportation Engineering*, *121*(6), 476–484.

Gorai, B., Jana, R. K., & Premchand. (2003). Characteristics and utilisation of copper slag—A review. *Resources Conservation and Recycling*, *39*, 299–313.

Gupta, H. V., Kling, H., Yilmaz, K. K., & Martinez, G. F. (2009). Decomposition of the mean squared error and NSE performance criteria: Implications for improving hydrological modelling. *Journal of Hydrology*, *377*(1–2), 80–91.

Hadzima-Nyarko, M., & Trinh, S. H. (2022). *Prediction of compressive strength of concrete at high heating conditions by using artificial neural network-based Bayesian regularization*. 13.

Haque, M. A., & Rasel-Ul-Alam, Md. (2018). Non-linear models for the prediction of specified design strengths of concretes development profile. *HBRC Journal*, *14*(2), 123–136.

Haranki, B. (2009). Strength, Modulus of Elasticity, Creep and Shrinkage of Concrete used in Florida. 176.

Hemmat Esfe, M., Wongwises, S., Naderi, A., Asadi, A., Safaei, M. R., Rostamian, H., Dahari, M., & Karimipour, A. (2015). Thermal conductivity of Cu/TiO2–water/EG hybrid nanofluid: Experimental data and modeling using artificial neural network and correlation. *International Communications in Heat and Mass Transfer*, *66*, 100–104.

Hespe, E. D. (1971). LEACH TESTING OF IMMOBILIZED RADIOACTIVE WASTE SOLIDS. A PROPOSAL FOR A STANDARD METHOD. *At. Energy Rev. 9: No. 1, 195-207(Apr 1971).*

Hope, J. A., Beaudoin, J. J., Brauson, D. E., Gamble, B. R., Geymayer, H. G., Goyalt, B. B., & Hope, B. B. (n.d.). *Prediction of Creep, Shrinkage, and Temperature Effects in Concrete Structures*. 47.

Ibrahim, A., Mahmoud, E., Yamin, M., & Patibandla, V. C. (2014). Experimental study on Portland cement pervious concrete mechanical and hydrological properties. *Construction and Building Materials*, *50*, 524–529.

James E. Cook. (1982). Research and Application of High-Strength Concrete Using Class C Fly Ash. *Concrete International*, *4*(7).

Kaur, H., & Salaria, D. S. (2013). *Bayesian Regularization Based Neural Network Tool for SoftwareEffort Estimation*. 7.

Khademi, F., Jamal, S. M., Deshpande, N., & Londhe, S. (2016). Predicting strength of recycled aggregate concrete using Artificial Neural Network, Adaptive Neuro-Fuzzy Inference System and Multiple Linear Regression. *International Journal of Sustainable Built Environment*, *5*(2), 355–369.

Khanzadi, M., & Behnood, A. (2009). Mechanical properties of high-strength concrete incorporating copper slag as coarse aggregate. *Construction and Building Materials*, *23*(6), 2183–2188.

Kim, J.-K., Han, S. H., & Song, Y. C. (2002). Effect of temperature and aging on the mechanical properties of concrete Part I. Experimental results. *Cement and Concrete Research*, 8.

Kockal, N., & Aydogdu, I. (2020). Estimation of rigidity of concrete based on multi parameters using artificial bee colony optimization method with levy flight distribution. *Filomat*, *34*(2), 583–590.

McKinney, D. C., (2009). *Numerical methdos for civil engineers* (Lecture Notes. CE 311K). The University of Texas at Austin.

Muhendisligi, Y. (n.d.). *YUKSEK LISANS TEZI Ins. Muh. Enver Burak TURKEL*. 92.

Neville, A. M., & Brooks, J. J. (2010). *Concrete technology* (2. ed). Prentice Hall.

Noguchi, T., & Tomosawa, F. (1995). RELATIONSHIP BETWEEN COMPRESSIVE STRENGTH AND MODULUS OF ELASTICITY OF HIGH STRENGTH CONCRETE. *Journal of Structural and Construction Engineering (Transactions of AIJ)*, *60*(474), 1–10.

NT BUILD 200. (1984). Concrete, hardened: Dimensions of test specimens. Espoo: Nordtest.

NT BUILD 201. (1984). Concrete: Making and curing of moulded test specimens for strength tests. Espoo: Nordtest.

NT BUILD 202. (1984). Concrete, hardened: Sampling and treatment of cores for strength tests. Espoo: Nordtest.

NT BUILD 203. (1984). Concrete, hardened: Compressive strength test specimens. Espoo: Nordtest.

NT BUILD 204. (1984). Concrete hardened: Tensile strength of test specimens. Espoo: Nordtest.

NT BUILD 205. (1984). Concrete hardened: Modulus of elasticity in compression. Espoo: Nordtest.

Ozturan, M., Kutlu, B., & Ozturan, T. (n.d.). *COMPARISON OF CONCRETE STRENGTH PREDICTION TECHNIQUES WITH ARTIFICIAL NEURAL NETWORK APPROACH*. 14.

Parrott, L. J., & British Cement Association. (1988). *A literature review of high strength concrete properties*. British Cement Association.

Plecas, I. B., & Dimovic, S. D. (2009). Mathematical Modelling of Immobilization of Radionuclides 137Cs and 60Co in Concrete Matrix. *The Open Waste Management Journal*, *2*(1), 43–46. https://doi.org/10.2174/1876400201002010043

Pliego Marugán, A., García Márquez, F. P., Pinar Pérez, J. M., & Ruiz-Hernández, D. (2018). A survey of artificial neural network in wind energy systems. *Applied Energy*, *228*, 1822–18bouk36.

Prediction of Efficiency Factor of Ground-Granulated Blast-Furnace Slag of Concrete Using Artificial Neural Network. (2011). *ACI Materials Journal*, *108*(1).

Price, W. F., & Hynes, J. P. (1996). In-situ strength testing of high strength concrete. *Magazine of Concrete Research*, *48*(176), 189–197.

Rajamane, N. P., Ambily, P. S., Nataraja, M. C., & Das, L. (2014). Discussion: Modified Bolomey equation for strength of lightweight concretes containing fly ash aggregates. *Magazine of Concrete Research*, *66*(24), 1286–1288.

Raphael, J. M. (1984). *Tensile Strength of Concrete*. 8.

Razak, H. A., & Wong, H. S. (n.d.). *RE-EVALUATION OF STRENGTH AND STIFFNESS RELATIONSHIPS FOR HIGH-STRENGTH CONCRETE*. 17.

Resheidat, M. R., & Ghanma, M. S. (1997). Accelerated strength and testing of concrete using blended cement. *Advanced Cement Based Materials*, *5*(2), 49–56.

Said Iravani. (1996). Mechanical Properties of High- Performance Concrete. *ACI Materials Journal*, *93*(5).

Sam, J. (2020). *Use of Correlation and Regression Analyses as Statistical Tools in Green Concrete Research*. *8*, 991.

Seitablaiev, E. (2019). Beton Dayaniminim Su/Cimento ve Agrega/Cimento Oranlarina Bagli Olarak Belirlenmesi, Yuksek Lisans Tezi, Trakya Universitesi, Edirne.

Shah, S. P., & Ahmad, S. H. (1985). Structural Properties of High Strength Concrete and its Implications for Precast Prestressed Concrete. *PCI Journal*, *30*(6), 92–119.

Suescum-Morales, D., Salas-Morera, L., Jiménez, J. R., & García-Hernández, L. (2021). A Novel Artificial Neural Network to Predict Compressive Strength of Recycled Aggregate Concrete. *Applied Sciences*, *11*(22), 11077.

Sutherland, A., Haldenwang, R., & Chhabra, R. (n.d.). *NEWTONIAN FLUIDS – USE OF RMSE and R^2 vs. AIC*. 10.

TS EN 12350-2. (2019). Testing fresh concrete – Part 2: Slump test. Turkish Standards Institute, Ankara.

TS EN 12350-6. (2019). Testing fresh concrete – Part 6: Density. Turkish Standards Institute, Ankara.

TS500. (2000). Requirements for design and construction of reinforced concrete structures. Turkish Standards Institute, Ankara.

TS802. (2016). Design Concrete Mixes. Turkish Standards Institute, Ankara.

Wills, M. H. Jr., (1967). How Aggregate Particle Shape Influences Concrete Mixing Water Requirement and Strength. *Journal of Materials*, 2(4), 843-865.

Wilson, J., Jones, E., & Dickson, M. (n.d.). *PREDICTION OF CONCRETE COMPRESSIVE STRENGTH USING MATHEMATICAL REGRESSION MODEL*. 8.

Xu, J., Zhao, X., Yu, Y., Xie, T., Yang, G., & Xue, J. (2019). Parametric sensitivity analysis and modelling of mechanical properties of normal- and high-strength recycled aggregate concrete using grey theory, multiple nonlinear regression and artificial neural networks. *Construction and Building Materials*, *211*, 479–491.

Yilmaz, Y. (n.d.). *BETON ÜRETİMİNDE UÇUCU KÜL VE YÜKSEK FIRIN CÜRUFU KULLANILMASININ ETKİLERİ VE MALİYET ANALİZİ*. 65.

Zain, M., Abd, S., Sopian, K., Jamil, M., & Che-Ani, A. (2008). *Mathematical regression model for the prediction of concrete strength* (p. 402).

Zhang, X., Deng, S., Deng, X., & Qin, Y. (2007). Experimental research on regression coefficients in recycled concrete Bolomey formula. *Journal of Central South University of Technology*, *14*(1), 314–317.

Ziółkowski, P., & Niedostatkiewicz, M. (2019). Machine Learning Techniques in Concrete Mix Design. *Materials*, *12*, 1256.

Ziolkowski, P., Niedostatkiewicz, M., & Kang, S.-B. (2021). Model-Based Adaptive Machine Learning Approach in Concrete Mix Design. *Materials*, *14*(7), 1661.

CURRICULUM VITAE

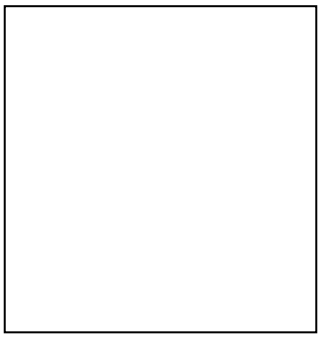

Name Surname **:** Muzaffer Umur DALGIC

Place and Date of Birth **:**

E-Mail **:**

EDUCATION **:**

- **B.Sc.** **:** 2017, Istanbul Technical University. Civil Engineering Faculty. Civil Engineering Department